A Shared Metabolic Basis for Parkinson's, Alzheimer's, and Huntington's

A thesis submitted to The University of Manchester for the degree of Doctor of Philosophy in the Faculty of Biology, Medicine and Health

2021

Melissa J. Scholefield

School of Medical Sciences

Division of Cardiovascular Sciences

Table of Contents

Table of Contents 2
List of Figures 10
List of Tables 13
Abbreviations 16
Abstract 22
Declaration 23
Disclaimer 24
Copyright Statement 25
Acknowledgements 26
Chapter One | Introduction 27
1. Introduction 28
1.1. Dementia in Neurodegenerative Diseases 28
1.2. Mechanisms of Dementias 35
1.3. -Omics 42
1.4. The Current Investigation 44
1.4.1. Use of the Alternative Thesis Format 46
1.5. Aims 47
Chapter Two | Mass Spectrometry Methods 48
2.1. Mass Spectrometry 49
2.1.1. Mass Spectrometry Overview 49
2.2. Mass Analysers 50
2.2.1. Quadrupole Mass Analysers 50
2.2.2. TOF Mass Analyser 51
2.2.3. Other Mass Analysers 52
2.2.4. Tandem MS 53
2.2.5. Comparison and Selection of Mass Analysers 55
2.2.6. Advantages & Disadvantages of MS 55
2.3. ICP–MS 56
2.3.1. Sample Preparation 57

2.3.2. Sample Introduction 58
2.3.3. Sample Ionisation 59
2.3.4. Interface Region 60
2.3.5. Collision/Reaction Cell 61
2.3.6. Data Analysis 62
2.3.7. Advantages and Disadvantages of ICP–MS 62
2.4. Chromatography–MS 64
2.5. Gas Chromatography–MS 64
2.5.1. Sample Preparation 64
2.5.2. Sample Introduction 69
2.5.3. Gas Chromatograph (GC) 69
2.5.4. Interface 72
2.5.5. Data Analysis 73
2.6. LC–MS 74
2.6.1. Sample Preparation 75
2.6.2. Sample Introduction 75
2.6.3. Liquid Chromatography 75
2.6.4. Interface 77
2.6.5. Data Analysis 79
2.6.6. Advantages & Disadvantages of Metabolomic MS Techniques 79
2.7. Summary 81

Chapter Three | Shared perturbations in the metallome and metabolome of Alzheimer's, Parkinson's, Huntington's, and dementia with Lewy bodies: a systematic review 82

3.1. Introduction 83
3.2. Methods 85
3.2.1. Approach to Literature Searching 85
3.2.1. Inclusion & Exclusion Criteria 85
3.2.2. Scoring of Included Papers 87
3.2.3. Evaluation of Findings 88
3.3. Results 88

3.3.1. Inclusion Criteria and Rating System for Selection of Studies 88
3.2.1. Rating of Papers 91
3.2.2. Findings in Brain Tissue 93
3.2.3. Findings in CSF 97
3.2.4. Findings in Blood 97
3.2.5. Summary of disease comparisons 100
3.2.6. Common Findings across Brain Tissue, CSF and Blood 101
3.2.2. Discussion of Comparisons of Metals and Metabolites in Four Dementias 107
3.3. Discussion of Scientific Findings 110
3.3.1. Strengths and Limitations of this Systematic Review 117
3.4. Summary 119
Chapter Four | Evidence that levels of nine essential metals in post mortem human-Alzheimer's-brain and ex-vivo rat-brain tissues are unaffected by differences in post mortem delay, age, disease staging, and brain bank location 120
4.1. Introduction 122
4.1.1. Alzheimer's Disease & Human Brain Studies 122
4.1.2. Metallomics in the Human Brain 124
4.2. Materials and methods 125
4.2.1. Reagents 125
4.2.2. Acquisition of human cingulate gyrus from AD cases and controls 125
4.2.3. Acquisition of rat-brain tissues 125
4.2.4. Diagnosis & Severity of Human Cases 126
4.2.5. Tissue Dissection 126
4.2.6. ICP–MS 127
4.2.7. ICP–MS Data Analysis 127
4.3. Results 128
4.3.1. Patient characteristics 128
4.3.2. Cohort comparisons 128
4.3.3. ICP–MS Metals Analysis 132
4.3.4. Wet-weight Tissue 143
4.3.5. Effect of *post mortem* delay on metallomic analysis of *ex-vivo* rat-brain tissues 147

4.4. Discussion 152
4.4.1. Human brain tissue 152
4.4.2. Effect of PMD on Metallomic Analyses in Rat Brain Tissues 156
Chapter Five | Widespread decreases in copper common to Parkinson's disease dementia and Alzheimer's disease human brains 159
5.1. Introduction 161
5.2. Materials and methods 162
5.2.1. Reagents 162
5.2.2. Acquisition of human brain tissues from PDD cases and controls 162
5.2.3. Diagnosis & Severity of Human Cases 162
5.2.4. Tissue Dissection 163
5.2.5. ICP–MS 163
5.2.6. ICP–MS Data Analysis 164
5.3. Results 166
5.3.1. Patient Characteristics 166
5.3.2. Control Groups 168
5.3.3. ICP–MS Metals Analysis 171
5.3.4. Comparison to AD Findings 181
5.4. Discussion 183
5.4.1. Copper (Cu) 183
5.4.2. Manganese (Mn) 184
5.4.3. Zinc (Zn) 185
5.4.4. Selenium (Se) 186
5.4.5. Magnesium (Mg) 186
5.4.6. Potassium (K) 187
5.4.7. Iron (Fe) 187
5.4.8. Sodium (Na) and Calcium (Ca) 188
5.5. Conclusions 188
Chapter Six | Effects of Alterations of Post mortem Delay and Other Tissue-collection Variables on Metabolite Levels in Human- and Rat-brain 189
6.1. Introduction 191

6.2. Methods 192
6.2.1. Acquisition of Brain Tissue 192
6.2.2. Diagnosis & Severity of Human Cases 192
6.2.3. Tissue Dissection 192
6.2.4. GC–MS 193
6.2.5. Data Acquisition 194
6.2.6. Data Analysis 194
6.3. Results 195
6.3.1. Cohort Comparisons in Human Brain Tissue 195
6.3.2. Human Brain Metabolite Analysis 198
6.3.3. Effect of PMD on Metabolomic Analysis of Rat Brain Tissue 201
6.4. Discussion 210
6.4.1. Metabolomic Analysis 210
6.4.2. Effect of PMD on Metabolomic Analyses in Rat Brain Tissues 212
6.5. Conclusions 215
Chapter Seven | Substantively lowered levels of pantothenic acid (vitamin B5) in several regions of the human brain in Parkinson's disease dementia 216
7.1. Introduction 218
7.2. Methods 219
7.2.1. Acquiring Tissue for Pantothenic Acid Quantification 219
7.2.2. Diagnosis & Severity of PDD Cases 220
7.2.3. Pantothenic Acid Quantification 220
7.2.4. UHPLC–MS/MS Data Analysis 222
7.3. Results & Discussion 222
7.3.1. Cohort Characterisation 222
7.3.2. Pantothenic Acid Analysis 223
7.3.3. Comparisons with ADD and HD 227
Chapter Eight | Severe and regionally widespread increases in tissue urea in the human brain represent a novel finding of pathogenic potential in Parkinson's disease dementia 234
8.1. Background 236

8.2. Methods 237
8.2.1. Obtaining Tissue for Urea Quantification 237
8.2.2. Diagnosis & Severity of PDD Cases 237
8.2.3. Tissue Dissection 237
8.2.4. Urea Quantification 237
8.2.5. UHPLC–MS/MS Data Analysis 239
8.3. Results & Discussion 240
8.3.1. Cohort Characterisation 240
8.3.2. Brain-tissue Urea Findings in PDD 240
8.3.3. Comparisons with Brain-urea Concentrations in AD and in HD 244
8.4. Conclusions 250
Chapter Nine | Untargeted Metabolomics Analysis of PDD 251
9.1. Introduction 252
9.2. Methods 254
9.2.1. Obtaining Tissue for LC–MS Metabolomics 254
9.2.2. Diagnosis & Severity of PDD Cases 254
9.2.3. Tissue Dissection 254
9.2.4. LC–MS Metabolomics 254
9.2.5. Data Analysis 256
9.3. Results 256
9.3.1. Cohort Characteristics 256
9.3.2. LC–MS Analysis 257
9.3.3. Comparison to AD and HD 266
9.4. Discussion 272
9.4.1. Glucose Metabolism 272
9.4.2. Purine Metabolism 274
9.4.3. Amino Acids 278
9.4.4. Other 278
9.4.5. Limitations of the Study 279
9.5. Conclusions 280
Chapter Ten | Discussion 281

10.1. Discussion 282
10.2. Designing Studies for –Omics 283
10.3. Metals in the PDD Brain 285
10.4. Metabolites in the PDD Brain 286
10.5. Where Metallomics and Metabolomics Meet 288
10.6. PDD, AD, and HD 291
10.7. Future Studies 293
10.8. Conclusions 294
References 296
Supplementary Material 314
Supplementary Table 1 – Search Terms 314
Supplementary Table 2A – Metals in AD 318
Supplementary Table 2B – Metabolites in AD 324
Supplementary Table 3A – Metals in PD 349
Supplementary Table 3B – Metabolites in PD 357
Supplementary Table 4A – Metals in DLB 372
Supplementary Table 4B – Metabolites in DLB 374
Supplementary Table 5A – Metals in HD 378
Supplementary Table 5B – Metabolites in HD 380
Supplementary Table 6: Characteristics of individuals in the Manchester AD cohort 397
Supplementary Table 7: Characteristics of individuals in the Newcastle cohort 400
Supplementary Table 8: Characteristics of individuals in the Auckland AD cohort 402
Supplementary Table 9: Characteristics of Manchester AD experimental cohort 404
Supplementary Table 10: Characteristics of Newcastle experimental cohort 405
Supplementary Table 11: Characteristics of Auckland AD experimental cohort 406
Supplementary Table 12: Characteristics of individuals in the PDD Metallomics cohort 407
Supplementary Table 13: Recorded comorbidities, causes of death, and neuropathological diagnoses of PDD Metallomics cohort 409
Supplementary Table 14: Characteristics of individuals in the PDD Metabolomics cohort 411
Supplementary Table 15: Individual Pantothenic Acid Concentrations in PDD Cohort 414

Supplementary Table 16: Individual Urea Concentrations in PDD Cohort 415
Supplementary Figure 1: Significantly Altered Metabolites in PDD 416
Electronic Appendix 421

Word Count: 65, 844

List of Figures

Figure 1. 1. Shared causes and symptoms across various dementia diseases **34**

Figure 1. 2. Mitochondrial electron transport chain and TCA cycle **38**

Figure 2. 1. Diagram of ICP–MS mass analyser and collision/reaction cell **50**

Figure 2. 2. Diagram of TOF mass analyser **52**

Figure 2. 3. Diagram of QQQ MS/MS **53**

Figure 2. 4. Overview of ICP–MS apparatus **57**

Figure 2. 5. Diagram of ICP–MS sample introduction apparatus **59**

Figure 2. 6. Diagram of ICP–MS ionisation apparatus **60**

Figure 2. 7. Silylation Reaction **69**

Figure 2. 8. Diagram of gas chromatograph **71**

Figure 2. 9. Diagram of GC–MS interface apparatus **73**

Figure 2. 10. Diagram of LC–MS Apparatus **74**

Figure 2. 11. Diagram of LC with Sample Introduction System **77**

Figure 2. 12. Diagram of LC–MS Interface with Electrospray Ionisation **79**

Figure 3. 1. Disease and matrix coverage of papers accepted for final review **90**

Figure 3. 2. Percentage of papers meeting Table 2 rating system requirements **92**

Figure 3. 3. Summary of evidence from all reports of altered metals and metabolites in AD brains accepted for this review **112**

Figure 3. 4. Summary of evidence from all reports of altered metals and metabolites in PD brains accepted for this review **113**

Figure 3. 5. Summary of evidence from all reports of altered metals and metabolites in DLB brains accepted for this review **114**

Figure 3. 6. Summary of evidence from all reports of altered metals and metabolites in HD brains accepted for this review **115**

Figure 4. 1. Braak staging of all controls registered on MRC brain bank database **123**

Figure 4. 2. Dry-weight metal concentrations in the Manchester, Newcastle, and Auckland cohorts **134**

Figure 4. 4. Wet-weight metal concentrations in the Manchester and Auckland cohorts **145**

Figure 4. 5. Essential metal concentrations in three rat-brain regions at four levels of *post mortem* delay **151**

Figure 5. 1. Metal concentrations in PDD cases vs controls **179**

Figure 5. 2. Number of altered metals per brain region **180**

Figure 5. 3. Regional comparison of metal perturbations observed in PDD and AD brains **182**

Figure 6. 1. CERAD Score vs tau Braak Stage **200**

Figure 6. 2. Metabolomic Analysis of Newcastle and Manchester Cohorts **200**

Figure 6. 3. Unaltered and Altered Metabolites in Rat Brain Tissue **207**

Figure 6. 4. PLS–DA Plots of Rat Brain Tissue Metabolites **209**

Figure 7. 1. Pantothenic Acid Concentrations in PDD Cases and Controls **224**

Figure 7. 2. Regional Distribution of Pantothenic Acid Decreases in the PDD, ADD, and HD Brain **229**

Figure 8. 1. Urea Concentrations in PDD Cases and Matched Controls **242**

Figure 8. 2. Regional Distribution of Measured Tissue Urea Increases in the PDD, AD, and HD Brain **246**

Figure 9. 1. Number of Altered Metabolites in PDD Brain Regions **262**

Figure 9. 2. Glucose Pathway Metabolites in the PDD Brain **263**

Figure 9. 3. Purine Pathway Metabolites in the PDD Brain **265**

Figure 9. 4. Updated: Glucose Pathway Changes in the PDD Brain **274**

Figure 9. 5. Updated: Purine Pathway Alterations in the PDD Brain **277**

Figure 10. 1. Updated Diagram of Metabolic and Metallomic Changes Reported in the PD/D Brain **290**

Figure 10. 2. Common features and findings between AD, PDD, and HD **292**

List of Tables

Table 1.1. A comparison of clinical and neuropathological presentation of PDD, DLB, AD, and HD **31**

Table 2. 1. Comparison of Metallomic Analytical Techniques **63**

Table 2. 2. Comparison of GC–MS Extraction Techniques **67**

Table 2. 3. Comparison of Metabolomic Analysis Techniques **81**

Table 3. 1. Inclusion criteria necessary for a published study to be considered for review **86**

Table 3. 2. Rating system of papers meeting inclusion criteria **87**

Table 3. 3. Perturbations in levels of metals & metabolites in dementia brain tissue **93**

Table 3. 4. Metals & metabolites reported in blood from patients with age-related dementia **99**

Table 3. 5. Number of Analytes Reported in Brain tissues & Biofluids of AD patients **103**

Table 4. 1. PMD, Braak stage and age of all brains listed in databases of the Manchester brain bank **129**

Table 4. 2. Comparison of group characteristics of cohorts from each brain bank **131**

Table 4. 3. Essential metal concentrations in dry cingulate gyrus tissue from the Manchester, Newcastle, Auckland, and combined cohorts **135**

Table 4. 4. Power analysis of individual and combined cohorts **138**

Table 4. 5. Table of MANCOVA analysis of combined-cohort metal concentrations **140**

Table 4. 6. Table of significant and borderline findings in tests of between-subjects effects of combined- cohort metal concentrations **142**

Table 4. 7. Essential metal concentrations in wet cingulate gyrus tissue from the Manchester, Auckland, and combined cohorts **146**

Table 4. 8. Two-way ANOVA analysis of essential metals in three rat-brain regions **148**

Table 4. 9. Essential metal concentrations in three rat-brain regions at four levels of *post mortem* delay **150**

Table 5. 1. Cohort Characteristics **167**

Table 5. 2. Comparison of cohort control characteristics **169**

Table 5. 3. Final Control Groups for each region **170**

Table 5. 4. Metal concentrations in the SN of PDD cases and controls **173**

Table 5. 5. Metal concentrations in the CG of PDD cases and controls **173**

Table 5. 6. Metal concentrations in the LC of PDD cases and controls **174**

Table 5. 7. Metal concentrations in the HP of PDD cases and controls **174**

Table 5. 8. Metal concentrations in the MED of PDD cases and controls **175**

Table 5. 9. Metal concentrations in the PVC of PDD cases and controls **175**

Table 5. 10. Metal concentrations in the MTG of PDD cases and controls **176**

Table 5. 11. Metal concentrations in the CB of PDD cases and controls **176**

Table 5. 12. Metal concentrations in the MCX of PDD cases and controls **176**

Table 6. 1. Comparison of Brain Bank Groups **197**

Table 6. 2.	Unaltered Metabolites in Rat Brain Tissue	**202**
Table 6. 3.	Metabolites Significantly Altered in Rat Brain Tissue	**206**
Table 7. 1.	UHPLC-MS/MS Gradient Elution Conditions	**222**
Table 7. 2.	UHPLC-MS/MS Transitions	**222**
Table 7. 3.	PDD Cohort Characteristics	**223**
Table 7. 4.	Pantothenic Acid Concentrations in PDD Cases and Controls	**226**
Table 7. 5.	Statistical Power of Pantothenic Acid Analyses	**227**
Table 7. 6.	Pantothenic acid fold-changes in PDD, ADD, and HD	**228**
Table 8. 1.	UHPLC-MS/MS Gradient Elution Conditions	**240**
Table 8. 2.	UHPLC-MS/MS Transitions	**240**
Table 8. 3.	PDD Cohort Characteristics	**240**
Table 8. 4.	Tissue Urea Concentrations in PDD Cases and Controls	**242**
Table 8. 5.	Statistical Power of Urea Analyses	**243**
Table 9. 1.	Summary of Metabolomic Perturbations Previously Reported in PD/PDD Brains	**253**
Table 9. 2.	Cohort Characteristics	**257**
Table 9. 3.	Significantly Altered Metabolites in PDD Brain	**261**
Table 9. 4.	Comparison of Metabolites in PDD, AD, and HD Brains	**271**

Abbreviations

AAS	Atomic absorption spectroscopy
AES	Auger electron spectroscopy
Acetyl CoA	Acetyl coenzyme A
AD	Alzheimer's disease
AMG	Amygdala
ANOVA	Analysis of variance
AntCG	Anterior cingulate gyrus
ATP	Adenosine triphosphate
APCI	Atmospheric pressure chemical ionisation
ApoE	Apolipoprotein E
BD10	Brodmann's area 10
Ca	Calcium
CAUD	Caudate
CB	Cerebellum
CBC	Cerebellar cortex
CERAD	Consortium to Establish a Registry for Alzheimer's disease
CG	Cingulate gyrus
CI	Confidence interval
CN	Caudate nucleus
Cu	Copper
CoV	Coefficient of variance

CSF	Cerebrospinal fluid
CV	Covariate
DLB	Dementia with Lewy bodies
DV	Dependent variable
ENT	Entorhinal cortex
ESI	Electrospray ionisation
FC	Frontal cortex
Fe	Iron
FDG-PET	Fluorodeoxyglucose-positron emission tomography
FDR	False discovery rate
FG	Frontal gyrus
FL	Frontal lobe
FWM	Frontal white matter
G-3-P	Glycerol-3-phosphate
GC–MS	Gas chromatography/mass spectrometry
GFC	Gel filtration chromatography
GP	Globus pallidus
GPC	Gel permeation chromatography
GSH	Reduced glutathione
GSSG	Oxidised glutathione
GTX2	Glutaredoxin 2
HD	Huntington’s disease

He	Helium
HP	Hippocampus
HPLC	High-performance liquid chromatography
HR-full scan	High resolution-full scan
HRMS	High resolution mass spectrometry
ICP–MS	Inductively-coupled plasma mass spectrometry
IEC	Ion exclusion chromatography
IHC	Immunohistochemistry
IMP	Inosine monophosphate
INAA	Instrumental neutron activation analysis
IPL	Inferior parietal lobe
ITG	Inferior temporal gyrus
IV	Independent variable
K	Potassium
LC	Locus coeruleus
LC/MS	Liquid chromatography/mass spectrometry
LC-LTQ-Orbitrap-MS	Liquid chromatography Orbitrap mass spectrometry
LOD	Limit of detection
LOQ	Lower limit of quantification
m/z	Mass-to-charge ratio
MCX	Motor cortex
MED	Medulla oblongata

MFG	Middle frontal gyrus
Mg	Magnesium
MMSE	Mini-Mental State Examination
Mn	Manganese
Mn-SOD	Manganese superoxide dismutase
MOX	Methoxamine
MRI	Magnetic resonance imaging
MRS	Magnetic resonance spectroscopy
MS	Mass spectrometry
MS/MS	Tandem mass spectrometry
MSTFA	N-trimethylsilyl-N-methyl trifluoracetamide
MTG	Middle temporal gyrus
Na	Sodium
NA	Nucleus accumbens
$NADP^+$	Oxidised nicotinamide adenine dinucleotide phosphate
NADPH	Reduced nicotinamide adenine dinucleotide phosphate
NC	Neocortex
NMR	Nuclear magnetic resonance spectroscopy
NS	Non-significant
OCC	Occipital cortex
OES	Optical omission spectrometry
OPC	Occipital primary cortex

OPLS–DA	Orthogonal partial least squares discriminant analysis
PALL	Pallidus
PC	Parietal cortex
PCA	Principal component analysis
PCG	Posterior cingulate gyrus
PCR	Polymerase chain reaction
PD	Parkinson’s disease
PDD	Parkinson’s disease with dementia
PINK1	PTEN-induced putative kinase 1
PLS–DA	Partial least squares discriminant analysis
ppb	Parts per billion
PPP	Pentose phosphate pathway
PPRP	Phosphoribosyl pyrophosphate
ppt	Parts per trillion
PUT	Putamen
PVC	Primary visual cortex
Q-TOF	Quadrupole-time of flight tandem mass spectrometer
QC	Quality control
QQQ	Triple quadrupole tandem mass spectrometry
qtPCR	Real time polymerase chain reaction
RF	Radio frequency
RN	Raphe nucleus

ROS	Reactive oxygen species
RT	Retention time
SEC	Size-exclusion chromatography
SCX	Sensory cortex
SD	Significant difference
Se	Selenium
SFG	Superior frontal gyrus
SG	Superior gyrus
SN	Substantia nigra
SNc	Substantia nigra pars compacta
SNr	Substantia nigra pars reticula
SPECT	Single-photon emission computed tomography
SPG	Superior parietal gyrus
SRM	Selected reaction mode
STR	Striatum
TC	Temporal cortex
TCA Cycle	Tricarboxylic acid cycle (AKA Kreb's cycle or citric acid cycle; CAC)
THAL	Thalamus
TOF-MS	Time-of-flight mass spectrometry
UHPLC	Ultra-high performance liquid chromatography
WM	White matter
Zn	Zinc

Abstract

The University of Manchester

Melissa J. Scholefield

Doctor of Philosophy

2021

A Shared Metabolic Basis for Parkinson's, Alzheimer's, and Huntington's

Parkinson's disease (PD) is the second most common neurodegenerative disorder following Alzheimer's disease (AD). In PD, extensive loss of dopamine neurons, mainly in the substantia nigra, is found in the brain alongside proteinaceous deposits of α-synuclein known as Lewy bodies. Although characterised primarily by motor dysfunction, up to 80% of individuals with PD go on to develop cognitive dysfunction within 20 years of initial diagnosis, in a condition referred to as Parkinson's disease dementia (PDD).

PDD shares many characteristics with other neurodegenerative diseases, such as AD and Huntington's disease (HD), including progressive dementia symptoms, neuronal loss which is initially region-specific but eventually spreads throughout the brain, and metabolic perturbations—including mitochondrial dysfunction, oxidative stress, and energy pathway disruption. Previous studies have identified specific metabolic and metallic dysregulations shared in AD and HD brains, including marked widespread increases in glucose and urea, and decreases in copper. This raised the question as to whether similar perturbations may be present in PDD.

Using mass spectrometric methods, this thesis aimed to perform parallel metabolomic and metallomic analyses of PDD brain tissues, the results of which could then be compared to those obtained in AD and HD. Firstly, investigations into the effects of tissue collection variables such as *post mortem* delay were carried out to ascertain the suitability of different donor tissues for metallomic and metabolomic analysis. Using the results of this preliminary study, suitable tissues were selected for investigations of metals and metabolites in PDD brain tissue obtained from both the UK and the US.

These investigations revealed strikingly similar findings to those observed in AD and HD, including widespread decreases in copper, increases in urea, and perturbations in metabolic pathways involved in energy production and purine metabolism, as well as regional-selective decreases in pantothenic acid. The results indicate, for the first time, a shared metabolic basis for three neurodegenerative diseases featuring dementia—raising the possibility not only of shared pathogenic mechanisms, but shared therapeutic targets for these conditions.

Declaration

I declare that no portion of the work referred to in this thesis has been submitted in support of an application for another degree or qualification of this or any other university or other institute of learning.

Disclaimer

I carried out all the work in this thesis with the following exceptions:

- Chapters Four and Six: Culling of Wistar Han rats was performed by Dr Natalie Gardiner
- Chapters Four to Nine: Previous analysis of Auckland AD samples by Dr Jingshu Xu
- Chapters Five & Seven to Nine: Previous analysis of Auckland HD samples by Dr Stefano Patassini
- Chapters Seven & Eight: Development of targeted LC-MS methods by Dr Stephanie Church
- Chapter Ten: Processing of PDD brain samples for untargeted HPLC–MS/MS metabolomics was performed by Dr George Taylor

Several chapters of this thesis have been published. The author contributions for these papers are as follows:

- Conception and design of experiments, development of methodologies, experimental work, writing and editing of manuscripts
- Stephanie Church: Development of methodologies, editing of manuscripts
- Jingshu Xu: Previous Auckland AD cohort experimental work, editing of manuscripts
- Stefano Patassini: Previous Auckland HD cohort experimental work, editing of manuscripts
- Natalie Gardiner: Conception and design of rat experiments, culling of rats
- Andrew Robinson: Provision of Manchester AD cohort brain samples, editing of manuscripts
- Federico Roncaroli: Conception of experiments, provision of Manchester AD cohort brain samples, editing of manuscripts, supervision
- Nigel Hooper: Conception of experiments, editing of manuscripts, supervision
- Richard Unwin: Conception and design of experiments, development of methodologies, editing of manuscripts, supervision
- Garth Cooper: Conception and design of experiments, editing of manuscripts, primary supervisor

All figures featured in this work were produced by me.

Melissa J. Scholefield **1st June 2021**

Copyright Statement

Acknowledgements

First and foremost, I would like to thanks Professor Garth Cooper for his extensive and unwavering support throughout my PhD, even at times from the opposite side of the world. Without his continuing assistance over an unexpected three and half years, much of this work would not have been possible. Secondly, I would like to thank Dr Richard Unwin, who has always been on hand to answer my (numerous) questions and offer guidance whenever I've needed it. Thirdly, I wish to thank Stephanie Church, who has helped me with yet more numerous questions, endless equipment issues, and has generally been unable to escape me over the course of this thesis.

I'd next like to thank Professor Nigel Hooper and Professor Federico Roncaroli for their indispensable supervision over this project, guidance, and assistance with the manuscripts that have resulted from this work. Here I also wish to thank Dr Natalie Gardiner, whose assistance in the conception, design, and execution of portions of this study was invaluable.

As well as this, I also had endless support from Anna Tiernley (who was trapped even closer than Steph—right next to me), Dr Michael Anderson (who made paperwork *much* less of a headache), Sasha Philbert (who has shared all my mass spec-based distress), John Griffiths, and Andrew Robinson—as well as Jingshu Xu, Stefano Patassini, and Cynthia Tse, who were all happy to lend a hand from continents away.

As well as those who have helped me at work, I'd also like to thank all the people who have helped support me and keep me in a generally acceptable level of sanity over a difficult period, which spanned everything from Brexit to thesis-writing to COVID. All my close friends in Manchester—Michael, Binh, Grace, Alison, Laura, Rowan, Jo, Dan, Phil, and Connor—and those from further afield, who gave me something to think about other than work; my family who put up with me for months during lockdown; and Ebru, who shared my PhD pain and disappointment with the lack of balcony weather in Manchester.

I'd also like to thank the Lee Trust for funding this study, and the numerous people who donated their brains to research so that research like this can happen, as well as their families and close ones.

Chapter One | Introduction

1. Introduction

1.1. Dementia in Neurodegenerative Diseases

Parkinson's disease (PD) is one of the most common neurodegenerative disorders, affecting around 1% of the world's population above the age of 60 (1). Clinically, PD is characterised by progressive motor dysfunction, resulting in bradykinesia, tremor, and rigidity, as well as non-motor symptoms such as anosmia, constipation, and orthostatic hypotension. Cognitive dysfunction is also prevalent in PD patients, with reports of around a third of *de-novo* cases showing symptoms of mild cognitive impairment (MCI) at the point of diagnosis and as many as 80% of sufferers developing dementia in the twenty years following (2). This latter condition is described as Parkinson's disease dementia (PDD).

PD/PDD are characterised neuropathologically by the degeneration of dopaminergic neurons in affected regions of the brain, most severely in the substantia nigra pars compacta (SN), an area of the midbrain involved in fine motor control and reward pathways. By the time Parkinsonian symptoms appear, damage to the SN is severe, with around 30% of dopaminergic neurons being already lost at the first point of diagnosis, as well as 50-60% of dopaminergic axon terminals (3).

Why such extensive neuronal loss occurs in PD has not yet been determined, but has been shown to develop alongside accumulation of abnormal protein inclusions known as Lewy bodies. Lewy bodies are intraneuronal protein aggregates composed primarily of α-synuclein, as well as other associated proteins including ubiquitin and neurofilament protein. These aggregates localise mainly to the presynaptic terminal and are used to stage the progression of the disease at *post mortem* examination by determination of its regional deposition patterns. Deposition usually begins in the vagal nerves and olfactory tract, moving upwards to the midbrain (at which point characteristic motor symptoms typically begin to present) and eventually across cortical regions (associated with development of cognitive impairment) (4). However, this typical progression is not followed in every case (5) and does not always reflect clinical progression of the disease (6).

Despite what appears to be a clear association between accumulation of Lewy bodies and dopaminergic neuronal loss, it remains unknown what the connection is between the two

or if the former can be targeted therapeutically in order to combat the latter. Native monomeric α-synuclein itself does not appear to be toxic and may play a role in regulating neurotransmitter release and synaptic function (7). In human brains with Lewy pathology however, up to 90% of α-synuclein is phosphorylated (8), resulting in aggregation of insoluble oligomers that occur in-line with Lewy body staging (9). Accumulation of such insoluble inclusions may have any number of toxic effects on neuronal cells including microtubule impairment, induction of mitochondrial dysfunction and oxidative stress, and synaptic dysfunction (10).

However, no treatment targeting α-synuclein, even where clearance of the protein is successful, has been able to slow or stop progression of the disease in clinical trials. Indeed, no treatment targeting any mechanism identified as contributing to PD has been successful in this regard, with only symptomatic therapeutics available at this time (11). This is not exclusive to PD/PDD but is also the case with other dementias. These include Alzheimer's disease (AD), dementia with Lewy bodies (DLB), vascular dementia (VD), frontotemporal dementia (FTD), Huntington's disease (HD), and amyotrophic lateral sclerosis (ALS), among others. Despite the collective impact of these devastating diseases, not a single one of them yet has a treatment that can slow, stop, or reverse its development.

All dementias are defined by a common characteristic: the presence of cognitive impairment, progressive or sudden, that is eventually severe enough to leave an individual unable to care for themselves, although the type of cognitive impairment is not always the same. In spite of some differences in clinical presentation and causative factors, cognitive impairment is not the only similarity between these conditions. Most are characterised by widespread deposition of toxic protein aggregates (α-synuclein in PD/PDD and DLB, amyloid-β and tau in AD, all three of these proteins in DLB, TDP-43 in ALS and FTD, huntingtin in HD), all have age as a primary risk factor (with the exception of HD, which is primarily caused by mutations in the *Huntingtin* gene, although symptoms gradually progress with age, as well as familiar forms of all these conditions which are associated with specific, rare gene mutations), and many have been proposed to involve similar pathogenic mechanisms. For example, PDD, AD, HD, and ALS all have been suggested to be affected by mitochondrial dysfunction and increased oxidative stress (12). Such similarities raise the possibility that several, if not all, dementias involve common molecular

mechanisms that affect different vulnerable regions of the brain, resulting in varying clinical presentations.

In fact, even with regard to clinical presentation there is significant overlap between neurodegenerative conditions (see Table 1.1 for a comparison of PDD, DLB, AD, and HD, which show several common features). In the case of PDD and DLB, the major distinguishing factor between the two is the order of onset of symptoms; in the former, motor symptoms precede cognitive impairment by more than a year, whereas in the latter cognitive impairment occurs first. At their respective end stages, these two conditions are virtually indistinguishable. Neuropathologically they are likewise very similar, both exhibiting Lewy body deposition, but with a somewhat more cortical pattern of spread in DLB (13). Even with both clinical and post mortem neuropathological data available, it can be difficult to make a reliable diagnosis of either PDD or DLB. Many differences between these dementias in terms of neuropathological presentation appear to consist largely of the regions affected and the extent to which they are affected rather than the character of the changes themselves (14).

Table 1.1. A comparison of clinical and neuropathological presentation of PDD, DLB, AD, and HD

Dementia Type	Typical Age of Onset	Clinical Presentation	Neuropathological Presentation	Pattern of Development
Parkinson's disease dementia (PDD)	> 70 years; ~*10 years following PD diagnosis*	**Motor**: *preceding onset of cognitive symptoms*; tremor, bradykinesia, rigidity, autonomic dysfunction **Cognitive**: *following onset of motor symptoms*; memory loss, difficulties with judgement and attention **Physical**: anosmia, dizziness and fainting, hyperhidrosis, insomnia **Psychological**: apathy, depression, anxiety, visual hallucinations, delusions	**Primary**: α-synuclein deposits (Lewy Bodies; LBs) *primarily within basal ganglia* **Secondary**: limited amyloid-β and tau deposits; *less extensive than in DLB or AD* **Atrophy:** within temporal, occipital, and parietal lobes; *particularly within midbrain*	- Gradual and progressive without fluctuations (except those caused by L-DOPA therapy) - Motor symptoms precede cognitive symptoms
Dementia with Lewy Bodies (DLB)	> 65 years	**Cognitive:** *preceding onset of motor symptoms;* memory loss, difficulties with judgement, executive function and attention **Motor**: *following onset of cognitive symptoms*; tremor, bradykinesia, rigidity, autonomic dysfunction **Physical**: falls and fainting, orthostatic hypertension, urinary incontinence **Psychologica**l: visual and/or auditory hallucinations, delusions, depression, REM sleep disorder	**Primary**: α-synuclein deposits (Lewy Bodies; LBs) *primarily within cortex* **Secondary**: limited amyloid-β and tau deposits; *less extensive than in AD, more than in PDD* **Atrophy:** within midbrain, frontal & temporal cortices, hypothalamus, and basal forebrain	- Progressive but fluctuating - Cognitive symptoms precede motor symptoms

Alzheimer's disease (AD)	> 65 years	**Cognitive:** Memory and learning impairments, deficits in executive function and language, agnosia, apraxia **Psychologica**l: Apathy or depression, psychotic features, wandering, labile effect, aggression, delusions **Physical**: *only in later stages of disease;* falls, urinary incontinence **Motor**: *only in later stages of disease*; gait disturbance, dysphagia	**Primary:** amyloid-β and tau deposits throughout brain; *more extensive than in PDD or DLB* **Secondary**: limited α-synuclein deposits; *less than PDD or DLB* **Atrophy**: global atrophy, *most severe in hippocampus*	- Gradual and progressive without fluctuations - Primarily characterised by cognitive symptoms; motor/ physical symptoms only occur at later stages
Huntington's disease (HD)	> 40 years	**Motor:** *Preceding onset of cognitive symptoms;* chorea, rigidity, abnormal posture, difficulties chewing and swallowing **Cognitive:** *following onset of motor symptoms*; executive dysfunction, memory impairment **Psychological:** Anxiety, depression, reduced emotional display, aggression, compulsive behaviour, increased risk of suicide **Physical:** muscle atrophy, cardiac failure, weight loss, osteoporosis	**Primary:** Mutant huntingtin deposits throughout body (not just brain) **Secondary:** Limited tau and α-synuclein inclusions; *less than PDD, DLB, or AD* **Atrophy:** within striatum *(particularly caudate nuclei),* hypothalamus, and cerebrum	- Gradual and progressive over average of ten years without fluctuations - Primarily characterised by motor symptoms, but cognitive and psychological symptoms also prominent

Such similarities across neurodegenerative diseases have led to the suggestion that they may in fact exist on a spectrum rather than being completely separate conditions (see Figure 1.1). Dementias may even be comorbid, with individuals showing symptoms of more than one neurodegenerative condition at a time. The majority of dementia cases are sporadic with genetic cases being rare (the exception to this being HD, which is always caused by a dominant mutation in the *Huntingtin* gene, and familiar forms of AD and other dementias), despite a positive family history increasing the risk of dementia (15). Some share common causative mutations; for example, *c9orf72* mutations in both ALS and FTD (16). Vascular conditions are also risk factors for most dementia conditions, not just for VD itself (17, 18). Type II diabetes has been linked to increased risk of VD, AD, and PD (19, 20). Many non-cognitive symptoms such as motor dysfunction and psychological/behavioural issues are common across multiple neurodegenerative diseases. As mentioned, PD and DLB are very similar in terms of motor symptoms, but hallucinations are also commonly observed in both conditions (21). Delusions are present in both DLB and AD, and many dementias show increased risk for psychological issues such as depression, apathy, or mood changes (22-24).

The existence of a dementia spectrum would indicate a potential both for shared pathogenic mechanisms between conditions and for development of therapeutics which may be effective in the treatment of several diseases. However, in order to determine whether such mechanistic similarities exist, findings must be compared across multiple dementias. It is currently rare to investigate more than one condition in any single investigation, and there are difficulties in doing so—particularly in obtaining the appropriate tissues from sufficient numbers of donors for each disease. However, by conducting experiments on individual conditions with comparable methodologies, these difficulties may be overcome. The aim of this thesis was to do this by performing investigations of PDD with methodologies comparable to those used in previous analyses on AD and HD. This was to allow not only for the discovery of brain changes in PDD, but also to see if they showed any similarities to those previously identified in AD and HD.

Figure 1.1. Shared causes and symptoms across various dementias

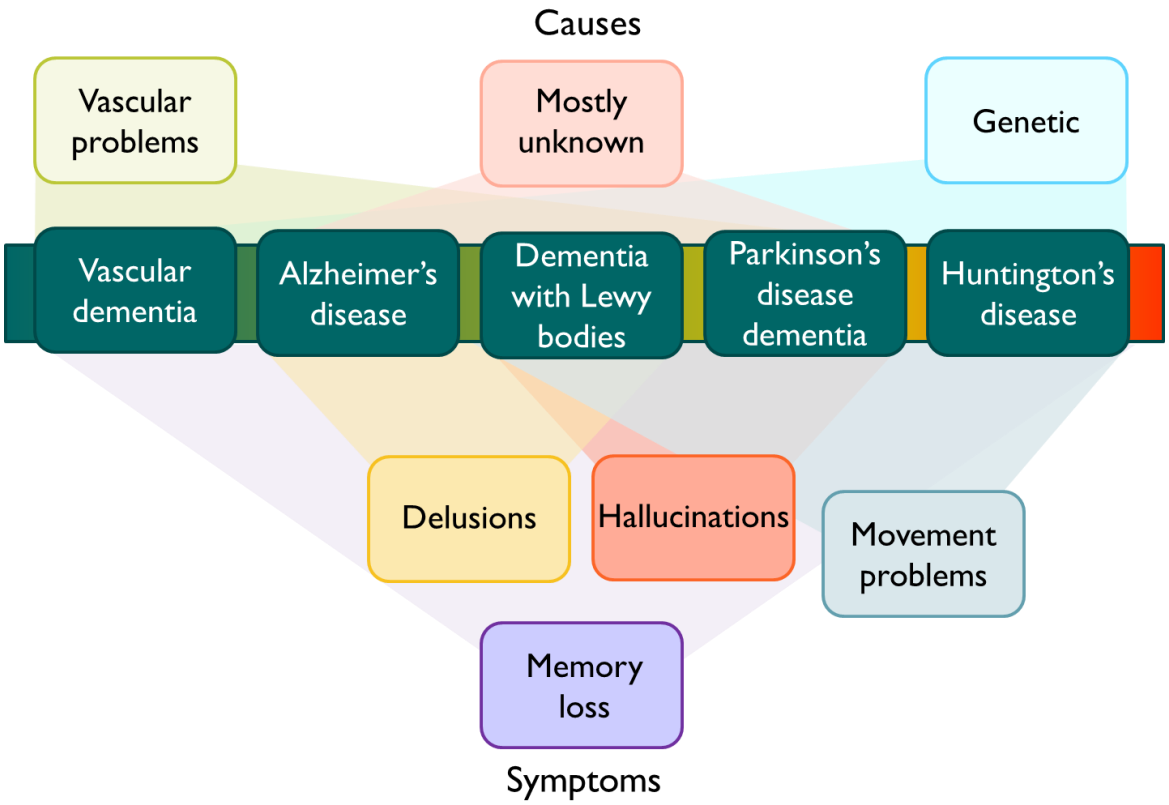

1.2. Mechanisms of Dementias

This investigation was designed around the theory that there may be considerable overlap between different dementias—not only in terms of symptomology and neuropathology but also mechanistic similarities. For example, previous investigations of AD, PD, DLB, and HD have observed shared perturbations in their cerebral metallome and metabolome, including increased iron and decreased copper, as well as increased glucose in comparison to the brains of healthy controls (see Chapter Three). These previous investigations suggested molecular pathways of interest for the current project, which could be analysed not only to look for disturbances in the PDD brain, but also to compare any such findings to those already observed in other dementias and look for further similarities and differences.

Such observations could contribute to shared neuropathology and symptomology across some dementias, as well as explain some of the differences between conditions. For example, there may be mechanisms shared by PDD, HD, and DLB, but not AD, which may help explain why motor dysfunction is characteristic of the former three illnesses but not of the latter. By contrast, cerebral perturbations shared by all these conditions could contribute to the memory loss characteristic of all dementias. In this investigation, we set out to discover such contributing factors within the metallome and metabolome of these conditions, and how they might interact with known mechanisms of disease in dementia.

1.2.1. Protein Aggregation

PD is a synucleinopathy, being neuropathologically characterised by extensive α-synuclein-containing inclusions known as Lewy bodies alongside areas of dopaminergic neuronal loss. Braak staging of α-synucleinopathy is a system used to classify the neuropathological progression inherent in PD, using the amount and localisation of Lewy bodies in the brain to determine the stage of the disease (25). Despite the substantia nigra pars compacta being the region most severely affected by neuronal loss and α-synuclein aggregation, it is not the first area of the brain to show deposits. In a typical PD progression, Lewy bodies are first seen in the dorsal motor nucleus and olfactory bulb; they then follow a caudo-rostral progression up through the brain stem and midbrain, and finally to wider neocortical spread – although not all cases follow this typical progression (25, 26). PD symptomology appears to follow this progression, with motor dysfunction occurring in

areas associated with fine motor control (e.g. the substantia nigra) and possible cognitive decline as deposits move into cortical regions (6).

Lewy bodies are proteinaceous structures primarily composed of α-synuclein, but also containing smaller amounts of other proteins including ubiquitin, neurofilament protein, and α-B crystallin (27). Despite being a characteristic component of PD, it remains unknown why α-synuclein forms in Lewy bodies in the brain of those with the disease. Similarly elusive is the endogenous function of α-synuclein, which is present in healthy cells as well as diseased tissues, although some studies have been uncovering varying functions for the protein. α-synuclein has been observed to participate in various cellular processes, including synaptic vesicle trafficking, fatty acid transport, and stabilisation of SNARE complexes (28). However, α-synuclein knockout in animal models is not lethal and appears to cause few effects (29). As such, the monomeric protein in and of itself appears to be neither essential nor toxic to cells. Moreover, α-synuclein deposits are sometimes observed in the brains of individuals not known to have PD or any other synucleinopathy; this condition has been termed incidental Lewy body disease, although it has been speculated that such cases may represent pre-clinical PD or DLB (30, 31).

However, α-synuclein is a flexible protein which is able to assume various different structures. Despite being an intrinsically disordered protein in its primary monomeric form, α-synuclein is able to fold and conform into an α-helix shape upon binding with membranes, or to aggregate into oligomers or amyloid fibrils (32). Initially, the observed presence of high numbers of fibrils in PD tissues and Lewy bodies led to the general acceptance that these were the primary toxic form of α-synuclein (33). However, increased levels of oligomers have also been observed in the brains of PD patients (34). PD mutations A53T and A30P have been linked to increased oligomerisation of α-synuclein, but not increased fibrillization (35). In one study, injection of oligomerisation-inducing α-synuclein mutants into rat brains resulted in more severe dopaminergic neuronal loss than other fibril-inducing mutants, whereas another study reported more drastic motor impairment and cell death with injection of α-synuclein fibrils than oligomers in rat brains (36, 37). As such, it appears that both forms are toxic to dopaminergic neurons, but it remains unclear which produces the most severe effects.

There has also been significant focus on trying to uncover the mechanisms by which α-synuclein may be toxic to neuronal cells in PD. As a protein primarily localised to the presynaptic terminal, α-synuclein participates in vesicle trafficking via interactions with soluble NSF attachment protein receptor (SNARE) complexes (38). Oligomerised α-synuclein however has been observed to disrupt SNARE complex formation, resulting in decreased dopamine release and vesicle motility (39); this indicates a loss of function in aggregated α-synuclein. However, α-synuclein is also found in other parts of the cell. For instance, α-synuclein oligomers have been observed to increase calcium uptake into mitochondria, resulting in complex I-dependent mitochondrial dysfunction (see section below for more detail) (40). Wild-type α-synuclein has also been observed in mitochondria-associated endoplasmic reticulum (ER) membranes (MAMs), with mutated α-synuclein reducing MAM contacts and resulting in mitochondrial fragmentation (41, 42). α-synuclein oligomers have also been found to associate with the ER itself in a PD mouse model, with administration of the anti-ER stress compound Salubrinal reducing α-synuclein accumulation and delaying onset of PD symptomology (43).

Despite being recognised as a central component of PD neuropathology, therapies targeting α-synuclein through mechanisms ranging from inhibition of aggregation, reduction of overall α-synuclein synthesis, or blocking transmission of the protein between cells have as yet failed to prevent, reduce, or reverse symptoms in humans – although trials remain ongoing (44). There are several challenges in employing α-synuclein as a therapeutic target in PD—reducing levels too low could be harmful if α-synuclein is involved in normal cellular process at healthy levels, it may be difficult to target only the regions of the brain that are affected by excessive accumulation of the protein, and it is not clear that clearance of α-synuclein itself will improve symptoms in PD. Trials targeting α-synuclein remain ongoing, with several currently in early phases of development (44, 45); however, the lack of positive results in trials so far has highlighted the need to consider other disease mechanisms and their suitability for therapeutic targeting.

1.2.2. Mitochondrial Dysfunction

Mitochondria are cellular organelles whose main function is energy production by the generation of adenosine triphosphate (ATP) molecules via the electron transport chain (ETC). This process not only provides ATP molecules, but also generates essential cofactors

for the tricarboxylic acid cycle (TCA cycle, AKA citric acid or Kreb's cycle), which produces ATP through oxidation of pyruvate, and in turn, also produces cofactors essential to the ETC (see Figure 1.2). The primary function of both these processes is to generate energy which can be used to fuel the essential metabolic functions of the cell, in the form of ATP and acetyl CoA respectively.

Figure 1.2. Mitochondrial electron transport chain and TCA cycle

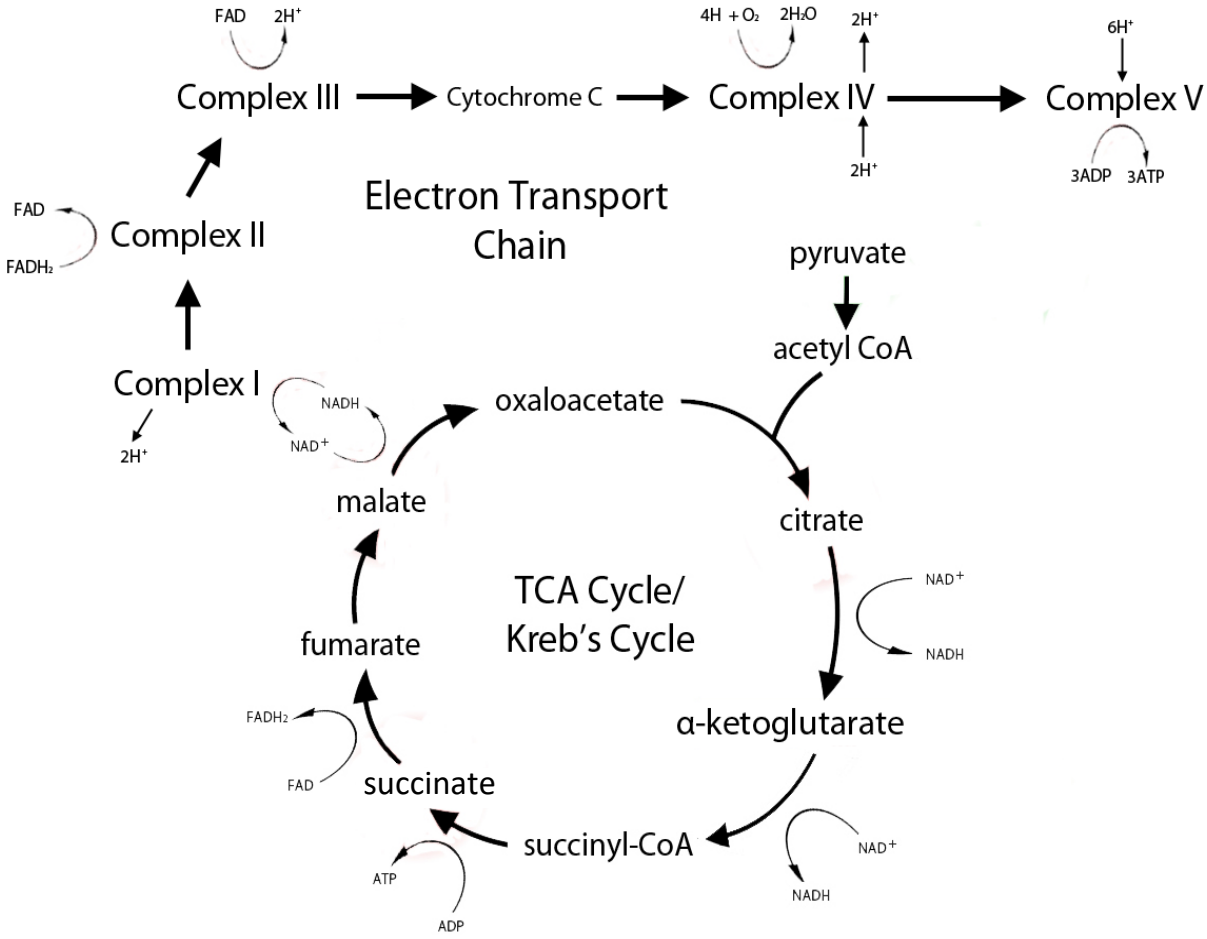

Mitochondrial function has been observed to be disrupted in PD. In particular, mitochondrial complex I of the ETC appears to show impaired activity in both humans with PD/PDD and animal models of the disease (46-49). Respiratory complex I, composed of NADH:ubiquinone oxidoreductase, is responsible for the first step in the ETC—oxidising NADH received from the TCA cycle in order to reduce ubiquinone to ubiquinol. The resultant redox energy is used to drive the proton gradient used by other complexes in the chain to produce ATP (50). Reduced complex I function can result in altered mitochondrial morphology, reduced ATP generation, disrupted calcium homeostasis, increased

mitochondrial permeability, and increased production of harmful reactive oxygen species (ROS) such as superoxide and hydrogen peroxide (51). A commonly used animal model for PD, created via injection of the toxin 1-methyl-4-phenyl-1, 2, 3, 6-tetrahydrodropyridine (MPTP), shows selective inhibition of complex I (52-54).

Loss of complex I activity has been reported to have dopaminergic neurone-selective effects, including impaired dopamine homeostasis stimulation and increased sensitivity of these neurons to toxins, although not all studies observe overt dopaminergic neuronal death (55-57). However, it has been reported elsewhere that dopaminergic sensitivity to PD model toxins such as rotenone, MPP(+), and paraquat are not complex I-dependent (58). PD-generating mutations such as the VPS35 and PINK1 mutation have been found to decrease complex I activity in cells from individuals with PD, resulting in mitochondrial dysfunction (59, 60). The A53T transgenic PD animal model has been observed to show α-synuclein accumulation within the inner mitochondrial membrane, resulting in complex I inhibition and increased mitophagy in dopaminergic neurons *in vivo* (61). Prolonged expression of A53T α-synuclein in SH-SY5Y cells has also been observed to result in altered mitochondrial morphology and increased formation of superoxide radicals (62).

ROS are highly reactive molecules that are formed as a by-product of respiration at several steps of the ETC; they include superoxide, hydrogen peroxide, and hydroxyl radicals. ROS are involved in several essential biological functions, including redox homeostasis, regulation of cell proliferation and apoptotic pathways, and immune function (63-66). However, excessive amounts of ROS are toxic to cells, and have been associated with a plethora of pathologies including autoimmune diseases, cardiac disease, and neurodegenerative diseases (12, 66, 67). Several PD-related genes including PINK1, PARK2, LRRK2, and DJ-1 are involved in regulation of mitochondrial function, and PD-associated mutations in these genes may lead to mitochondrial dysfunction and increased ROS production (68-70). Dysregulation of antioxidative processes has also been reported in PD, including decreases in reduced glutathione (71) and increases in glutathione peroxidase levels in the substantia nigra (72).

Despite the many studies showing disturbances in mitochondrial function, energy production, and oxidative stress in PD, there is less information concerning the molecular

pathways associated with these processes. However, some studies are beginning to focus on this area. For example, decreased α-ketoglutarate has been observed in the brains of individuals with PD, but other TCA cycle intermediates have yet to be reported on (73). Other pathways have received more attention, such as the glycolytic pathways and those associated with ROS production; increased glucose (74) and decreased glucose-6-phosphate (75) observed in the PD brain may reflect not only reduced mitochondrial energy production, but also a decrease in glycolytic pathway activity. Decreases in oxidised glutathione within the substantia nigra of PD patients may reflect an increase in antioxidative stress (71). Iron, which is capable of producing superoxide radicals via the Fenton reaction, has also been reported to be elevated in PD brains (76-81). Considering the currently limited coverage on these pathways, they may prove to be of particular interest for future metabolomics studies—particularly as drug trials aimed at directly targeting disruptions in mitochondrial function and oxidative stress, for example antioxidant treatments, have to date failed to slow or stop the course of PD (82). The current literature covering metabolic pathways in the PD brain are discussed in more detail in Chapter Four, as well as those in similar dementias including AD, HD, and DLB. This systematic review of the literature is used as a starting point for determining molecular pathways of interest in PDD and selection of analytes for investigation in this thesis.

In addition to energy production, the mitochondria are involved in other important cellular processes including amino acid and lipid metabolism, calcium ion storage and signalling, and in neuronal cells, cellular quality control via signalling to glial cells (83). Although these mechanisms have been less thoroughly investigated in PD/PDD, disruptions in these functions have also been linked to mitochondrial dysfunction and cell death (84-86)

1.2.3. Neuroinflammation

Neuroinflammation has been consistently observed in the brains of individuals with PD, with increases in cytokines and complement factors such as interleukins (ILs) and tumour necrosis factor (TNF) reported in areas of the brain affected in PD, such as the substantia nigra (87). Inflammation in the brain is usually led by microglia—non-neuronal immune cells which account for up to 15% of all cells within the brain (88). Microglia are able to respond to changes in the cellular environment, and can respond to pathogenic insults via phagocytosis or signalling to other cells of the immune system in order to activate a B- or

T-cell response (89). Microgliosis, an increase in the number of activated microglia at the site of a lesion or insult, has been observed in early-stage PD (90) and the microglia-expressed human leukocyte antigen gene (HLA-DRA) has been associated with increased risk of developing PD (91). Microglial activation has even been observed in idiopathic rapid-eye-movement sleep behaviour disorder (IRBD), a condition which often pre-dates PD and is sometimes considered to be a pre-clinical form of the disease (92). This suggests that neuroinflammation contributes to pathology in PD, rather than being a consequence of other pathogenic processes.

Interestingly, upregulation of the pentose phosphate shunt, an alternative glucose metabolism pathway, has been observed to increase neuroinflammation, dopaminergic neuronal loss, and ROS production in several PD mouse models (93). In this study, glucose-6-phosphate dehydrogenase, a pentose phosphate pathway intermediate, was found to be upregulated exclusively in microglia. As such, this pathway presents a target of interest for future metabolomic studies of PD. Additionally, iron accumulation has been associated with microgliosis in the substantia nigra of PD patients and a rat model of PD, suggesting a role for metals in neuroinflammation (94, 95).

1.2.4. Bringing Mechanisms Together

It is clear from this brief overview of the current literature on PD that whilst several mechanisms have been implicated in disease pathogenesis, there is less information on how these mechanisms interact with one another, or through what pathways and intermediates they do so. Metabolic pathways such as glycolysis, the TCA cycle, and the pentose phosphate pathway, as well as metals such as iron, copper, and manganese, have been suggested to participate in many of these processes. This suggests the possibility that these pathways and molecules may be the common factors which link these different pathogenic mechanisms together. In order to further elucidate this idea, a more comprehensive understanding of the individual components of these pathways and how they interact in PD is required. This thesis aims to address this issue with a series of experiments that will capture a wide view of the metabolic and metallic factors that are altered in PD, using an approach called ‘multi-omics.’

1.3. -Omics

'-Omics' is a term used to describe a branch of science covering several fields of study which broadly target a particular family of molecules, such as proteins, metabolites, and genes, whose name ends with the suffix 'omics', e.g. proteomics, metabolomics, genomics, metallomics, transcriptomics, etc. -Omics approaches are generally wide-reaching in scope, being capable of describing up to hundreds or thousands of molecules within the targeted molecular pool (e.g. the proteome, metabolome, genome, etc.) but methodologies can be as targeted or untargeted as required. 'Multi-omics' describes an approach where multiple -omics investigations are combined to build a broader picture of the molecular pathways within a cell or tissue of interest. There is often overlap or interactions between the different molecular pools targeted by each individual approach, so investigating multiple pools can provide a deeper understanding of how different molecules and their associated pathways function and interact within a disease. This thesis employs this philosophy by incorporating two -omics approaches, metallomics and metabolomics, in order to build a picture of the molecular pathways involved in PDD.

1.3.1. Metallomics

Metallomics is a term describing the study of the metallome of a tissue/biofluid or cell, covering the distribution of all physiologically necessary or essential metals and metal ions within the sample. Metals serve several essential functions within the human body and are a dietary requirement for survival (hence 'essential'). Such essential metals include five major minerals: sodium, magnesium, potassium, calcium, and phosphorus, as well as trace elements including iron, copper, zinc, manganese, and selenium, among others (96). These metals are necessary for the proper functioning of the entire human body, including the brain itself—being involved in functions as varied as neurogenesis, cell-to-cell communication, antioxidation, enzyme function, and neurotransmitter release to name only a few (96). Necessary levels of these metals are usually easily available through consumption of a balanced diet.

Almost all of these metals have been investigated in one or several dementias, including PD, with several observed to show altered concentrations in one or more brain regions. Such perturbations may reflect disturbed metal homeostasis in the dementia brain, with resultant dysregulation of metal-dependent cerebral processes. An extensive systematic

review of current metallomic findings in PD, AD, DLB, and HD is here presented in Chapter Three (97).

1.3.2. Metabolomics

Metabolomics describes the study of the metabolome—the small molecules involved in life-sustaining metabolic processes of the cell, covering a huge number of molecules including amino acids, sugars, fatty acids, and cofactors. Metabolomics may be targeted to investigate individual pathways of interest or may aim to cover as broad a range of molecules as the chosen methodology allows.

Several metabolic pathways have found to be dysregulated in PD/PDD, including glucose metabolism, redox homeostasis, neurotransmitter regulation, and purine metabolism among others (97-99). A review of currently identified metabolite disruptions in PD, AD, DLB, and HD is presented in chapter three (97).

1.3.3. Mass Spectrometry

Mass spectrometry (MS) is an analytical method often employed in -omics studies due to its ability to investigate a wide range and number of molecules in a sample simultaneously. It functions by ionising the sample of interest and measuring the mass-to-charge ratios (*m/z*) of the product ions, detecting the time it takes for ions to pass through the apparatus (their retention time) and using this information to determine their structure and molecular identity. MS can be used as an isolated technique, such as in the case of inductively-coupled plasma mass spectrometry (ICP–MS), which is particularly useful for determining metal levels within a sample (100). At other times, MS is coupled with chromatographic apparatus, such as in gas Chromatography–MS (GC–MS) or liquid-Chromatography–MS (LC–MS). This pairing allows for more accurate detection of larger numbers of different molecules by providing additional separation based on a molecule's chemical properties, such as volatility and polarity, based on their interactions with the stationary and mobile phases within the chromatograph. This additional degree of separation is important for approaches like metabolomics where several analytes of interest may have very similar *m/z*, and so be difficult to distinguish using MS alone.

A detailed outline of the three MS methods used in the investigations in this thesis: ICP–MS, GC–MS, and LC–MS, can be found in Chapter Two, where an analysis of the advantages and disadvantages of each of these approaches is presented.

1.4. The Current Investigation

As current clinical trials targeting various proposed disease mechanisms in dementias continue to fail, investigations are beginning to widen beyond more traditional targets such as α-synuclein inclusions. -Omics analyses have revealed not only multiple proteomic disturbances in conditions such as AD and HD, but also perturbations in metabolites and essential metals. The benefits of using multiple -omics approaches for this investigation are not only the possibility of investigating a wide number of analytes simultaneously, but also that findings from different approaches can be brought together to build a better picture of what is happening within a diseased system. For example, disruptions in metabolomic pathways may measurably alter regulation of intracellular metal levels, or conversely, changes in available metal cofactors may alter enzyme activity and reduce or increase activity in relevant metabolic pathways. Here, a combination of metabolomics and metallomics was used to aim to build this bigger picture in the PDD brain, based on alterations that have been previously identified in AD and HD. Chapter Two discusses the different types of mass spectrometry employed, how these methods work and why they were chosen for this project, and Chapter Three then outlines the methods as they were used for each part of the investigation.

Chapter Three contains a systematic review which was carried out in order to bring together current metallomic and metabolomic findings in AD, PD, HD, and DLB. This allowed for the identification of promising analytes that show similarities across multiple diseases, as well as of gaps in the literature which could be addressed by the current investigation. This review identified a few consistent findings across AD, PD, and HD, but also highlighted a lack of consensus across most findings in different diseases and brain tissues. It additionally showed several areas where data is currently lacking, particularly in investigations of DLB. These findings were used to select analytes of interest in PDD and direct the course of the following metallomic and metabolomics analyses. This review was published as a full paper in *Ageing Research Reviews* (97).

Chapter Four describes a preliminary study conducted to determine if tissues obtained from different geographical locations under differing conditions would be suitable for direct comparison of metallomic findings in order to determine the suitability of UK-derived tissues for the analysis performed in this thesis. Due to the nature of human brain tissue collection, tissues can vary across several parameters including length of post mortem delay, age of donors, disease staging of cases and controls, etc. Without first determining the effect of such variables on brain metals and metabolites, findings from resulting analyses could not be reliably compared to those previously obtained in AD and HD. Results from this analysis were used to determine the suitability of UK brain bank tissues for our metallomic analysis of PDD brains, and were published as a full paper in *Metallomics* (101).

The metallomic analysis of PDD is described in Chapter Five, in which nine essential metals including sodium, potassium, magnesium, calcium, manganese, iron, copper, zinc, and selenium were quantified in nine brain regions from nine PDD cases and nine controls free from any kind of dementia. Metal concentrations were quantified using ICP–MS and findings were compared to those previously obtained in a similar analysis on AD brains performed by our lab. This investigation has been accepted by the journal *Frontiers in Aging Neuroscience (102)*.

The metabolomics portion of the investigation is commenced in Chapter Six. Similar to the preliminary metallomics study, an investigation of the effects of tissue collection variables such as post mortem delay was carried out on rat and human tissues obtained from different brain banks. Using the results from this investigation, the suitability of brain tissues obtained from UK and international brain banks for metabolomic analysis was assessed. This chapter was published as a full paper in *Metabolites* (103).

Following the identification and acquisition of appropriate tissues, a metabolomics analysis of PDD brain tissues commenced. This was initially to be carried out using only an untargeted methodology, however multiple factors necessitated the development of a new two-step plan using both targeted and semi-targeted analyses. Chapter Seven covers the first of these: a targeted LC/MS analysis of pantothenic acid (AKA vitamin B5). Following identification of decreased B5 levels in AD and HD brain tissues by our lab, and the

discovery of localisation of B5 to myelin-containing neurons in rat brains—the data analysis of which I assisted with—this became another analyte of interest in PDD brains (104). This data was accepted for publication in *Metabolites*. Chapter Eight then reports on the targeted analysis of urea levels within the PDD brain tissues. Urea was previously identified as showing dramatic, widespread increases in both AD and HD, and so was chosen as a metabolite of particular interest for comparison of PDD with these two conditions. The data from this chapter was accepted by *Frontiers in Molecular Neurodegeneration* for publication.

A new method was also developed in order to carry out a semi-targeted LC–MS metabolomics analysis of PDD brains, as described in Chapter Nine. This method was developed to focus on analytes of interest to this investigation, including sugars and sugar phosphates, as well as multiple other metabolites that have not been previously targeted in PDD. The findings from this analysis were compared to those previously observed in AD and HD metabolomic studies to look for similarities and differences between different dementia conditions.

Finally, Chapter Ten discusses the investigation carried out in this thesis, the findings reported, what these findings contribute to the current knowledge of PDD and other dementias, the strengths and limitations of the project, and what further research would have been carried out if time and resources had allowed.

1.4.1. Use of the Alternative Thesis Format

As the work for this thesis was carried out, several experiments that were conducted yielded positive results suitable for publication. As such, these experiments are presented here as paper-format results chapters, formatted and adapted appropriately to fit into the overall thesis. Each of these chapters includes an introductory statement explaining where they were published or submitted for publication, what changes have been made (including additional relevant data obtained after publication), and how the chapter fits into the overall arc of the thesis. These include a systematic review (Chapter Three), which here takes the place of a traditional thesis literature review, as well as five results chapters (Chapters Four to Eight). The final results chapter (Chapter Nine) as well as the introduction, methodology, and discussion chapters are presented in traditional thesis

format. The use of a separate methodology chapter allows for the explanation and critical evaluation of the selected methods used in this thesis, which is not generally allowed for in publications.

The role of co-authors in any manuscripts included here is described in the acknowledgements section. All experiments conducted in these manuscripts were carried out by myself, with assistance from co-authors in experiment design, method development, and editing of manuscripts.

1.5. Aims

Following this outline, the aims of this thesis are:

1) To characterise in greater depth similarities and differences already identified between different dementias including PDD, AD, HD, and DLB, and establish gaps in the current literature, and to use this new information to select analytes of interest for metallomic and metabolomic analyses of PDD brains (Chapter Three).
2) To determine the effects of tissue collection variables such as post mortem delay, disease staging, and age and sex-matching, for example, on the metallomes of both human and rat brains, and use the findings to select suitable human brain tissues for metallomic analysis of PDD (Chapter Four).
3) To perform a metallomic analysis of PDD brains using ICP–MS in order to identify any alterations in essential metal levels, and compare any findings with those already identified in previous analyses of AD (Chapter Five).
4) To determine the effects of tissue collection variables on the metabolome of rat and human tissues, and use this data to select appropriate human tissues for metabolomic analysis of PDD brains (Chapter Six).
5) To perform untargeted and semi-targeted metabolomic analyses of PDD in order to determine any changes in key analytes of interest, and compare findings with those previously observed in AD and HD (Chapters Seven to Nine).

Chapter Two | Mass Spectrometry Methods

2.1. Mass Spectrometry

Mass spectrometry (MS) is an analytical technique that can be used to separate different ions within a sample based on their mass-to-charge ratios (*m/z*). It is a technique which is able to simultaneously identify large numbers of different analytes within biological and non-biological samples, in either a targeted, semi-targeted, or untargeted manner, with highly precise quantitation. Targeted MS can be used to confidently quantify particular analytes within a sample to concentrations as low as parts per trillion (ppt) (105), whereas semi- or untargeted MS can be used to apply a 'shotgun' approach that can measure 100's or even 1000's of analytes simultaneously—either quantitatively or semi-quantitatively. It can be adjusted and combined with other techniques to measure different types of molecules as diverse as proteins, metabolites, or metals. The high sensitivity and wide target molecule range of MS makes it ideal for the metallomic and metabolomic analyses performed in this thesis, and this chapter focuses on an explanation and evaluation of the various types of MS used in the experiments here.

2.1.1. Mass Spectrometry Overview

Mass spectrometers involve three main components: the ion source, the mass analyser, and the detector. The source is used to vaporise the sample molecules into a gaseous phase which can then be transported into the mass analyser by magnetic or electric fields. The vapourised sample molecules separated based on their *m/z.* Ions of different *m/z* are directed through the mass analyser to reach the detector, which generates a current proportional to the abundance of ions at each *m/z*. The data from the detector is then used to generate a mass spectrum, which shows the *m/z* of ions present in the sample and their relative abundance.

There are many different types of mass spectrometer, with varying types of ion sources and mass analysers, and the possibility of having multiple mass analysers in a single spectrometer. Some of these mass analysers are described in detail below.

2.2. Mass Analysers

Mass analysers are the main component of the apparatus used to perform MS. There are various types of mass analysers available, including quadrupole, time-of-flight (TOF), magnetic sector, ion trap, Orbitrap, and tandem mass spectrometers, among others. These are covered here, with a focus on quadrupole, TOF, and triple quadrupole (QQQ) tandem mass analysers.

2.2.1. Quadrupole Mass Analysers

A commonly used mass analyser is the quadrupole mass analyser. Quadrupoles consist of four hyperbolic metallic rods; on one pair a direct current field is applied while an RF field is applied to the opposite pair. The positive/negative bias on these fields is selected to allow ions of a specific *m/z* ratio to move through the spectrometer and reach the detector at any one time. These ions are converted into an electromagnetic impulse and counted by a multi-channel analyser (detector). The use of multiple channels is used to construct a profile of the ion which corresponds to its spectral peak. The magnitude of the impulse reflects the number of ions detected. Ions of the incorrect ratio will be ejected and not counted by the detector. This process can then be repeated with varying direct current-RF voltages in order to allow ions of different *m/z* ratios to reach the detector in untargeted analyses. However, this can lead to a loss in sensitivity and resolution. A turbomolecular pump is used to maintain the analyser in a vacuum to prevent interference with the separation and guidance of ions to the detector at the end of the device.

Figure 2. 1. Diagram of ICP–MS mass analyser and collision/reaction cell

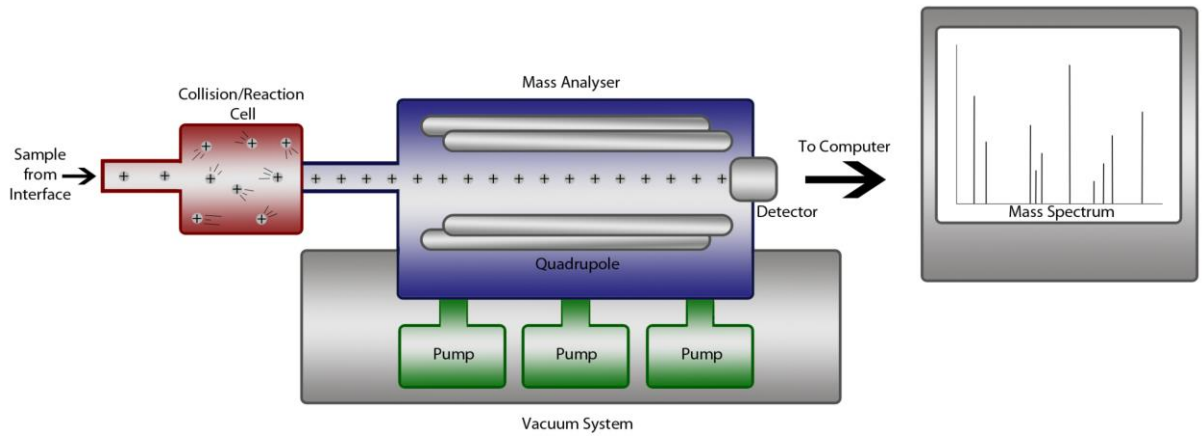

2.2.2. TOF Mass Analyser

TOF mass analysers separate ions of different *m/z* based on the time it takes for them to move through the analyser and reach the detector, i.e. their time of flight. Analyte ions are introduced into the flight tube of the MS in pulses and accelerated by application of a voltage to electrodes placed at the ion source. Each ion should then move through the flight tube at a velocity proportional to the square root of its *m/z* ratio (the smaller the ratio, the faster it travels). A reflectron is used to reflect the ion beam towards the detector using a constant electrostatic field. The purpose of this is to diminish the spread of flight times between ions with the same *m/z* but different kinetic energies, as more energetic ions will move further into the reflector, and so take a slightly longer path to the detector than less energetic ions. It also doubles the length of the flight path, which increases the resolution. By measuring each ion's TOF, the detector can then determine its *m/z* and from that generate its mass spectrum. As there is no upper limit to the TOF, this method of MS can theoretically cover any mass range.

Figure 2. 2. Diagram of TOF mass analyser

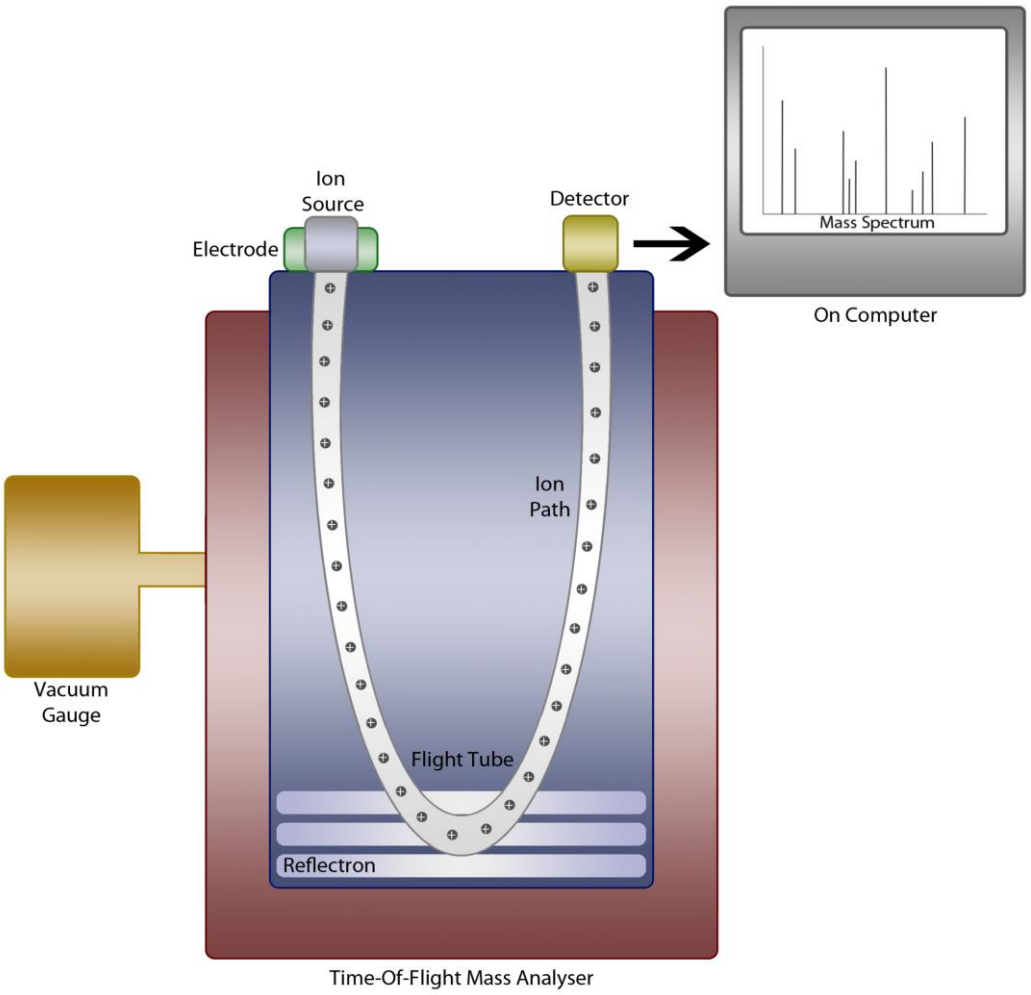

2.2.3. Other Mass Analysers

As well as quadrupole and TOF, there are other types of mass analyser available, including ion trap mass spectrometers, such as the Orbitrap and magnetic sector analysers. Like TOF analysers, magnetic sector analysers also identify ions based on time of flight. However, unlike TOF analysers, they use a magnetic field in order to separate ions. Magnetic sector analysers have very high resolution, but can be relatively expensive and difficult to interface to complementary apparatus such as chromatographs, and as such are not commonly used for omics studies (106).

Ion trap mass spectrometers use magnetic and electric fields to manipulate ions and 'trap' them inside an electrode contained within the analyser. Orbitraps use two outer electrodes to form a barrel-like enclosure around a spindle-like electrode, which traps ions into an orbital motion around itself. Ions of different *m/z* oscillate at different frequencies, and so

these frequencies can be used to identify different ions. Orbitraps have very good resolution, but do not scan as quickly as some tandem mass analysers (107).

2.2.4. Tandem MS

Multiple analysers can also be combined in order to perform tandem mass spectrometry (MS/MS), in which more than one mass measurement is carried out by the MS instrument. Ions which enter the MS are separated once by the first mass analyser, further fragmented by the second, and separated a second time by the third. For example, in the case of the triple quadrupole, this involves a primary set of rods which separate ions based on *m/z*, and a second set which is used as a collision cell which causes further fragmentation of this first set of ions. A third set of quadrupole rods then analyses the *m/z* of these smaller ion fragments, which finally pass on to the detector. This double mass measurement allows for separation and identification of different ions that would have very similar *m/z* in regular MS machines using a single mass analyser – a critical quality in analysis of complex mixtures, such as those in omics studies.

Figure 2. 3. Diagram of QQQ MS/MS

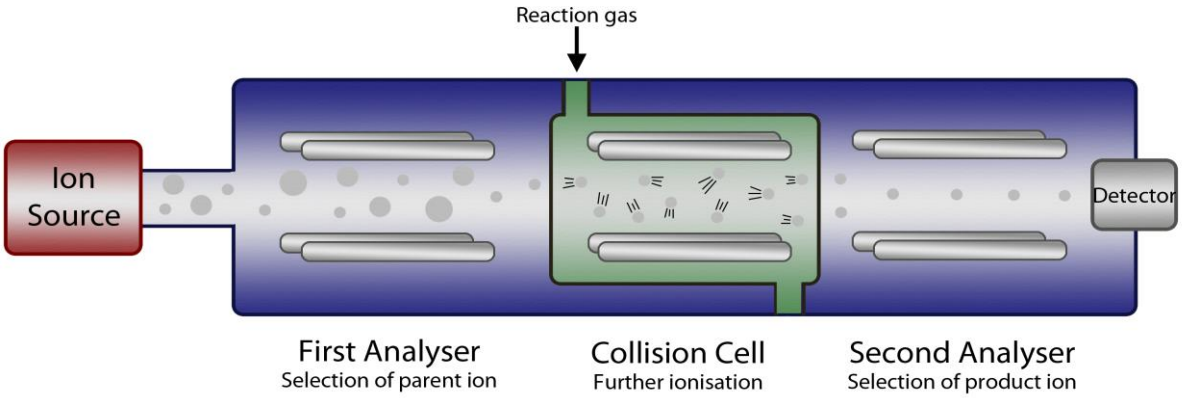

This can be used for selected reaction monitoring (SRM), in which an ion of a particular mass is selected in the first mass analyser, fragmented in the second, and then a specific product ion of that fragmentation is selected for detection in the final analyser. This method does however require additional method development, as the ion fragment(s), or transitions (the specific *m/z* values associated with the precursor and fragment ions), with the best sensitivity and specificity must be selected for each individual analyte of interest. The transitions need to be unique as possible to the analyte of interest – preferably with a

high signal intensity and low number of interfering signals. Online libraries can be used to determine the ideal transitions for many small molecules, although these libraries are not yet as extensive as those available for proteomics, and does not cover all metabolites (108).

In contrast, in full scan mode, instead of selecting one/a few fragments, a wide scan spanning a large range of fragments can be carried out. Although this allows for the identification of as many unknown molecules as possible within the selected range, it comes with the trade-off of lower sensitivity, due to loss of scan speed. This approach is used for global, untargeted analyses due to its ability to identify unknown analytes.

As well as QQQ, different types of mass analysers can also be combined. For example, in quadrupole time-of-flight (Q-TOF) MS, a quadrupole first separates ions based on *m/z*, followed by further separation of ions based on their time of flight. Different types of MS/MS are more suitable for different applications however. QQQ-MS is usually employed for selected reaction monitoring SRM, or other more targeted analyses, where it has greater sensitivity as a result of its lower signal:noise ratio in comparison to other mass analysers (107). Q-TOF on the other hand is a much faster, higher resolution MS/MS technique which is more suitable for global assays covering a wide range of analytes, such as high-resolution full scan (HR-full scan) analysis (107). Orbitraps can also be paired with other analysers to perform Orbitrap-MS/MS, which has superior resolution to Q-TOF, but is not as fast-scanning (107). Both these methods however have lower sensitivity than QQQ in SRM, making them less suitable for targeted analyses (107). For this reason, QQQ was more suitable for the semi-targeted analysis of PDD tissues performed here.

2.2.5. Comparison and Selection of Mass Analysers

When selecting an appropriate mass analyser, several factors need to be considered, such accuracy, resolution, range, scan speed, and cost. The importance of these factors then needs to be evaluated based on the type of analysis being performed (e.g. SRM, HR-full scan, etc.).

Analysers with higher range and scan speed are more suitable for untargeted 'shotgun' assays, which may require separation of multiple analytes with the same *m/z*. Conversely, in more targeted analyses, higher sensitivity, quantitation, and minimisation of missing values are preferred at the expense of identifying higher numbers of analytes.

Based on these criteria, a quadrupole mass analyser was considered suitable for our metallomics study, in which smaller numbers of analytes are easily separated by *m/z*, and so higher resolution did not warrant a higher cost. TOF was chosen for the untargeted gas chromatography–mass spectrometry (GC–MS) metabolomics analysis in order to benefit from higher mass resolution, *m/z* range, and scan speed for HR-full scan analysis. QQQ was chosen as suitable for the semi-targeted liquid Chromatography–mass spectrometry (LC–MS) metabolomics analysis due to its superior sensitivity in SRM mode in comparison to other MS/MS techniques.

2.2.6. Advantages & Disadvantages of MS

MS is a powerful technique with high resolution and sensitivity. It can detect 1000's of analytes simultaneously in a single sample, with analysis being as targeted or untargeted as desired. In these aspects, MS is superior to other commonly-used metabolomics techniques such as nuclear magnetic spectroscopy (NMR) (118). However, NMR requires much less sample preparation, and is capable of analysing tissue samples directly without extraction. This allows for multiple analyses to be carried out on the same sample, and contributes to the higher reproducibility seen in NMR analyses (118). It can also be used for *in vivo* investigations, such as in magnetic resonance spectroscopy (MRS) or magnetic resonance imaging (MRI) studies, which is of particular use in biomarker investigations (119). In the current investigation of *post mortem* tissues, which requires analysis of as

wide a range of analytes of possible, with high resolution and sensitivity, MS is the preferred method.

One of the other primary advantages of MS is the ability to combine it with other analytical techniques or otherwise adjust it to further its range, resolution, and sensitivity. For example, metallomics studies often employ inductively-coupled plasma MS (ICP–MS), which is powerful enough to ionise metals and measure their abundance in samples to levels as low as ppt (120). In metabolomics, MS is often combined with chromatographic techniques such as GC or LC in order to enhance separation of analytes with similar *m/z* – which is essential in studies covering 100s or even 1000s of metabolites simultaneously. These techniques are covered in detail below.

2.3. ICP–MS

ICP–MS is a technique that breaks samples down to atomic and small polyatomic ions in order to quantify the concentrations of the resulting elemental ion masses. This allows for the detection of multiple analytes simultaneously in a sample.

The ICP–MS functions quite simply (see Figure 2.4. for outline). First, the sample must be digested prepared for introduction into the apparatus. This typically involves digestion of the sample in enzymes, alkalis, or strong acids, most commonly nitric acid (121), to break it down to a liquid form. The liquidated sample is then introduced into the ICP–MS as an aerosol, which is carried through the instrument on a carrier gas. The sample is carried to the spray chamber where it is introduced to an argon gas plasma, which is heated up to 6,000-7,000 K. It is this extremely high temperature which allows the argon gas to atomise and ionise metals so efficiently, whereupon they move through to the MS portion of the instrument.

Figure 2. 4. Overview of ICP–MS apparatus

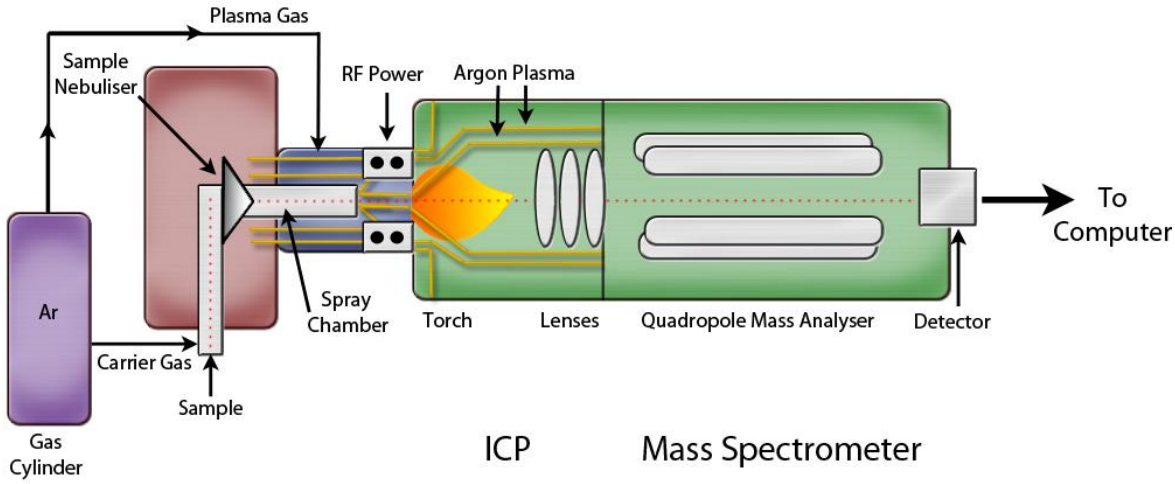

The optimal function of the ICP–MS relies on optimisation of all its components, including the sample preparation, sample introduction, sample ionisation, interface, MS, detection, and data analysis.

2.3.1. Sample Preparation

Before being introduced to the ICP, solid samples must be digested into a liquid form. They can then be nebulised and injected in aerosol form in the ICP. Solid samples require digestion in enzymes, alkalis, or strong acids at a high temperature. In our case concentrated nitric acid is used, which is a strong oxidiser able to digest tissue and convert metals to highly soluble nitrate salts, which will not cause build-up or interference in the instrument. Other acids such as hydrochloric acid (HCl) or hydrofluoric acid (HF) are also not uncommon and may be better for digestion of some particular metals, such as mercury, but may also be more likely to cause matrix interferences and require more extensive safety measures during use (121). Combinations of acids, such as aqua regia (1:3 nitric acid:HCl) may even be used where appropriate; for example in the detection of precious metals such as gold or platinum – but it is not necessary for the detection of essential metals (121). Enzyme digestion may also be suitable for analyses in which acid digestion may lead to nanoparticle aggregation or dissolution (122). Nitric acid was chosen as our

digestion method as it is able to effectively digest all our elements of interest, without risking machine build-up or interference.

Digestion with nitric acid is carried out at high temperatures; first at 60°C and then at 100°C. This is important to ensure as many large molecules as possible are removed from the samples, as these will otherwise build up in the instrument and cause damage. An environmental calibration standard, containing non-biological, chemically stable metals that are not present in the sample (a common example is scandium), is added to each sample to correct for the effects of matrix interference in samples, variations in sample introduction efficiency, and any instrumental variations that may occur over the course of the run, such as instrument drift. This ensures optimal performance.

2.3.2. Sample Introduction

The sample introduction system comprises of the autosampler, peristaltic pump, nebuliser, spray chamber, and sample injector (see Figure 2.5). The purpose of this component is to nebulise liquid samples into an aerosol spray fine enough to be ionised by the argon plasma. Sample retention as this point is very low, with only 1 – 2% of the introduced sample being retained into the plasma (123). However, this amount is still sufficient for quantitation of metals from samples even of just a few millilitres.

The sample is first taken up by an injector before moving through a peristaltic pump, which contains several minirollers that create a constant pressure and flow of liquid into the nebuliser despite any differences in viscosity between samples, standards, or blanks. The borosilicate glass nebuliser breaks the introduced liquid up into a fine aerosol by application of an argon gas flow. The resulting droplets move through a double-pass spray chamber. In here the droplets move through a long tube, during the passage of which larger droplets (< 10 µm) will fall out due to gravity, allowing only the finer droplets (5- 10 µm) to pass through to the sample injector at the plasma torch. Although not as efficient as a conventional cyclonic spray chamber, which can have 2-3 times lower detection limits, the double pass is more flexible in the variety of shapes, sizes, and materials available, allowing for better optimisation with some sample types (124).

Figure 2. 5. Diagram of ICP–MS sample introduction apparatus

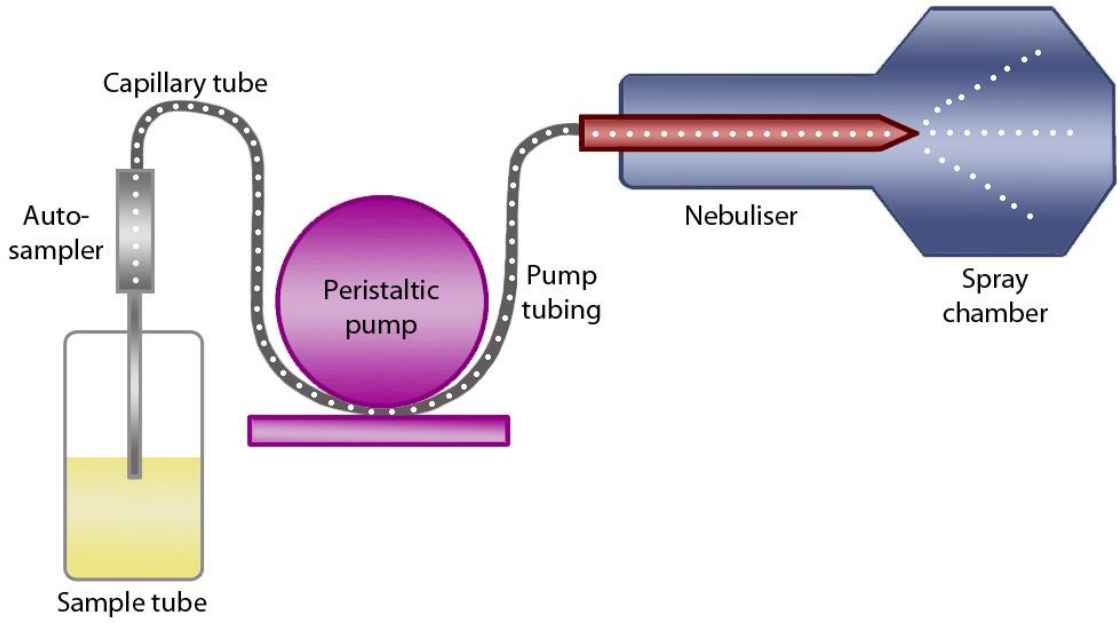

2.3.3. Sample Ionisation

In ICP–MS, a superheated argon plasma is used to atomise, and then ionise samples. The components required to do this are the plasma torch, the radio frequency (RF) coil, and the RF power supply (see Figure 2.6). The plasma torch is composed of an outer and middle tube, and sample injector made of quartz. The argon gas passes between the outer and middle tubes, while a second auxiliary gas passes between the middle tube and the injector, and third nebulizer gas flow carries the sample. The purpose of the auxiliary gas is to position the argon gas between the middle tube and injector. Due to its high velocity, the nebulizer gas is capable of punching a hole through the centre of the argon gas in order to allow sample droplets to pass through.

At the top of the argon torch is a load coil connected to an RF generator. As RF power is loaded onto the coil, it produces an alternating current corresponding to the frequency of the generator. The resulting oscillating current produces an electromagnetic field around the torch. As argon gas is directed through this, a high-voltage spark is applied. This spark causes some electrons to be stripped from the argon atoms. These electrons accelerate within the electromagnetic field and collide with other argon atoms, in turn causing them to lose electrons and ionise. This causes a chain reaction which leads to ionisation of more

and more argon atoms within the plasma. The resulting discharge is maintained as the aerosol sample is introduced via the sample injector.

As the sample moves through the plasma it undergoes several changes. First, it is stripped of water molecules to produce a stream of small, solid particles. These particles first change to a gaseous form, then to a stream of ground-state atoms as they are atomised by the plasma gas. Collisions with energetic argon ions then cause metallic complexes within the sample to break up and the resulting atoms to ionise, allowing metals to be introduced into the mass analyser in their elemental state. The ions produced are then directed into the mass spectrometer. The overall purpose of this stage is to convert the introduced sample aerosol into a stream of metal ions that can be directed into the mass spectrometer.

Figure 2. 6. Diagram of ICP–MS ionisation apparatus

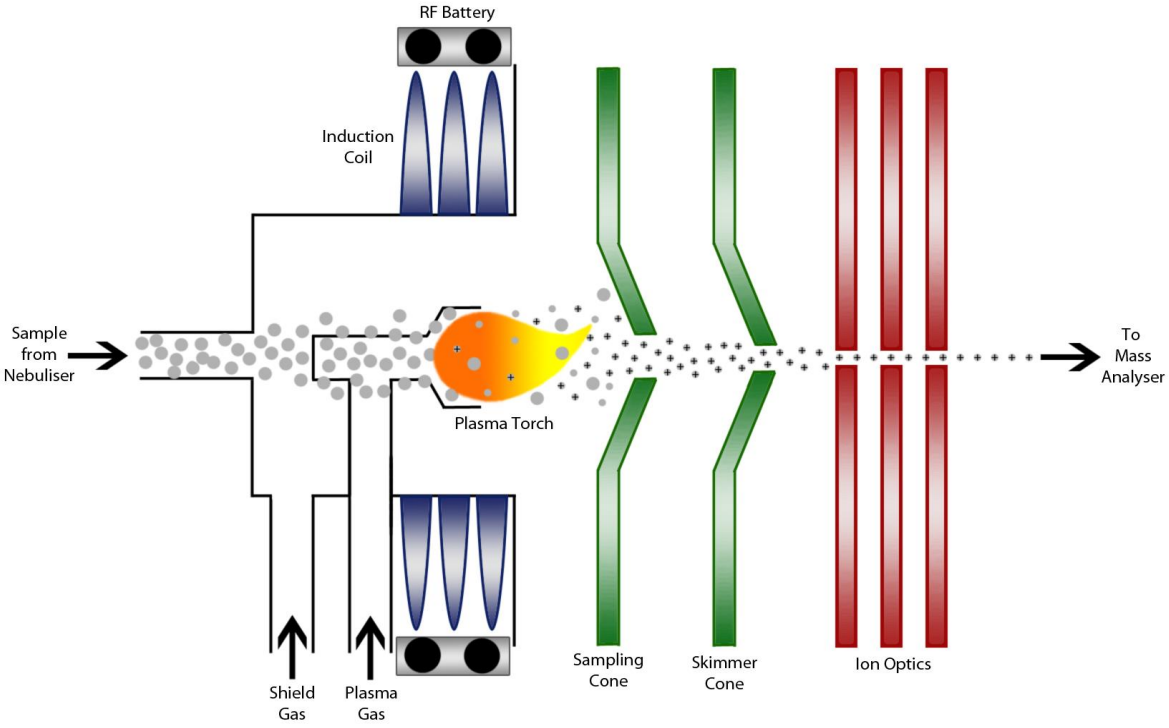

2.3.4. Interface Region

The purpose of the interface region is to efficiently direct ions from the argon plasma and focus them into the mass spectrometer. This is done by focusing the ions through water-cooled metallic cones with extremely small orifices through which the ions are directed. The sampler cone is the first of these, with an orifice of around 0.8 – 1.2 mm, and the

second is the skimmer cone with a smaller diameter of 0.4 – 0.8 mm. These cones are usually made of nickel or copper to avoid corrosion and interference with analysed metals. Platinum is an alternative that is more resistant to corrosion but can be prohibitively costly (125).

After moving through the skimmer cone the ions are directed through the ion optics, a series of lenses which remove interfering particles such as UV photons from the ion beam and further concentrate the ions into a narrow beam. This is done by placing a voltage on the lenses which steer the ions towards the centre of the beam. The purpose of the interface region is to guide ions into this concentrated beam, which can then be directed to move through the quadrupole while also removing any interfering particles that may reduce sensitivity.

The importance of this step is in removing inefficiency in the number of ions reaching the detector. Out of every million ions generated in the argon plasma, only one may actually reach the detector after moving through the mass analyser (106). One reason for this can be interference from matrix elements, which can defocus the ions. The interface regions counters this, and also removes unwanted matrix components from the beam which can add to background noise and disrupt optimal system performance. Although this process increases sensitivity, stability may be sacrificed if samples are not diluted before introduction to the ICP–MS due to the high concentration of matrix components (106). Such dilution is necessary to avoid performance degradation, but is a limitation in organic samples which may already contain very low metal concentrations. The degree of dilution must take both of these issues into account.

2.3.5. Collision/Reaction Cell

One issue that may arise during ICP–MS analysis is the formation of interference from polyatomic species generated from the argon plasma, solvent, or sample. Polyatomic interferences result from the combination of multiple isotopes generated from different elements, either from the samples itself or from the matrix, diluent, or argon plasma. Argon-based interference is especially problematic for determination of particular metals including potassium, iron, calcium, and selenium – metals which we aim to measure in our

analyses. This is due to the large number of polyatomic interferences that can be formed for these ions – for example, $^{40}Ar^{16}O^{+}$, $^{40}Ca^{16}O^{+}$, $^{40}Ar^{15}N^{1}H^{+}$, $^{38}Ar^{18}O^{+}$, $^{38}Ar^{17}O^{1}H^{+}$, and $^{37}Cl^{18}O^{1}H^{+}$ are all polyatomic interferences that can be formed which would interfere with the signal for ^{56}Fe (126). This issue can be addressed by the use of collision/reaction cell technology, which aims to prevent such interfering species from being formed. This is done by use of a collision/reaction cell which is positioned before the quadrupole analyser. The cell consists of an octapole surrounded by an RF field which is used not to separate ions, but to focus them into a beam. A non-reactive collision/reaction gas (in this case He, for which the instrument is optimised) is then bled into the cell, where it collides with the ions in the focused beam. This can either convert polyatomic species into non-interfering species, or convert the analyte itself into an ion that the argon cannot interfere with.

2.3.6. Data Analysis

The MS detector generates electromagnetic pulses upon detecting an ion, which are then counted by the multi-channel analyser and used to generate a mass spectrum of the metals present in the sample. The size of a spectral peak is proportional to the quantity of a certain ion detected within the sample.

Determination of sample concentrations relies on comparison of spectral peaks against standard solutions that contain known concentrations of each analyte of interest. These standards are used to generate standard curves which the sample concentrations can be compared against. Analyte signals that fall far outside the standard curves cannot be reliably quantified. The standards also provide information on the lower limit of quantitation in any single batch for each metal. Blanks containing nitric acid and internal standards but no sample are used to determine the lower limit of detection in individual batches, and also to identify any issues with the machine that may occur mid-analysis. Once the concentration of each metal of interest has been reliably determined using these methods, statistical analysis can be performed to compare concentrations between sample groups.

2.3.7. Advantages and Disadvantages of ICP–MS

ICP–MS is particularly useful for analysis of metals as it is able to detect them in extremely low concentrations, as low as ppt (127). This makes it much more sensitive than alternative

quantitative methods such as inductively coupled plasma optical emission spectrometry (ICP–OES) or atomic absorption spectroscopy (AAS), which can generally only detect concentrations down to parts per billion (ppb) (128). This low detection limit is especially important in organic samples, which can have particularly low concentrations of essential metals. This sensitivity is however traded for slightly lower precision, at < 5% in comparison to < 3% in ICP–OES (128). ICP–MS is able to detect a similar number of metals as ICP–OES, at > 75 elements, whereas AAS is able to detect between 50 – 68 elements (128). AAS is also incapable of performing quantitative analysis, unlike ICP–MS or ICP–OES, although this makes method development relatively simple for AAS, with cheaper capital and operating costs (128).

Table 2. 1. Comparison of Metallomic Analytical Techniques

	ICP–MS	ICP–OES	AAS
Detection Limits(129)	ppt	ppb – 100s ppt	100s ppb
Sensitivity[128]	< 5%	< 3%	0.1 – 5%
Speed[128]	All elements 2 – 6 minutes	5 – 30 elements per minute	15 seconds – 4 minutes per element
Number of Elements[129]	~70	~70	~50-60
Quantitative[128]	Yes	Yes	No
Cost[128]	High	High	Low/Medium

AAS = Atomic absorption spectroscopy; ICP–MS = Inductively-coupled plasma-MS; ICP–OES = Inductively-coupled plasma-optical emission spectrometry (ICP–OES); ppb = parts per billion; ppt = parts per trillion.

In the current metallomic analysis, detection limits, speed of analysis, and the ability to quantify metals were the top priorities, due to the high number of samples to be analysed and the low physiological concentrations of some metals and metalloids of interest in human tissues – as low as the ng/g range for manganese and selenium for example (130). As such, ICP–MS was decided upon as the most suitable method for this investigation.

2.4. Chromatography–MS

MS can be combined with chromatographic techniques such as GC and LC in order to enhance separation of similar compounds. These methods work by separating analytes based on their chemical properties. This is done based on relative affinities of different sample molecules for either the stationary or mobile phases, which vary depending on properties such as polarity, hydrophobicity and boiling point. These molecules can be collected in fractions, but are most commonly eluted from the column directly into the source of the MS, where they ionised and separated further based on their *m/z*. This allows for a greater degree of separation, and can distinguish analytes with the same *m/z*, polarity, or boiling points, which is not possible with either technique alone. This is particularly important in metabolomics, in which large numbers of analytes may be identified and require two-step separation in order to be effectively distinguished from one another.

2.5. Gas Chromatography–MS

GC–MS separates analytes by both chemical properties and *m/z*. The first step for this is the extraction and derivitisation of sample metabolites. Upon introduction into the GC–MS itself, the sample is vaporised and carried onto a chromatographic column by the carrier gas. As the analytes pass through this column, they will separate depending on their affinity for the coating of the column (the stationary phase) or the carrier gas (mobile phase). Analytes with low affinity for the stationary phase will pass through the column quickly, whereas those with a high affinity will take longer to do so. As they pass through the farther part of the column the analytes move through a heated transfer line and into the collision cell, where they are ionised by bombardment with high-energy electrons. The resulting ions then move into the mass spectrometer.

2.5.1. Sample Preparation

Although ideal for analysis of small and volatile compounds, some metabolites present challenges in GC–MS; in particular nonpolar compounds (131, 132). Derivitisation of samples is required to volatize nonpolar compounds before introduction into the GC–MS.

First, solid samples are lysed and metabolites extracted by precipitation and removal of proteins. This can be done in several ways, including several types of liquid-liquid extraction (LLE), solid-liquid extraction (SLE) and solid-phase extraction (SPE). SPE usually involves the use of a solid sorbent within a cartridge (the solid phase), and a liquid mobile carrier phase to separate components in samples based on their chemical properties such as polarity. The desired analytes are retained on the sorbent and can be eluted using an organic solvent. SLE is similar to SPE, using a sorbent through which the liquid sample is passed. However, in SLE, the sorbent is composed of an inert material which retains the entire sample – analytes are then selectively eluted off the sorbent using an organic solvent which leaves matrix components in the media. LLE separates compounds based on their relative solubility in polar and non-polar liquids, producing separate layers of polar and nonpolar analytes, which can then be extracted as desired. Advantages and disadvantages of these methods are summarised in Table 2.2.

LLE is the simplest extraction method, requiring no specialised equipment to perform with good extraction efficiency and reproducibility (133). Although SLE and SPE have higher selectivity and efficiency (133, 134), these factors may not outweigh the need for specialised equipment and associated costs unless the analysis requires better separation than is already being achieved with LLE (134). For these reasons, we used LLE for our GC–MS analysis.

LLE was performed here using 50:50 chloroform:methanol, which separates metabolites into a lower chloroform phase containing nonpolar molecules (mostly lipids) and an upper methanol phase containing polar molecules and amino acids. The polar methanol phase was then taken for analysis by GC–MS. This process concentrates the more volatile and lower mass compounds in the sample while removing nonpolar compounds that cannot be effectively analysed by GC–MS. During extraction, internal standards – analytes that would not be expected to occur naturally in the investigated sample but are chemically similar to analytes of interest (for example, norleucine is commonly used in investigations of amino acids (135)) – are also added to the samples in known concentrations. These can be used to monitor instrument performance during a run, and can also be used to quantify relative concentrations of analytes against the inserted standards, which are spiked into the samples at a known concentration.

Following extraction, the metabolites in the methanol phase must be derivatised. in order to make them more amenable to detection, by increasing volatility and thermal stability, or ‘tagging’ compounds that would otherwise fail to be detected. There are many derivatising methods available, including silylation, acylation, and alkylation.

Table 2. 2. Comparison of GC–MS Extraction Techniques

	LLE	SLE	SPE
Advantages	No special equipment required More straightforward to perform Conditions such as pH and ionic strength easily adjusted as required Good extraction efficiency Reproducible	Faster than LLE; can be automated No emulsion Can have higher recovery/ reproducibility than LLE	Faster than LLE; can be automated Analytes can be stored on sorbent until analysis More selective than LLE or SLE No emulsion
Disadvantages	Large quantities of organic solvent required; environmental pollution Difficult to extract highly water-soluble components Lower selectivity Cannot be automated Emulsion formation	Less selective than SPE Requires additional evaporation and reconstitution steps Specialised equipment required Higher consumable costs	More complicated than LLE; requires specialised equipment Matrix-sorbent interactions can reduce analyte recovery Solvent flow rate can affect recovery Heavily contaminated samples can cause analyte break through

LLE = Liquid-liquid extraction; SLE = Solid-liquid extraction; SPE = Solid-phase extraction

The most common of these is silylation, which uses a silyl reagent (such as N-Trimethylsilyl-N-methyl trifluoroacetamide [MSTFA] as used here) to donate silyl molecules to compounds containing active hydrogens (see Figure 2.9). The resulting silylation derivatives are generally more volatile and thermally stable, and less polar, making them more suitable for GC–MS analysis. One benefit of silylation is the wide range of molecules that can be targeted, making it suitable for untargeted analyses (136). Silyl molecules are also fairly low molecular weight substitutions, which should prevent increases in boiling point that would make the compound unsuitable for GC analysis (136). Silylated derivatives can be highly moisture sensitive though, and so are unsuitable for long-term storage and must be kept dry using reagents such as pyridine (137).

In acylation, acylating reagents react with highly polar functional groups (e.g. carbohydrates or amino acids) to replace active hydrogen with acyl groups. Like silylation, this reduces analyte polarity, but is not as effective at increasing volatility (136). Alkylation, in which the active hydrogen group is replaced by an aliphatic or aliphatic-aromatic group, produces very stable derivatives, and shows greater reproducibility than silylation for some groups such as amino acids (138). However, alkylation is generally restricted to amine and acidic hydroxyls, making it less suitable for untargeted analyses aiming to investigate as many molecules as possible. For these reasons, silylation was chosen as the most suitable method of derivitisation for the current investigation.

Additional reagents are added during this process in order to prevent formation of multiple derivatives. For example, methoxyamine hydrochloride (MOX) does this by reacting with carbonyl groups following silylation to form an oxime derivative, which also improves detectability of the sample molecule and improves peak shapes for carbonyl-containing molecules. An appropriate catalysing agent, such as pyridine, will also speed up and improve derivatisation reactions as well as improve solubility of derivatised compounds.

Figure 2. 7. Silylation Reaction

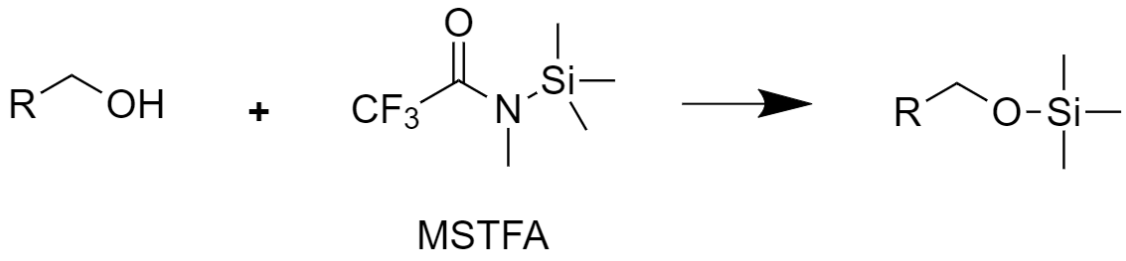

Finally, retention markers are added to the samples before GC–MS. Retention markers contain molecules with a known retention time (RT) that can be used as references during analysis of GC–MS spectra. This allows for more accurate identification of analytes on a mass spectrum by calculation of their relative RT, as relative to the standard marker.

Following derivitisation, samples will only remain stable enough for analysis for around 48 hours and so GC–MS must be performed immediately.

2.5.2. Sample Introduction

The sample is injected into the GC at the injection port by the autosampler. High temperatures of 150-250°C are applied to the port which instantaneously vaporise the sample. There are different modes of injection which can be used: split, splitless, and direct. Split-mode injection only allows a small portion of the sample to be injected via small vent, whereas splitless-mode introduces the entire sample. Whilst the former is better for avoiding overloading of the column, the latter is more suitable for accurate determination of trace analytes, and so was used here (139). Direct, or on-column, injection modes bypass the injection port and introduce the sample straight onto the column. This is the best method for low volatility samples, but not for samples containing high volatility compounds (139).

2.5.3. Gas Chromatograph (GC)

The GC is comprised mainly of a long cylindrical tube, usually ranging between anywhere from 15 to 60 m, through which the sample travels (see Figure 2.8). The sample is transported by the carrier gas; with helium, hydrogen, and nitrogen being the most

commonly used. Carrier gases must be inert and purified to extremely high levels (up to 99.999-99.9999%) to prevent contamination and degradation of the GC column. Helium is generally the least reactive and most sensitive of the three, and so is usually the best option when available (140) – however at times of helium shortage (as have occurred in recent years), an alternative may be necessary. Hydrogen is a more reactive gas and may degrade some compounds, and so is may not be suitable for all types of analysis (140). Nitrogen is less reactive than hydrogen but is only efficient at its optimum flow rate, with helium being more efficient at higher flow rates, and hydrogen being the most efficient at higher ranges (141). In our case, helium was available and so was used for our analyses due to its flexibility, lack of reactivity, and higher sensitivity.

The carrier gas acts as the mobile phase, whereas the coating of the column itself acts as the stationary phase. Depending on the chemical properties of the sample compound, such as volatility and polarity, it will have a different affinity for the stationary phase. Samples will low volatility and polarity will have a higher affinity for the stationary phase and so will take longer to elute from the column and move through to the detector, whereas compounds with higher volatility and polarity will move through faster. The time is takes for a compound to travel from the sample injector to the detector at the end of the column is referred to as its RT.

There are various types of column available for use in GC analysis. Currently the most common type of column used is the capillary column, which provides shorter run times, higher efficiency and resolution (up to 3-5,000 vs ~2,000 plates per metre), and requires less sample than more traditional packed columns (142). While the latter consist of columns packed with solid particles which act as the stationary phase, in a capillary column only the surface is coated with the liquid stationary phase. Capillary columns are much longer than packed columns (~30-60 metres vs a maximum of ~2 meters) which contributes to more efficient separation of compounds (142). However, as the sample does not have to move through solid particles as it would in a packed column, the compounds are still able to move faster through these longer capillary columns, resulting in faster analyses (142).

The temperature of the column is carefully controlled by the GC oven, which can be kept at a constant temperature (isothermal) or programmed to alter over the course of a cycle. Isothermal temperature control is easier to run and control, but may not be sufficient to separate all compounds in a sample – particularly if a wide range of analytes are being investigated (143). A temperature programme needs to be carefully designed to balance separation of samples and sensitivity of detection. Samples theoretically would be separated better at low temperatures, as if the temperature is too high, many components will not interact with the stationary phase. However, low temperatures can result in broader peaks and lower signal height (i.e. lower sensitivity), as well as increasing run times. Temperature programmes can also be set to 'ramp' meaning they begin at a low temperature and are then increased to a maximum pre-determined temperature. The initial low temperature allows for efficient injection (low starting temperatures are required for splitless injection), and as the temperature increases, less volatile compounds will be able to elute from the column. In our case, this involved a temperature cycle beginning at 50°C, which was then ramped up to 300°C, followed by cooling back to 50°C for the next sample. This cycle allowed for sufficient separation of analytes and sensitivity with an acceptable run time (42 minutes per sample).

Figure 2. 8. Diagram of gas chromatograph

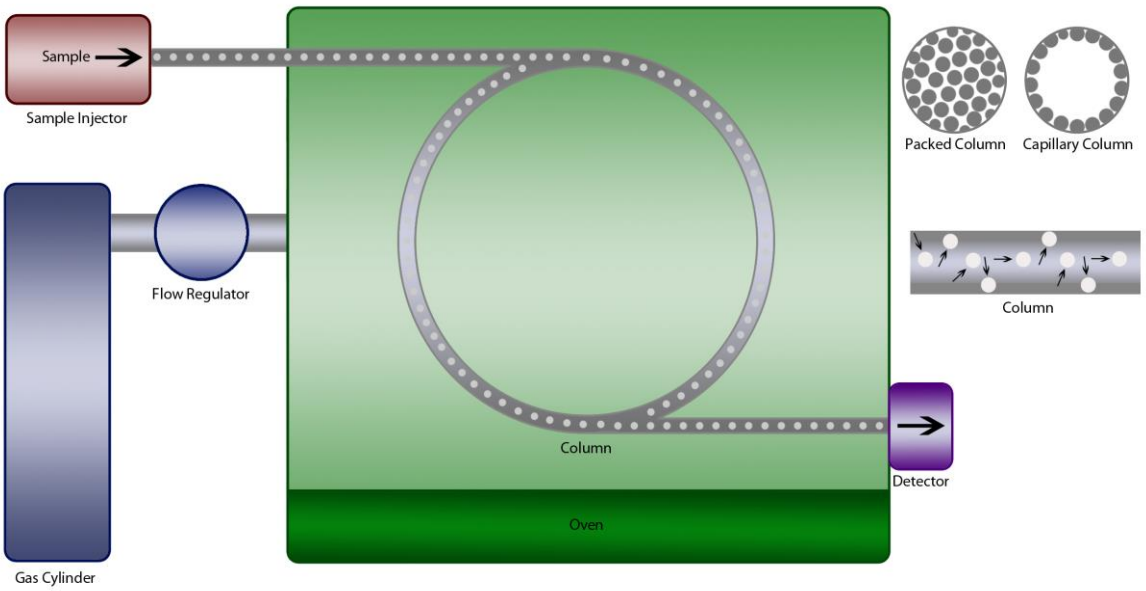

2.5.4. Interface

Coupling a GC with an MS allows for better separation of compounds and quantitation of analytes within a compound. However, there are challenges in linking these two systems, as they do not operate under all the same conditions. The purpose of the interface is to transport compounds from the GC and introduce them into the MS with minimal loss of sample (see Figure 2.9). One important condition is that the MS operates under a high vacuum, as opposed to the GC which works at atmospheric pressure. The interface creates the required vacuum using pressure pumps, and a high temperature is maintained to keep eluted compounds in a gaseous phase. Another useful attribute of capillary columns is that their relatively low pressure and flow rate allow them to be directly interfaced between the GC and MS, minimising loss of compounds.

The MS also requires ionisation of analytes before they move through the mass analyser. This can be achieved by electron ionisation (EI), chemical ionisation (CI), or field ionisation (FI). FI, or field desorption, applies a high-potential electric field to a sharp metal surface, resulting in ionisation of analytes applied to the surface. This results in a soft ionisation that does not result in fragmentation. This produces very clean spectra, but is far less sensitive than either EI or CI (144). CI is also a soft ionisation technique, which ionises the molecules of the reagent gas molecules, which the subsequently react with and ionise analyte molecules. CI is sensitive and produces fragment ions, but less than in EI (144). This lack of fragment ions produces cleaner spectra, but does not provide structural information for molecules (144). EI is the most commonly used ionisation mode, and achieves ionisation by colliding fast-moving electrons with sample molecules. The fragment ions provided by this hard ionisation method provides structural information on analyte molecules. These fragments decay reproducibly into characteristic fragments which can be used for automated identification of molecules using widely-available spectrum libraries (144). For these reasons, EI was selected as the most suitable method for our untargeted metabolomics analyses, in which we would need to identify large numbers of molecules with the sample.

In GC–MS, EI is achieved by use of a heated filament which produces electrons. These electrons then move from the filament to an anode on the other side of the column. As they do so they move perpendicular to the GC sample flow and collide with sample

analytes, causing them to fragment and ionise. The ionisation voltage is usually maintained at -70 eV to maximise ion intensity and resultant compound fragmentation, as well as for easy reference of GC–MS spectra to existing mass spectral library databases.

The sample flow is concentrated by the skimmer cones before entering the ionisation source and further focused by a series of lenses following ionisation before moving into the mass analyser (see section 2.3.4 for more detailed description of cones and lenses).

Figure 2. 9. Diagram of GC–MS interface apparatus

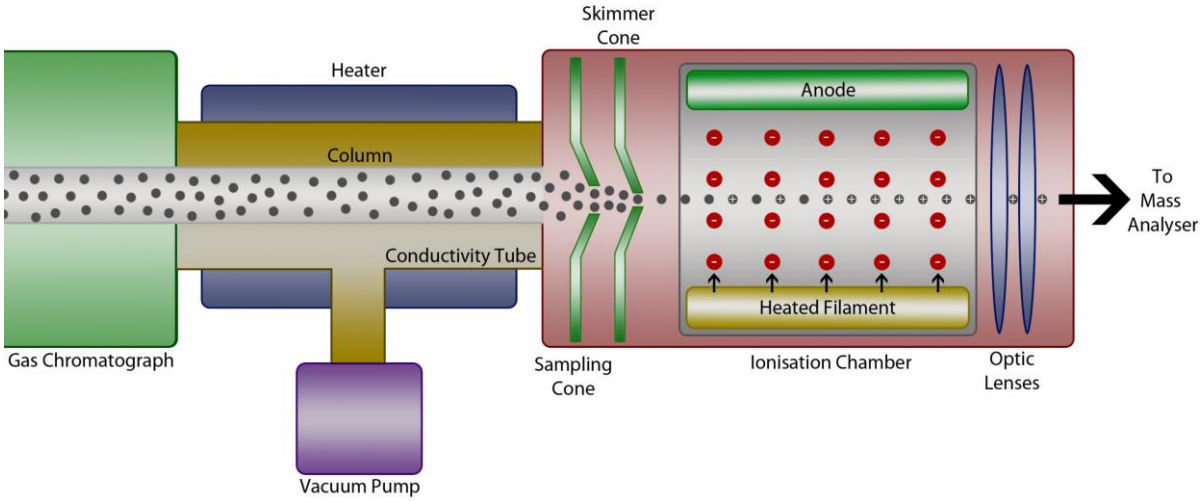

2.5.5. Data Analysis

As in ICP, the data collected by the GC–MS detector is used to generate a mass spectrum. On this, the x-axis represents *m/z*; this reflects the mass-to-charge ratio of the detected analyte and can be used for identification by reference to an existing mass library. However, as several factors such as flow rate, oven temperature, and column type can influence RT, retention markers with a known RT must be used to determine the relative RT of each analyte. This ensures more accurate alignment of distinct sample chromatograms and identification of analytes.

The y-axis represents the signal intensity of an ion; the higher the peak, the higher the ion count. Based on the peaks generated, software can be used to determine analyte identity and concentration. However, such software is not infallible and must be checked manually for unidentified peaks, inaccurate peak identification, and incorrect labelling of background noise. This must be done for each sample spectrum. This process introduces an element of human variability in analysis of the data, which must be minimised to ensure

consistent peak identification and quantitation. Making sure that peaks are well separated by proper sample extraction and derivitisation is important in minimising the influence of human variability during this step.

Once these steps have been completed, the relative concentrations of each analyte (as relative to the spiked standards) can be used to compare quantities of each analyte between samples using statistical analysis.

2.6. LC–MS

LC–MS broadly works in a very similar fashion to GC–MS, with the primary difference being that the mobile phase in LC–MS is liquid, rather than gaseous (see Figure 2.10 for overview). First, samples are extracted without derivitisation and introduced into the LC as a liquid. In the LC, different component molecules move through the column at different rates based on their affinities for the stationary and mobile phases. They then pass through the interface, where the liquid mobile phase is removed and the sample molecules are ionised for delivery into the MS. In the MS, the analyte ions are separated based on their *m/z*. The LC–MS then generates a mass spectrum based on the molecular weight and RT of ions within the sample, and their relative concentrations to internal or external standards.

Figure 2. 10. Diagram of LC–MS Apparatus

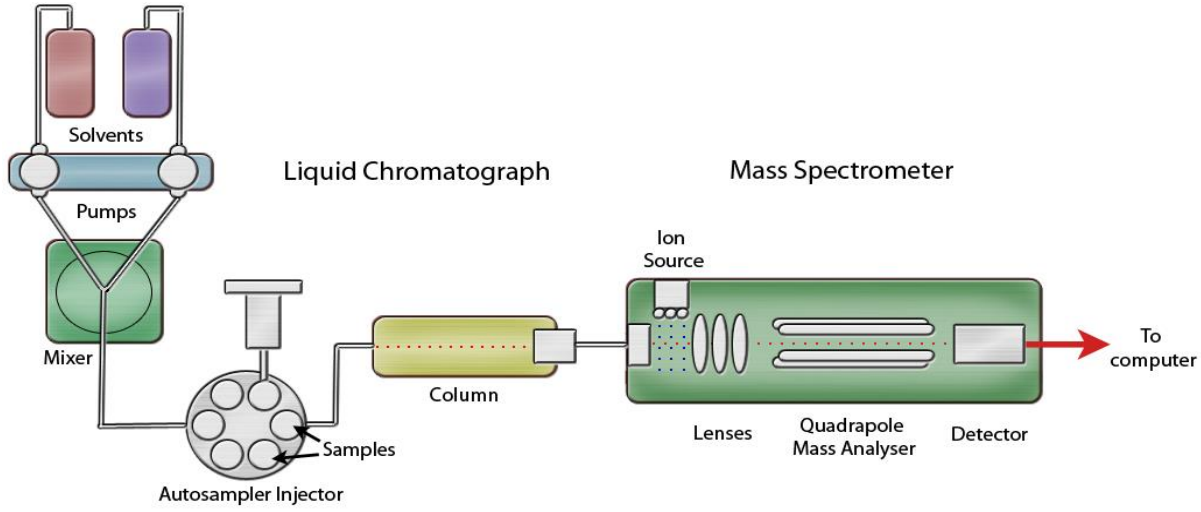

2.6.1. Sample Preparation

Sample preparation is minimal for LC–MS. The analytes of interest must be extracted from samples to remove matrix components and proteins that may clog the instrument. Comparison of different extraction methods are covered in section 2.5.1. In the case of the current analyses, liquid-liquid extraction into 50:50 chloroform:methanol allows separation of polar analytes from non-polar molecules and matrix components that are not of interest with good efficiency and reproducibility. Internal standards are added at this stage, following which the polar methanol phase is transferred and dried. This is the same extraction process used in the GC–MS analyses, but without derivitisation due to LC–MS' suitability for analysis of non-volatile compounds. Extracted samples are reconstituted in 0.1% formic acid for delivery into the LC–MS, as samples must be delivered as a liquid. Formic acid maintains a low pH in the mobile phase, which maximises ionisation of analytes by ensuring the analytes are more basic than the solvent.

2.6.2. Sample Introduction

The sample is injected into the LC at the injection port by the autosampler syringe. Loop injectors are most commonly used for this purpose in LC–MS, in which the sample is injected into the loop, which is then switched onto the flow path of the LC and into the column. In full loop injectors, excess sample is used to overfill the loop which ensures a precise injection volume, but results in some sample wastage. Partial loop injectors only fill 10-50% of the loop. This allows for greater flexibility as different sample volumes can be injected, but this variability can also result in decreased precision of injected sample volume compared to full loops (145).

2.6.3. Liquid Chromatography

Upon entering the LC, the sample is carried by the liquid mobile phase through a column to the detector at the end of the column (see Figure 2.11 for diagram of LC and LC introduction system). Unlike in GC, where only affinity to the stationary phase affects an analyte's elution time, affinity for both the mobile and stationary phase is key in LC. This makes the selection of both a suitable mobile phase and column important for maximising

performance. LC columns are most commonly made of cylinders of stainless steel, polymers, or occasionally glass, with a silica gel or polymer particle packing which acts as the stationary phase. The relative polarity of the stationary and mobile phases can depend on the type of column used. The length of the column can be selected to find the best balance between higher resolution for more complex samples (longer columns, up to ~300mm) and maximisation of throughput (shorter columns, down to ~15mm).

There are various types of columns available for use in LC–MS, the most common of which is the reverse-phase column. A reverse-phase column is one in which the mobile phase is more polar than the stationary phase, which causes more polar analytes to elute more rapidly from the stationary phase than less polar analytes. This is achieved by modifying the stationary phase to be non-polar or hydrophobic, for example with an alkyl-based bonding phase such as C_{18}, and using a more polar liquid for the mobile phase. This type of column is most suitable when highly polar compounds are of interest (146). These include molecules such as urea or pantothenic acid, which are the molecules of interest in this thesis for LC–MS analysis, making reverse-phase the most suitable column type for the analyses here.

By contrast, in normal phase LC, the stationary phase is more polar than the mobile phase. This is often achieved by coating the stationary phase with highly polar molecules, for example, if silica-packed columns are used, the silica can be coated with a layer or strongly polar silanol groups. This type of column works best for water-insoluble analytes (146). The buffers used in normal phase LC are less problematic for pairing with MS, but can produce less reproducible spectra than reverse-phase columns (147). Hydrophilic-interaction chromatography (HILIC) is similar to normal-phase LC, but with inclusion of water in the mobile phase in order to separate polar compounds that would otherwise be strongly retained in normal phase LC. HILIC can provide higher sensitivity than reverse phase or standard normal phase LC (147). However, HILIC can have solubility issues due to its reliance on acetonitrile as a mobile phase, and methods are less well established than those for reverse phase LC (148).

Somewhat less commonly, columns may need to be selected for size exclusion chromatography (SEC). SEC is used to determine the molecular weight and distribution of

polymers using columns packed with gels, cross-linked polymers, or silica particles, with no interaction of the analytes with the stationary phase. This separates molecules based on their size rather than their polarity or charge, which makes it particularly useful for separating macromolecules from smaller molecules, but unsuitable for separating molecules of similar sizes (136). This makes it unsuitable for the current analysis, in which small molecules are the main focus.

Figure 2. 11. Diagram of LC with Sample Introduction System

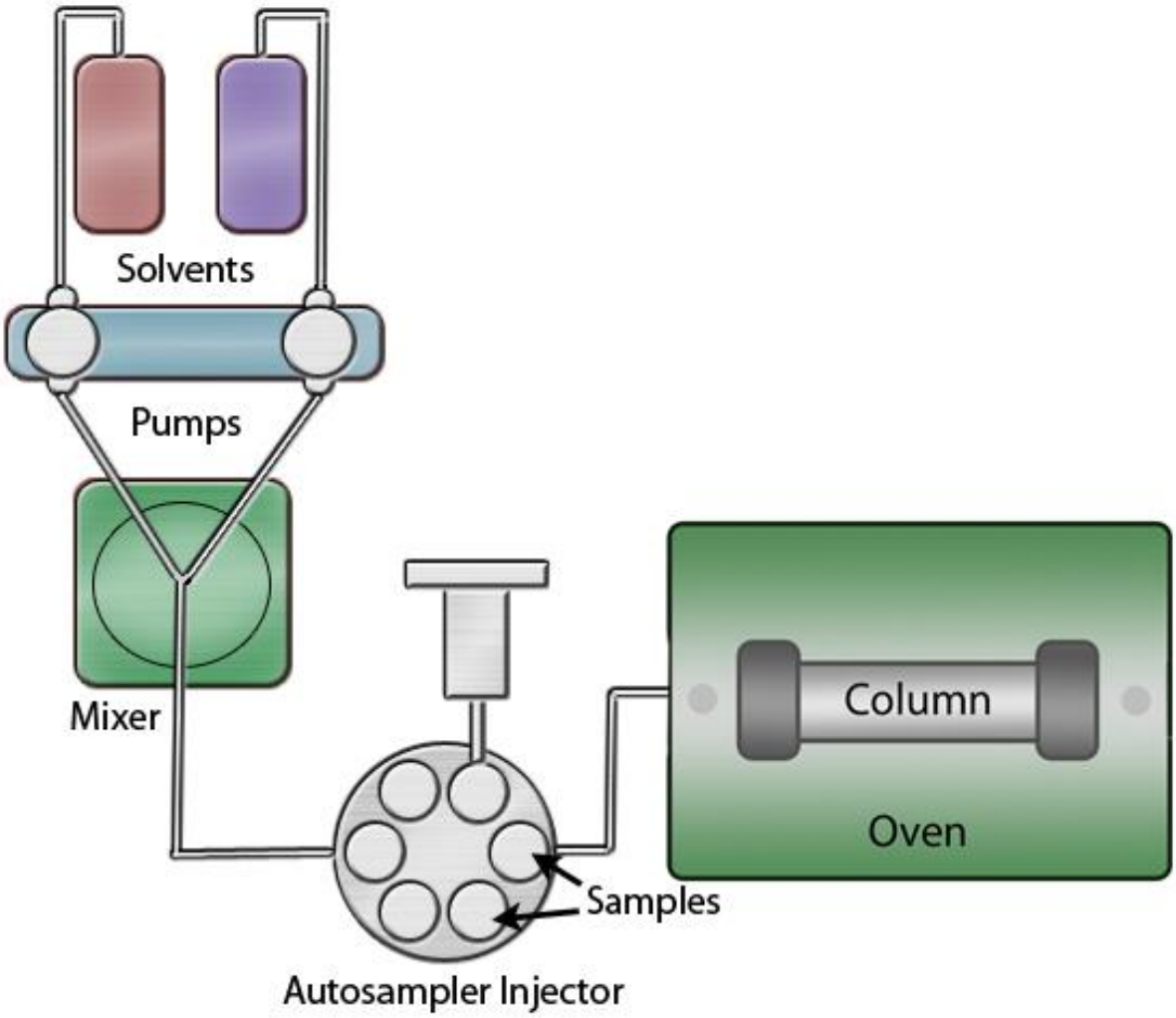

2.6.4. Interface

The interface is a key component of LC–MS, as the two techniques cannot be linked directly due to the liquid mobile phase of the LC. The MS must operate at very low pressures (~10^{-5} to 10^{-6} torr) in order to ensure ions reach the detector (see Figure 2.12). This requires the

removal of most, if not all, of the liquid mobile phase in order to function. This must be done whilst minimising loss of sample analytes.

In current instruments, this is most commonly done using either electrospray ionisation (ESI) or an atmospheric pressure chemical ionisation (APCI). In the ESI, the sample is sprayed into an electric field that desolvates the sample and turns it into a fine aerosol. The resulting droplets then evaporate in a vacuum that is maintained by a pump attached to the LC. The vacuum maintains the voltage applied to the droplets, causing them to become increasingly smaller and multiply charged. The presence of multiple charges on the ions reduces their *m/z*, making it easier to obtain spectra from large macromolecules (149). This 'soft ionisation' is often preferred in metabolomics as it can form intact molecular ions that assist in identification of the initial molecule (150).

In APCI, the sample is vapourised in a heated nebuliser, producing an aerosol carried by the N_2 nebuliser gas. This aerosol is converted into a gas stream by the combined heat and nebuliser gas flow. The ions then move through a cloud of solvent ions that can either donate or receive protons from the ions, causing them to become protonated or deprotonated respectively. The solvent ion cloud is produced by a corona discharge needle, which creates an electrical discharge via the ionisation of the solvent. Following de/protonation, the ions pass through a skimmer cone into the MS.

ESI is able to cover a much wider range of molecules, including more polar molecules than API (149). For this reason, it was considered more suitable for the untargeted and semi-targeted analyses conducted in this thesis.

Figure 2. 12. Diagram of LC–MS Interface with Electrospray Ionisation

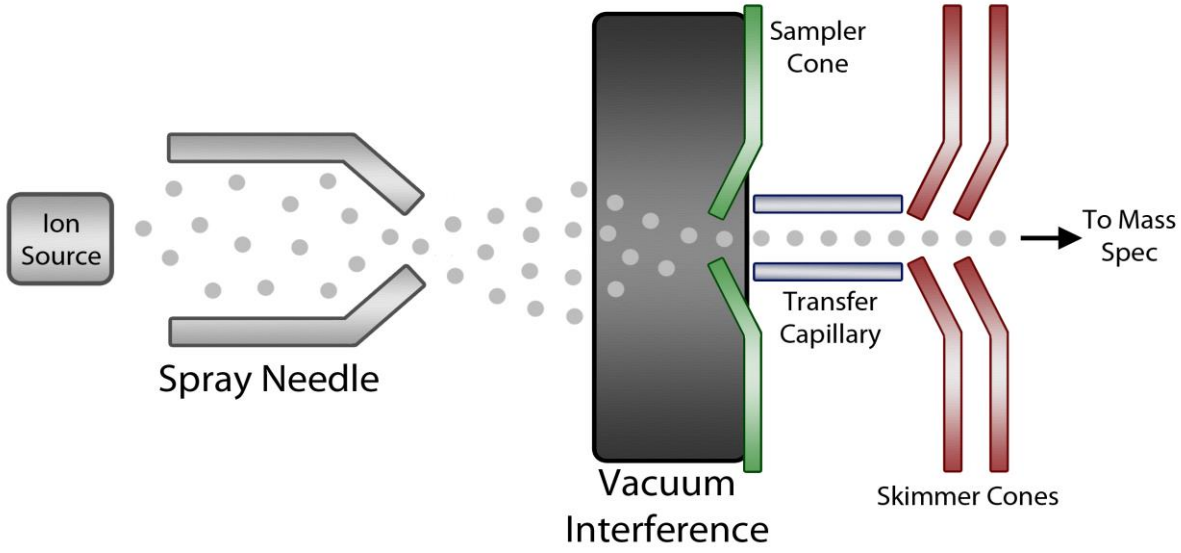

2.6.5. Data Analysis

Data analysis for the LC–MS methods used in this thesis is very similar to that used for GC–MS, and will not be reiterated again in detail here. In the case of the urea/vitamin B5 analyses, the targeted approach with use of spiked internal standards meant that the absolute concentrations of these analytes could be determined, in contrast to the untargeted approach used in the GC–MS.

2.6.6. Advantages & Disadvantages of Metabolomic MS Techniques

GC–MS and LC–MS are both commonly used techniques in metabolomics studies. Both are able target a much wider range of analytes than MS alone, due to their two-stage separation of sample molecules, but have their own advantages and disadvantages that make their more suitable for different types of analyses.

GCs often use capillary columns, which can provide better resolution than the packed columns generally used in LC–MS (see Table 2.3) (142). However, GC–MS generally has lower sensitivity to more polar and less volatile molecules, which require derivitisation before they can be detected (131). This is due to the high thermal stability required in the GC column, which can be heated up to 300°C. LC–MS applies little to no heat to sample analytes, and so is more suitable for analysis of thermally unstable compounds such as

polar molecules (151). This means derivitisation is not required, resulting in simpler sample preparation. Many polar molecules can still be detected using GC–MS though so long as the correct derivitisation procedure is carried out, and it is more adept at detecting nonpolar compounds than LC–MS (131, 132). Compound identification is assisted by the wide availability of comprehensive spectral libraries for GC–MS, which are more limited in LC–MS (152) – this can make it more difficult to make confident metabolite IDs in LC–MS. GC–MS is also typically cheaper than LC–MS due to simpler operation and relatively less maintenance required (153). However, GC–MS is unable to detect as many features as LC–MS due to its difficulty in identifying non-volatile, polar compounds, and so the relative importance of either the overall number of features detected vs the ease of identifying features against spectral libraries must be weighed up when selecting a technique.

Both these techniques are more sensitive than the common alternative method of NMR, as they are able to detect metabolites down to nanomolar concentrations, whereas NMR is restricted to high micromolar concentrations at best (see Table 2.3) (118, 154). MS techniques are also capable of detecting a wider range of metabolites than NMR, and can be performed using very low sample volumes (down to the nanolitre range) (155). This makes up for the lack of sample recovery in MS and more complicated analysis that is required. For more targeted analyses NMR may be a viable option, but GC–MS and LC–MS are more suitable for semi- or untargeted investigations due to their far superior mass range (see Table 2.3). This compensates for the lower level of reproducibility in MS in comparison to NMR, in which the same samples can be used to perform multiple analyses (118).

Table 2. 3. Comparison of Metabolomic Analysis Techniques

	GC–MS	LC–MS	NMR
Sensitivity[156]	mM-nM	mM-pM	mM-µM
Limit of Detection[156]	ng-pg	pg-fg	µM
Mass Range[156]	1,000,000	1,000,000	10,000
Speed[156]	Slow (~30 mins)	Moderate (5-9 mins)	Fast (1-5 mins)
Resolution[142]	Highest	High	Moderate
Other Advantages	Cheaper than LC–MS; wide availability of spectral libraries	Simpler sample preparation than GC–MS	Can be used in-vivo; higher reproducibility than MS

GC–MS = Gas Chromatography–mass spectrometry; LC–MS = Liquid Chromatography –mass spectrometry; NMR = Nuclear magnetic resonance spectroscopy.

GC–MS analysis was initially selected for the metabolomic analysis of tissues in this investigation due to its high resolution and availability of spectral libraries for analyte identification. However, LC–MS methods were later developed for analysis of PDD tissues, and may provide a higher degree of sensitivity. However, these methods were limited to analytes that could be identified using a specially-constructed in-house spectral library, and as such does not cover as wide a range of potential molecules as the GC–MS analysis.

2.7. Summary

There are several advantages to using MS methods for metallomic and metabolomics analysis of biological samples, including simultaneous identification of a broad range of analytes, high sensitivity, and quantitative capacity. These advantages are further strengthened by the pairing of MS with chromatographic techniques such as GC and LC, which allow identification of an even wider pool of molecules. In this thesis, these methods allowed for the analysis of a wide range of metals and metabolites in human brain samples, with the identification of metallomic and metabolomics perturbations that had not been previously described in PDD.

Chapter Three | Shared perturbations in the metallome and metabolome of Alzheimer's, Parkinson's, Huntington's, and dementia with Lewy bodies: a systematic review

3.1. Introduction

This chapter was published in Ageing Research Reviews: Scholefield M, Unwin RD, Cooper GJS. Shared perturbations in the metallome and metabolome of Alzheimer's, Parkinson's, Huntington's, and dementia with Lewy bodies: A systematic review. Ageing Res Rev. 2020;63:101152 (97). It is included in this thesis with only minor amendments.

Despite the high and increasing prevalence of chronic dementing diseases, both the mechanisms that underpin neurodegeneration and effective disease-modifying treatments remain elusive. Treatments for many dementing diseases, including Alzheimer's disease (AD), Parkinson's disease (PD), dementia with Lewy bodies (DLB), and Huntington's disease (HD), remain purely symptomatic, and despite decades of research the molecular pathways leading to neurodegeneration in these disorders remain unclear.

Research has however indicated several similarities amongst these diseases, both clinical and pathological. The greatest risk factor for the majority of dementing disorders is age (with the exception of HD, which is more common in aged individuals but is primarily determined by possession of an autosomal dominant mutation in the *Huntingtin* gene), and all are clinically characterised by a progressive reduction in cognitive function amongst other symptoms more specific to individual conditions. Neuropathologically, most dementias are associated with some degree of cerebral protein aggregation (for example, of amyloid-β in AD, α-synuclein in PD/DLB, and huntingtin in HD). Several studies have also pointed to possible shared metabolic and metallomic disturbances, such as increased iron deposition, glucose and lipid dysregulation, inflammation, and mitochondrial functional impairment. Considering the number of molecular similarities reported across these diseases, it becomes worthwhile to review the current literature in order to conduct a direct comparison of existing findings across multiple dementias. Identification of common findings may point to shared mechanisms in these diseases. This in turn could assist in the identification of common therapeutic targets that may be utilised in the development of treatments, which could potentially be administered for not just one, but up to several dementing disorders.

This review focuses on metallomic and metabolomic investigations of four dementing diseases: AD, PD, DLB, and HD, both in cerebral tissue and biofluids. Measures have been taken to try to account for variations in coverage of different diseases and matrices, and quality of the available literature. Each manuscript included in this analysis has been rated according to a-priori-defined criteria based on matching, methodology, and appropriate reporting of patient data and statistical analyses. Papers that did not meet the minimum criteria for inclusion were excluded from further consideration.

'Omics analyses allow for wide determination of multiple molecules within a tissue simultaneously, either by targeting a specific group or by an untargeted analysis which does not specifically focus on a chosen group of analytes – although this is usually restricted to groups of molecules which are identifiable using a chosen method, and so is not a truly global approach. This process generates a wider picture of what is occurring within a disease, rather than being limited to one or a few selected targets. By including results from two 'omics approaches, this picture is widened further, allowing connections to be drawn between different classes of analytes, metals and metabolites, and illustrating how such linkages may be involved in the pathogenesis of the disease.

The emergent focus here is on pathways involved in the metabolism of glucose and purines, both of which have been extensively implicated in multiple dementing diseases by network and pathway analyses (157-161). Enzymes in these pathways often require essential metal cofactors including manganese, magnesium, potassium, calcium, and selenium (162); the dysregulation of which can affect enzymatic activity and therefore metabolite concentrations. Other metals such as iron, copper, and zinc can also act as regulators of these pathways but, in addition, may also participate directly in disease mechanisms through their binding and down-stream interactions with the pathogenic, self-aggregating proteins that characterise many age-related dementing diseases (157).

As the glucose and purine pathways overlap and interact with one another, and given that they may even compensate for deficiencies in the other (158), analysis of changes in one would not be complete without analysis of the other. Additionally, as alterations in these pathways have been identified across several dementing diseases, it becomes possible to compare findings and identify similarities or differences in these pathways across different

conditions. These pathways include the polyol, pentose phosphate, purine, and glycolytic pathways, as well as the TCA and urea cycles; most have been individually suggested to be disturbed in dementing diseases (159, 160). These pathways are closely linked to regulation of mitochondrial energy production and oxidative stress and have been identified as disrupted across several dementing diseases. Comparison across the four dementias will enable both similarities and differences between diseases to be identified, and therefore potentially employed in, diagnosis, mechanistic research, identification of biomarkers, and eventual therapeutic development.

3.2. Methods

3.2.1. Approach to Literature Searching

A systematic literature search was conducted using the PubMed database to identify peer-reviewed English-language articles on the topic of metallomic and metabolomic analyses of AD, HD, PD, and DLB within the last three decades (1989 – 2019). For avoidance of doubt, this study was limited to human cases and controls, and does not discuss findings in animal models of disease. Here, the metallome is defined as the distribution of metal species, and the metabolome as the complete set of metabolites, present within an investigated tissue. Additional searches using Google Scholar were performed to ensure that as many available articles as possible were included. Search terms included variations of disease names (e.g. "Parkinson's disease", "Parkinson disease", "Parkinson's" for PD) as well as the terms "metals", "metallomics", "metabolites", and "metabolomics". In addition to the –omics terms, all individual metals/metabolites included in the study were searched for independently (e.g. "Parkinson's disease" AND "glucose") to ensure as full a coverage as possible (a full list of the search terms employed is provided in Supplementary Table 1, p314–317). The final search was conducted on 18/06/19.

3.2.1. Inclusion & Exclusion Criteria

All papers identified as relevant were assessed based on the inclusion/exclusion criteria shown in Table 3.1. These were selected on the basis of a minimum number of criteria (e.g. minimum N number of 5 in each group, inclusion of patient data covering factors such as cause of death, disease stage, and/or comorbidities, explanation of statistical analyses

employed, and either sex- or age-matching) for a comparison of metal and metabolite concentrations between diseased human cases and controls. N number was selected not as an ideal sample number, but as a minimum sample size on which statistical analysis can be reliably performed, and which was usually achievable even for scarce sample types. Although previous reviews investigating these dementing diseases have included some of these criteria, particularly those involving case–control matching and sufficient N values, this appears to be the most extensive group of inclusion criteria used to date to the best or our knowledge. Papers investigating tissues not covered in a sufficient number for comparison, such as urine, hair, and nails, were also excluded for the purpose of this review. Investigations on serum, plasma, and whole-blood were grouped together into a single category named 'blood', as investigations of directional changes (e.g. increases/decreases) that occur in one are generally reflected by the others, although absolute concentrations of analytes may differ.

Table 3. 1. Inclusion criteria necessary for a published study to be considered for review

Inclusion Criteria
Human study
Brain, CSF, plasma, serum, or whole-blood measurements
Inclusion of healthy controls
N (for each group) ≥ 5
Both males and females included
Description of statistical analyses included in text
Either age- and/or gender-matching
Significant patient data provided (e.g. cause of death, comorbidities, stage of disease)
Separation of different dementias (e.g. no grouping of separate conditions: for example, PDD and DLB into one Lewy body dementia [LBD] group)
Direct comparison of metals/metabolites in different groups (e.g. correlational data or metabolite ratios were excluded)

3.2.2. Scoring of Included Papers

Papers that were included in the study were then rated and scored based on the criteria shown in Table 3.2, whereby a minimum of four points was required for inclusion in the final review. This process ensured that each source met the minimum criteria for inclusion in the review, and to determine how many papers included in the review met each of the criteria. Criteria were selected on the basis of a) potential for affecting experimental results (e.g. age and gender have both been shown previously to have effects on certain metals and metabolites); b) potential for affecting the statistical power (i.e. adequate N numbers); c) feasibility (e.g. exact age matching is very difficult to achieve, and so was not included); d) sufficient coverage in the literature (e.g. years of education may be a variable which could affect results, but to date very few studies report this variable, it is not routinely available in tissue bank data, and so was not included). Although some potentially confounding variables may be omitted on this basis, an effort has been made to include all that are present in the literature in sufficient number to make comparisons between diseases and tissues both feasible and meaningful (e.g. level of education was not included because it was included in insufficient numbers of studies to merit inclusion).

Table 3. 2. Rating system of papers meeting inclusion criteria

Rating System (1 point each; minimum of 4 points required for final inclusion; 8 total)
N ≥ 20 in each group
Age-matching
Gender-matching
PMD available (where applicable)*
PMD matching (where applicable)*
Cause of death available (where applicable)*
Statement of exclusion conditions/evidence of checking for comorbidities in cases AND controls
Data available on disease staging or progression (e.g. Braak stage, MMSE, etc.)

*Where not applicable (e.g. with tissues taken from living individuals) a point was automatically awarded. MMSE = Mini-Mental State Examination.

Based on these criteria, a total of 198 papers have been included in this review, whereas 86 were excluded. Tables of findings from each source accepted for inclusion in the review are presented in the Supplementary Tables 2-5, p318–396.

3.2.3. Evaluation of Findings

Following the collection of the accepted manuscripts, each was individually evaluated for its findings. For each analyte investigated it was recorded whether an increase, decrease, or no change was observed. This was done separately for each dementia condition and each matrix included in a manuscript. These findings were recorded in Supplementary Tables 2–5 (p318–396), along with information regarding sample numbers, matrix type, brain region (where applicable), and methodology used. A count was then made of the number of reports observing increases, decreases, and no change for each analyte (with reports in each disease and each matrix type counted separately). Findings for each individual manuscript were counted equally, with no weighting attributed based on criteria such as sample number, methodology, etc. as this was considered outside the scope of this review. Reports of changes/no changes are also considered equally when looking for consensus between sources. Once counted, it was then identified where consensus did or did not exist among reports in individual, and then between differing, matrices and diseases. These results are the primary focus of this review.

3.3. Results

3.3.1. Inclusion Criteria and Rating System for Selection of Studies

A total of 284 papers were identified and considered for inclusion in this systematic review. Following assessment of each paper by the inclusion, exclusion, and rating criteria (Table 1 and 2), 198 papers were finally accepted and 86 excluded. These papers varied in number corresponding to the four dementia diseases under study, as well as for differences in the material analysed: brain tissue, CSF or blood (we will use the term matrix hereinafter to refer to these biological materials). A summary is shown in Figure 3.1, and the full list of accepted papers is shown in Supplementary Tables 2-5 (p318–396). Figure 3.1 shows how many papers were reported for each matrix in each disease, as well as the average number

of sources per reported metal/metabolite, and the average number of points awarded to each source.

As became clear, analysis of different diseases and of different matrices is unequal in the samples studied. The analysis of metals and metabolites in DLB was substantively underrepresented in the literature in comparison with the other three dementias, with only 11 studies included in this review. In comparison, 69 sources were included for PD and 92 for AD. HD also had fewer accepted sources, which numbered 26.

In the case of PD, the number of studies reporting analysis of brain tissue and blood was similar, but there were only five studies of CSF that met the inclusion criteria (Table 2). Analysis of blood (50 sources) was much more extensive than either for brain or CSF in AD (29 and 20 sources respectively). In the case of HD, publications were heavily skewed towards brain and blood investigations, with very few CSF papers. Due to the low number of DLB studies, reports of blood, brain, and CSF were all low: with regard to blood investigations, not a single serum study reached criteria for acceptance and only two of plasma.

These variations in coverage were associated with large differences in the number of molecules reported for each disease. Whereas over 70 analytes were identified in PD and AD out of a total of 91, 60 were recorded for HD and only 22 in DLB. These observations highlight the large gaps in the available research investigating metabolomic and metal analytes in HD and especially DLB in comparison to the much more widely studied PD and AD; this was both with respect to the matrices studied and the analytes covered in individual reported studies.

Of the 86 excluded papers, 41% lacked either age- or gender-matching between cases and controls, making this the most prominent cause for rejection (data not shown). Sixteen per cent of excluded papers lacked any healthy controls; instead, only comparing between different dementing diseases, and 6% had $N < 5$ in one or more groups, or grouped two or more dementias together (e.g. PD and DLB linked together into 'Lewy body dementias'). Studies that compared analyte concentrations against symptom severity or disease staging rather than between cases and controls were also excluded.

Figure 3. 1. Disease and matrix coverage of papers accepted for final review

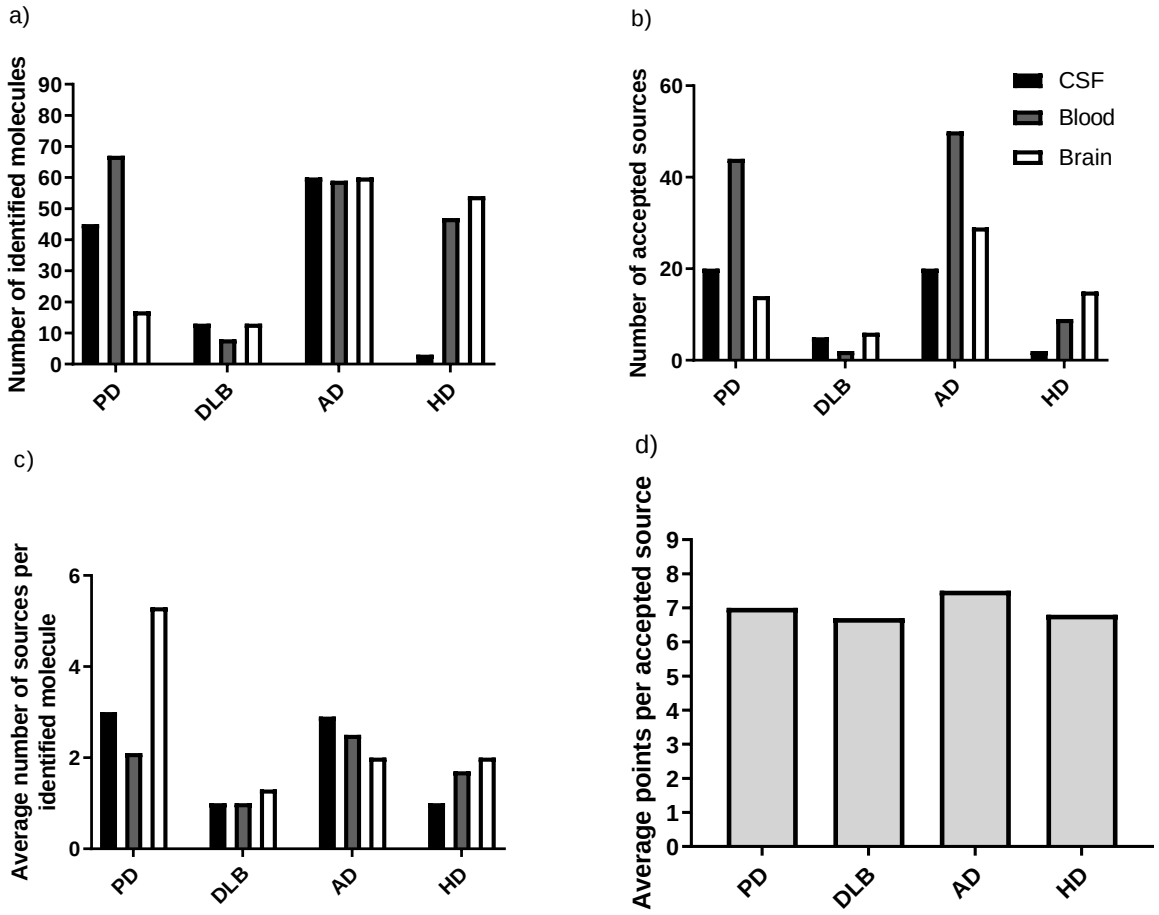

a) Number of identified molecules per matrix in each disease from total of 91 investigated. b) Number of accepted sources per matrix in each disease. c) Average number of source per identified molecule per matrix in each disease. d) Average number of points per accepted source in each disease as awarded by rating system. Abbreviations: PD, Parkinson's disease; DLB, Dementia with Lewy bodies; AD, Alzheimer's disease; HD, Huntington's disease; CSF, cerebrospinal fluid.

3.2.1. Rating of Papers

With regard to the quality of papers, the average rating score for each disease averaged around 6 points out of a possible 8. The minimum acceptance criterion was 4 points. Prevalent limiting factors were a low N-value (less than half had N ≥ 20; see Figure 3.2), lack of age- and gender-matching, and lack of data on the cause of death in post mortem experiments. The latter made it difficult to determine whether there are patterns in causes of death in cases or differences in patterns between cases and controls, or if factors such as inflammation or vascular issues show higher prevalence in cases compared to controls. All included sources had either gender- or age-matching, but only 82% had both (see Figure 3.2); there was a greater tendency towards use of age- vs gender-matching (95% and 86% respectively) in studies meeting Table 3.2 rating system requirements. Exclusion criteria/data on incidence of any comorbidities were included in 66% of studies, and 73% of post mortem studies were matched for PMD. It is acknowledged that some issues, for example low N-values, can be difficult to overcome, as samples are scarce and difficult to obtain in quantities sufficient to perform such analyses. Where suitable samples are not available, statistical tests of power may be able to provide confidence in findings from smaller numbers, and appropriate statistical analyses can be employed to investigate potential effects of unmatched or unrecorded variables (as undertaken in some reports).

Some issues were more prevalent in research on certain diseases. Relatively few studies on DLB in particular were included and there were lower percentages of papers with gender-matching or cause-of-death data. In addition to the relatively sparse coverage of DLB, these factors may also contribute to limited descriptions of metallomic and metabolomic alterations in this disease.

Figure 3. 2. Percentage of papers meeting Table 3.2 rating system requirements

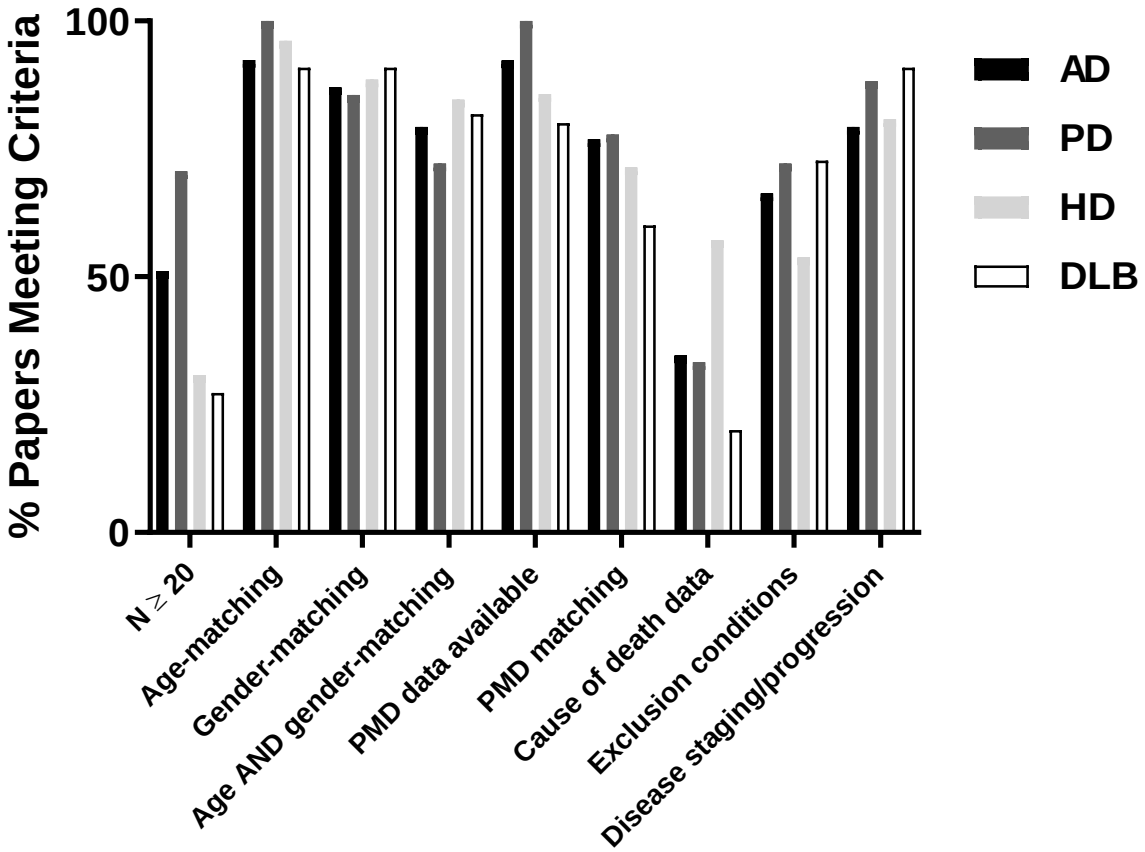

N ≥ 20 for *each* of the case and control groups. Abbreviations: PD, Parkinson's disease; DLB, Dementia with Lewy bodies; AD, Alzheimer's disease; HD, Huntington's disease; PMD, Post mortem delay.

3.2.2. Findings in Brain Tissue

A total of 75 of the 91 analytes identified in this review were reported from a total of 58 papers describing metallomic and metabolomic studies of brain tissue in AD, PD, HD, and DLB (see Supplementary Tables 2-5, p318–396, for complete list of reports). These studies covered 13 named brain regions in PD, eight in DLB, 24 in AD, and 25 in HD. In total, samples were obtained from the brains of 1146 donors with dementia (484 with AD, 363 with PD, 58 with DLB, and 241 with HD) and 1098 controls free from dementia. Of these 75 analytes, nine were reported on in all four conditions; adenosine, copper, hypoxanthine, inosine, iron, manganese, uric acid, xanthine, and zinc in one or more brain regions (see Table 3.3; and Supplementary Tables 2-5, p318–396, for details of specific regions). Of these nine, only changes in copper were found consistently across all four diseases.

Table 3. 3. Perturbations in levels of metals & metabolites in dementia brain tissue

Analyte	PD	DLB	AD	HD
Adenosine	1* / 0 / 0	1* / 0 / 0	1 / 1 / 2	0 / 0 / 1
Copper	0 / 3 / 2	0 / 2 / 2	1 / 4 / 4	0 / 1 / 1
Glucose	1 / 0 / 0	-	3 / 0 / 0	1 / 0 / 1
Hypoxanthine	0 / 0 / 1	0 / 0 / 1	0 / 2 / 2	0 / 1 / 2
Inosine	1* / 0 / 0	1* / 0 / 0	1 / 0 / 2	1 / 0 / 2
Iron	7 / 0 / 5	0 / 0 / 2	5 / 1 / 1	4 / 2 / 2
Manganese	0 / 0 / 1	0 / 0 / 1	1 / 1 / 3	0 / 1 / 1
Uric Acid	0 / 1* / 0	1 / 0 / 0	0 / 0 / 1	0 / 2 / 2
Xanthine	1† / 0 / 0	0 / 0 / 1	0 / 2 / 2	1 / 0 / 2
Zinc	0 / 0 / 1	0 / 0 / 2	3 / 3 / 4	1 / 0 / 1

Order of reports is **increases** / **decreases** / unchanged. The number in each box signifies the number of sources for each molecule in each disease; presence of a dash – indicates where there are no available sources. A list of all analytes and specific brain regions reported in the included studies is presented in Supplementary Tables 2-5 (p318–396). * In males only; † in females only.

3.2.2.1. Essential Metals

Copper: Most reports of copper in AD, PD, HD, and DLB noted decreases in some brain regions and no change in others (76, 78, 161, 163-166). In AD, hippocampal copper was reported to be decreased by four papers with no contradictory reports, despite differences in methodology (161, 163, 167, 168). Similar consistency was noticed in investigations of copper in the amygdala, with both available reports observing decreased levels in AD brains (163, 168). Observations in the cerebellum however were conflicting where one source reported decreases (168) and another no change (163). Similar discrepancies were present in investigations of the frontal cortex, with one source reporting increases (169) and another no change in copper (170).

In investigations of PD tissues, three sources reported that copper is decreased in the substantia nigra, with no conflicting findings (76, 78, 171). In DLB, only three brain regions were covered; however, hippocampal copper was reported to be both decreased (161) and unchanged (164). Only one study was accepted investigating copper in HD brains, which reported decreases in the anterior cingulate gyrus and no change in any of the other six investigated regions (166). This analysis highlights varying levels of consistency reported by different sources, even within the same brain regions. However, it is worth noting that regions strongly associated with high levels of neurodegeneration in each disease (for example, the hippocampus in AD and substantia nigra in PD) have produced more consistent findings than regions considered to be relatively spared, such as the cerebellum.

Iron: Iron has also been reported to show consistent increases in various brain regions across AD, PD, and HD; particularly within heavily affected regions such as the hippocampus, substantia nigra, and caudate respectively (see Supplementary Table 2A (p318–323), 3A (p349–356) & 5A (p378–379)). There were no studies of iron levels in the AD substantia nigra or in the PD hippocampus, which unfortunately prevented comparison of these heavily-affected regions (substantia nigra in PD and hippocampus in AD) between the two diseases. Two studies in DLB have reported iron to be unchanged in the hippocampus, amygdala, and neocortex (161, 172). Decreases in iron have been reported in the corpus callosum, frontal white matter, and genu white matter in HD (173, 174), in contrast with other regions reported to show increases (166, 174-176). One contradictory

finding was reported in AD by Corrigan and colleagues who observed decreased iron in the hippocampus (167), in contrast to three other reports that reported increases in this region (163, 168, 177). There are no reports of decreased iron in any of the 12 regions investigated in the PD brain.

Considering this high level of consistency, increases in cerebral iron may play a role in the pathogenesis of three of these dementias, a possibility made even more likely by the fact that these changes are more often reported in heavily affected regions of each disorder. As it is possible to image iron in the brain of living individuals, iron could also therefore serve as a biomarker both of general dementia (observing general increases in iron) and specific conditions (observing increases in heavily affected regions of a disease). It would also be of interest to conduct further investigations covering more areas of the DLB brain, as the two reports included in this review covered only three regions (161, 178). It may be that other regions of the DLB brain, or further studies looking at the same regions, might produce findings similar to those seen in the other three dementias.

Manganese: Manganese was reported to be unchanged by the majority of sources across all four diseases. However, there was a single report of increased manganese in the AD hippocampus (168), conflicting with the other source that reported no change in this region (167). Only one source was accepted for each of the other three dementias, and there were no brain regions investigated in common across three or more diseases, preventing region-specific comparisons across diseases.

3.2.2.2. Metabolites

Hypoxanthine: Most sources (4/6) reported hypoxanthine to be unchanged in the PD, DLB, AD, and HD brains, although there were again conflicting reports in some brain regions. In AD brains, hypoxanthine in the frontal cortex and the cerebellum was reported to be either decreased or unchanged by three differing sources (179-181). Similarly, both decreases and a lack of change in hypoxanthine were reported in HD across differing brain regions; however, no single region was reported on by more than one source (182, 183). Only one report by McFarland and colleagues was included for hypoxanthine measurements in both PD and DLB, which reported a lack of change in the cortex and striatum of both conditions

(181). The lack of common brain regions investigated precludes area-specific comparison across all four dementias.

Glucose: It is also possible that other molecules may show some consistency across the four dementias; however, incomplete coverage precludes full comparison at present. For example, glucose shows region-dependent increases in PD (74, 179, 180), AD (184), and HD (183) brain tissues, but there is no equivalent study on DLB. As the only dementia with multiple accepted sources, reported glucose changes from three investigations in AD were largely in agreement, although two sources reported increases in the cerebellum (180, 184) whilst another reported no change (185). Interestingly, PD (74), AD (180, 184), and HD (183) all had reports of glucose increases within cortical regions, suggesting a possible susceptibility of the cortex for glucose dysregulation across multiple dementing diseases, in contrast to more specific vulnerability of deeper grey matter regions in different conditions.

Uric acid: Another particularly interesting finding in this comparison is that of the differences in uric acid changes reported in PD and DLB brain tissues (decreases in the former and increases in the latter), particularly as they are reported by the same source (181). These two diseases closely resemble each other, and are distinguishable only by the order of onset of motor and cognitive symptoms and pattern of α-synuclein deposition within the brain, with controversy over whether the two should be considered separate conditions at all (14). As such, the differences reported in brain uric acid levels could indicate why these subtle differences occur and help to better distinguish these two diseases at post mortem. Decreased uric acid levels have been reported repeatedly in PD biofluids (79, 186-189), but parallel studies have yet to be conducted on brain tissue. PD and DLB have also both been observed to have increased inosine and adenosine levels in the brains of males, with both metabolites being involved in purine metabolism.

Summary: Taken together, these results highlight *inter alia* that studies using different methods, different levels of matching, etc. do not necessarily produce the same results; as such, these are factors that should be considered in the interpretation of results and design of future experiments. However, there are some findings, such as regional increases in brain glucose and decreases in copper that show striking consistencies across multiple

sources and across multiple dementias. Another factor limiting the comparisons here, which is also present in investigations of the other matrices, is the number of reports covering each analyte. As can be seen in Table 3.3 and as has been highlighted here, many molecules are only reported by a single source. Additional validation studies will be required to establish whether these changes are in fact genuine and can be replicated in larger cohorts and by other groups. Wider coverage of metallic perturbations, particularly in AD, makes the metal findings more reliable than those for metabolites, although discrepancies between sources still exist.

3.2.3. Findings in CSF

Out of 91 investigated analytes, a total of 62 were reported in CSF in at least one dementing disease. However, only a single one – copper – was reported in all four. There were some consistencies in the changes reported in copper; both sources investigating CSF copper in AD reported no change (190), as did the single report in HD (191). The majority of investigations in PD also reported no change(192-195), although there were two reports of increased CSF copper (190, 196) and a single source reported decreased levels (197). The single source reporting on DLB CSF copper observed increased levels (198). If this finding were to be replicable, CSF copper could perhaps be used as a biomarker to distinguish DLB from other dementias.

Comparisons of CSF measurements across all four diseases were made difficult by the sparse coverage in both DLB and HD. In DLB, a total of five included papers investigated 14 molecules (198-202) whilst in HD two papers reported on only three molecules (190, 203). In comparison, there were 18 sources investigating PD CSF and 20 in AD (see Tables 3.1 & 3.2). There is a clear gap in the literature here, where comparisons across dementing diseases could greatly benefit from more investigations into HD and DLB CSF.

3.2.4. Findings in Blood

Taken together, blood measurements (whole blood, plasma, and/or serum) have the most complete coverage of any matrix, with a total of 198 included papers reporting on 84 analytes in at least one dementia. However, only one source reported on HD serum and none at all in DLB. As serum is often used to model plasma, it might be expected that

plasma and serum reports would indicate similar observations. As such, the two have been combined in this analysis along with whole-blood measurements into the single category 'blood'. However, it is not always the case that findings in the serum and plasma agree in every single case, even within studies investigating them simultaneously (194).

Only two analytes were reported in the blood in all four dementias; arginine and citrulline (Table 4). Observations of these two metabolites were not consistent across diseases. Citrulline was largely reported to be unchanged in PD blood (204-206), with only a single report of increases in serum (207). In the single report on DLB plasma, no change were observed (200). Increases were reported in both AD plasma (208) and serum (209) by one source each, although another report observed no change in the plasma (210). Observations in HD plasma were also inconsistent, with reports of increases (211) and of no change (212) in citrulline levels.

Arginine showed a somewhat better level of consistency than citrulline, with more reports of levels being unchanged than increased or decreased in all four diseases (see Supplementary Tables 2-5, p318–396). However, once again there were some contradictory findings in PD, AD, and HD; with decreases reported by a single source in all three (211, 213, 214), as well as single reports of increases in both AD (215) and HD (216). The single source on DLB plasma reported no change (200).

Every metabolite reported to be consistent across at least three diseases was an amino acid, with the majority of reports observing no change in any of them in any disease (see Table 3.4). The strength of evidence supporting decreased uric acid in PD is already widely accepted (217, 218). What is perhaps of more interest are the number of sources also reporting decreased uric acid in AD patient blood measurements: three reports observed decreases (219-221); however three other investigations reported increases or no change (222-224). These differing findings occurred in both plasma and serum investigations, and so it would be of interest if additional studies were to be performed to validate whether uric acid levels change in AD blood. The single report on uric acid in HD plasma found no change (225). Depending on the findings of such repeat investigations, decreased blood uric acid may be of use as part of a generic biomarker panel for dementia, or as a specific marker of PD.

Table 3. 4. Metals & metabolites reported in blood from patients with age-related dementia

Analyte	PD	DLB	AD	HD
Asparagine	0 / 1 / 2	-	1 / 2 / 2	0 / 1 / 2
Aspartate	1 / 1 / 1	-	1 / 1 / 1	0 / 0 / 2
Arginine	0 / 1 / 2	0 / 0 / 1	1 / 1 / 8	1 / 1 / 3
Calcium	0 / 0 / 1	1 / 0 / 0	0 / 0 / 1	-
Citrulline	1 / 0 / 3	0 / 0 / 1	2 / 0 / 1	1 / 0 / 1
Creatinine	1 / 0 / 2	-	1 / 0 / 2	0 / 0 / 1
Glucose	2 / 0 / 0	-	2 / 0 / 0	0 / 0 / 2
Glutamate	2 / 1 / 2	-	1 / 0 / 2	0 / 0 / 1
Glutamine	1 / 1 / 3	-	1 / 1 / 7	0 / 1 / 2
Glycine	2 / 1 / 2	-	2 / 0 / 4	1 / 0 / 1
GSH	1 / 0 / 0	-	0 / 3 / 2	0 / 1 / 1
Histidine	0 / 0 / 2	-	0 / 1 / 5	0 / 1 / 3
Hypoxanthine	0 / 3 / 0	-	1 / 0 / 1	0 / 0 / 1
Iron	2 / 3 / 9	0 / 1 / 0	2 / 3 / 5	-
Isoleucine	2 / 0 / 3	-	0 / 1 / 5	0 / 2 / 1
Kynurenine	1 / 1 / 2	-	0 / 1 / 4	0 / 0 / 1
Kynurenic Acid	1 / 0 / 0	0 / 0 / 1	0 / 2 / 2	-
Leucine	2 / 2 / 2	-	0 / 1 / 5	0 / 1 / 3
Lysine	0 / 0 / 2	-	1 / 0 / 4	0 / 0 / 3
Methionine	2 / 2 / 1	-	1 / 1 / 4	0 / 1 / 2
Ornithine	1 / 0 / 3	-	0 / 2 / 4	1 / 0 / 3
Phenylalanine	1 / 1 / 3	-	1 / 2 / 5	1 / 0 / 2
Serine	0 / 1 / 2	-	0 / 0 / 4	0 / 1 / 3
Taurine	0 / 1 / 2	-	0 / 1 / 4	0 / 1 / 1
Threonine	2 / 1 / 1	-	1 / 0 / 3	0 / 1 / 3
Tryptophan	1 / 4 / 2	-	0 / 4 / 5	0 / 0 / 3
Tyrosine	2 / 0 / 3	-	0 / 1 / 7	1 / 0 / 4

Urea	1 / 1 / 1	-	0 / 2 / 0	1 / 0 / 0
Uric Acid	0 / 5 / 0	-	1 / 3 / 2	0 / 0 / 1
Valine	0 / 1 / 6	-	0 / 1 / 6	0 / 2 / 2
Xanthine	0 / 0 / 1	-	0 / 1 / 0	0 / 1 / 0
Zinc	2 / 4 / 5	0 / 1 / 0	2 / 4 / 5	-
α-aminobutyric Acid	0 / 1 / 0	-	0 / 1 / 0	0 / 0 / 1

Order of reports: **increases** / **decreases** / unchanged. The number in each box signifies the number of sources for each molecule in each disease; – : indicates where there are no available sources. For a list of all reported analytes, see Supplementary Tables 2-5 (p318–396).

3.2.5. Summary of disease comparisons

A lack of consistency in the level of coverage across the four diseases investigated in this review precluded a full comparison of analyte changes across the spectrum of dementing diseases, from those caused by known genetic mutations such as HD, to those that are most commonly sporadic in form such as AD. In particular, sparse coverage of DLB and HD in comparison to PD and AD suggests areas in which future research may be beneficial. However, it should also be noted that even in more widely-covered diseases, individual analytes are often reported only by a single source, and those that have multiple sources often show discrepancies depending on the cohorts and methodologies used. This observation highlights not only the importance of replication of results, but also how different methods may affect findings in metallomic and metabolomics investigations.

Despite these drawbacks, some interesting consistencies have been revealed. Both increased iron and glucose have been reported across three diseases: AD, PD, and HD (insufficient studies have been published in DLB). Increased glucose is particularly interesting as it appears to occur not only within brain tissue, but also in the blood and CSF of at least AD and PD. Copper has also been consistently reported to be decreased in brain tissues of PD, DLB, and AD cases, with a lack of change observed in HD. Investigations of analytes in biofluids across the four dementias have produced little consistency other than reports of unchanged levels of multiple amino acids; this finding may preclude

development of metal- or metabolite-based biomarkers for application in biofluids, which are usually considered to have better utility for such development due to their accessibility.

In summary, increased glucose, increased iron, and decreased copper in the brain show the best current potential as analytes involved in the pathogenesis of several dementias. Glucose and iron also show potential as *in vivo* biomarkers, as they can be imaged directly in the brain (226, 227). However, such a biomarker would require extensive development to assess whether either of these analytes show a suitable level of sensitivity and specificity for either one or several dementia diseases.

Investigations using brain tissue usually involve the selection of regions traditionally associated with the condition being investigated (for example, the hippocampus in AD or the substantia nigra in PD), which results in more coverage, and the concomitant neglect of other areas. As such, it should prove fruitful to design studies that directly compare a selection of brain regions across AD, PD, HD, and DLB using the same methodologies. The presence of altered analytes across different regions in different dementias may indicate shared pathogenic processes in multiple diseases, with the varied clinical presentations being caused by their respective regional susceptibilities. Not only would this assist in understanding the processes involved in the development of dementia, but may also indicate potential therapeutic targets that could be beneficial across multiple disorders.

3.2.6. Common Findings across Brain Tissue, CSF and Blood

3.2.6.1. Alzheimer's Disease

A total of seventy analytes were reported in at least one matrix in AD, from a total of 92 papers. Of these analytes, 39 were reported in all three matrices (Table 3.5). Six of these analytes showed consistency across both biofluids and brain tissue, including glutamine, isoleucine, leucine, phenylalanine, tryptophan, and tyrosine. However, these molecules generally showed a lack of change in AD, despite some conflicting reports.

The only molecule for which a majority of reports (4/5) indicated increases across multiple matrices was glucose, which was reported to be increased in plasma (185), serum (219), and brain tissue (180, 184); with only a single source reporting no change in brain regions (185). The single source investigating CSF glucose in AD reported no change (208). It is

interesting that one of the few molecules showing consistent change across multiple dementias is also the only one that appears to show consistent change across several matrices within a single dementia, indicating not only the possibility of shared alterations in glucose metabolism across AD, HD, and PD, but also that these alterations may cross the blood–brain-barrier.

Taken together, the data in Table 3.5 show a general lack of consistency between matrices, presumably reflecting the fact that pathological changes occurring within the brain are rarely mirrored in biofluids. However, the few consistent changes may point towards promising peripheral biomarkers, such as increased glucose as discussed. Lowering of reduced glutathione (GSH) in the brain and plasma (228-232) has also been reported in AD, with only one report of no change in plasma (222). Selenium has also been reported to decrease in both brain (167, 168) and blood by three sources (233-235). However, the reports for blood are conflicting, with three and six sources reporting a lack of change in either GSH (222, 236) or selenium (237-240) respectively; further validatory investigations are required to determine whether these changes occur on both sides of the blood–brain-barrier, or whether they are largely confined to the brain itself. If changes are replicable in biofluids, they may have potential as biomarkers for disease incidence or progression. The few reports on CSF measurements of either GSH (241) or selenium (233, 238) observed no change .

In contrast, findings that differ between brain tissue and biofluids may also be informative. Copper was decreased in some brain regions according to four reports (161, 163, 167, 168), whereas one report showed an increase in the frontal cortex (169). Most investigations on biofluids reported increases (235, 239, 242-247) or a lack of change (190, 191, 212, 248-252), although three reports found decreases in blood measurements (234, 253, 254). This may indicate that copper decreases are localised to the brain tissue, whereas increases may be present in the blood, although current data on blood copper levels are too conflicting to be conclusive. As such, although copper may be involved in disease pathogenesis, it may not be suitable for use as a peripheral biomarker. The same could be the case for other molecules where changes are only reported in the brain.

Increases in iron have been reported in seven reports on the AD brain, with only one investigation observing a decrease within the hippocampus (167) in direct contradiction to three reports of an increase in the same region (76, 163, 168). Reports in the blood are conflicting though, with three observing an increase (235, 239), three finding a decrease (247, 248, 254) and nine finding no change (191, 212, 252, 253, 255). The single study looking at the CSF reported no change (191). Given the strength of evidence behind increased iron in AD brains, particularly within the hippocampus, it may be that iron changes are restricted to heavily affected brain regions. As such, they may also have a role in the pathophysiology of the disease, although it is not possible to tell from these data alone whether the changes observed are causative or an effect of the disease course.

Both reports identifying ornithine in the AD brain included here reported a decrease, although in four differing regions (214, 256). Decreases have also been reported in the CSF and blood (219, 257, 258), but the majority of sources observed no change in either of these biofluids (210, 259-261).

Table 3. 5. Number of Analytes Reported in Brain tissues & Biofluids of AD patients

Analyte	CSF	Blood	Brain
Adenosine	0 / 0 / 1	1 / 1 / 0	1 / 1 / 2
Alanine	0 / 0 / 5	1 / 0 / 3	0 / 0 / 3
Arginine	1 / 0 / 6	1 / 1 / 7	1 / 1 / 1
Asparagine	0 / 0 / 3	1 / 2 / 2	0 / 0 / 1
Aspartate	1 / 0 / 1	1 / 1 / 1	0 / 1 / 2
Carnitine	0 / 0 / 2	0 / 1 / 0	0 / 1 / 1
Citrulline	1 / 1 / 2	2 / 0 / 1	0 / 0 / 1
Copper	0 / 0 / 2	6 / 4 / 1	1 / 3 / 2
Creatinine	1 / 1 / 0	1 / 0 / 2	1 / 0 / 1
Ethanolamine	0 / 1 / 1	0 / 1 / 0	0 / 1 / 1
Glucose	0 / 0 / 1	2 / 0 / 0	3 / 0 / 1
Glutamate	1 / 1 / 1	1 / 0 / 2	2 / 3 / 3
Glutamic Acid	0 / 0 / 2	0 / 3 / 2	1 / 0 / 1

Glutamine	0 / 0 / 5	1 / 1 / 7	2 / 0 / 3
Glycine	1 / 1 / 3	2 / 0 / 4	0 / 2 / 2
GSH	0 / 0 / 1	0 / 3 / 2	0 / 2 / 1
GSSG	0 / 0 / 1	2 / 0 / 1	0 / 0 / 1
Hypoxanthine	0 / 0 / 2	1 / 1 / 0	0 / 2 / 3
Iron	0 / 0 / 1	2 / 3 / 5	5 / 1 / 3
Isoleucine	0 / 0 / 6	0 / 1 / 5	0 / 0 / 1
Leucine	0 / 1 / 5	0 / 1 / 6	0 / 0 / 1
Lysine	2 / 0 / 4	1 / 0 / 4	0 / 1 / 1
Manganese	0 / 0 / 1	0 / 1 / 3	1 / 1 / 3
Methionine	1 / 1 / 4	1 / 1 / 4	0 / 2 / 2
Ornithine	0 / 1 / 3	0 / 2 / 4	0 / 2 / 0
Phenylalanine	1 / 1 / 4	1 / 2 / 5	1 / 0 / 1
Potassium	0 / 0 / 1	1 / 0 / 1	1 / 2 / 2
Proline	0 / 0 / 2	2 / 0 / 2	0 / 1 / 1
Selenium	0 / 1 / 2	1 / 5 / 5	0 / 2 / 1
Serine	2 / 0 / 4	0 / 0 / 4	1 / 1 / 1
Taurine	1 / 0 / 5	0 / 1 / 4	0 / 0 / 2
Threonine	1 / 0 / 4	1 / 0 / 3	1 / 0 / 1
Tryptophan	0 / 2 / 6	0 / 3 / 5	1 / 0 / 1
Tyrosine	1 / 0 / 6	0 / 1 / 7	0 / 0 / 1
Urea	0 / 0 / 2	0 / 2 / 0	2 / 0 / 0
Uric Acid	0 / 0 / 3	1 / 3 / 2	0 / 0 / 1
Valine	0 / 1 / 5	0 / 1 / 6	0 / 0 / 1
Xanthine	0 / 0 / 2	0 / 1 / 0	0 / 2 / 2
Zinc	0 / 1 / 0	2 / 4 / 4	3 / 3 / 4

Order of reports is **increases** / **decreases** / unchanged. The number in each box signifies the number of sources for each molecule in each disease; a – indicates where there are no available sources. A list of all reported analytes is presented in Supplementary Table 2 (p318–348). Abbreviations: GSH, reduced glutathione; GSSG, oxidised glutathione.

3.2.1.1. Parkinson's Disease

From a total of 69 papers, 81 out of possible 98 searched-for analytes were reported in at least one PD matrix. Out of these 81, only five have been reported in all matrices investigated here: copper, glucose, iron, manganese, and zinc (a complete list is presented in Supplementary Table 3, p349–371). There are few consistencies across multiple matrices in PD, with only manganese (193, 194, 197, 262, 263) and zinc (192, 264-266) being reported as unchanged by a majority of sources. Manganese was however reported to be decreased in the CSF (197) and increased in the plasma (267) by single reports. Zinc was also reported to be decreased in PD CSF by Sanyal and colleagues (197). There was a higher level of inconsistency within measurements of blood zinc, with three reports of decreases (268-270) and one of an increase (194).

Increased glucose has been reported in the PD cortex (34). There have also been three reports of increases in the CSF (271-273), although one report observed no change (274). Plasma reports observed no change (273, 275) and a single report found decreased glucose in the serum (204).

There are several reports of decreased copper in PD brains, primarily in the substantia nigra (76, 78, 171) but also in the caudate nucleus and locus coeruleus (171). There are also reports of no change in the cortex (76), occipital cortex and frontal gyrus (78), but no such reports for the substantia nigra. CSF copper was largely reported to be unchanged (192-195) although there were two reports of increases (190, 196) and one of decreases (197). Investigations of copper in the blood were conflicting, with four reports of increases (194, 263, 264, 269), six of decreases (194, 197, 265, 266, 270, 276) and one finding of no change (277). As such, biofluid findings aren't conclusive enough to suggest viability of blood copper as a biomarker in PD.

Increased iron was observed in several regions of the brains of PD cases, although this increase was only consistently reported in the substantia nigra (76-81, 278). Increases were also reported in the globus pallidus (278) and putamen (81), but other sources observed no change in these regions (77, 252). No change in the raphe nucleus (77, 252) and caudate nucleus (81, 278) was reported by two sources, and no change was seen in the white

matter (77), cortex (76), cerebellum (278), occipital lobe and frontal gyrus (78). The substantia nigra is one of the regions with the highest α-synuclein load and levels of neuromelanin in the PD brain. Neuromelanin is an iron-chelating pigment that gives the substantia nigra and locus coeruleus their characteristic deep red-brown colouration (279). It is possible that chelation of iron by neuromelanin itself may be related to the observed increases of the metal within the substantia nigra, or even that neuromelanin may interact with and cause accumulation of α-synuclein itself (280). Findings in biofluids were again inconsistent, with both increases (194, 270) and decreases (77, 197, 269) reported in blood, although the majority of sources reported no change (186, 192, 194, 264, 265, 277, 281-283).

Decreases in uric acid have been observed in plasma (186-188), serum (79, 189), and in the brains of males only (181). Decreases in biofluid uric acid have long been linked to PD, with several reports linking decreased uric acid levels to increased risk of developing the disease (186, 217, 284). That decreases have also been reported in the cortex and striatum in males (see Supplementary Table 2B, p324–348, for details of regions) suggests that diminished uric acid levels may not only serve as a potential biomarker, but may also play a role in PD pathogenesis.

3.2.1.2. Dementia with Lewy Bodies

Of the 22 molecules reported in DLB from 11 qualifying sources, only copper, iron, manganese, and zinc were reported in all three matrices, although most only in one report each (see Supplementary Table 4A, p372–373, for full list). Investigations of glucose levels in DLB could not be found for any matrix. A single source reported increased copper and no change in iron, zinc, or manganese in the CSF, and decreased plasma iron and zinc with no change in copper or manganese (198). Decreased copper was reported once in the hippocampus (161) but elsewhere found to have no change (164). Decreased copper has also been reported once in the frontal cortex (164) but unchanged in the amygdala (161). No other molecules suggest themselves as targets for further investigation. Some of the metals identified across all DLB matrices may however lend themselves as possible markers for distinguishing patients with similarly-presenting diseases such as PD and AD. For example, normal levels of blood zinc may help distinguish DLB patients from PD patients

with decreased blood zinc, and unchanged concentrations of copper in the blood may differentiate DLB from AD, where copper is decreased in the blood.

3.2.1.3. Huntington's Disease

Of the 58 analytes reported from 26 qualifying studies, only two, homovanillate and lactate, were reported in brain, plasma, and CSF (a full list is shown in Supplementary Table 5, p378–396). Unlike in other conditions, copper and glucose have been the subject much investigation across different matrices, with the former only covered by single reports in brain tissue (166) and CSF (190), and the latter investigated only in the brain (183) and plasma (216, 285). Iron levels have received some attention in the HD brain (166, 173-176), but has not been covered in other matrices, making comparisons impossible. Plasma homovanillate was reported to be increased by two sources (225, 286) whilst only one source found no change in the brain (287) and CSF (288). Lactate was observed to be increased in the occipital lobe and cerebellum (289), but decreased in plasma (216) and unchanged in CSF (290). As such, increased plasma homovanillate is the only analyte that has been reported consistently by more than one source, and shows most promise as a biomarker for HD. Increased lactate in the brain may play a role in HD pathogenesis but requires validation.

3.2.2. Discussion of Comparisons of Metals and Metabolites in Four Dementias

As in the comparison across multiple dementias, the comparison of matrices within single diseases is limited by sparse coverage of some matrices—particularly serum and CSF. More studies investigating these two in HD and DLB will be required to identify perturbations common across multiple matrices. It is, however, important to note that not all the metabolites and metals covered by this review are likely to be detectable in all matrices. For example, indoleacetate is primarily produced by the breakdown of tryptophan by bacteria in the gut, although it can also be produced endogenously in smaller amounts (291). So although it has been detected in biofluids, such as in the serum of PD patients or CSF of individuals with AD, it is possible that it may not cross the blood–brain-barrier and enter brain tissue (204, 292). Some intermediates in metabolic pathways may be metabolised too quickly to be detectable or may be present in concentrations too low for

current techniques to detect. Additionally, methodologies for accurately detecting these molecules may still be in development, such as that for detection of acetyl CoA using mass spectrometry (293). This precludes the inclusion of some metabolites in 'omics investigations.

AD and PD have received better coverage than either HD or DLB, and this has led to some interesting findings. In particular, the increases in glucose levels reported across several matrices in both of the former. The presence of increased glucose in biofluids suggests potential as an accessible biomarker, and the cerebral findings indicate that glucose accumulation contributes to pathogenesis within the brain in both AD and PD. Indeed, glucose dysregulation and hypometabolism has been repeatedly observed in both diseases (99, 294-296). Both glucose increases and glucose hypometabolism have been reported in HD brains as well (Patassini et al., 2016; Morea et al., 2017), but not in the blood (Nambron et al., 2016; Pena-Sanchez et al., 2015). Even though investigations on glucose levels have not uncovered increases in DLB brains, glucose hypometabolism has also been reported in this condition (297, 298). This contributes to the debate on mechanistic overlaps between different forms of age-related neurodegenerative diseases. Due to the many neuropathological and clinical similarities observed across multiple dementias, it may be that they share some pathological mechanisms, and glucose increases could be one such common molecular perturbation. That these alterations are not only seen in both AD and PD, but across several matrices within both diseases, makes glucose an even more promising marker of pathogenesis. Since glucose can be directly measured *in vivo*, this makes it even more promising as a biomarker both of disease incidence and progression, or even as a prodromal marker (299).

The comparison of findings in PD tissues brought up another interesting metabolite: uric acid. Decreases have been reported across all the blood and brain with no discrepancies between sources (79, 181, 186-189), although levels in CSF have not yet been reported. As such, it may have potential as a biomarker and as a metabolite contributing to the disease process. However, decreases were only observed in male brains and there were no accepted studies in CSF (181). Similar decreases in uric acid were not observed in any other disease, and so it could potentially contribute to a diagnostic panel used to distinguish PD

from other dementias. This could be particularly helpful for DLB, which has a closely similar clinical presentation to PD, but was observed to show increases in uric acid within the brain by the same research group (181). However, investigations of uric acid in DLB are generally lacking, with no qualifying reports in CSF or blood, and only the aforementioned one in brain. Alternatively, if further studies were to find that both PD and DLB show decreases in uric acid, it may be involved in pathogenic processes that result in similar clinical presentations for these two diseases.

Also of interest are analytes that differed between brain and biofluids. Such an analyte may not be particularly useful in the development of biomarkers due to the inaccessibility of brain tissue, but could suggest molecules involved in disease mechanisms. In AD, decreased copper (161, 163, 167-169), GSH (228, 231), selenium (167, 168), and ornithine (214, 256) were all observed in several regions of the brain without concurrent decreases being reported in biofluids. Changes in these molecules appeared to be particularly consistent in regions heavily affected by neurodegeneration, with reductions in all four reported at least once in the hippocampus (161, 167, 168, 228, 229, 256). It would be of interest to determine whether changes in these four analytes reflect alterations in a shared metabolic pathway that may be pathogenic in AD. Indeed, copper, GSH and selenium are all involved in glutathione regulation of oxidative stress. Selenium is a component of glutathione peroxidases, which oxidise GSH to oxidised glutathione (GSSG), possibly lowering GSH-related production of reactive oxygen species (ROS)(300). In contrast, both GSH and GSSG are able to bind copper and regulate its transport, forming complexes which are both capable of generating ROS molecules (301, 302). As such, alterations in GSH, selenium, and copper together could disrupt glutathione-mediated regulation of oxidative stress. Decreased brain copper has not only been observed in AD, but also in PD (76, 78, 171). These reductions were not consistently observed in PD biofluids such as CSF or blood (see Supplementary Table 3A, p349–356).

Increases in iron have been reported in both AD and PD brain tissues, without concurrent increases in biofluid levels (Table 3.5 and 3.6). Both diminished copper and increased iron have been reported within the same heavily-affected regions of the brain in both diseases, suggesting not only a role in pathogenesis, but possibly an interaction between the two

metals themselves. This is further bolstered by reports of copper decreases in DLB brains (161, 164) and both copper decreases (166) and iron increases (174-176) in HD brains. This could indicate a mechanism that is shared across all four diseases, and explain the presentation of similar symptoms. In the case of iron which can be imaged *in vivo* using MRI, there is also the potential for a biomarker of generic dementia – a possibility which is already under investigation in both Alzheimer's and vascular dementia (252, 303, 304). Depending on the outcome of such investigations, iron measurements could potentially be used alongside glucose imaging to identify individuals in the early stages of dementia or those at risk of going on to develop it.

3.3. Discussion of Scientific Findings

This systematic review has highlighted several intriguing findings observed across AD, PD, HD, and DLB, and in different matrices including blood (whole, plasma or serum), CSF, and the brain. These findings are summarised in Figures 3.3 – 3.6. Perhaps the most promising of all are multiple reports of increased glucose both in the brain and biofluids of AD, PD, and HD, making glucose a promising molecule both as a biomarker and as an aetiological molecule. Studies looking into glucose levels in DLB tissues and biofluids would determine whether this disease also shows similar increases. As well as changes in glucose levels, decreases in glucose metabolism are a widely recognised feature of several dementing diseases, with suggestions that resultant increases in glucose provide a link between diabetes and AD (305-308). This could also be the case in PD, which has also been linked to diabetes (309). Hypometabolism of glucose could lead to deficiencies in energy production and mitochondrial function, as well as increased production of ROS; all of these features have been observed in multiple dementing diseases and could contribute to neuronal loss (310).

Uric acid levels have additionally been reported to be decreased in both AD and PD biofluids. Uric acid is an important antioxidant able to scavenge oxygen radicals and stabilise other antioxidant systems (311). However, production of uric acid via the purine catabolism pathway itself produces ROS: conversion of hypoxanthine to xanthine by xanthine oxidase (XO) produces superoxide radicals, and production of uric acid from xanthine by the same enzyme produces hydrogen peroxide (312, 313) (Figure 3.3 – 3.6).

Increases in XO activity have been reported in PD patients (314). This may be linked to reports of increased iron in the PD brain, as iron is a component of XO and has been observed to regulate its activity in cultured lung cells (315). Should XO activity favour the production of xanthine from hypoxanthine rather than uric acid from xanthine, it would result both in increased levels of harmful superoxide radicals and reduced levels of uric acid. However, there is nothing in the published literature to either confirm or refute this.

Hypoxanthine is upstream of uric acid in the purine catabolic pathway, and so diminished hypoxanthine, as observed in PD blood (188, 316, 317), may contribute to the downstream reductions observed in uric acid. Studies looking at the enzymatic activity of xanthine oxidase in PD might help determine which, if any, of those possibilities is correct.

GSH is the oxidised form of glutathione, another antioxidant molecule that neutralises ROS including hydrogen peroxide (318). GSH is oxidised to GSSG as a result of neutralising anti-oxidant species, and an increased GSSG:GSH ratio is considered an indication of oxidative stress (319). Two reviewed papers not only found decreased plasma GSH, but also increased GSSG plasma levels in AD (222, 320). This might suggest that GSH-mediated antioxidative activity has increased in response to oxidative stress. However, there is currently no evidence that GSSG levels increase in the brain itself (228).

Figure 3. 3. Summary of evidence from all reports of altered metals and metabolites in AD brains accepted for this review

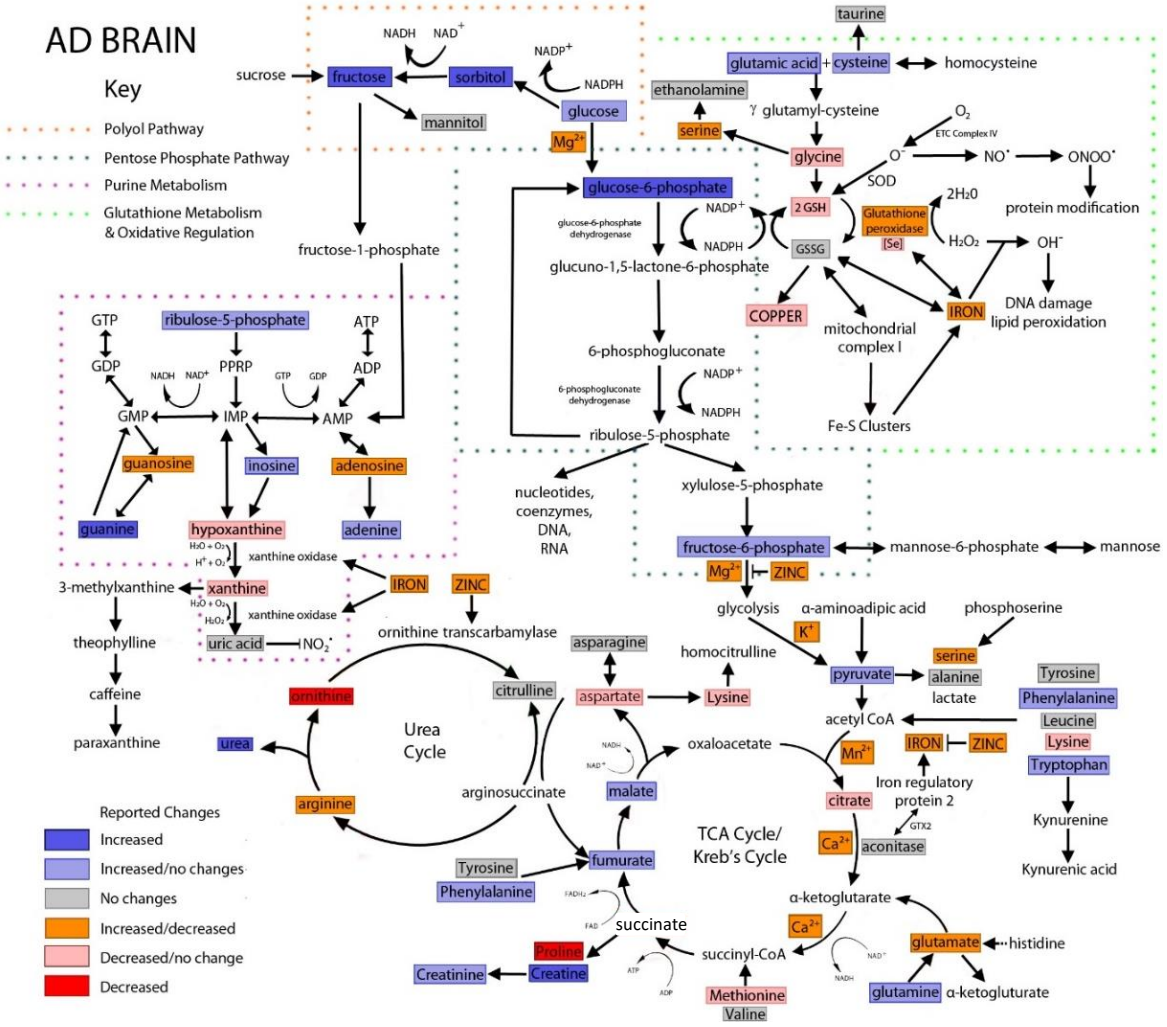

Notable findings include increases in glucose pathway metabolites (particularly the polyol pathway), decreases in metabolites of the purine pathway, and decreases in copper. Reports on many of the metabolites and metals here show high variability between reports, making conclusions difficult to draw. Reports of changes/lack of changes are all equally weighted. Acetyl CoA, acetyl coenzyme A; ADP, adenosine diphosphate; AMP, adenosine monophosphate; ATP, adenosine triphosphate; Ca^{2+}, calcium ion; ETC, electron transport chain; GMP, guanosine monophosphate; GSH, reduced glutathione; GSSG, oxidised glutathione; GTP, guanosine triphosphate; H_2O_2, hydrogen peroxide; IMP, inosinic acid; Mg^{2+}, magnesium ion; K^+, potassium ion; Mn^{2+}, manganese ion; NAD, oxidised nicotinamide adenine dinucleotide; NADH, reduced nicotinamide adenine dinucleotide; NADP, oxidised nicotinamide adenine dinucleotide phosphate; NADPH, reduced nicotinamide adenine dinucleotide phosphate; NO^-, nitric oxide radical; O^-, superoxide radical; OH^-, hydroxide radical; $ONOO^-$, peroxynitrite; PPRP, phosphoribosyl pyrophosphate; Se, selenium; SOD, superoxide dismutase.

Figure 3. 4. Summary of evidence from all reports of altered metals and metabolites in PD brains accepted for this review.

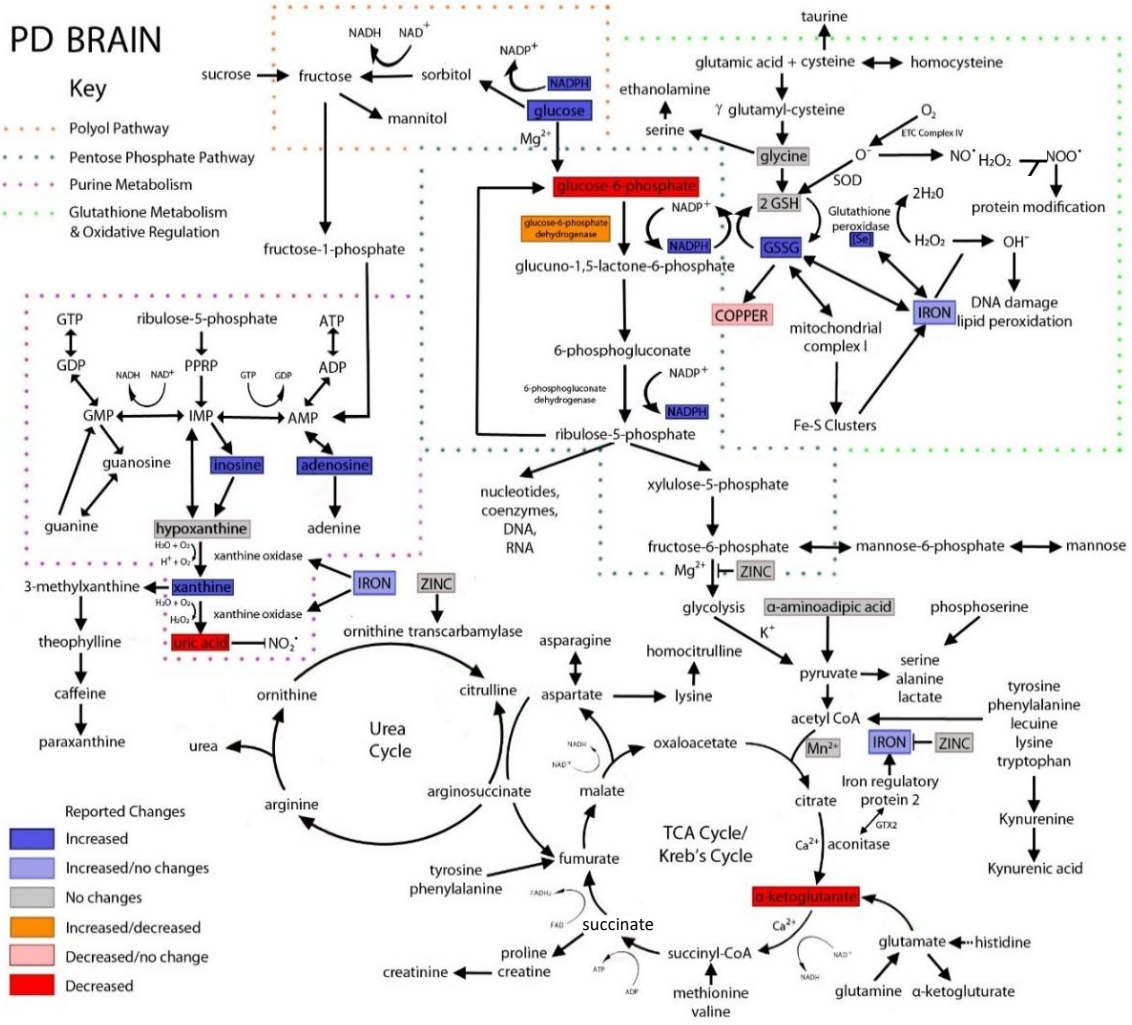

Few consistent findings were identified in reports on PD brains, but there were several reports of increased glucose, increased iron, decreased copper, and increased purine pathway metabolites. Reports of changes/lack of changes are all equally weighted. Acetyl CoA, acetyl coenzyme A; ADP, adenosine diphosphate; AMP, adenosine monophosphate; ATP, adenosine triphosphate; Ca^{2+}, calcium ion; ETC, electron transport chain; GMP, guanosine monophosphate; GSH, reduced glutathione; GSSG, oxidised glutathione; GTP, guanosine triphosphate; H_2O_2, hydrogen peroxide; IMP, inosinic acid; Mg^{2+}, magnesium ion; K^+, potassium ion; Mn^{2+}, manganese ion; NAD, oxidised nicotinamide adenine dinucleotide; NADH, reduced nicotinamide adenine dinucleotide; NADP, oxidised nicotinamide adenine dinucleotide phosphate; NADPH, reduced nicotinamide adenine dinucleotide phosphate; NO^-, nitric oxide radical; O^-, superoxide radical; OH^-, hydroxide radical; $ONOO^-$, peroxynitrite; PPRP, phosphoribosyl pyrophosphate; Se, selenium; SOD, superoxide dismutase.

Figure 3. 5. Summary of evidence from all reports of altered metals and metabolites in DLB brains accepted for this review.

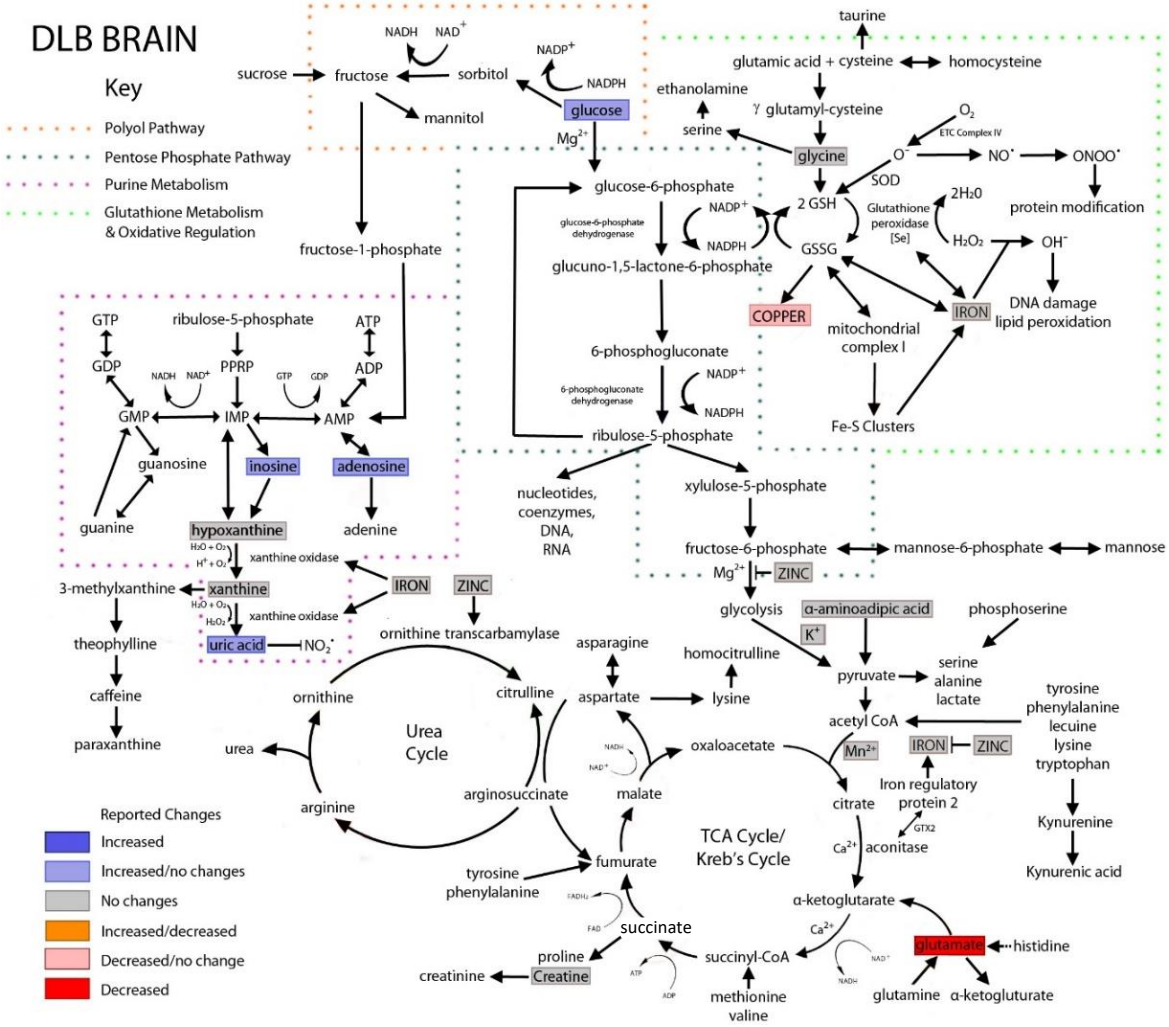

Due to a lack of coverage, few conclusions can be drawn concerning metals and metabolites in the DLB brain, although increases in purine pathway metabolites and glucose have been reported, as well as decreased copper and glutamate. Reports of changes/lack of changes are all equally weighted. Acetyl CoA, acetyl coenzyme A; ADP, adenosine diphosphate; AMP, adenosine monophosphate; ATP, adenosine triphosphate; Ca^{2+}, calcium ion; ETC, electron transport chain; GMP, guanosine monophosphate; GSH, reduced glutathione; GSSG, oxidised glutathione; GTP, guanosine triphosphate; H_2O_2, hydrogen peroxide; IMP, inosinic acid; Mg^{2+}, magnesium ion; K^+, potassium ion; Mn^{2+}, manganese ion; NAD, oxidised nicotinamide adenine dinucleotide; NADH, reduced nicotinamide adenine dinucleotide; NADP, oxidised nicotinamide adenine dinucleotide phosphate; NADPH, reduced nicotinamide adenine dinucleotide phosphate; NO^-, nitric oxide radical; O^-, superoxide radical; OH^-, hydroxide radical; $ONOO^-$, peroxynitrite; PPRP, phosphoribosyl pyrophosphate; Se, selenium; SOD, superoxide dismutase.

Figure 3. 6. Summary of evidence from all reports of altered metals and metabolites in HD brains accepted for this review.

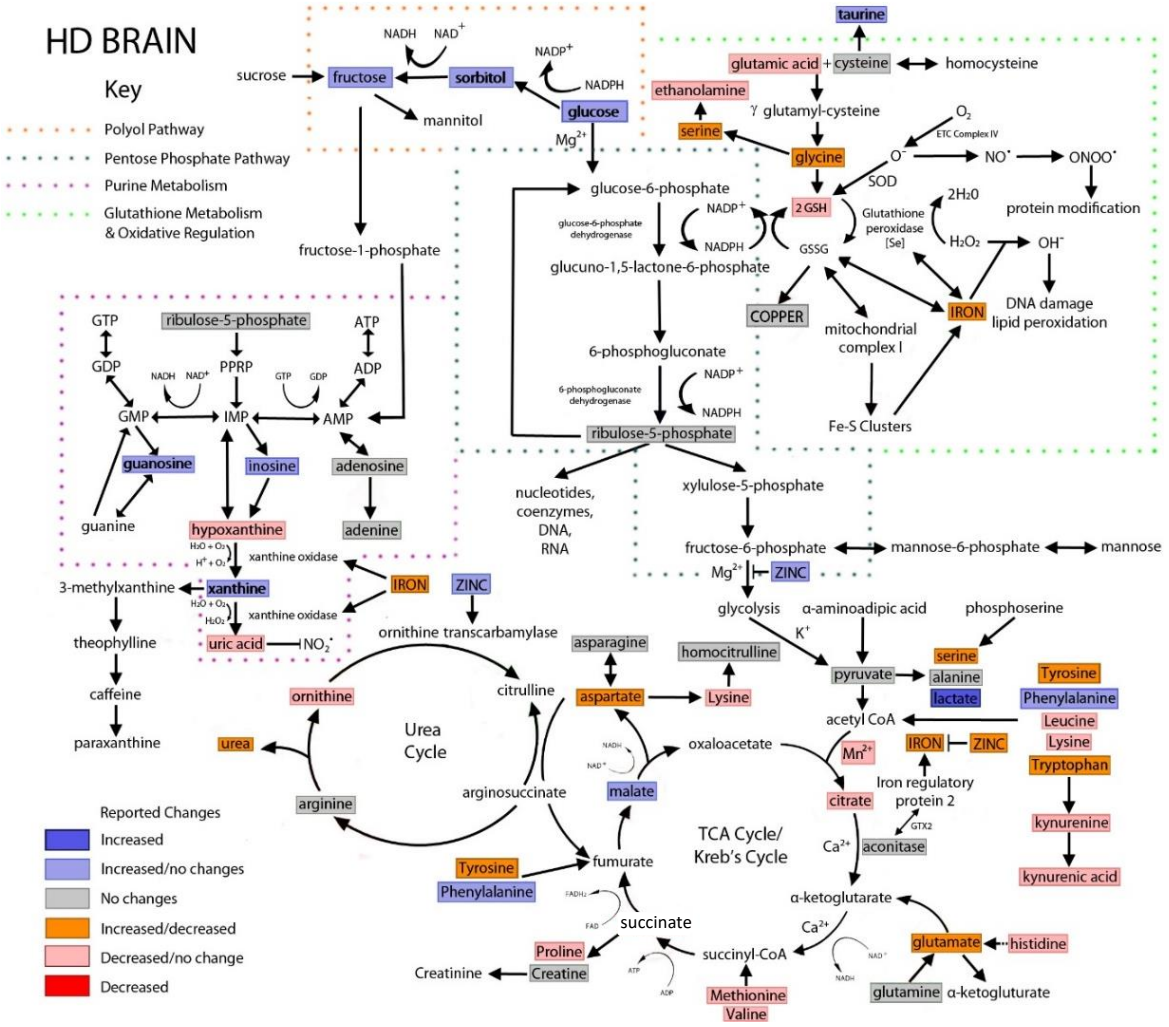

Notable findings in the HD brain include increased polyol pathway metabolites, decreased TCA cycle metabolites, many decreased amino acids, and both increases and decreases in metabolites of the purine pathway. Reports of changes/lack of changes are all equally weighted. Acetyl CoA, acetyl coenzyme A; ADP, adenosine diphosphate; AMP, adenosine monophosphate; ATP, adenosine triphosphate; Ca^{2+}, calcium ion; ETC, electron transport chain; GMP, guanosine monophosphate; GSH, reduced glutathione; GSSG, oxidised glutathione; GTP, guanosine triphosphate; H_2O_2, hydrogen peroxide; IMP, inosinic acid; Mg^{2+}, magnesium ion; K^+, potassium ion; Mn^{2+}, manganese ion; NAD, oxidised nicotinamide adenine dinucleotide; NADH, reduced nicotinamide adenine dinucleotide; NADP, oxidised nicotinamide adenine dinucleotide phosphate; NADPH, reduced nicotinamide adenine dinucleotide phosphate; NO^-, nitric oxide radical; O^-, superoxide radical; OH^-, hydroxide radical; $ONOO^-$, peroxynitrite; PPRP, phosphoribosyl pyrophosphate; Se, selenium; SOD, superoxide dismutase.

As well as regulating the activity of oxidative enzymes such as XO, iron is also able to produce ROS itself via a process called the Fenton reaction, and by doing so can contribute to oxidative stress (321). This is because in the Fenton reaction, hydrogen peroxide is converted into toxic hydroxyl free radicals, with ferrous iron acting as a vital oxidation reagent. Increased iron levels may exacerbate this process, and indeed iron-selective antioxidant probes which target and chelate iron in the mitochondria in order to reduce antioxidant production have been synthesised with the aim of producing a novel therapeutic for AD and PD (322).

The decreases in copper reported in AD, PD, and HD brains may also drive ROS production by iron. Copper is an essential component of ceruloplasmin, a ferroxidase that can oxidase ferrous iron (Fe^{2+}) to less reactive ferric iron (Fe^{3+}), which can then be taken up by transferrin (323, 324). Diminished copper levels could lead to reduced iron chelation, freeing up more iron to participate in ROS production via the Fenton reaction. The observation that copper decreases and iron increases occur within similar regions further supports this (76, 78, 161, 163, 168). Copper is also an important cofactor for several antioxidants, including superoxide dismutase 1 (SOD1) (325). A recent study reported that although SOD1 is effective at preventing oxidative stress in the early stages of AD, its effect diminishes by as much as 90% as tau levels increase (326). If changes in copper also occur during early disease, these changes may be linked to alterations in tau levels and/or the decreased effectiveness of SOD1 as an antioxidant. However, the decreases in SOD1 were observed in CSF rather than brain tissue, so quantification of SOD1 in the brain is required to establish any such associations. Taken together, these findings suggest that not only may decreases in copper lead to increased ROS production, but also to reduced ROS clearance.

As well as its role in antioxidation, copper is also a vital component of cytochrome c oxidase in the mitochondrial electron transport chain (ETC). Cytochrome c oxidase is the last enzyme of the ETC, responsible for converting oxygen to water, and in doing so creating the electrochemical potential by which ATP is synthesised. Reductions in copper may, alongside glucose hypometabolism, contribute to reduced energy production due to mitochondrial dysfunction. Indeed, reduced activity of complex IV of the ETC has been

observed in both AD and PD brains, although not all groups report these findings (47, 327, 328).

Tryptophan, in combination with kynurenine, is involved in the production of vitamin B_3. Vitamin B_3 insufficiency can lead to a condition called pellagra that is characterised by dementia, amongst other symptoms (Prakash et al, 2008) (329). Treatments targeting vitamin B_3, (niacin), or its receptors have been proposed as therapeutic targets in PD, although research is at a preliminary stage and case studies have indicated possible harmful side-effects (330-332).

The changes in glucose, iron and copper observed within the brains of multiple dementias seem to indicate pathogenic mechanisms involving oxidative stress, mitochondrial dysfunction, and decreased energy production in affected regions of the brain, although it is difficult to determine whether these processes are causative or symptomatic based on these observations alone. The ability to image both iron and glucose *in vivo* using MRI should contribute to this discussion by determining whether such changes are apparent in early stages of disease.

In addition to the possibilities for diagnosis and monitoring of non-specific dementia using increased iron and glucose, a simple yet effective biomarker panel using blood samples might be possible to aiding the diagnosis of specific diseases such as decreased hypoxanthine, uric acid, and tryptophan in PD, or reduced GSH in AD. This may be of particular use when clinical symptoms are insufficient to discriminate between two or more dementias. Identification of specific metabolic biomarkers for HD and DLB using blood would make such a panel more viable, but will not be possible without more investigations.

3.3.1. Strengths and Limitations of this Systematic Review

The strengths of this review are the collating of a large number of separate reports, which to the authors' knowledge has not previously been carried out to this extent. This has allowed the identification of similarities and differences between datasets in order to select the most promising to pursue in future experiments. Additionally, strict inclusion and exclusion criteria made the results of experiments performed across different cohorts

with differing methodologies as comparable as possible. An additional strength of a systematic review of this nature is to identify gaps in knowledge, such as the lack of reports about DLB, which therefore requires more attention to further understanding of both DLB itself and to enable comparisons with AD, PD, and HD. Investigations covering these gaps using methods that have already been validated in previous studies could quickly provide useful data to advance our knowledge of these diseases. Additionally, summarised data for multiple molecules enables the identification of pathways that may be affected in one or more conditions. For example, several of the altered metabolites in the four dementias are involved in energy metabolism and antioxidant pathways, suggesting shared mechanisms across diseases.

The inclusion/exclusion criteria employed here are however also a limitation of this review. Data collected from studies correlating analyte levels to disease progression, from comparisons of different dementing diseases without comparison to healthy controls; and from studies grouping diseases together (e.g. PD and DLB into Lewy body diseases), were not included. Such data would be difficult to incorporate into this review, but should be used in tandem to gain the fullest possible picture of current knowledge of metals and metabolites in these four age-related dementias. It was not possible to include longitudinal data, despite their usefulness for identifying biomarker candidates. As such, although the comparisons made here have highlighted potential candidate molecules, they lose the more nuanced information that can be obtained from correlational and longitudinal data. To overcome this limitation, a more in-depth review of longitudinal data can be performed on these candidates to determine their suitability for further study. This would save significant time in contrast to having to undertake an in-depth review of all 91 analytes. Another limitation of this review was that, although papers met a minimum criterion to be included, there was no weighting of papers based on criteria such as a large N number or inclusion of more in-depth patient data. Considering the number of papers involved and the number of criteria assessed, some of which only applied to certain tissues, this would have been infeasible for this review. Having a minimum requirement for inclusion should have negated this issue to a certain extent, but would not completely eradicate it.

3.4. Summary

Although differences in coverage and methodologies in available studies of the metallomes and metabolomes of AD, PD, HD, and DLB can limit comparisons between these diseases, several common findings were identified: glucose elevations in both brain tissue and biofluids of AD, PD, and HD; decreased copper and increased iron in AD, PD, and HD brains; and decreased uric acid in AD and PD biofluids. However, DLB currently suffers from wide gaps in the published literature that preclude a full comparison with the other dementing diseases. Changes in brain analyte levels are often not present in the blood, and vice versa. There are many inter-study differences in individual metabolites reported, and in terms of levels and changes. Larger-scale studies using standardised methods will be required to replicated and extend these findings. In conclusion, this investigation has highlighted perturbations in pathways regulating copper, iron, glucose and purine metabolism that might potentially be part of overlapping pathogenic processes in these age-related dementias, and points to potential biomarkers that could assist in the identification and monitoring of these conditions.

Chapter Four | Evidence that levels of nine essential metals in post mortem human-Alzheimer's-brain and ex-vivo rat-brain tissues are unaffected by differences in post mortem delay, age, disease staging, and brain bank location

This chapter includes data from the publication(101). Following this publication, data from a third brain bank cohort (Newcastle, UK) was collected and are included here. Additional data obtained from wet-weight brain tissues are also included here.

The comparison of multiple dementias in the systematic review indicated several shared perturbations across diseases, including alterations in metals such as decreased copper. However, metals have never been investigated in multi-regional studies of PDD, and so present interesting targets for study and comparison with other neurodegenerative conditions. However, it is of upmost importance that the tissues obtained for analysis of PDD are of sufficient quality to a) produce reliable measurements of metal concentrations in the brain and b) be comparable to previous investigations in order to allow a comparison of multiple dementia diseases. To ascertain this, a pilot study investigating the effect of tissue collection variables on metal and findings in Alzheimer's disease (AD) tissues was performed. Previous studies on AD and Huntington's disease (HD) tissues have been performed using the same methodologies as described here using tissues obtained from New Zealand (168, 180, 183). New Zealand brain donor samples are generally characterised by a lower average age and post mortem delay (PMD) than tissues from the United Kingdom. As such, this pilot study made it possible to determine if UK tissues were suitable for metallomic analysis and comparison with previous studies in AD and HD. This was done by comparing three AD human brain cohorts including the previously analysed New Zealand group(168), as well as two UK-derived cohorts.

4.1. Introduction

4.1.1. Alzheimer's Disease & Human Brain Studies

AD is a neurodegenerative condition characterised by extensive neuronal loss, especially in the cerebral cortex and in certain subcortical regions, for example the limbic system (333-335). The diagnosis of AD requires "the presence of an appropriate AD phenotype (typical or atypical) and a pathophysiological biomarker consistent with the presence of Alzheimer's pathology" (336). Currently, a definitive diagnosis can only be made following *post mortem* investigation, in which extensive deposition of amyloid-β and tau protein in typical regions is recorded (225).

As a disease which primarily affects the brain and which can only be definitively diagnosed at post mortem examination, there are clear advantages to the use of brain tissues to examine mechanisms of AD pathology. Unlike model systems, investigations of the human samples allow direct investigation of affected *ex vivo* tissues taken directly from their individual physiological environment, without isolation from neighbouring cell types or systems. However, there are also several potential limitations to such studies. For example, they can only provide a snapshot of the disease, which makes it difficult to distinguish between causative and down-stream factors. Additionally, experiments are constrained by the limited availability of appropriate brain tissues from both cases and matched controls. Such constraints are not limited to the quantity of samples available, but also potentially by specific potentially-confounding variables including matching for PMD, age, sex, and brain weight, as well as case and control disease staging; these considerations make the achievement of well-matched experimental cohorts challenging.

These variables may differ significantly between jurisdictions, depending on several factors. For example, PMD can be affected by legal constraints that have systematic effects on the timeliness of obtaining consent to collect tissue, meaning that countries with lengthier or more complicated processes can struggle to harvest tissues within short time frames, leading to longer PMDs and hence potentially affecting experimental outcomes and interpretation thereof. Additionally, there may be fewer donations of tissues from cases without dementia, particularly from younger individuals who may not have

considered tissue donation at their time of life. As a corollary, this may limit the availability of Braak stage 0 controls, which in turn may affect studies of dementing diseases if it becomes apparent for example that any pathological changes occur within the lower, pre-symptomatic Braak stages. A smaller quantity of control tissues may also make controlling for age and sex more difficult as it limits availability of suitably matched samples. Finally, there may be true phenotypic differences between cases from different jurisdictions.

Although efforts have been made to standardise tissue collection, processing, and storage practices, there is not yet any formally adhered-to standard for these procedures. Different brain banks (even within the same jurisdiction) may differ in their handling of tissues in many ways such as whether samples are stored whole or immediately dissected, methods of freezing samples, and how quickly the availability of staff and facilities allow tissues to be harvested. Before comparisons between tissues from different locations can be made, it needs to be determined to what degree such variables could affect comparability.

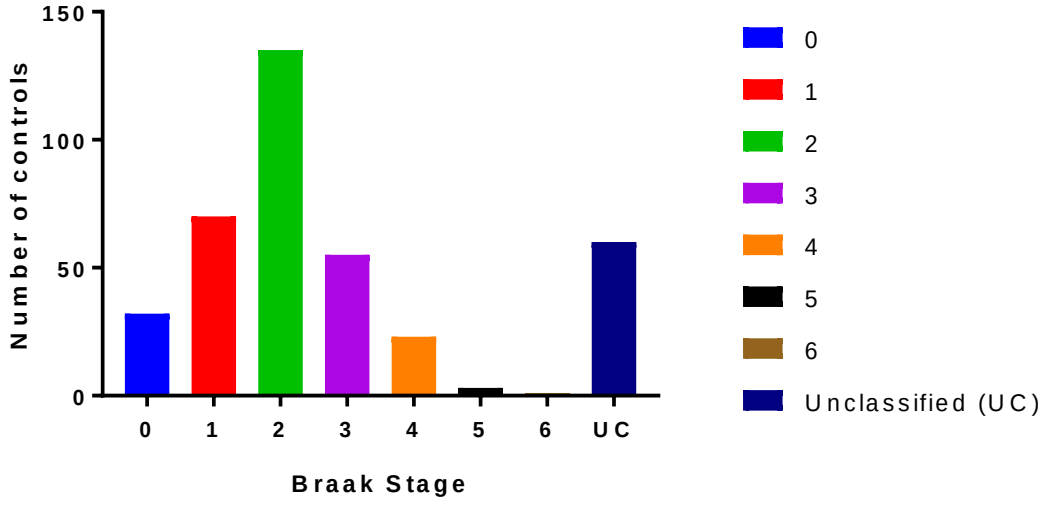

Figure 4. 1. Braak staging of all controls registered on MRC brain bank database

Braak staging of Alzheimer's disease-associated neurofibrillary pathology (hyperphosphorylated tau) in *all* brain-tissue samples listed on the online MRC Brain Bank database as 'controls' or as having 'no abnormality detected.' We studied all relevant brains in the MRC Brain Bank (N = 379) with data collection on 08/01/2019.

4.1.2. Metallomics in the Human Brain

The metallome is a term used to refer to the metal and metalloid species within a cell, tissue, or organism, inclusive of metal-containing biomolecules as well as free metals themselves. This includes essential metals, the roles of which in the development and progression of AD have been under investigation for some time, with those such as Fe, Cu, and Zn implicated in the pathogenesis of the disease (157, 158). Essential metals are those which occur physiologically in tissues and which must be present in adequate amounts to support health and survival. Here we report measurements of essential metals that fall into two groups: the bulk essential metals (Na, K, Ca and Mg), and the essential trace metals (Fe, Zn, Cu, Mn, and Se). Strictly speaking, Se is in fact a metalloid: that is, an element whose chemical properties are intermediate between those of typical metals and non-metals.

This study was designed to investigate the presence and effects of significant variables that might act as potential confounders on levels of essential metals between two brain- bank networks from distinct jurisdictions, the UK MRC brain bank network (Manchester and Newcastle brain banks) and the Neurological Foundation Human Brain Bank (Auckland, New Zealand); the latter has previously provided brain tissues used by our laboratories for metallomic investigations into AD. (159) Here, we conducted investigations using human cingulate gyrus tissue from both AD and non-demented controls from the three brain banks in order to determine the putative effects that variation in matching of age, sex, PMD, and Braak stage may have on tissue-metal concentrations. *Analyses were additionally conducted on wet-weight brain tissue to see if observations looked the same or differed from those carried out on dry-weight tissue.* The potential effects of PMD were further investigated under more controlled conditions using healthy adult rat cortex, hippocampus, and cerebellum by analysing metal concentrations over 0 to 72 hours' PMD. These investigations show that metal levels are not significantly affected by variation in these factors, which therefore did not act as confounders for measurements of essential metals under the conditions studied herein.

4.2. Materials and methods

4.2.1. Reagents

All reagents were purchased from Sigma-Aldrich (UK) unless otherwise stated.

4.2.2. Acquisition of human cingulate gyrus from AD cases and controls

In the current study, we obtained *post mortem* human brain tissue from the cingulate gyrus of cases with AD and non-demented controls from the Manchester Brain Bank (Salford Royal Hospital) and the Newcastle Brain Tissue Resource (University of Newcastle). All samples were taken from flash-frozen, non-fixed brain tissue. The effects of different parameters on the metallomic status of the human cingulate gyrus as a representative brain tissue were compared (see Table 4.2. for comparison of parameters between tissues obtained from the Manchester and Newcastle Brain Banks, and data from our earlier case–control study of brain metals from the New Zealand National Brain Bank in Auckland).[2]

The cingulate gyrus was chosen on the basis of our previous metallomic findings in AD as well as its greater availability than some other tissues (e.g. hippocampus), although the latter manifests greater metallomic perturbations. (161) It has been shown previously by our group that Cu concentrations in cingulate gyrus were significantly lowered in AD as compared to control tissue (mean ± 95% CI, μmol Cu/dry-kg cingulate-gyrus tissue: controls, 346 (264–454); AD cases, 198 (141–280); p = 0.010) in a study based on tissues from the New Zealand National Brain Bank (76) so considered it likely that it would also show informative changes in further case–control contrasts.

4.2.3. Acquisition of rat-brain tissues

Animal experiments were performed in accordance with the U.K. Animal (Scientific Procedures) Act 1986 and related institutional ethics policies, with approval from The University of Manchester's Animal Welfare Ethics Review Body (AWERB).

Cortical and cerebellar tissues were acquired from twenty healthy adult-female and twenty adult-male Wistar Han rats (initial weights ~300-400 g; Charles River, UK). Rats were

terminally anesthetized (2% volume for volume [v/v] isoflurane in oxygen) as previously described. (163) Experimental procedures were designed to replicate methods employed for the acquisition of *post mortem* human-brain tissues by brain banks. After culling, rat carcases were separated into four groups of five males and five females (i.e. 10 per time-point). It was determined *a priori* that, should analytical values not differ between males and females at any time-point, then the two groups would be combined for final analysis. The first group was immediately decapitated by guillotine following culling and whole brains collected to represent zero-hours PMD. The remaining groups were stored at 4°C (to replicate mortuary temperatures) for 24, 48, and 72 hours respectively before respective decapitation and harvesting of brain tissue. After decapitation, samples were stored at -80°C until dissection of the cortex, hippocampus, and cerebellum. Thereafter, dissected brain tissues were stored at -80°C until time of analysis.

4.2.4. Diagnosis & Severity of Human Cases

All cases had a histopathologically-confirmed diagnosis of AD, whereas controls were free from diagnosis of any dementia or other neurodegenerative disorder. Neuropathological severity was determined by assignment of Braak stage (78) to each brain by a consultant neuropathologist. Characteristics of individual cases and controls in the Manchester cohort are shown in Supplementary Table 6 (p397–399), for the Newcastle cohort in Supplementary Table 7 (p400–401), and for the Auckland cohort in Supplementary Table 8 (p402–403). APOE status was also recorded in AD cases and controls, except for a single AD case in the Newcastle cohort for which the APOE status was not known. No significant difference was found in the prevalence of the APOE4 allele, which is associated with increased likelihood of developing AD. Additional data concerning pH of the brain tissue, CERAD score, and cause of death were available and recorded for the Newcastle cohort. These data were unavailable for some of the Manchester cohort, but are recorded where available.

4.2.5. Tissue Dissection

Brain tissue was sectioned into 50 mg (± 5%) samples for ICP–MS using a ceramic scalpel before being placed into 'Safe-Lok' microfuge tubes (Eppendorf AG; Hamburg, Germany)

and stored at -80°C. This scalpel obviated the potential for metal contamination that might otherwise occur with use of a steel blade.

4.2.6. ICP–MS

A detailed description of our ICP–MS metals analysis has been published previously and was performed as described. (164) Briefly, samples were centrifuged before being dried to a constant weight (*dry-weight samples only*) and digested in nitric acid in a heat block. Digestion blanks containing nitric acid but no sample were also processed by the same methods (see Electronic Appendix A, Tables A1 & A3, p2 & 8–9). Samples were stored at 4°C overnight before ICP–MS analysis, which was performed using a 7700x ICP–MS spectrometer (Agilent, Santa Clara, USA) equipped with a MicroMist nebulizer and Scott double-pass spray chamber (Glass Expansion, Melbourne, Australia) and nickel sample and skimmer cones. Serial dilutions of calibration standard were used as multi-element calibration for each batch and periodic quality controls (see Electronic Appendix A, Figures A1 & A2, p5–7 & 11–13). Germanium was used as the internal standard for Zn and Se, with all other elements standardised against scandium.

Operation mode selections, integration times, and internal standard assignments were made according to Agilent's recommendations for the measured elements and samples were introduced using an integrated autosampler (Agilent, Santa Clara, CA, USA). Helium was used as the collision gas with all elements analysed in helium mode (5.0 ml/min helium), with the exception of Se which was analysed in high-energy helium mode due to its state as a polyatomic ion (10 ml/min helium). Limits of detection (LODs), limits of quantitation (LOQs), and background equivalent concentrations (BECs) for each of the measured metals were automatically calculated (see Electronic Appendix A, Tables 2 & 4, p3 & 9).

4.2.7. ICP–MS Data Analysis

Individual values from each sample were normalised to the corresponding wet-weight. For human samples, mean values (±95 % CI) were calculated and significance of intra- and inter-group differences in individual and combined cohorts determined by nonparametric Mann–Whitney U test, as normality of small sample sizes could not be assumed. Case vs

controls and inter-cohort differences in metal levels were analysed individually as interactions between metals were not of interest here, but only the effects of the independent variables. Statistical power of the analyses was then calculated using the DSS Statistical Power and Sample Size Calculators. (Link: https://www.dssresearch.com /resources/calculators/statistical-power-calculator-average/). Following analysis of human tissues, mean values (±95 % CI) of rat samples were calculated and significance of inter- and intragroup differences determined by two-way ANOVA followed by Tukey's multiple comparisons test. This allowed interpretation of any interactions between PMD and brain region affecting metal levels, as identical effects of PMD could not be assumed across different regions. Inter-group differences were analysed individually as interactions between metals were again not of interest for the purposes of this study, but only the effects of PMD and brain region on individual metals. GraphPad v6.04 (Prism; La Jolla, CA) was used to perform Mann–Whitney U calculations and two-way ANOVAs; p-values < 0.05 were considered significant.

4.3. Results

4.3.1. Patient characteristics

Cingulate gyrus tissue was obtained from each brain bank from nine cases diagnosed clinically and neuropathologically with AD and nine controls without a diagnosis of AD or any other form of dementia or neurodegenerative disease.

4.3.2. Cohort comparisons

The characteristics of UK-derived tissues were compared with those from our group's previous case–control study of an Auckland AD cohort (Table 4.2). The Braak staging of controls obtained from both UK cohorts was more advanced than those from the Auckland group (Table 4.2; $p < 0.0001$). This finding is consistent with the older average age at death of the Manchester controls compared to the Auckland controls, although the Newcastle controls were not found to be significantly older. As higher Braak pathology is also found in the brains of healthy aged individuals, it is possible that the lower age at death for the Auckland samples is directly related to the higher availability of Braak stage 0 controls. In

the UK MRC brain bank database, individuals listed as having Braak stage 0 are younger than those with Braak stage I/II pathology in both Manchester (mean age 68 vs 85 years; $p = 1.4 \times 10^{-6}$) and Newcastle (mean age 61 vs 78 years; $p = 8.5 \times 10^{-12}$; see Table 4.2).

Table 4. 1. PMD, Braak stage and age of all brains listed in databases of the Manchester brain bank

Variable	Manchester Samples			Newcastle Samples		
PMD†	82 (4 – 279)[1]			46 (4 – 432)[2]		
	Manchester Brain Bank			Newcastle Brain Bank		
Braak Stage	**0**	**I/II**	**P-Value**	**0**	**I/II**	**P-Value**
Age†	68 (44 – 90)	85 (55 – 103)	1.4×10^{-6}****	61 (18 – 83)	78 (48 – 102)	6.5×10^{-2}****

Values are mean (range). † Data taken from all individuals in database, irrespective of diagnosis. [1]Data obtained from MRC Brain Bank database on 07/06/2019 from 420 cases with available PMD data; data unavailable for 20 individuals. [2] Data obtained from MRC Brain Bank database on 07/06/2019 from 1051 cases with available PMD data; data unavailable for 47 individuals. **** $p < 0.0001$. MRC database does not cover Auckland samples.

Due to the nature of brain tissue collection in the UK, PMDs for both AD cases and controls are significantly longer than those for tissues from Auckland ($p = 0.0001$ and $p < 0.0001$ respectively). Samples with the lowest available PMD were sought from tissues which satisfied the other *a priori*-specified criteria, and PMD was lower than average for both the Manchester and Newcastle brain banks (82 and 46 hours respectively; see Tables 4.1 & 4.2).

Inspecting differences between individual cohorts, the largest variation was between the Auckland and Manchester cohorts, with significant differences in control age ($p = 0.006$; Table 4.2), case and control Braak staging ($p = 0.0046$ and $p < 0.0001$, respectively), as well as case and control PMD ($p < 0.0001$ in both cases). However there was also a significant

difference between Newcastle and Auckland ages in both cases and controls ($p = 0.0055$ and $p < 0.0001$ respectively), and between Newcastle and Manchester control Braak staging ($p < 0.0001$) and PMD in both cases and controls ($p = 0.018$ and $p < 0.0001$, respectively).

It is also important to note that cases and controls in the Manchester cohort were not age-, PMD-, or sex-matched; and that Auckland cases and controls were not PMD-matched (see Supplementary Tables 9–11, p404–406, for cohort characteristics). Although substantive efforts were made to match these characteristics as closely as possible, the limited availability of tissues precluded full matching. These factors could affect the analyses within these groups, and subsequently the comparability of such results between cohorts.

Table 4. 2. Comparison of group characteristics of cohorts from each brain bank

Variable	Manchester Controls	Newcastle Controls	Auckland Controls
Number	9	9	9
Age	89 (82 – 95)	85 (76 – 94)	73 (61 – 78)[a,c]
Male Sex, n (%)	6 (66.7)	6 (66.7%)	7 (53.8)
Braak Stage	I – II	I – II	0[a,c]
PMD (hours)	75 (49 – 130)	25 (9 – 40)[b]	12 (5.5 – 15.0)[c]
Whole-Brain Weight (g)†	1160 (1020 – 1494)	1235 (1064 – 1406)	1260 (1094 – 1461)
Variable	**Manchester Cases**	**Newcastle Cases**	**Auckland Cases**
Number	9	9	9
Age	83 (61 – 89)	83 (70 – 95)	72 (60 – 80)[a]
Male Sex, n (%)	3 (33.3)	6 (66.7%)	5 (55.6)
Braak Stage	IV – V	VI[b]	V – VI[c]
PMD (hours)	39 (12 – 70)	25 (9 – 41)[b]	7 (4.0 – 12.0)[c]
Whole-Brain Weight (g)†	1066 (900 – 1359)	1155 (959 – 1351)	1062 (831 – 1355)

Sample-group characteristics are consistent with properties of brains in each brain bank. Age, male percentage, and PMD are means (range); p-values for significance of between-group differences were calculated by one-way ANOVA followed by Tukey's post hoc test. [a] $p < 0.05$ between Newcastle and Auckland cohorts; [b] $p < 0.05$ between Newcastle and Manchester cohorts; [c] $p < 0.05$ between Manchester and Auckland cohorts.

4.3.3. ICP–MS Metals Analysis

The concentrations of eight essential metals (Na, Mg, K, Ca, Mn, Fe, Cu, Zn) and Se were measured in dry tissue from the cingulate gyrus of nine AD cases and nine controls with no diagnosis of dementia or other brain disease in each cohort. The statistical power and minimum sample size for the metals analyses were then determined. Cingulate gyrus tissue was selected as a region that has previously been found to show changes in metal concentrations in AD and for which samples are widely available in the majority of brain banks.

4.3.3.1. Manchester cohort

K levels were found to be decreased in AD cases compared to the control group ($p = 0.0005$; Table 4.3 and Figure 4.2), as was Cu (Cu; $p = 0.03$) and Se (Se; $p = 0.04$) in the Manchester cohort. There was also a non-significant trend towards decreased Zn (Zn) cases compared to controls ($p = 0.09$).

4.3.3.2. Newcastle cohort

Due to a shortage of available tissue, only a single replicate was performed in this cohort. No significant differences were found between cases and controls (Table 4.3 and Figure 4.2).

4.3.3.3. Comparisons among all three cohorts

Case–control differences in the Auckland and Manchester cohorts were consistent, with significantly decreased K ($p = 0.0005$ and $p = 0.03$, respectively), decreased Cu ($p = 0.03$ and $p = 0.010$, respectively), and decreased Se ($p = 0.004$ and $p = 0.019$, respectively in AD cases versus controls (see Table 4.3 and Figure 4.2). However, no equivalent differences were present in the Newcastle cohort. This could be due to a lack of sufficient tissue to enable repeated measurements, which might have compensated for any unusually high or low measurements that may skew statistical analysis, or could simply be due to real differences between the cohorts. However, when all three cohorts were pooled, the significant differences from the Manchester and Auckland cohorts persisted (see Table 4.3). This suggests that rather than an actual difference between the cohorts, the lack of significant effects observed in the Newcastle cohort may be due to the lower number of

available replicates, resulting in insufficient statistical power to find differences between cases and controls.

This view is supported by comparing the actual metal concentrations across the three cohorts. Where the few significant differences occur, they are almost exclusively between the Manchester and Auckland cohorts (see Table 4.3). There was only one borderline-significant difference observed between the Manchester and Newcastle cohorts in the case of Ca concentrations ($p = 0.046$) and no differences observed between the Newcastle and Auckland cohorts. Taking these observations into account, it seems unlikely that the lack of significant changes observed between Newcastle cases and controls could be due simply to concentrations in the Newcastle cohort being different to those in the other two cohorts.

Power analyses were conducted to determine the statistical power of the experiment as conducted in each separate cohort and with all three cohorts combined (see Table 4.4). As reflected in the table, all of the metals which showed a significant difference between cases and controls (K, Cu, and Se) required an overall minimum sample number of 18 or less in both the Manchester and Auckland cohorts, but not in the Newcastle cohort, suggesting that higher numbers would have been required in this cohort in order to observe significant changes in these same metals. Similarly, every metal but one (Zn) required an overall minimum sample size of 54 or less in the combined cohort. However, the table also shows that a statistical power of 80% or more was only obtained for all three significant metals in the combined cohort, whereas only K reached this threshold in the Manchester cohort, and Cu in the Auckland cohort (power of 99.8% and 84.8% respectively). These observations confirm the need for higher statistical power present in larger cohorts (when they are obtainable). However, only K in the Manchester cohort retained a power of over 80% when the significance level was adjusted to two-σ ($p < 0.01$; data not shown), highlighting the need for selecting sample sizes with adequate statistical power, particularly where effect sizes may be small, but also to avoid wastage of tissues in limited supply.

Figure 4. 2. Dry-weight metal concentrations in the Manchester, Newcastle, and Auckland cohorts

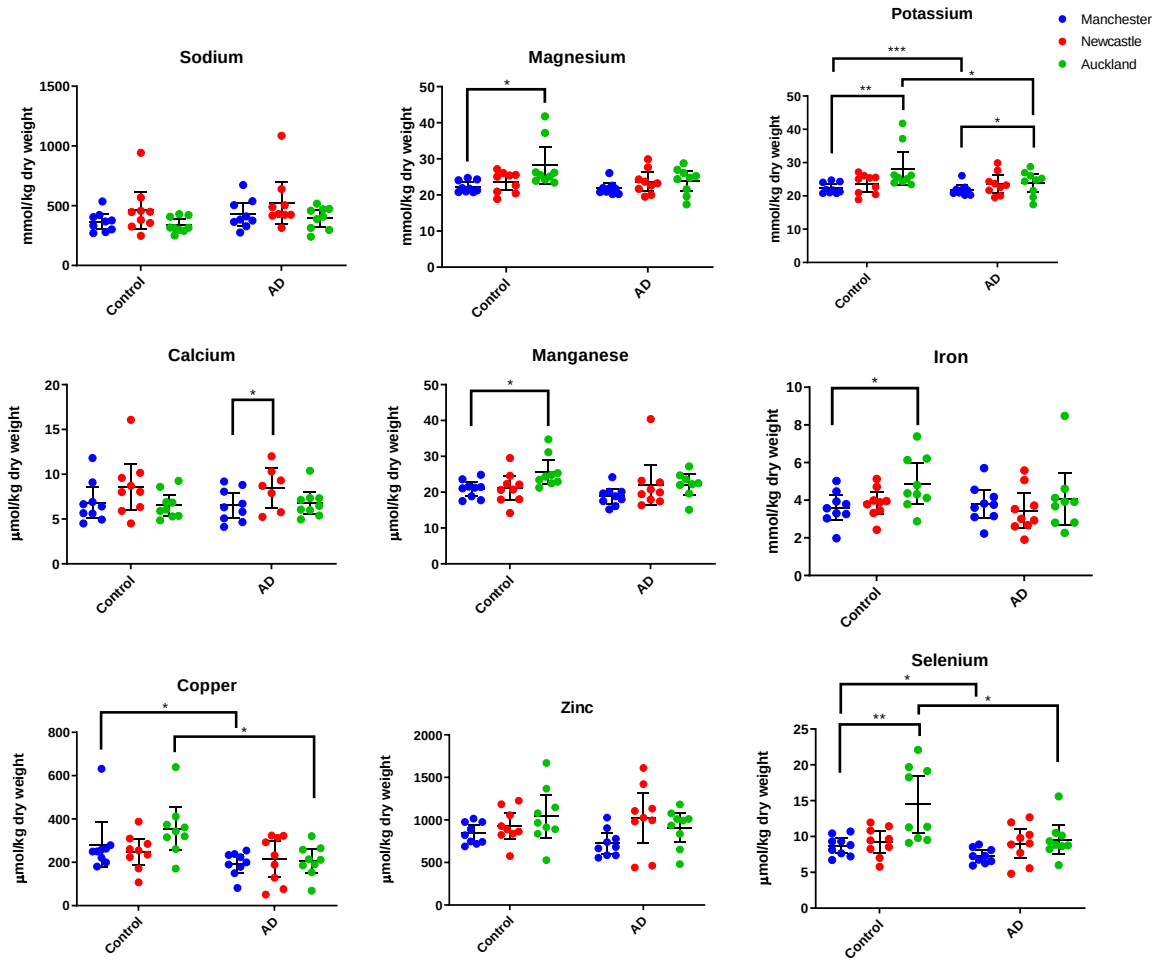

Dry-weight metal concentrations in cingulate gyrus from AD cases (n = 27) and controls (n = 27) in the combined Manchester, Newcastle, and Auckland cohorts. Values are means ± 95% CIs. Values from Auckland and Manchester cohorts are taken from 3 replicate analyses; values from the Newcastle cohort are from a single replicate. Intra- and intergroup p-values determined by two-way ANOVA followed by Tukey's multiple comparisons tests: * $p < 0.05$; ** $p < 0.01$.

Manchester Cohort	Newcastle Cohort				Auckland Cohort				Combined	
Element	**Controls (n = 9)**	**AD Cases (n = 9)**	**P-Value**	**Controls (n = 9)**	**AD Cases n = 9)**	**P-Value**	**Controls (n = 9)**	**AD Cases (n = 9)**	**P-Value**	**P-Value**
Na	**365.9** (301.9 – 429.8)	**428.4** (334.2 – 522.7)	**0.3**	**463.7** (308.7 – 618.7)	**525.5** (350.8 – 700.2)	**0.5**	**338.2** (288.4 – 388.0)	**396.3** (323.9 – 468.7)	**0.2**	**0.09**
Mg	**22.3** (21.0 – 23.5)	**21.8** (20.4 – 23.2)	**0.6**	**23.6** (21.3 – 25.8)	**23.6** (21.0 – 26.2)	**0.9**	**28.2** (23.1 – 33.2)[a]	**23.9** (21.1 – 26.7)	**0.09**	**0.3**
K	**285.9** (271.9 – 299.9)	**240.3** (223.6 – 257.0)	**0.00005**	**318.1** (259.9 – 376.3)	**299.0** (243.6 – 354.5)	**0.7**	**413.8** (320.7 – 506.8)[a]	**305.7** (260.8 – 350.7)[a]	**0.03**	**0.007**
Ca	**6.8** (5.1 – 8.6)	**7.9** (3.8 –	**1**	**8.6** (6.0 –	**12.4** (6.1 –	**0.4**	**6.6**	**6.8**	**0.7**	**0.8**

		12.1)		11.2)	18.6)[b]		(5.4 – 7.7)	(5.6 – 8.0)		
Mn	**20.9** (19.0 – 22.8)	**18.9** (16.8 – 20.9)	**0.1**	**21.1** (17.8 – 24.5)	**22.0** (16.4 – 27.6)	**0.8**	**25.6** (22.2 – 29.0)[a]	**26.8** (15.7 – 37.9)	**0.9**	**0.1**
Fe	**3.6** (2.9 – 4.3)	**3.8** (3.0 – 4.5)	**0.7**	**3.8** (3.2 – 4.4)	**3.4** (2.5 – 4.4)	**0.3**	**4.9** (3.8 – 6.0)[a]	**4.1** (2.7 – 5.5)	**0.2**	**0.3**
Cu	**281.5** (177.7 – 385.4)	**194.3** (153.3 – 235.3)	**0.03**	**248.5** (187.1 – 309.9)	**214.4** (131.3 – 297.4)	**0.8**	**365.4** (265.1 – 465.6)	**213.5** (156.3 – 270.7)	**0.0101**	**0.0011**
Zn	**841.9** (745.3 – 938.5)	**724.8** (603.3 – 846.2)	**0.09**	**931.2** (777.7 – 1084.7)	**1019.8** (724.9 – 1314.6)	**0.4**	**1044.5** (792.1 – 1296.9)	**908.9** (740.1 – 1077.6)	**0.4**	**0.2**
Se†	**8.7** (7.6 – 9.8)	**7.3**	**0.04**	**9.2** (7.6 –	**9.0** (6.9 –	**1**	**14.5** (10.5 –	**9.6** (7.6 –	**0.019**	**0.006**

	(6.5 – 8.1)		10.8)	11.0)	18.5)[a]	11.6)

Table 4. 3. Comparison of group characteristics of cohorts from each brain bank

Dry-weight metal concentrations are means (±95% CI); p-values for significance of case vs control differences were calculated by Mann–Whitney U test of AD and control brain sample measurements. Values taken over 3 replicate runs for Manchester and Auckland cohorts; 1 replicate run for the Newcastle cohort. Na, Mg, K, Ca, and Fe are measured in mmol per kg dry tissue; Mn, Cu, Zn, and Se are measured in µmol per kg dry tissue. P-values for significance of between-cohort differences were calculated by one-way ANOVA followed by Tukey's post hoc test of dry-weight Manchester and Auckland brain sample measurements; [a] significant difference ($p < 0.05$) between Newcastle and Auckland cohorts; [b] significant difference ($p < 0.05$) between Newcastle and Manchester cohorts. † P-value of between-cohort differences calculated by Kruskal-Wallis test followed by Dunn's multiple comparisons test due to unequal variance as determined by Brown-Forsythe's *post hoc* test.

Table 4. 4. Power analysis of individual and combined cohorts

Element	Manchester Cohort (N = 9 v 9)	Newcastle Cohort (N = 9 v 9)	Auckland Cohort (N = 9 v 9)	Combined Cohorts (N = 27 v 27)
Statistical Power ($p < 0.05$)				
Na	24.5	9.4	32.5	50.9
Mg	9	5	39.5	44.6
K	**99.8**	8.5	66.3	**88.7**
Ca	6.2	25.3	5.8	35.4
Mn	38.7	6.2	5.6	34.2
Fe	7.2	13.4	17.4	25.9
Cu	43.7	11.9	**84.8**	**89.4**
Zn	41.4	9.4	17.6	13.9
Se	67.8	5.5	70.2	**84.1**
Sample Size Required ($p < 0.05$)				
Na	**15**	65	**11**	**19**
Mg	71	21591	**8**	**22**
K	**1**	82	**4**	**7**
Ca	226	**15**	348	**29**
Mn	**9**	240	482	**30**
Fe	129	35	24	**29**
Cu	**8**	42	**3**	**7**
Zn	**8**	65	23	98
Se	**4**	520	**4**	**8**

Test of statistical power for individual and combined-cohort metal concentrations in dry-weight cingulate gyrus tissue. Values highlighted in bold satisfy statistical power minimum requirement of 80% or sample size required of ≤ 18 in individual cohorts or ≤ 54 in combined cohort. Values determined using the DSS Statistical Power and Sample Size Calculators. Link: https://www.dssresearch.com/resources/calculators/statistical-power-calculator-average/.

4.3.3.4. MANCOVA analysis

A multivariate analysis of covariance (MANCOVA) was carried out on the combined results from all three cohorts (N = 54) in order to determine the effects of patient and *post mortem* variables on the findings. It was not possible to conduct this on individual cohorts due to the insufficient numbers. An initial MANCOVA was performed using the nine metals as dependent variables (DVs); cohort, sex, and disease status as independent variables (IVs); and age, Braak staging, and PMD as covariates (CVs).

The multivariate analysis of all nine metals revealed a significant contribution of status (AD vs control; Wilks' $\Lambda = 0.579$; $F[9,31] = 2.503$; $p = 0.028$) and Braak staging (Wilks' $\Lambda = 0.569$; $F[9,31] = 2.609$; $p = 0.023$) on differences in metal concentrations within the combined cohort (see summary in Table 4.5). No other variables were found to be significant, including PMD. This suggests that while Braak staging had an effect on metallomic findings, PMD did not. It should be noted that the effect of Braak staging was not strong enough to prevent replication of findings in the two control cohorts with significant differences in Braak staging (i.e. the Manchester and Auckland cohorts).

Table 4. 5. Table of MANCOVA analysis of combined-cohort metal concentrations

Effect	Wilks' Lambda (Λ)	F	P-Value	Significance
Intercept	0.082	38.763	0.0	-
Age	0.844	0.635	0.8	NS
Braak	0.569	2.609	0.02	*
PMD	0.702	1.461	0.2	NS
Status	0.579	2.503	0.03	*
Cohort	0.475	1.553	0.1	NS
Sex	0.860	0.559	0.8	NS
Status * Cohort	0.477	1.543	0.1	NS
Status * Sex	0.716	1.369	0.2	NS
Cohort * Sex	0.613	0.954	0.5	NS
Status * Cohort * Sex	0.612	0.958	0.5	NS

Design: Intercept + Age + Braak + PMD + Status + Cohort + Sex + Status + Status * Cohort + Status * Sex + Cohort * Sex + Status * Sex * Cohort. * $P < 0.05$; NS = not-significant

The tests of between-subjects effects showed that K (F[14,39] = 3.713; p = 0.001), Cu (F[14,39] = 2.349; p = 0.018), and Se (F[14,39] = 3.592; p = 0.001) remained statistically significant following correction for IVs and CVs (see Table 4.6). Mg (Mg) also became significant (F[14,39] = 2.018; p = 0.042) in the corrected model. No other metals were found to be significant in the corrected model.

A significant interaction between Braak stage and K (F[1,39] = 9.573; p = 0.004) and Zn (F[1,39] = 5.163; p = 0.029) concentrations was observed, as well as a possible interaction with Cu concentrations (F[1,39] = 3.969; p = 0.053). There were additional significant interactions between K concentration and status (F[1,39] = 8.859; p = 0.005), status * cohort (F[2,39] = 3.897; p = 0.029), and cohort * sex {F[2,39] = 3.534; 0 = 0.039). Cohort * sex also had significant interactions with Cu (F[2,39] = 2.503; p = 0.032), and status * cohort * sex had significant interactions with Fe (F[2,39] = 4.771; p = 0.014) and Se (F[2,39] = 3.486; p = 0.04) concentrations. There were no other significant interactions.

These results suggest an effect of Braak staging, status, cohort, and sex on K; Braak staging, cohort, and sex on Cu; Braak staging on Zn; and status, cohort, and sex on Fe and Se concentrations. No individual IV or CV was found to have a significant interaction with Na, Ca, or Mn. No significant interactions were found for Mg either, despite its significance level in the corrected model. This suggests that changes in Mg are only significant when all variables are taken into account together.

Table 4. 6. Table of significant and borderline findings in tests of between-subjects effects of combined- cohort metal concentrations

Source	DV	Type III Sum of Squares	F	P-Value	Significance
Corrected Model	Mg	0.099	2.018	0.04	*
	K	0.380	3.713	0.001	**
	Cu	1.043	2.349	0.02	*
	Se	0.549	3.592	0.001	**
Braak stage	K	0.070	9.573	0.004	**
	Cu	0.126	3.969	0.053	NS
	Zn	0.076	5.163	0.03	*
Status	K	0.065	8.859	0.005	**
Status * Cohort	K	0.057	3.897	0.03	*
Cohort * Sex	K	0.052	3.534	0.04	*
	Cu	0.239	2.503	0.03	*
Status * Cohort * Sex	Fe	0.147	4.771	0.014	*
	Se	0.076	3.486	0.04	*

* $P < 0.05$; ** $p < 0.01$; NS = not-significant.

4.3.4. Wet-weight Tissue

Essential metal concentrations were also measured in wet-weight tissue from the Auckland and Manchester cohorts, in a single run each, to see if observations were consistent with analyses of dry-weight tissue. There were not sufficient quantities of the Newcastle tissues to include in this analysis.

4.3.4.1. Manchester Cohort

Significantly increased Na was observed in AD cases from the Manchester cohort ($p = 0.0016$; see Figure 4.3 and Table 4.7), as well as significantly decreased K ($p = 0.03$) and Mn ($p = 0.02$). There was a trend towards decreased Se in cases, but this was not significant ($p = 0.08$).

4.3.4.2. Auckland Cohort

Significantly increased Na was also found in Auckland cases ($p = 0.016$; see Figure 4.3 and Table 4.7), but neither decreased K or Mn were observed. There was however a significant decrease in Se ($p = 0.009$) in cases.

4.3.4.3. Comparisons between Cohorts

There were some differences observed between cases and control between the two cohorts. In cases, Mg levels ($p = 0.0033$; see Figure 4.3) and Mn levels ($p = 0.0164$) were significantly higher in the Auckland cohort. Auckland controls also showed increased Fe ($p = 0.047$), Cu ($p = 0.048$), Zn ($p = 0.019$), and Se ($p = 0.0007$) compared to Manchester controls, although differences in Fe and Cu were of borderline significance. The differences observed in control Se levels and Mn case levels between cohorts may contribute to significant case–control differences being present in only one cohort for each of these metals.

Interestingly, when data from both the Manchester and Auckland cohorts were combined into a single cohort (see Table 4.7), a significant decrease in Cu was observed in cases ($p = 0.004$), as well as increased Na ($p < 0.0001$), and decreased K ($p = 0.009$) and Se ($p = 0.004$). As such, all three significant differences observed in AD dry-weight tissues (decreased K,

Cu, and Se) are present in wet-weight tissues when both Manchester and Auckland cohorts are combined. However, this is not the case in individual cohorts.

The only finding that was consistent across individual cohorts and the combined cohort in wet-weight tissues was significantly increased Na in cases ($p < 0.0001$ in combined cohort). This was not observed in dry-weight tissues, although there was a non-significant trend in the combined cohort ($p = 0.09$; see Table 4.3). As such it appears that Na levels may be sensitive to the drying process.

Figure 4. 3. Wet-weight metal concentrations in the Manchester and Auckland cohorts

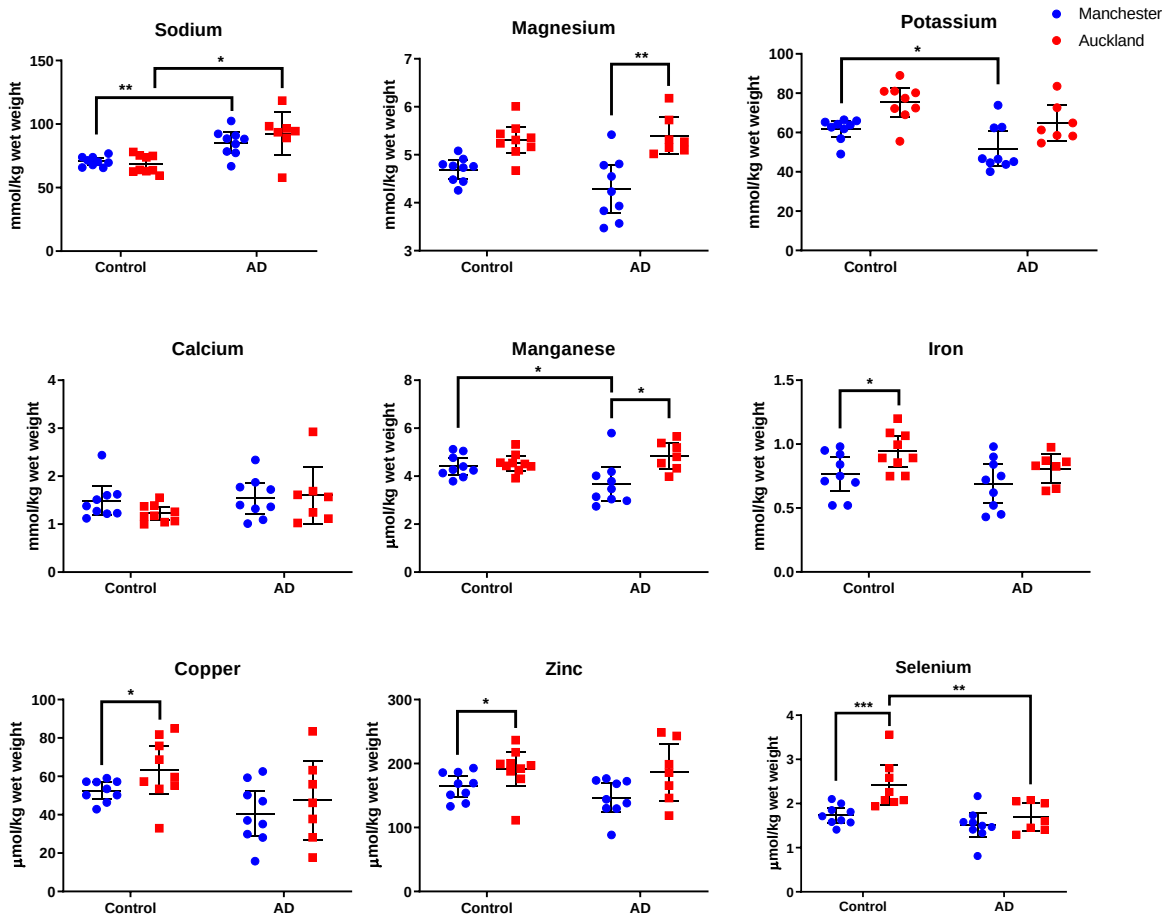

Wet-weight metal concentrations in cingulate gyrus from AD cases (n = 16) and controls (n = 18) in the combined Manchester and Auckland cohorts. Values are means ± 95% CIs. Values are taken from single replicates. Intra- and intergroup p-values determined by Mann–Whitney U test. * $p < 0.05$; ** $p < 0.01$, *** $p < 0.001$.

Table 4. 7. Essential metal concentrations in wet cingulate gyrus tissue from the Manchester, Auckland, and combined cohorts

	Manchester Cohort			Auckland Cohort			Combined
Element	**Controls (n = 9)**	**AD Cases (n = 9)**	**P-Value**	**Controls (n = 9)**	**AD Cases (n = 9)**	**P-Value**	**P-Value**
Na	**70.6** (68.1 – 73.1)	**85.5** (78.8 – 92.2)	**0.002**	**68.3** (63.7 – 72.9)	**92.6** (79.3 – 105.9)	**0.016**	**<0.0001**
Mg	**4.7** (4.5 – 4.9)	**4.3** (3.9 – 4.7)	**0.2**	**5.3** (5.1 – 5.5)	**5.4** (5.1 – 5.7)	**1.0**	**0.6**
K	**61.8** (58.2 – 65.4)	**51.8** (44.2 – 59.3)	**0.03**	**75.3** (69.1 – 81.6)	**64.8** (57.3 – 72.3)	**0.1**	**0.009**
Ca	**1.5** (1.2 – 1.7)	**1.5** (1.3 – 1.8)	**0.7**	**1.2** (1.1 – 1.3)	**1.6** (1.1 – 2.1)	**0.2**	**0.2**
Mn	**4.4** (4.1 – 4.7)	**3.7** (3.1 – 4.3)	**0.02**	**4.5** (4.3 – 4.8)	**4.8** (4.4 – 5.3)	**0.4**	**0.3**
Fe	**0.8** (0.7 – 0.9)	**0.7** (0.6 – 0.8)	**0.4**	**0.9** (0.8 – 1.0)	**0.8** (0.7 – 0.9)	**0.09**	**0.08**
Cu	**52.6** (49.0 – 56.3)	**40.6** (30.5 – 50.6)	**0.2**	**63.3** (52.6 – 74.0)	**47.5** (31.0 – 64.0)	**0.2**	**0.02**
Zn	**164.4** (150.2 – 178.6)	**146.8** (127.8 – 165.8)	**0.2**	**190.9** (168.3 – 213.5)	**186.7** (151.1 – 222.3)	**0.8**	**0.2**
Se†	**1.7** (1.6 – 1.9)	**1.5** (1.3 – 1.7)	**0.08**	**2.4** (2.1 – 2.8)	**1.7** (1.4 – 1.9)	**0.009**	**0.004**

Wet-weight metal concentrations are means (±95% CI); p-values for significance of case vs control and inter-cohort differences were calculated by Mann–Whitney U test of AD and control brain sample measurements. Values taken over single replicate runs for both cohorts. Na, Mg, K, Ca, and Fe are measured in mmol per kg dry tissue; Mn, Cu, Zn, and Se are measured in µmol per kg dry tissue.

4.3.5. Effect of *post mortem* delay on metallomic analysis of *ex-vivo* rat-brain tissues

The concentrations of nine essential elements: Na, Mg, K, Ca, Mn, Cu , Fe, Zn, and Se were measured in the cerebral cortex, cerebellum, and hippocampus of forty healthy adult Wistar Han rats with PMDs of 0, 24, 48, and 72 hours.

The effects of PMD and brain region on metal concentrations were determined by two-way ANOVA. PMD was found to have a significant effect on Na ($F [3, 107] = 5.905$, $p = 0.0009$; see Table 4.8), K ($F[3, 107] = 6.117$, $p = 0.0007$), Mn ($F[3, 107] = 4.014$, $p = 0.0095$), and Cu ($F [3, 104] = 4.264$, $p = 0.007$). Effects of PMD on these metals accounted for 13.3%, 10.3%, 4.4%, and 9.9% of variation in these metal concentrations respectively. However, multiple comparisons tests found only one significant difference in metal concentrations between different PMD groups within the same brain region; with 48-hour PMD cerebellar Ca being significantly lower than 72-hour PMD cerebellar levels ($p = 0.04$; see Table 4.9).

Brain region was shown to have a significant effect on the following: Mg ($F[2, 107] = 11.75$, $p < 0.0001$; see Table 4.8); K ($F[2, 107] = 24.84$, $p < 0.0001$); Ca ($F[2, 94] = 5.003$, $p = 0.009$); Mn ($F[2, 107] = 76.37$, $p < 0.0001$); Fe ($F[2, 106] = 10.98$, $p < 0.0001$); Zn ($F[2, 106] = 43.88$, $p < 0.0001$); and Se ($F[2, 107] = 10.69$, $p < 0.0001$). Brain region accounted for 17.4%, 27.8%, 8.1%, 55.3%, 16.2%, 43.7%, and 15.6% of variation in concentrations of these metals respectively. No significant effect of brain region was found on either Na or Cu. *Post hoc* multiple comparisons tests also found multiple significant differences between metal concentrations among regions, particularly for K, Mn, and Zn (see Table 4.8). K and Zn levels were lower in the cerebellum than in the cortex or hippocampus, and Mn levels were lower in the cortex than in the hippocampus or cerebellum (see Table 4.9 and Figure 4.4).

As such, PMD appears to have small effects on Na, K, Mn, and Cu levels, and brain region appears to have an effect on K, Mn, and Zn, as well as smaller effects on Mg, Ca, Fe, and Se.

Table 4. 8. Two-way ANOVA analysis of essential metals in three rat-brain regions

Metal	Interaction		Region		PMD	
	P- Value	% Variation	P-Value	% Variation	P- Value	% Variation
Na	0.2	6.6	0.9	0.06	0.0009	13.3
Mg	0.7	2.9	<0.0001	17.4	0.9	0.5
K	0.7	1.9	<0.0001	27.8	0.0007	10.3
Ca	0.04	11.4	0.009	8.1	0.07	6
Mn	0.5	2	<0.0001	55.3	0.0095	4.4
Fe	0.9	1.7	<0.0001	16.2	0.2	3.6
Cu	0.2	6.4	0.1	3.5	0.007	9.9
Zn	0.7	1.9	<0.0001	43.7	0.2	2.4
Se	0.7	2.8	<0.0001	15.6	0.2	3.9

P-values determined by two-way ANOVA followed by Tukey's *post hoc* multiple comparisons tests

Metal	Cortex				Hippocampus				Cerebellum			
	0 Hours PMD	24 Hours PMD	48 Hours PMD	72 Hours PMD	0 Hours PMD	24 Hours PMD	48 Hours PMD	72 Hours PMD	0 Hours PMD	24 Hours PMD	48 Hours PMD	72 Hours PMD
Na	**232.1** (202.6 – 271.6)	**248.7** (219.2 – 278.3)	**264.1** (227.3 – 301.0)	**269.7** (252.3 – 287.1)	**234.1** (202.8 – 265.4)	**244.9** (225.5 – 264.2)	**272.3** (238.1 – 306.5)	**272.0** (255.5 – 288.5)	**230.5** (213.4 – 247.5)	**274.3** (241.6 – 307.0)	**236.2** (216.0 – 256.4)	**274.2** (245.3 – 303.0)
Mg	**30.6** (27.3 – 34.0)	**28.9** (25.5 – 32.2)	**28.8** (26.3 – 31.3)	**29.6** (27.0 – 32.2)	**33.5** (29.1 – 38.0)	**31.5** (29.0 – 34.0)	**33.5** (29.2 – 37.8)	**32.1** (30.3 – 33.9)	**26.5** (25.0 – 28.0) [e, g]	**28.2** (24.9 – 31.5)	**28.7** (26.1 – 31.3)	**28.7** (24.1 – 33.3)
K	**467.4** (409.1 – 525.7)	**446.6** (386.3 – 502.9)	**424.2** (385.7 – 462.8)	**406.6** (384.7 – 428.5)	**502.6** (438.8 – 566.3)[d]	**460.9** (424.1 – 497.6)	**466.6** (417.7 – 515.5)	**440.1** (414.8 – 465.5)	**397.6** (367.8 – 427.4)[e]	**383.1** (340.4 – 425.8)[a, d, e]	**403.6** (374.9 – 432.3)[c, e]	**338.0** (310.3 – 365.6)[a, b, e, f, g ,h]
Ca	**5.1** (3.1 – 7.1)	**4.7** (2.7 – 6.7)	**5.2** (4.0 – 6.3)	**5.6** (4.1 – 7.2)	**5.7** (4.8 – 6.5)	**5.4** (4.8 – 6.0)	**6.2** (5.4 – 6.9)	**5.8** (5.4 – 6.3)	**5.4** (4.8 – 6.1)	**8.0** (5.6 – 10.4)	**5.7** (4.2 – 7.2)	**8.1** (6.2 – 10.0) [b, c, i]
Mn	**25.5** (23.2 – 27.8)	**26.7** (24.4 – 29.0)	**23.8** (21.9 – 27.7)	**22.1** (20.1 – 24.0)	**41.1** (36.1 – 46.1)[a, b, c, d]	**36.8** (32.8 – 40.7)[a, b, c, d]	**41.0** (36.9 – 45.1)[a, b, c, d]	**35.4** (32.1 – 38.8)[a, b, c, d]	**34.5** (31.8 – 37.2) [a, b, c, d]	**35.9** (31.4 – 40.4) [a, b, c, d]	**35.2** (32.7 – 37.7) [a, b, c, d]	**31.9** (28.9 – 35.0) [a, d, e, g]
Fe	**1.5** (1.3 – 1.7)	**1.4** (1.2 – 1.7)	**1.5** (1.3 – 1.7)	**1.3** (1.1 – 1.5)	**1.5** (1.3 – 1.7)	**1.6** (1.4 – 1.7)	**1.7** (1.5 – 1.9)	**1.5** (1.4 – 1.6)	**1.8** (1.5 – 2.0)[d]	**1.7** (1.4 – 1.9)	**1.9** (1.7 – 2.0)[d]	**1.7** (1.5 – 1.9)

Cu	**160.2** (141.9 – 178.5)	**156.0** (137.7 – 174.3)	**167.3** (142.4 – 192.2)	**151.0** (144.1 – 157.9)	**180.9** (152.0 – 209.7)	**168.4** (156.3 – 180.5)	**175.6** (158.7 – 192.5)	**157.6** (146.0 – 169.2)	**176.7** (148.3 – 205.2)	**189.9** (145.9 – 234.0)	**151.0** (134.5 – 167.4)	**135.6** (121.4 – 149.9)[e]
Zn	**1044.8** (924.4 – 1165.2)	**1057.4** (937.0 – 1177.8)	**985.9** (866.5 – 1105.2)	**982.6** (919.1 – 1046.0)	**952.0** (842.8 – 1061.2)	**927.2** (812.8 – 1041.5)	**986.6** (858.7 – 1114.6)	**913.0** (854.2 – 971.9)	**763.1** (716.6 – 809.5)[a, b, c, d, g]	**802.1** (717.8 – 886.3)[a, b]	**729.0** (667.4 – 790.6)[a, b, c, d, e, g]	**743.3** (579.2 – 907.5)[a, b, c, d, e, f, g, h]
Se	**11.6** (10.3 – 13.0)	**10.8** (9.5 – 12.1)	**10.8** (9.8 – 11.9)	**10.6** (9.9 – 11.2)	**12.7** (10.9 – 14.5)	**11.8** (11.0 – 12.5)	**12.6** (11.3 – 14.0)	**11.9** (11.1 – 12.7)	**10.6** (9.8 – 11.3)	**10.8** (9.6 – 12.1)	**11.5** (10.5 – 12.4)	**10.2** (9.0 – 11.4)[e, g]

Table 4. 9. Essential metal concentrations in three rat-brain regions at four levels of *post mortem* delay

Dry-weight metal concentrations are means (±95% CI); p-values for significance of case vs control differences were calculated by two-way ANOVA followed by Tukey's *post hoc* multiple comparisons tests. Na, Mg, K, Ca, and Fe are displayed in units of mmol/kg dry-weight tissue; Mn, Cu, Zn, and Se are displayed in units of µmol/kg dry-weight tissue. [a] Significantly higher concentration ($p < 0.05$) than in the cortex at 0 hour PMD group; [b] Significantly higher concentration ($p < 0.05$) than in the cortex at 24 hour PMD group; [c] Significantly higher concentration ($p < 0.05$) than cortex 48 hour PMD group; [d] Significantly higher concentration ($p < 0.05$) than in the cortex at 72 hour PMD group. [e] Significantly higher concentration ($p < 0.05$) than in hippocampus at 0 hour PMD group; [f] Significantly higher concentration ($p < 0.05$) than in the hippocampus at the 24 hour PMD group; [g] Significantly higher concentration ($p < 0.05$) than hippocampus in the 48 hour PMD group; [h] Significantly higher concentration ($p < 0.05$) in the hippocampus 72 hour PMD group; [i] Significantly higher concentration ($p < 0.05$) than in the cerebellum 48 hour PMD group.

Figure 4. 4. Essential metal concentrations in three rat-brain regions at four levels of *post mortem* delay

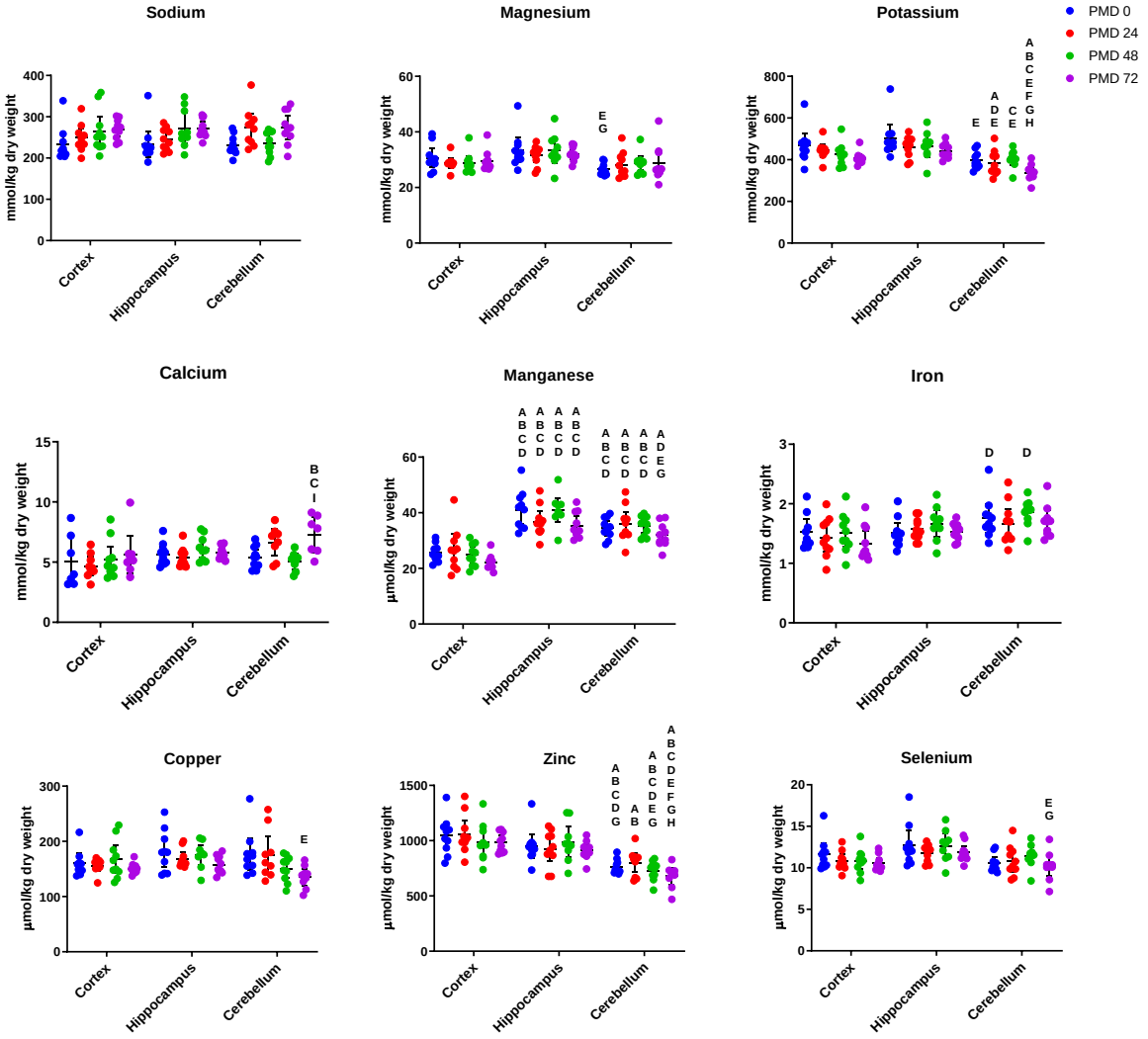

Dry-weight metal concentrations in adult-rat cortex, cerebellum, and hippocampus at 0, 24, 48, and 72 hours *post mortem* delay (PMD, h). Values determined in a single replicate for each region. Intra- and intergroup differences determined by two-way ANOVA followed by Tukey's multiple comparisons tests. A = Significantly higher concentration ($p < 0.05$) than cortex in 0 hour PMD group; B = Significantly higher concentration ($p < 0.05$) than cortex in 24 hour PMD group; C = Significantly higher concentration ($p < 0.05$) than in cortex 48 hour PMD group; D = Significantly higher concentration ($p < 0.05$) than in cortex 72 hour PMD group; E = Significantly higher concentration ($p < 0.05$) than hippocampus 0 hour PMD group; F = Significantly higher concentration ($p < 0.05$) than hippocampus 24 hour PMD group. G = significantly higher concentration ($p < 0.05$) than in hippocampus 48 hour PMD group; H = significantly higher concentration ($p < 0.05$) than in hippocampus 72 hour PMD group; I = significantly higher concentration ($p < 0.05$) than in cerebellum 48 hour PMD group.

4.4. Discussion

4.4.1. Human brain tissue

Studies conducted using human tissues have had to address several issues in the locating and obtaining of samples that are available in sufficient quantities to fulfil multiple exclusionary criteria, and requiring extensive matching. Due to the extremely limited availability of some tissues, such as brain tissue, it can be difficult to meet all these challenges. Studies performing metallomic investigations of such tissues often report contradictory results that are difficult to replicate. For example, although Cu levels in the AD brain have been investigated by several separate research teams, their methodologies, sample numbers, selected brain regions, and subsequent observations have differed greatly, with some reporting decreases in cerebral Cu levels in selected regions, (161, 167, 337-340) some reporting no change in some regions, (165, 169, 170) and one source reporting increases in some regions. (169) Of those studies which have used ICP–MS methodologies similar to our own, all have reported either decreases or lack-of-changes in Cu levels in various regions of the brain, whereas the source that reported an increase (163) used atomic absorption spectroscopy (AAS), suggesting that there may be less comparability between investigations using different methodologies. However, Cu decreases similar to those observed by our own laboratory using ICP–MS, were also reported in the hippocampus by investigations employing neutron activation analysis (NAA); thus methodological differences are not the only reason for discrepancies between different reports. (169, 170) It is also possible that, among other factors, challenges in constructing well-matched and well-defined cohorts can contribute to such mixed findings. As such, it is of importance to determine the effects of variable cohort characteristics on such experiments, which is the key aim of this investigation.

Previous studies conducted by our group have indicated perturbations of multiple metals in the Alzheimer's brain using an age-, PMD-, and sex-matched cohort of 9 cases vs 9 controls.(76) PMD was well below 24 hours for all samples and all but one control had Braak stage 0 (with one control having Braak stage II). Metal changes were reported across several regions, including the cingulate gyrus, where decreases in K, Se, and Cu were

observed. To our knowledge, no similar analyses on these metals have been carried out on the cingulate gyrus. Cu level analyses on different regions of the brain have reported decreases (161, 167, 337-340) no change, (165, 169, 170) or increases (163) as already discussed, and experiments looking at levels of K across different brain areas are similarly inconsistent. Reports have been made both of decreases or lack of change in K within the frontal cortex, as well as increases in the cerebellum. (78, 171) Roberts and colleagues reported decreased brain K measured using an ICP–MS methodology similar to ours but their study examined different regions, making direct comparisons difficult .(161) Similarly, although this and our previous report (164) found decreased K in the cerebellum, the reported increases found in this region by others were determined by flame photometry, (166) which is not a reference method for such measurements. As such, these different observations might simply result from differing methodologies. With regard to reports of measured cerebral levels of Se, only a single previous investigation could be found in our investigation of the literature: this reported decreased Se levels in the hippocampus using ICP–MS, (161) consistent with our own findings in this region. (172)

In the current analysis, all three of these metals were also found to be altered in analysis of the separate Manchester cohort, despite several differences in cohort variables including age, control Braak stage, and PMD; as well as lack of age, PMD, or sex-matching. However, none of these differences were found in the third Newcastle cohort, although pooling of data from all three cohorts retained all three significant observations. There are a few possibilities for the lack of changes observed within the Newcastle cohort in comparison to the Manchester and Auckland groups. The first possibility is simply real variation in metal concentrations within the individuals of each cohort. However, this seems unlikely as a comparison of the concentrations between cohorts revealed only one significant difference between the Newcastle and Manchester cohorts, and none between Newcastle and Auckland (see Table 4.3).

The second possibility is the influence of cohort characteristics, such as age, sex, PMD, etc. The cases and controls in the Newcastle cohort are significantly older than those in the Auckland group and Newcastle controls have higher Braak staging than controls in the

latter group (see Table 4.2). Additionally, PMD in the latter is also lower than cases and controls in the Manchester cohort and Braak staging higher in Newcastle than Manchester cases. However, there were many more differences observed between the Manchester and Auckland cohorts, including control age, case and control Braak staging, and case and control PMD. Despite this, the Manchester and Auckland cohorts still had similar findings. This suggests that the discrepancy between these two cohorts and the Newcastle group are also not due to variations in cohort characteristics. Additionally, MANCOVA analysis of the combined-cohort metal results revealed no significant interactions between age, sex, or PMD with metal concentrations. Metallomic analysis of rat brains at intervals of up to 72 hours PMD also found only small effects of PMD on a few metals (see Table 4.6), a time frame which covers the majority of the human samples used in this study.

However, significant interactions were observed for Braak staging as well as for AD vs control status. Our findings support reported semi-quantitative histochemical observations that some individuals even with early stage (Braak I/II) tangle pathology had increased iron deposition in the brain compared with Braak 0 individuals, and that iron levels correlated with Braak stage. (173) This correlation has also been observed by other groups, as well as association of Braak staging with decreased Mn and Zn levels in AD brain tissue. This group however did not find significant associations between Braak staging and Cu or Mn levels, and Se was not investigated in their experiment. This provides additional support to the findings in the Manchester and Auckland cohorts, suggesting that they are not caused by variables in control Braak staging. What we cannot determine from the MANCOVA analysis is exactly how Braak staging or status effect different metal concentrations or to what degree, only that there is some sort of interaction. However, as Braak staging is often used to give a definitive diagnosis of AD neuropathologically *post mortem*, it follows that a significant effect of either Braak staging or AD status should be reflected by a significant effect of the other.

Another, third possibility for the discrepancies between results is differences in the statistical power of each cohort. Although statistical power analyses showed that N-values of 18 or less were sufficient to find statistically significant differences between cases and

controls for K, Cu, and Se in the Manchester and Auckland cohorts; this was not the case in the Newcastle cohort (Table 4.4). This suggests that the N-value was too low to find significant changes in these metals within the Newcastle cohort, particularly if those changes are of a small effect size. The same power analysis showed that N-values of 54 or less were required to observe significant changes in every metal but Zn in the combined cohort, supporting the higher statistical power of these findings, which would be expected with larger sample numbers. Furthermore, it was only in the combined cohort that the statistical power for all three of K, Cu, and Se passed the threshold of 80% (see Table 4.4), whereas this was only observed for one of these metals in the Manchester and Auckland cohorts separately, and for none in the Newcastle cohort. This is perhaps not surprising due to the large differences in N-value, but highlights the importance of the careful selection of sample numbers in order to optimise the balance between avoiding wastage of precious tissues in short supply, and in achieving sufficient levels of statistical power. One way around this issue could be to combine cohorts from multiple studies where possible in order to boost N-values, and consequently statistical power, without requiring further usage of tissue. However this requires tissues that can either be re-analysed, or that have undergone analysis by standardised, comparable methodologies, which often hitherto has not been the case.

This is supported by observations made from analysis of wet-weight brain tissues from the same cohorts as those used for dry-weight analyses. Here, wet-weight brain tissues showed the same significant case–control differences as dry-weight tissue (decreased K, Mn, and Se), but only when samples from both the Manchester and Auckland cohort were combined. When taken individually, only the Manchester cohort showed decreased K and Mn in cases and only the Auckland cohort showed decreased case Se. This may indicate that the wet-weight tissue analyses are more sensitive to the effects of low sample numbers. As such, dry-weight analysis may be preferable where sample numbers are low. However, significant increases in Na AD cases, which were observed in both cohorts individually as well as when they were combined into a single cohort, were only observed in wet-weight tissue. This indicates that concentrations of Na specifically are sensitive to

the drying process, and that targeted measurements of this metal may be more suited to wet-weight analysis.

When there are multiple variables present to be analysed, it can be difficult to distinguish the effects of each one. As such, being able to study the influence of single factors in more controlled ways is desirable. This is difficult to do with human tissues due to the large degree of individual variability, but can be done using animal models for some variables such as PMD.

4.4.2. Effect of PMD on Metallomic Analyses in Rat Brain Tissues

Although results from animal studies must be interpreted with care in relation to experiments using human tissues, they can provide important information which is difficult to obtain from human studies due to the large numbers of variations that exist between individual human samples. Using animal tissues provides the opportunity to design a more controlled experiment in order to investigate the effects of single parameters. This is not possible for all factors, due to intrinsic differences between humans and animals in factors such as life-span, and the absence of human pathological markers (e.g. amyloid-β or tau deposition) in animals. However it is possible for factors such as PMD. Here we used healthy adult rat tissues to examine the effect of different PMDs on cerebral metals, a parameter which varied greatly between different brain banks and individual human samples, with better control over other variables such as age and sex.

To the best of our knowledge, there have been no previous investigations into the effect of PMD on rat brain-tissue metal concentrations published to date. The present analysis found only a small effect of PMD on concentrations of Na, K, Mn, and Cu in the rat-brain cortex, cerebellum, or hippocampus, accounting for a maximum of 13.3% of the variation in these metals (see Table 4.6). Na levels increased from 0 to 72 hours PMD by 16.2%, 16.2%, and 19.1% in the cortex, hippocampus, and cerebellum respectively, showing a very consistent change across brain regions (data not shown). Despite this, multiple comparisons tests found no significant differences within any of these time points within the same regions (see Table 4.7). K levels decreased in each region by 13%, 12.4%, and 15% respectively by 72 hours PMD, again showing high consistency. As with Na, multiple

comparisons tests found no differences between K levels at different time points within the same region. Due to a lack of available studies in this area, it is difficult to determine why extended PMDs could be causing these changes in Na and K levels. As the brains were left in situ in the otherwise-intact bodies of the rats during the *post mortem* intervals, it seems most likely that Na had leeched in, and K leeched out of the brain from another tissue, most likely the blood, possibly as a consequence of post mortem absence of chemical energy generation. To determine if this was definitely the case could perhaps be done by taking concurrent measurements from both blood and adjacent brain tissue at the same time points, which was not carried out here. Changes in Mn and Cu were less consistent across regions, and did not follow a clear pattern across time points. Taken together along with the findings from the human samples, these results suggest a minimal impact of PMD on levels of these metals up to a period of 72 hours in *post mortem* brain tissues.

In comparison to PMD, brain region appeared to have a more extensive effect on some metal concentrations; having a significant effect on Mg, K, Ca, Mn, Fe, Zn, and Se. Variation accounted for by region ranged from 8.1% (Ca) to 55.3% (Mn; see Table 4.7). Only three metals had more than 25% of their variation accounted for by brain region: K (27.8%), Mn (55.3%), and Zn (43.7%). These metals also showed the highest number of significant differences between regions as found by multiple comparisons tests. The cerebellum showed an average of 14.1% less K than the hippocampus at each time point (data not shown). The cerebellum also showed a mean of 12.2% and 19.5% less Zn than the cortex and hippocampus respectively at each PMD interval. The cortex however showed an average of 18.7% and 25.6% less Mn than the cerebellum and hippocampus respectively. This evidence indicates lower concentrations of K and Zn in the cerebellum and lower Mn levels in the cortex. Future studies investigating these metals in rat models might reasonably consider the regions chosen for experiments. Previous studies have reported lower endogenous Mn in the hippocampus in comparison to the cortex and cerebellum in rats with non-supplemented diets, contradictory to the result observed here. (174) Similar studies comparing K levels in these regions of healthy rat brains could not be found in the literature. However, a comparison of Fe, Cu, and Zn levels within the cortex and cerebellum

of rat brains reportedly found somewhat higher levels of all three in the cerebellum, although statistical tests were not performed in order to examine this further. [174] To our knowledge, the current manuscript reports the first study to systematically compare levels of all nine physiological metals investigated here across the rat cortex, cerebellum, and hippocampus.

Taken together, the studies reported here of both human and rat brain tissues suggest that metal concentrations are robust to differences in tissue-collection variables including age and PMD. Braak staging does appear to have a small effect on metal levels, but not enough to influence interpretation of findings within the cohorts studied here. Notably, metal concentrations differ significantly between regions in both human and rat brains, and so regions of interest for study of brain metal metabolism should be selected carefully.

These results indicate that UK tissues are suitable for metallomic analysis, despite differences to New Zealand cohorts in age, PMD, and Braak staging. As such, the decision was made to source Parkinson's disease dementia PDD brain tissues from the UK for metallomic analysis. It was also determined that dry-weight analysis of these tissues should be performed as observations using these methods remain largely consistent, with wet-weight samples showing higher sensitivity to low n numbers.

Chapter Five | Widespread decreases in copper common to Parkinson's disease dementia and Alzheimer's disease human brains

This chapter was published as a paper in Metallomics: Scholefield M, Church SJ, Xu J, Kassab S, Gardiner NJ, Roncaroli F, et al. Evidence that levels of nine essential metals in post-mortem human-Alzheimer's-brain and ex vivo rat-brain tissues are unaffected by differences in post-mortem delay, age, disease staging, and brain bank location. Metallomics. 2020;12(6):952-62 (102). It is presented here with minor adjustments. Following the previous pilot study, in which it was ascertained that tissue collection variables such as PMD should not affect metallomic findings, Parkinson's disease dementia (PDD) tissues were obtained from a UK brain bank in order to analyse levels of essential metals in PDD and compare them with those in both AD and HD. This represents the first multi-regional metallomic analysis of PDD brains.

5.1. Introduction

Parkinson's disease (PD) is one of the most common neurodegenerative diseases, affecting around 1% of the world's population above the age of 60 (1). Clinically, PD is characterised by progressive motor dysfunction resulting in bradykinesia, tremor, and rigidity. Cognitive impairment is also common, with cohort studies reporting around a third of patients as showing mild cognitive impairment (MCI) at the time of diagnosis, and up to 80% developing dementia twenty years following (2). This condition is described as PDD.

PD and PDD are characterised by the degeneration of dopaminergic neurons in the substantia nigra and the accumulation of misfolded α-synuclein to form Lewy bodies and neuropil threads. However, research is ongoing on exactly how these inclusions develop or how they lead to neuronal death. Although clinical trials targeting the aggregation and binding of α-synuclein, and/or aiming to changes its levels are ongoing, to date no drugs modifying misfolded α-synuclein have been developed (341). As such, research is beginning to focus on other mechanisms that may contribute to pathogenesis, including the roles of mitochondrial dysfunction and oxidative stress (342), autophagy (343), genetic factors (344), lipid dysfunction (345), inflammation (342), and metal homeostasis (346). Perturbations of metals have been reported in PD brain tissues; increases in iron (Fe) have been consistently found in the substantia nigra (SN), the region most severely affected in PD (76-81). Likewise, there have been several reports of reduced copper (Cu) within the same region (76, 78, 171). Some studies examined other brain regions, usually observing no changes in Cu outside the SN (76, 78) but with one study showing decreases in the caudate nucleus (CN) and locus coeruleus (LC) (171). Additionally, most investigations did not distinguish between PD and PDD and primarily focus on the former. It remains unknown if different or additional metal alterations characterise PDD.

This study investigated perturbations in nine essential metals (sodium (Na), magnesium (Mg), potassium (K), calcium (Ca), manganese (Mn), Fe, Cu, zinc (Zn), and selenium (Se)) across nine brain regions (cerebellum at the level of the dentate nucleus (CB), cingulate gyrus (CG), hippocampus (HP), LC, motor cortex (MCX), medulla (MED), middle temporal gyrus (MTG), occipital cortex at the level of the primary visual cortex (PVC), and SN) in nine confirmed cases of PDD and nine age-matched control brains. Essential metals were

chosen for investigation due to the physiological necessity of tightly-controlled levels for health and survival in humans, as well as on the basis of previous reports of alterations of such elements not only in PD, but also across multiple brain regions in other neurodegenerative conditions such as Alzheimer's (AD) (163, 168, 169) and Huntington's disease (HD) (166, 174, 347). The regions selected here should cover areas highly affected by degeneration in PD/PDD (SN, MED, LC), moderately affected regions (MCX, HP, PVC, CG), as well as relatively spared regions (CB, MTG). As well as allowing direct comparison of areas differently affected by neurodegeneration, this selection should also allow comparison of results to previous parallel studies investigating metallomic perturbations in AD, to identify any similarities or differences between the two dementias. Any identified similarities could point towards shared disturbances or pathogenic mechanisms between diseases, whilst differences could aid in distinguishing between conditions in cases where clinical presentation may make diagnosis and treatment difficult.

5.2. Materials and methods

5.2.1. Reagents

Except where otherwise stated, all reagents were obtained from Sigma-Aldrich (UK).

5.2.2. Acquisition of human brain tissues from PDD cases and controls

Flash-frozen brain tissues from nine neuropathologically confirmed PDD cases and nine age-matched controls were obtained from the Multiple Sclerosis & Parkinson's Tissue Bank, Imperial College, London (UK). Tissues from the SN, CG, LC, HP, MCX, CB, PVC, MED, MTG were obtained. The regions were selected on the basis of their varying levels of involvement in PDD and for direct comparison with previous metallomic studies in AD. Post mortem delay was 48 hours or shorter (see Supplementary Table 12 & 13, p407–410, for individual donor characterisation).

5.2.3. Diagnosis & Severity of Human Cases

The extent of amyloid, α-synuclein, and tau-related pathologies was determined in all cases; these were assessed using CERAD and Thal phase for amyloid, and Braak grading

systems for tau and for α-synuclein. In all cases, dementia only developed at least one year following the onset of motor symptoms, ruling out a diagnosis of dementia with Lewy bodies (DLB) (13). Co-morbidities, cause of death, smoking status, post mortem delay, Thal and CERAD scores, presence of signs of small vessel disease, brain weight, age at onset and duration of disease in PDD cases, were recorded. Cases with signs of other dementia conditions, such as Alzheimer's disease, were excluded.

Control brains only showed age-related changes and no evidence of cognitive impairment was reported in the clinical records. Characteristics of individual donors are shown in Supplementary Table 12 & 13 (p407–410).

5.2.4. Tissue Dissection

Brain tissue was stored at -80°C upon delivery. On the day of the experiment, the specimens were thawed slightly on ice and dissected into 50 mg (± 5%) samples for ICP–MS using a metal-free ceramic scalpel and placed into 'Safe-Lok' microfuge tubes (Eppendorf AG; Hamburg, Germany). Tubes were weighed before adding tissues to allow samples to be dried and weighed without the need for transferring to new tubes. The use of a ceramic scalpel prevented contamination from metals during sectioning. Following dissection, tissues were immediately dried as detailed below.

5.2.5. ICP–MS

Freshly-dissected samples were briefly centrifuged before being dried to a constant weight using a Savant Speedvac (Thermo Fisher Scientific; MA, USA). Nitric acid digestion of samples was then performed in a heat block, along with digestion blanks containing nitric acid alone (see Appendix B, Table B1 & B3, p2-10 & 31–33). Following digestion, samples were refrigerated overnight at 4°C before undergoing ICP–MS analysis with a 7700x ICP–MS spectrometer (Agilent; Santa Clara, CA, USA) equipped with a MicroMist nebulizer and Scott double-pass spray chamber (Glass Expansion; Melbourne, Australia), and nickel sample and skimmer cones. Samples were separated into batches of either one or two regions, with multi-element calibration using calibration standard dilutions and periodic quality controls included for each batch (see Appendix B, Figures B1 & B2, p17–30 & 36–

42). All elements were standardised against scandium, with the exception of Zn and Se which were standardised against germanium.

Agilent's recommendations were followed for selection of operation mode, integration times, and internal standard assignments. Samples were introduced to the instrument using an integrated autosampler (Agilent). All elements were analysed using helium as the collision gas; Se was analysed in high-energy helium mode (10 ml/min helium) due to its state as a polyatomic ion, and all other elements were analysed using standard helium mode (5.0 ml/min helium). For each of the quantified metals, limits of quantitation (LOQs), detection limits (DLs), and background equivalent concentrations (BECs), were automatically calculated by the instrument (see Appendix B, Table B2 & B4, p11–16 & 34–35). Measured metal concentrations from individual runs were disregarded where lower than the detection limit calculated for that run.

5.2.6. ICP–MS Data Analysis

Mean metal values (±95 % CI) were calculated and differences between cases and controls determined by non-parametric Mann–Whitney U tests due to the small sample size. Mann–Whitney U calculations were performed using GraphPad v8.1.2 (Prism; La Jolla, CA, USA) and p-values < 0.05 were considered significant.

Where possible, control values from previous experiments on AD (obtained from the New Zealand National Brain Bank; Auckland, New Zealand; Manchester Brain Bank; Salford Royal Hospital, UK; and the Newcastle Brain Tissue Resource; University of Newcastle, UK) and Huntington's disease (obtained from the New Zealand National Brain Bank) were combined with the current PDD control group values in order to obtain the largest available sample size. Details of individual donors from these cohorts are also included in Supplementary Tables 6–8 & 12 (p397–403 & 407–408). Suitability of previous control groups for combination with the current control group was determined by comparison of cohort characteristics as well as metal concentrations in each region. This included comparisons of sex, age, and post mortem delays between control groups as determined by Mann–Whitney U test, as well as separation analysis by principal component analysis (PCA) and partial least squares discriminant analysis (PLS–DA; see Electronic Appendix C).

Orthogonal PLS–DA (OPLS–DA) was used where only two control groups were being compared. Extra controls were accepted where they did not differ significantly across control-cohort variables and were not separated from the current control group by PCA or PLS–DA. PCA and PLS–DA analyses were performed using MetaboAnalyst (McGill University; Montreal, Canada).

5.3. Results

5.3.1. Patient Characteristics

Tissue from nine different brain regions was obtained from nine clinically-diagnosed and neuropathologically-confirmed cases of PDD and nine age-matched controls. Where possible, additional control samples derived from previously-described cohorts used in investigations of AD and HD were also included in the analysis (see section 'Control Groups').

No significant differences were found between cases and controls when sex, PMD, tau Braak stage, Thal and CERAD scores, brain weight, and smoker status were compared (see Table 5.1). PDD cases were about ten years younger than controls (mean 77.0 years vs 87.6 years respectively). The cause of death of PDD and control cases is reported in Supplementary Table 12 (p407–408). Smoking status was unknown for three cases (PD5, PD8, and PD9). PDD cases showed a higher incidence of psychiatric symptoms such as anxiety and depression, whereas hypertension and type II diabetes were more common in controls (see Supplementary Table 13, p409–410). One control had a family history of PD, but no recorded signs and symptoms or neuropathological features α-synucleinopathy or any other neurodegenerative disease were observed (C4).

Table 5. 1. Cohort Characteristics

Variable	PDD Cases (n = 9)	Controls (n = 9)	P-Value
Male Sex, n (%)	5 (55.5)	4 (44.4)	0.7
Age	78 (66 – 93)	87 (79 – 95)**	**0.005**
PMD (hours)	27 (9 – 48)	25 (15 – 48)	0.8
α-synuclein Braak	6 (5 – 6)	0****	**< 0.0001**
tau Braak	2 (0 – 4)	2 (1 – 3)	0.9
Thal	2 (0 – 5)	2.5 (0 – 1)	0.4
CERAD	0 (0 – 2)	0 (0 – 1)	0.7
Disease Duration (years)	13 (6 – 23)	N/A	N/A
Age Onset	67 (49 – 69)	N/A	N/A
Whole Brain Weight (g)	1371 (960 – 1402)	1126 (946 – 1338)	0.0503
Never smoked, n (%)	4 (44.4)	2 (22.2)	0.3

Comparison of PDD case and control variables. All variables are medians (range); p-values for significance of between-group differences were calculated by Mann–Whitney U test. ** p < 0.01; **** p < 0.0001. CERAD = The Consortium to Establish a Registry for Alzheimer's disease score; PMD = post mortem delay.

5.3.2. Control Groups

Our group has previously carried out metallomic analyses of human brains with AD and HD using the methods employed here. These studies included three AD cohorts obtained from the New Zealand National Brain Bank, Manchester Brain Bank, and Newcastle Brain Bank; as well as an HD cohort from the New Zealand National Brain Bank. Where possible, controls from these cohorts have been combined with the controls from the current PDD cohort in order to maximise sample size and improve reliability of the analysis.

The characteristics of each of these control groups is shown in Table 5.2 (details of individuals from each cohort are provided in Supplementary Tables 6–8 & 12, p397–403 & 407-408). Whilst the Newcastle and Manchester-derived AD groups and Auckland-derived HD group did not differ significantly across any of the comparable variables from the PDD controls, the Auckland-derived AD group showed significantly lower age, tau Braak staging, and PMD than the PDD controls. However, we have previously shown that these variables do not significantly alter metal concentrations in human AD and control brain tissues (348) and as such are not considered grounds for exclusion.

Whether these control groups were suitable for inclusion in this study was assessed on a region-by-region basis (see Table 5.3). Controls from the Manchester and Newcastle cohorts were available for the CG. Controls from an Auckland-derived AD cohort were available for the CG, MCX, HP, CB and MTG. Controls from an Auckland-derived HD cohort were available for the MC, HP, and CB. PCA and PLS–DA plots of available control groups were performed to determine whether metal measurements produced separation of different cohort controls (see Electronic Appendix C). If separation occurred, the dissimilar control group would not be included; otherwise, all controls were included in the final analysis for that region. On this basis, Manchester and Newcastle controls were accepted in the CG control group; Auckland AD controls were accepted in the HP control group, but excluded from the CG analysis; and the HD controls were accepted in the HP control group but excluded from the SN analysis (see Table 5.3).

Table 5. 2. Comparison of cohort control characteristics

Variable	Manchester AD Controls	Newcastle AD Controls	Auckland AD Controls	PDD Controls	HD Controls
Number	9	9	9	9	9
Age	89 (82-95)	85 (76-94)	73 (61-78)**	87 (79 – 95)	66 (49 – 81)**
Male Sex, n (%)	6 (66.6)	6 (66.6)	5 (55.4)	5 (44.4)	6 (66.6)
Tau Braak Stage	I-II	I-II	0****	II	NA
PMD (hours)	75 (49 – 130)	25 (9 – 40)	12 (5.5-15.0)**	25 (15 – 48)	12 (6.5 – 15)**
Whole-Brain Weight (g)†	1160 (1020 – 1494)	1235 (1064 – 1406)	1260 (1094 – 1461)	1126 (946 – 1338)	1315 (1210 – 1495)

Comparison of control group characteristics between each brain bank cohort. Age, male percentage, tau Braak stage, PMD, and whole brain weight are medians (range); p-values for significance of between-group differences were calculated by the Kruskal-Wallis test followed by Dunn's post hoc multiple comparisons test against the PDD control group. ** $p < 0.01$; **** $p < 0.0001$.

Table 5. 3. Final Control Groups for each region

Control Group	MTG	CB	CG	SN	HP	LC	MED	PVC	MCX
Manchester AD (n = 9)	-	-	Accepted	-	-	-	-	-	-
Newcastle AD (n = 9)	-	-	Accepted	-	-	-	-	-	-
Auckland AD (n = 9)	Accepted	Excluded	Excluded	-	Accepted	-	-	-	Accepted
Auckland HD (n = 9)	Accepted	Excluded	-	Excluded	Accepted	-	-	-	Accepted
Final number	**27**	**9**	**27**	**9**	**27**	**9**	**9**	**9**	**18**

A dash indicates that the region was not investigated in the indicated cohort. MTG = middle temporal gyrus; CB = cerebellum; CG = cingulate gyrus; SN = substantia nigra; HP = hippocampus; LC = locus coeruleus; MED = medulla; PVC = primary visual cortex (occipital lobe); MCX = motor cortex.

5.3.3. ICP–MS Metals Analysis

The concentrations of eight essential metals including Na, Mg, K, Ca, Mn, Fe, Cu, Zn, and Se, strictly a metalloid) were determined in dry tissue from nine regions of the brain in nine PDD cases and nine controls without dementia or other neurodegenerative disease. Where possible, measurements from additional controls from previously-analysed cohorts were also included for analysis (see Table 5.3).

Metal concentrations for each region are shown in Tables 5.4 – 5.12 and Figure 5.2. Cu concentrations were the most consistently perturbed, being found to be decreased in the CG ($p = 0.009$), SN ($p = 0.003$), HP ($p = 0.0010$), MED ($p = 0.008$), PVC ($p= 0.008$), MTG ($p = 0.0050$), and MCX ($p = 0.0010$) of cases in comparison to controls. Cu levels also trended lower in cases than controls in the remaining two regions, but not significantly. Cu concentrations in control regions were largely consistent, averaging around 300 µmol/kg dry-weight, although the MCX had a slightly (but not significantly) higher concentration than other regions (403.5 µmol/kg dry-weight).

Mn was also decreased in several regions, including the SN ($p = 0.04$), HP ($p = 0.04$) LC ($p = 0.03$), MED ($p = 0.007$), MTG ($p = 0.006$), and MCX ($p = 0.003$). In the remaining regions, there was a non-significant trend towards lower levels in cases compared to controls. Like Cu, Mn concentrations were consistent across control regions, averaging around 20 µmol/kg dry-weight, with the exception of the LC which showed slightly lower values (16.7 µmol/kg dry-weight).

As with Cu and Mn, K levels were lower in cases than controls in every region, but this decrease was only significant in three areas: the HP ($p = 0.04$), MTG ($p = 0.04$), and MCX ($p = 0.03$). K levels were lowest in MED controls at 215.8 mmol/kg dry-weight and highest in the MCX of controls at 362.6 mmol/kg dry-weight.

Mg and Se were found to be decreased only in the MCX ($p = 0.03$ and $p = 0.002$ respectively). Control Mg concentrations were also highest in the MCX (26.4 mmol/kg dry-weight) and lowest in the SN (20.0 mmol/kg dry-weight). Se was higher than average in three regions; the MTG (12.6 µmol/kg dry-weight), HP (11.3 µmol/kg dry-weight), and MCX (12.7 µmol/kg dry-weight). All other control regions showed Se levels below 10 µmol/kg

dry-weight. It is possible that the decreases observed in Mg and Se in the MCX are partially attributable to higher baseline levels compared to other regions.

Zn was only seen be to be lowered in the HP ($p = 0.009$). There was a marked variation in Zn levels across control regions, with a particularly low concentration in the LC (355.4 µmol/kg dry-weight) and the highest concentration in the HP itself (1095.5 µmol/kg dry-weight).

No significant differences were found between cases and controls for Na, Ca, or Fe in any region. Na concentrations in control brains were highly variable, with the highest levels observed in the HP (419.4 mmol/kg dry-weight) and the lowest in the LC (196.8 mmol/kg dry-weight). Control Fe concentrations were also highly variable, ranging from 5.8 mmol/kg dry-weight in the MCX to 1.3 mmol/kg dry-weight in the MED, an almost four-fold difference. Control Ca levels were however fairly similar across regions, with few significant differences between individual areas (data not shown).

The regions with the highest number of altered metals were the MCX, HP, and MTG (see Figures 5.1 – 5.2). Interestingly, the SN showed changes in only two metals, Cu and Mn, despite being the region most heavily affected by neurodegeneration in PDD. This indicates a pattern for metal changes that doesn't necessarily reflect α-synuclein deposition or neurodegeneration patterns. The CB also completely lacked alterations in any of the metals analysed here. The MED showed changes in two metals, Cu and Mn, like the SN. The CG and PVC both only showed decreases in Cu.

Table 5. 4. Metal concentrations in the SN of PDD cases and controls

Metal	PDD (n = 9)	Controls (n = 18)	p-value
Na	248.3 (219.3 – 277.2)	252.3 (229.5 – 275.1)	0.7
Mg	19.7 (18.8 – 20.6)	20.0 (19.3 – 20.7)	0.3
K	246.0 (226.6 – 265.4)	249.3 (235.0 – 263.7)	0.6
Ca	6.0 (3.8 – 8.3)	5.3 (3.9 – 6.7)	0.7
Mn	19.3 (15.2 – 23.5)	25.2 (20.6 – 29.9)	**0.04**
Fe	4.8 (3.1 – 6.5)	4.6 (3.4 – 5.8)	1.0
Cu	201.8 (174.1 – 229.6)	306.8 (248.4 – 365.2)	**0.003**
Zn	595.0 (550.7 – 639.2)	669.7 (579.4 – 759.9)	0.2
Se	6.6 (6.0 – 7.3)	7.1 (6.4 – 7.8)	0.2

Data are means (±95% CI) taken over three replicate runs; P-values for significance of between-group differences were calculated by Mann–Whitney U test. $P < 0.05$ is considered significant.

Table 5. 5. Metal concentrations in the CG of PDD cases and controls

Metal	PDD (n = 9)	Controls (n = 27)	p-value
Na	350.1 (286.5 – 413.7)	386.8 (340.1 – 433.4)	0.6
Mg	22.2 (21.1 – 23.3)	22.8 (22.0 – 23.7)	0.5
K	274.6 (258.9 – 290.3)	295.5 (277.7 – 313.4)	0.13
Ca	6.0 (5.0 – 7.0)	7.2 (6.3 – 8.1)	0.3
Mn	18.4 (15.8 – 21.1)	21.4 (20.2 – 22.6)	0.06
Fe	3.8 (3.2 – 4.3)	3.5 (3.3 – 3.8)	0.5
Cu	181.6 (152.5 – 210.8)	249.0 (216.4 – 281.6)	**0.009**
Zn	746.5 (652.2 – 840.8)	845.8 (786.4 – 905.2)	0.13
Se	7.7 (6.8 – 8.6)	8.4 (7.8 – 9.0)	0.3

Data are means (±95% CI) taken over three replicate runs; P-values for significance of between-group differences were calculated by Mann–Whitney U test. $P < 0.05$ is considered significant. This region includes controls from the Manchester and Newcastle AD cohorts.

Table 5. 6. Metal concentrations in the LC of PDD cases and controls

Metal	PDD (n = 9)	Controls (n = 9)	p-value
Na	213.7 (197.6 – 229.8)	196.8 (163.9 – 229.8)	0.5
Mg	18.7 (17.8 – 19.6)	19.4 (18.6 – 20.2)	0.30
K	244.4 (229.8 – 259.1)	253.3 (234.3 – 272.3)	0.5
Ca	4.2 (2.9 – 5.4)	5.1 (4.8 – 5.4)	0.3
Mn	14.7 (13.2 – 16.2)	16.7 (15.4 – 18.1)	**0.02**
Fe	1.6 (1.4 – 1.7)	1.5 (1.3 – 1.7)	0.6
Cu	168.8 (88.1 – 249.5)	214.7 (171.0 – 258.3)	0.7
Zn	348.3 (339.3 – 357.4)	355.4 (294.6 – 416.2)	0.3
Se	7.0 (6.5 – 7.6)	6.9 (6.3 – 7.6)	0.8

Data are means (±95% CI) taken over three replicate runs; P-values for significance of between-group differences were calculated by Mann–Whitney U test. $P < 0.05$ is considered significant.

Table 5. 7. Metal concentrations in the HP of PDD cases and controls

Metal	PDD (n = 9)	Controls (n = 27)	p-value
Na	465.1 (426.1 – 504.1)	419.4 (350.5 – 488.3)	0.3
Mg	24.8 (22.9 – 26.8)	26.7 (25.4 – 27.9)	0.1
K	287.1 (247.0 – 327.1)	345.9 (315.5 – 376.2)	**0.04**
Ca	9.5 (8.3 – 10.6)	8.5 (6.8 – 10.2)	0.2
Mn	23.4 (10.7 – 26.1)	27.0 (25.1 – 28.9)	**0.04**
Fe	4.1 (3.6 – 4.7)	4.0 (3.4 – 4.6)	0.3
Cu	177.4 (120.8 – 234.0)	303.1 (274.1 – 332.2)	**0.0010**
Zn	774.2 (623.7 – 924.8)	1095.5 (989.6 – 1201.4)	**0.009**
Se	8.9 (7.5 – 10.4)	11.3 (10.5 – 12.0)	0.1

Data are means (±95% CI) taken over three replicate runs; P-values for significance of between-group differences were calculated by Mann–Whitney U test. $P < 0.05$ is considered significant. This region includes controls from the Auckland AD and HD cohorts.

Table 5. 8. Metal concentrations in the MED of PDD cases and controls

Metal	PDD (n = 9)	Controls (n = 9)	p-value
Na	278.2 (249.8 – 306.6)	268.0 (238.0 – 298.1)	0.3
Mg	19.6 (19.1 – 20.2)	20.4 (19.7 – 21.0)	**0.03**
K	204.2 (188.6 – 219.7)	215.8 (205.1 – 226.4)	0.1
Ca	5.1 (4.2 – 6.1)	6.9 (4.7 – 9.1)	0.1
Mn	15.8 (13.7 – 17.8)	19.8 (16.8 – 22.9)	**0.007**
Fe	1.2 (1.0 – 1.4)	1.3 (1.2 – 1.4)	0.3
Cu	158.1 (141.4 – 174.8)	236.6 (125.8 – 347.4)	**0.008**
Zn	736.4 (643.2 – 829.7)	812.8 (704.2 – 921.5)	0.1
Se	7.5 (7.0 – 8.0)	7.7 (6.9 – 8.4)	0.8

Data are means (±95% CI) taken over three replicate runs; P-values for significance of between-group differences were calculated by Mann–Whitney U test. $P < 0.05$ is considered significant.

Table 5. 9. Metal concentrations in the PVC of PDD cases and controls

Metal	PDD (n = 9)	Controls (n = 9)	p-value
Na	347.0 (299.0 – 395.0)	353.6 (316.0 – 391.2)	0.5
Mg	22.9 (22.1 – 23.6)	24.2 (22.4 – 26.0)	0.2
K	319.6 (301.4 – 337.9)	332.1 (288.8 – 375.5)	0.4
Ca	6.7 (6.0 – 7.4)	11.7 (4.2 – 19.2)	0.2
Mn	20.1 (17.9 – 22.2)	22.8 (20.2 – 25.4)	0.06
Fe	5.1 (4.6 – 5.7)	4.8 (4.1 – 5.4)	0.5
Cu	237.8 (215.6 – 259.9)	316.4 (239.9 – 393.0)	**0.008**
Zn	938.8 (855.5 – 1022.0)	963.9 (817.3 – 1110.5)	0.3
Se	9.9 (9.3 – 10.4)	9.9 (8.6 – 11.1)	0.8

Data are means (±95% CI) taken over three replicate runs; P-values for significance of between-group differences were calculated by Mann–Whitney U test. $P < 0.05$ is considered significant.

Table 5. 10. Metal concentrations in the MTG of PDD cases and controls

Metal	PDD (n = 9)	Controls (n = 27)	p-value
Na	439.3 (326.5 – 552.2)	353.9 (302.5 – 405.3)	0.10
Mg	24.2 (22.3 – 26.0)	25.3 (23.1 – 27.5)	0.2
K	299.9 (278.8 – 320.9)	359.7 (322.0 – 397.3)	**0.04**
Ca	12.6 (8.6 – 16.6)	11.3 (7.4 – 15.3)	0.8
Mn	16.5 (14.4 – 18.6)	21.9 (19.2 – 24.6)	**0.006**
Fe	4.5 (4.0 – 5.0)	4.8 (4.3 – 5.2)	0.6
Cu	225.4 (182.2 – 268.7)	337.7 (289.1 – 386.4)	**0.0050**
Zn	1107.6 (940.4 – 1274.8)	1055.3 (948.2 – 1162.4)	0.6
Se	9.5 (8.8 – 10.2)	12.6 (10.3 – 14.9)	0.3

Data are means (±95% CI) taken over three replicate runs; P-values for significance of between-group differences were calculated by Mann–Whitney U test. $P < 0.05$ is considered significant.

Table 5. 11. Metal concentrations in the CB of PDD cases and controls

Metal	PDD (n = 9)	Controls (n = 9)	p-value
Na	222.4 (161.6 – 283.1)	214.3 (184.8 – 243.9)	0.8
Mg	20.7 (18.4 – 23.0)	20.1 (18.5 – 21.7)	0.9
K	275.3 (226.5 – 324.1)	267.7 (224.8 – 310.5)	1.0
Ca	4.2 (3.4 – 5.0)	4.4 (3.9 – 4.9)	0.4
Mn	19.6 (14.1 – 25.1)	20.8 (16.6 – 25.0)	0.6
Fe	4.2 (2.9 – 5.4)	3.8 (2.3 – 5.2)	0.6
Cu	324.2 (256.5 – 391.8)	328.3 (161.5 – 495.2)	0.6
Zn	736.4 (595.0 – 877.9)	698.4 (582.5 – 814.4)	0.8
Se	8.0 (6.8 – 9.1)	7.1 (6.2 – 8.0)	0.2

Data are means (±95% CI) taken over three replicate runs; P-values for significance of between-group differences were calculated by Mann–Whitney U test. $P < 0.05$ is considered significant.

Table 5. 12. Metal concentrations in the MCX of PDD cases and controls

Metal	PDD (n = 9)	Controls (n = 26)	p-value
Na	339.3 (217.2 – 461.4)	403.3 (251.4 – 555.2)	0.3
Mg	20.7 (18.7 – 22.7)	26.4 (17.6 – 35.2)	**0.003**
K	270.9 (218.3 – 323.5)	362.6 (225.1 – 500.1)	**0.03**
Ca	6.5 (3.4 – 9.6)	7.0 (4.3 – 9.7)	0.4
Mn	17.7 (14.4 – 21.1)	25.5 (16.4 – 34.5)	**0.003**
Fe	4.5 (3.4 – 5.7)	5.8 (3.6 – 8.0)	0.07
Cu	219.1 (174.5 – 263.6)	403.5 (171.7 – 635.3)	**0.0010**
Zn	689.0 (470.6 – 907.5)	954.9 (585.0 – 1324.8)	0.06
Se	7.9 (6.2 – 9.6)	12.7 (5.9 – 19.6)	**0.002**

Data are means (±95% CI) taken over three replicate runs; P-values for significance of between-group differences were calculated by Mann–Whitney U test. $P < 0.05$ is considered significant. This region includes controls from the Auckland AD and HD cohorts.

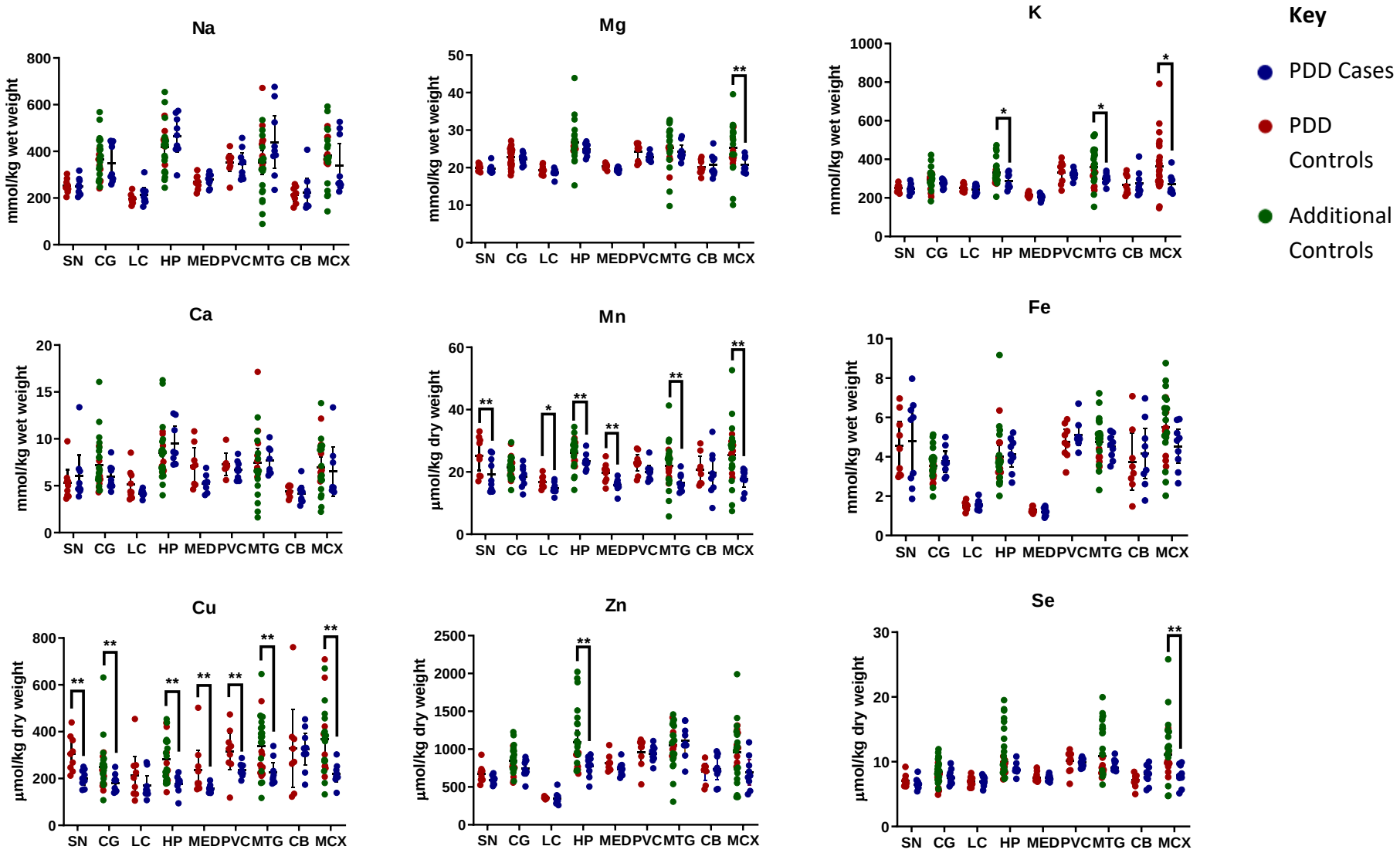
Na
mmol/kg wet weight
Mg
mmol/kg wet weight
K
mmol/kg wet weight
Key
PDD Cases
PDD Controls
Additional Controls
Ca
mmol/kg wet weight
Mn
µmol/kg dry weight
Fe
mmol/kg wet weight
Cu
µmol/kg dry weight
Zn
µmol/kg dry weight
Se
µmol/kg dry weight
SN CG LC HP MEDPVC MTG CB MCX

Figure 5. 1. Metal concentrations in PDD cases vs controls

Case–control differences determined by Mann–Whitney U test. * $p < 0.05$; ** $p < 0.01$. Abbreviations: SN = substantia nigra; CG = cingulate gyrus; LC = locus coeruleus; HP = hippocampus; MED = medulla; PVC = primary visual cortex; MTG = middle temporal gyrus; CB = cerebellum; MCX = motor cortex. Na = sodium; Mg = magnesium; K = potassium; Ca = calcium; Mn = manganese; Fe = iron; Cu = copper; Zn = zinc; Se = selenium.

Figure 5. 2. Number of altered metals per brain region

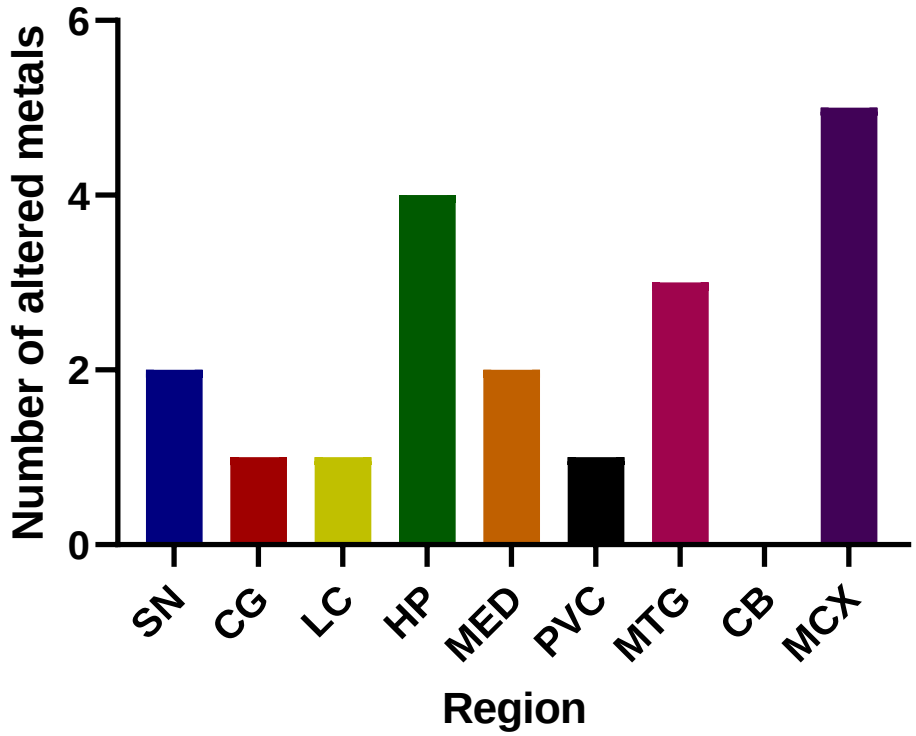

SN = substantia nigra; CG = cingulate gyrus; LC = locus coeruleus; HP = hippocampus; MED = medulla; PVC = primary visual cortex; MTG = middle temporal gyrus; CB = cerebellum; MCX = motor cortex. Na = sodium; Mg = magnesium; K = potassium; Ca = calcium; Mn = manganese; Fe = iron; Cu = copper; Zn = zinc; Se = selenium.

5.3.4. Comparison to AD Findings

We compared our results in PDD with AD cohort investigated with the same methodology (168) in five regions including the HP, MTG, MCX, CG, and CB. The SN, LC, PVC, and MED were only investigated in PDD, and the entorhinal cortex (ENT) and sensory cortex (SCX) only investigated in AD.

The widespread decreases in Cu in the MCX, CG, HP, and MTG was the most striking similarity between the PDD and AD (see Figure 5.3). Cu was also decreased in the SCX, ENT, and CB of AD brains, and in the SN, MED, and PVC of PDD brains. CB was the only region with dissimilar Cu concentration, with decreases in AD and no change in PDD brains. Several perturbations including decreased Mg, K, Mn, Zn, and Se were found in the CB of AD brains but no changes were found at all in the PDD CB, indicating a relative sparing of the CB in PDD compared to AD.

There were no other shared perturbations in metals between AD and PDD. Decreased K was observed in both conditions, however, with regional differences: in the MCX, HP, and MTG of PDD brains, and the CG and CB in AD cases. Likewise, although decreases in Mg, Mn, Zn, and Se were found in both PDD and AD brains, they occurred in differing regions (see Figure 5.3). Increases in Na, Mg, Ca, Fe, Mn, and Zn were identified in some regions of the AD brain, but not in any region of the PDD brain.

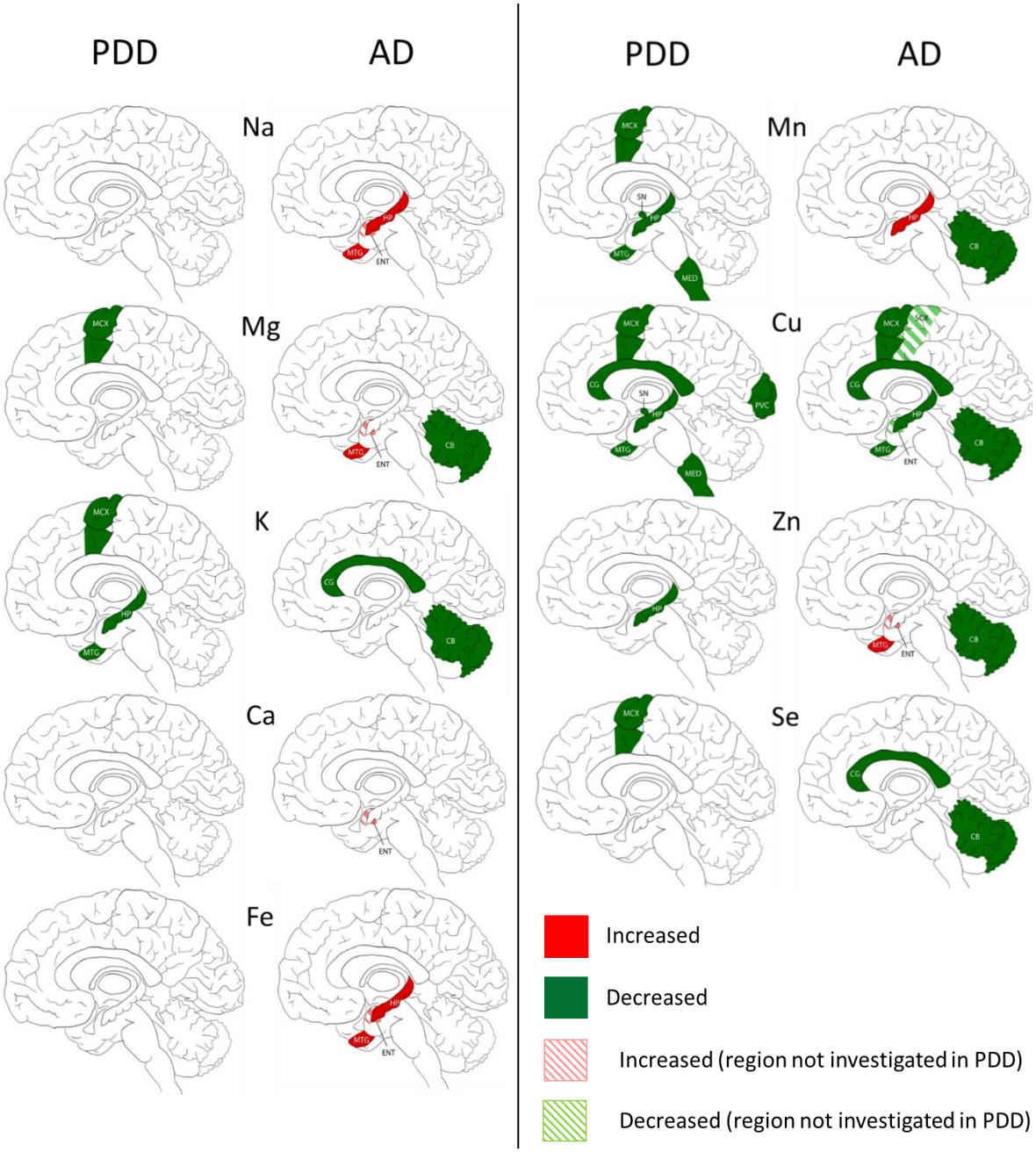

Figure 5. 3. Regional comparison of metal perturbations observed in PDD and AD brains

Abbreviations: SN = substantia nigra; CG = cingulate gyrus; LC = locus coeruleus; HP = hippocampus; MED = medulla; PVC = primary visual cortex; MTG = middle temporal gyrus; CB = cerebellum; MCX = motor cortex. Na = sodium; Mg = magnesium; K = potassium; Ca = calcium; Mn = manganese; Fe = iron; Cu = copper; Zn = zinc; Se = selenium.

5.4. Discussion

We investigated nine essential metals across nine brain regions in a cohort of clinically and neuropathologically defined PDD cases and documented reduction in Cu levels compared to controls and brains with AD.

Several studies have examined the role of individual metals in the brains with PD or PDD but none have described levels of multiple metals across several brain regions in PDD brains.

5.4.1. Copper (Cu)

That there are widespread decreases in Cu levels across seven of the nine regions investigated represents the most striking observation of this study. Decreased Cu has been reported within the SN (76, 78, 171, 349), CN and LC (171) of brains with α-synucleinopathy and clinical features of PD but never proved in patients with PD and dementia. Other studies that tested the neocortex (76), occipital cortex (OCC) and frontal gyrus (FG) (78), frontal cortex (FC), CN and CB (349) have reported no change.

Notably, decreases in Cu levels were observed in several brain regions that we previously found to be affected in AD brains (168), including the MCX, CG, HP, and MTG. Comparisons could not be made between the SN, MED, PVC, SCX, or ENT as they were each only investigated in one of the two conditions. One previous study reported no change within the SN in AD (169) but no data are available to the best of our knowledge on the MED, and PVC in AD, or on the SCX or ENT in PDD.

One region that clearly distinguished PD from AD in this study was the CB, which has previously shown substantive Cu decreases in AD (168), but showed no change here in PDD for Cu or any other metal. It is possible that this dissimilarity contributes to some of the symptomatic differences between AD and PD, either by cerebellar involvement in the more aggressive cognitive decline seen in AD, or by protection against typical Parkinsonian symptoms that are not often observed in AD such as hallucinations, motor symptoms, or rapid eye movement sleep behaviour disorder (350). A protective role for the CB is supported by proteomic and metabolomic findings in the AD brain, which have shown that although there are many protein and metabolite changes in the AD CB, they are drastically

different from those observed in regions heavily affected by neuronal loss in AD such as the HP (180, 351). This protective function may be lost in PDD.

Cu is an essential co-factor for several important antioxidants, including superoxide dismutase 1 (SOD1), which is responsible for removing harmful superoxide ions and hydrogen peroxide species from cells. Cu is also an essential component of ceruloplasmin, a ferroxidase which oxidises reactive ferrous Fe (Fe^{2+}) to its non-toxic ferric form (Fe^{3+}). This prevents production of hydroxyl radicals by ferrous Fe via the Fenton reaction (352). As such, decreases in Cu may lead to less effective removal and increased production of reactive oxygen species (ROS), resulting in increased oxidative stress in AD and in PDD (353). Indeed, increased oxidative stress has been reported widely in PD cases (354). SOD1 itself has been shown to display metal deficiency and to misfold in the SN and LC of PD cases (355). Indeed, decreased Cu binding to SOD1 has been proposed to contribute directly to build-up of misfolded and dysfunctional SOD1 in PD brains independently of mutations (356).

Cu is also an essential component of cytochrome *c* oxidase, which is responsible for transferring electrons between subunits III and IV of the mitochondrial electron transport chain (ETC). As such, decreased Cu could impair cytochrome *c* oxidase function and by extension ATP production via the mitochondrial F_1F_0 ATP synthase (also known as the H^+-ATPase or complex V). Mitochondrial dysfunction in PD is widely recognised (354) and experiments in a paraquat-exposed mouse model of PD have reported involvement of cytochrome *c* oxidase in α-synuclein oligomerisation and radical formation (357).

Together these observations suggest that decreased Cu in PD and AD could result in mitochondrial dysfunction, decreased energy production, increased oxidative stress, and perhaps even increased α-synuclein oligomerisation.

5.4.2. Manganese (Mn)

Another common finding in this study was decreased Mn, which was observed in six of nine regions investigated here: the MCX, SN, HP, MTG, LC and MED. Previous studies have reported no change in Mn levels in the SN (78, 349), OCC, FG (78), FC, CN or CB (349) of PD patients. No studies investigating any of the other regions covered here could be found.

PD has previously been suggested to be linked to increased Mn levels due its clinical similarity to manganism. Manganism is a condition caused by environmental exposure to Mn and is characterised by Parkinsonian symptomology and increased Mn levels in the brain. However, manganism patients do not display neuropathological signs of PD (358) or respond to dopaminergic drug treatment (359). Mn exposure has been shown to cause dopaminergic neuronal loss (360) and motor impairments in rats (361). However, surveys on humans show little support for the role of Mn exposure in the risk of developing PD itself, and increased levels have not been reported in the brain (362).

Mn is a cofactor for SOD2. This form of SOD is largely localised to the mitochondria in eukaryotic cells, where it can remove ROS produced by the mitochondrial ETC. As such, decreased Mn may also lead to increased oxidative stress in PDD. Combined with Cu decreases, this could lead to a dramatic decrease in SOD anti-oxidative function. Mn is also required for proper functioning of the urea cycle, with catalyses the break-down of toxic ammonia-containing compounds to urea for excretion. This requires the enzyme arginase, a Mn-containing enzyme which catalyses the final step of the urea cycle, converting arginine to ornithine and urea. Decreased Mn could lead to a reduction in arginase activity, resulting in toxic accumulation of ammonia-containing compounds. At present, little to no research has been done investigating a role for the urea cycle in PD or PDD.

5.4.3. Zinc (Zn)

Zn is the last of the three SOD metal cofactors. Cu/Zn-SOD1 is primarily localised to the cytosol but is also found in the mitochondria of cells (363), where it serves the same antioxidative function as Cu-SOD1/3 and Mn-SOD2. This study found decreased Zn in the HP of PDD brains, with no other region affected. Zn has been previously reported to be unchanged in the SN of PD brains (78, 349) as well as the OCC and FG (78) and the FC, CN, and CB (349). These reports agree with our own observations in the SN and CB, but no other investigations have yet been performed on the HP.

In these experiments, the HP of PDD cases was the only region found to have simultaneously decreased Cu, Mn, and Zn, meaning that all three SOD metal cofactors were diminished in this area. Cumulatively, this could have a dramatic effect on SOD function in

the PDD HP, resulting in increased oxidative stress. It is possible that this cumulative effect in an area heavily involved in cognitive function contributes to the increase in hippocampal neuronal loss and dysfunction observed in PDD compared to PD without dementia (364).

5.4.4. Selenium (Se)

Se was observed here to be decreased in the MCX only of PDD brains. A single report on Mn in the PD brain reported no change in the FC, CN, SN, or CB (349). There have been no previous investigations of Mn in the PD MCX.

Like Cu, Zn, and Mn, Se contributes to anti-oxidation in the cell by acting as a regulatory cofactor of antioxidative enzymes such as glutathione peroxidases, which are involved in removal of hydrogen peroxide via the oxidation of reduced glutathione (GSH) to oxidised glutathione (GSSG). Previous investigations have observed upregulated glutathione peroxidase 4 (GPX4) around surviving dopaminergic cells in the PD SN despite decreased levels of the enzyme overall, suggesting that GPX4 may play a neuroprotective role in PD (72). Se is also a cofactor for several other antioxidative enzymes, including thioredoxin reductases, the first of which has been reported to be decreased in the SN of PD mouse models (365).

5.4.5. Magnesium (Mg)

Like Se, Mg was also found to be decreased only in the MCX of PDD cases. Previous studies have reported decreased Mg in the CN but not in the FC, CN, CB (349), SN, (78, 349), OCC or FG (78). There are no previous reports on Mg in the PDD MCX.

Restricting Mg intake in the rat over several generations has been shown to result in SN-exclusive dopaminergic neuron loss, although the effects on the MCX have not been reported (366). Mg is also bound to a specific site in cytochrome *c* oxidase and regulates release of the complex into the mitochondria, as well as increasing NADH oxidation in the ETC (367). As such, lowering of Mg may result in dysfunction of the mitochondrial ETC and diminished ATP production. This could be compounded by simultaneous decreases in Cu and Mg in the PDD MCX.

5.4.6. Potassium (K)

Decreased K was found in three PDD brain regions investigated in this study; the MCX, HP, and MTG. A single previous investigation has reported no change in K levels in the PD FC, CN, SN, or CB (349). This corresponds with the lack of change observed by ourselves in the PDD SN and CB. Other investigations on the MCX, HP, or MTG could not be found.

During neuronal apoptosis, K channels are upregulated, resulting in increased K efflux from the cell. This in turn promotes apoptosis itself, contributing to widespread neuronal loss in neurodegenerative conditions such as AD or stroke (368). Decreased K levels in the MCX, HP, and MTG may reflect and contribute to increased apoptosis in these areas.

5.4.7. Iron (Fe)

One of the most common reports in the current literature investigating metal changes in PD are of increased Fe in the substantia nigra (SN (76-81, 278, 369). Some studies however have found no change in Fe levels within the SN of PD cases (349, 370, 371). Where additional regions have been investigated, a lack of change has generally been observed, including in the white matter (77); the OCC and FG (78); and the FC (349). Two sources have found no change in the raphe nucleus (77, 81), the CB (278, 349), the putamen (77, 369), and the cortex (77, 278), and three reports have also observed no change in the CN (81, 278, 349) and globus pallidus (77, 81, 369). There are however one reports of increased Fe in the putamen of PD patients (81) and in the globus pallidus (278). These observations largely agree with our own here, as we also observed no Fe changes in the PVC (located in the OCC), CB, or other cortical regions.

However, we also did not observe any change in the SN, where Fe increases are frequently reported. These reports are not universal though, with others observing no change in this region (349, 370, 372). These discrepancies have prompted a consideration of factors which may contribute to such disparate findings. One possibility is that whilst there may be differences in labile Fe, this may not be reflected by a change in total Fe concentration, which was measured in this study (372). Fe levels have also been observed to be highly heterogeneous between PD patients (373). This may contribute to differing findings between studies, especially as investigations of human brain tissues are generally only

possible on small cohorts of patients, either due to the limited availability of post mortem tissue or the practical difficulties of imaging large numbers of volunteers. Of additional note, two studies which investigated the substantia nigra pars compacta (SNpc) and substantia nigra pars reticula (SNpr) separately, observed increased Fe in the former and no change in the latter (77, 369). This is contrary to observations of increased Fe in both the SNpc and SNpr elsewhere (81). As such, it is possible that the area of the SN selected for study may affect observed metal levels. The effect of this possibility on the current study is indeterminable as different sub-regions of the SN were not distinguished during tissue dissection.

5.4.8. Sodium (Na) and Calcium (Ca)

Na and Ca were not found to change in any region of the PDD brain investigated here. This supports previous reports of no change in Ca or Na levels in the PD FC, CN, SN, and CB (349).

5.5. Conclusions

This study is the first to investigate differences in essential metals across multiple regions of the PDD brain. Although several studies looking at specific metals such as Cu, Fe, and Zn have been conducted in PD, these usually focus on the substantia nigra and do not distinguish between PD cases with and without dementia. PDD has not been as widely investigated as PD without dementia. The observations from this study confirm that PDD is driven by increased oxidative stress and mitochondrial dysfunction due to a loss of antioxidative and ETC enzyme metallomic co-factors including Cu, Mn, Zn, Se, K, and Mg. This includes widespread Cu decreases in PDD brains, reported for the first time here, affecting seven of the nine regions investigated, including the SN, CG, HP, MED, PVC, MTG, and MCX. This report also includes the first direct comparison of multiple essential metals across several brain regions in AD and PDD—observing shared decreases in Cu levels in the CG, HP, MTG, and MCX, as well as the relative sparing of the CB in PDD compared to AD. These findings indicate both shared mechanisms and regional variations between these two conditions that have not been previously observed.

Chapter Six | Effects of Alterations of Post mortem Delay and Other Tissue-collection Variables on Metabolite Levels in Human- and Rat-brain

This chapter was published as a manuscript in Metabolites: Scholefield M, Church SJ, Xu J, Robinson AC, Gardiner NJ, Roncaroli F, et al. Effects of alterations of post-mortem delay and other tissue-collection variables on metabolite levels in human and rat brain. Metabolites. 2020;10(11) (103), and is presented here with minor amendments. As with the metallomic analysis, it was necessary to determine whether metabolomic findings would remain consistent across multiple cohorts differing across different variables, such as PMD, disease staging, age- and sex-matching, etc. As such, a pilot study was carried out using AD brain tissues obtained from Manchester and Newcastle brain banks in order to compare findings to the previously-analysed Auckland AD cohort, and see if metabolite alterations differed or remained consistent.

In addition, an untargeted metabolomic analysis of healthy rat brains was carried out in order to more closely look at the effects of PMD on metabolite levels over a 72-hour period in a more controlled setting, where samples were age- and sex-matched, and were free from the effects of any disease. This data was used to determine the suitability of UK brain banks for supply of PDD samples for metabolomic analysis, as low donor numbers make it difficult to obtain such tissue with low PMD or extensive matching.

6.1. Introduction

Alzheimer's disease (AD) is the most common form of age-related dementia and currently affects more than 44 million people worldwide. Its incidence is projected to more than triple by the year 2050 (374). Despite AD being a leading cause of death in many countries, including the UK (375), there is still no treatment that can slow or halt the condition.

A lack of understanding of the pathogenesis of AD impacts current progress in developing effective treatments. Although research has aimed to determine the contributors to AD pathogenesis, including deposition of misfolded amyloid-β and tau, oxidative stress, inflammation, mitochondrial dysfunction, and protein and lipid dysregulation, such investigations have not yet led to the development of effective disease-modifying interventions (376). Many of the identified perturbations involve metabolic processes such as purine catabolism, glucose metabolism, and amino acid pathways (159, 333, 377-379). Such pathways may link seemingly disparate mechanisms provide potential explanations for AD pathogenesis, and suggest new therapeutic targets.

Currently, much research examining the role of these pathways in AD relies on pre-clinical models. However, human post mortem brain tissue is vital for investigating the mechanisms of AD. Although post mortem brains cannot represent a dynamic living system, tissues taken from individuals who died with AD can provide direct insight into the disease and can be compared to tissue from matched controls (380).

There are 'known unknowns' that apply to the use of human brain tissues for the investigation and modelling of AD in case–control studies. Factors that can vary either randomly or systematically among individual donors or institutions include: cause of death, post mortem delay (PMD), tau Braak stage (381), extent and severity of amyloid deposits, vascular pathology and other co-existent pathologies, age, and gender. There is little information currently available on the impact of these factors on the metabolome—the composition of all metabolites in a tissue—which has not yet been investigated.

This investigation aimed to determine the effects of identified variables on tissue-metabolite concentrations from human AD and control-brain tissue, with cingulate gyrus

as the representative brain tissue. The effects of PMD in particular were further examined under controlled conditions by using healthy adult rat-brain tissues.

6.2. Methods

6.2.1. Acquisition of Brain Tissue

The cohorts used in this study have been extensively characterised in a previous metallomics study (348). In brief, human cingulate gyrus samples were obtained from 9 AD cases and 9 normal controls without neurological conditions, from each of three geographically-distinct brain banks: the Manchester Brain Bank based at Salford, UK; the Newcastle Brain Bank based at Newcastle, UK; and the New Zealand National Brain Bank based at Auckland, New Zealand. Patient metadata were obtained for variables including the following: age at death, gender, tau Braak stage, CERAD, Thal phase, small vessel disease (SVD) score, cerebral amyloid angiopathy (CAA) score, and PMD for each donor.

Cortical and cerebellar tissues from twenty healthy adult Wister Han rats were also investigated for this study using a previously described protocol (348). Rats were terminally-anaesthetized (isoflurane), culled by decapitation, and stored at 4^{o}C for post mortem intervals of 0, 24, 48, and 72 hours before collection of brain tissues.

6.2.2. Diagnosis & Severity of Human Cases

All cases and controls were diagnosed at post mortem examination by consultant neuropathologists at the respective brain bank. All cases had a confirmed diagnosis of AD, whereas controls had only showed age-related changes. Characteristics of individuals and cohorts are included in Supplementary Tables 6–11 (p397–406).

6.2.3. Tissue Dissection

Brain tissues were dissected into samples of 50 mg (± 5 mg) for GC–MS (gas chromatography/mass spectrometry) analysis using a metal-free ceramic scalpel. Samples were placed in ‘Safe-Lok’ microfuge tubes (Eppendorf AG; Hamburg, Germany) and stored at -80°C until analysis.

6.2.4. GC–MS

Samples from each brain bank were analysed in separate runs. In brief, brain tissue was extracted in 800 µl 50:50 (v/v) methanol:chloroform containing 0.016 mg/ml labelled internal standards (citric acid-d_4, $^{13}C_6$-D-fructose, L-tryptophan-d_5, L-alanine-d_7, stearic acid-d_{35}, benzoic acid-d_5, and leucine-d_{10}; Cambridge Isotopes Inc.; Tewksbury, MA). Tubes containing 800 µl of the methanol:chloroform solvent (without any sample) were prepared for extraction blanks. Samples were lysed in a TissueLyser batch bead homogeniser (Qiagen, Manchester, UK) at 25 Hz for 10 min with a 3 mm tungsten carbide bead before addition of 0.4 ml water and separation of polar and non-polar phases by centrifugation at 2400 x g for 15 min. 200 µl of the polar phase was transferred to a new tube and dried overnight in a Speedvac centrifugal concentrator (Savant Speedvac, Thermo Scientific, UK) at ~25°C for 16–18 hours. An additional 200 µl was taken from each sample and pooled in order to create a quality control (QC), which was used to monitor any variation in GC readings over the course of the run. Quality control leads (QLs) were quality controls included at the beginning of the run as lead-ins in order to avoid variation in GC readings of samples during start-up. Samples were stored overnight at 4°C before derivatisation. Methlyoxime/trimethysilyl (TMS) derivatisation was used, and retention markers added to each sample before centrifugation. Samples were taken immediately for GC–MS analysis.

GC–MS analysis was performed using 7890A gas chromatograph with split/splitless inlet (Agilent; Santa Clara, CA) fitted with an Agilent/J&W DB17-MS column (30 m × 0.25 mm × 0.25 µm) with a 3 m × 0.25 mm retention gap, an MPS2 autosampler (Gerstel; Mulheim an der Ruhr, Germany), and Pegasus HT time-of-flight mass spectrometer (LECO; Stockport, UK). A helium carrier gas was used at a constant flow of 1.4 ml/min. Injections of 1 µl of sample were made in splitless mode at an inlet temperature of 270°C; the initial temperature inside the column was 50°C for 6 min, followed a ramp up to 300°C at 10C/min, and held at 300°C for 4 min before cooling to the initial temperature in the next cycle. Each cycle took 42 min after the initial 450 second solvent delay.

Ten spectra per second were acquired over the mass range of 45–800 Da in order to detect TMS derivatives of amino acids, sugars, sugar alcohols, organic acids, and miscellaneous organic molecules. QL samples were placed as a lead-in before samples and QCs were

interleaved evenly (every four samples) throughout the run. Extraction blanks were included at the beginning and towards the end of the run to confirm absence of carryover in each run. Samples were randomised in each run.

6.2.5. Data Acquisition

Data were prepared by a 'Reference Compare' method in ChromaTOF 4.5 (LECO; UK), using the NIST Mass Spectral Reference Library (NIST08/2008; National Institute of Standards and Technology/Environmental Protection Agency/National Institutes of Health Spectral 262 Library; NIST, Gaithersburg, MD, USA); and the Golm Metabolome Database (Max Planck Institute of Molecular Plant Physiology, Potsdam-Golm, Germany). Chromatographic retention-time data were obtained through our own in-house library reference standards.

Expected retention time (based on the library retention times) and peak shape were manually integrated to constitute a definitive molecular identification, using identified metabolites from QC pooled samples as a representative reference list for the human cingulate gyrus. After removal of ambiguous and low-quality spectra, a total of 83 unique signals were identified and selected from the GC–MS chromatogram for use in the reference list. This list was then applied to every sample, using a tolerable retention-time deviation of 6 seconds and manual validation to ensure correct peak integration. Instead of raw peak areas, internal standard ratios were used for each metabolite; this was achieved by determining the heavy internal standard which yielded the lowest variance for each individual metabolite across all the QC injections.

6.2.6. Data Analysis

Multivariate principal-component analysis (PCA) and partial least squares discriminant analysis (PLS–DA) were performed on the entire list of identified metabolites in order to identify any separation of the samples into groups by applying MetaboAnalyst software (metaboanalyst.ca; Canada). Samples located far away from the sample clusters on plots were identified as outliers and removed from the final analysis (See Electronic Appendices E & G for plots both with and without outliers). Statistical significance of individual metabolites was calculated using multiple 2-tailed t-tests corrected for potential effects of

multiple comparisons by applying a false-discovery rate (FDR) of 10% using GraphPad v6.04 (Prism; La Jolla, CA). Metabolites with a coefficient of variation (CV) ≥30% in quality controls were disregarded. Where multiple signals were identified for a single metabolite, the adduct with the strongest signal was used in this analysis. However, a list of all identified signals is included in Electronic Appendices D & F.

6.3. Results

6.3.1. Cohort Comparisons in Human Brain Tissue

A comprehensive description and comparison of the human brain cohorts has been reported previously, with details for each individual sample (348). In brief, the cingulate gyrus was obtained from nine AD cases and nine controls from each of three geographically-distinct brain banks based in Auckland, New Zealand, and Manchester and Newcastle, UK. Cingulate gyrus tissue was selected as it is a region that is widely available from brain banks and has also been reported to show changes in several metabolites in AD (180). It was also chosen as a more suitable pilot region for validation than more in-demand regions, such as the hippocampus.

Tau Braak staging at time of death was on average found to be more advanced in Manchester (I-II; see Table 6.1) and Newcastle (I-II) controls than Auckland controls (0). Manchester controls (83 years) were older than Auckland controls (72 years) by around a decade on average. Both Newcastle cases (85 years) and controls (83 years) were on average older than Auckland samples by around a decade. Average PMD for the Manchester (82 hours) and Newcastle (46 hours) was also higher than Auckland samples (11 hours).

Consortium to Establish a Registry for Alzheimer's Disease (CERAD), SVD, Thal, and CAA scores were also acquired where available from brain bank databases (see Table 6.1 for CERAD and CAA cohort scores). Due to the limited availability of this data, this information could not be obtained for some samples in the UK cohorts, or for any of the Auckland samples. Thus, comparisons between cohorts were not possible. However, individual data are shown in Supplementary Tables 6–8 (p397–403) where available. Many cases from the Manchester and Auckland cohorts (three and fourteen respectively) had moderate to

severe CAA. Five Manchester cases had moderate to severe SVD. Severity of CAA did not significantly differ between cases and in either cohort, nor did severity of SVD in the Manchester cases (data not shown). Where available, CERAD scores showed a significant correlation with Braak stage ($p < 0.0001$; see Table 6.1).

Table 6. 1. Comparison of Brain Bank Groups

Variable	Manchester Controls	Newcastle Controls	Auckland Controls
Number	9	9	9
Age	89 (82-95)	85 (76-94)	73 (61-78)[a,c]
Male Gender, n (%)	6 (66.7)	6 (66.7%)	7 (53.8)
Braak Stage	I-II (0-I – II)	I-II (I – II)	0 (0 – II)[a,c]
PMD (hours)	75 (49 – 130)	25 (9 – 40)[b]	12 (5.5-15.0)[c]
Whole Brain Weight (g)†	1160 (1020 – 1494)	1235 (1064 – 1406)	1260 (1094 – 1461)
CAA Score	None/Mild	Moderate*	NA
CERAD	0 (0 – A)	0 (0)	NA
Variable	**Manchester Cases**	**Newcastle Cases**	**Auckland Cases**
Number	9	9	9
Age	83 (61-89)	83 (70-95)	72 (60-80)[a]
Male Gender, n (%)	3 (33.3)	6 (66.7%)	5 (55.6)
Braak Stage	IV-V (IV – VI)	VI (VI – VI)[b]	V-VI (IV – VI)[c]
PMD (hours)	39 (12 – 70)	25 (9 – 41)[b]	7 (4.0-12.0)[c]
Whole Brain Weight (g)†	1066 (900 – 1359)	1155 (959 – 1351)	1062 (831 – 1355)
CAA Score	Mild/Moderate	Moderate/Severe*	NA
CERAD	C (B – C)	C (B – C)*	NA

Age, male (%), Braak stage, PMD are means (range); CERAD scores are modes (range); CAA scores are modes; p-values for significance of between-group differences were calculated by one-way ANOVA followed by Tukey's test. [a] $p < 0.05$ between Newcastle and Auckland cohorts; [b] $p < 0.05$ between Newcastle and Manchester cohorts; [c] $p < 0.05$ between Manchester and Auckland cohorts. See Supplementary Tables 6–8 for details of individual cases and controls. CAA = Cerebral amyloid angiopathy; PMD = post mortem delay; NA = Not available. *Data not available for some samples (see Supplementary Tables 6–8).

Figure 6. 1. CERAD Score vs tau Braak Stage

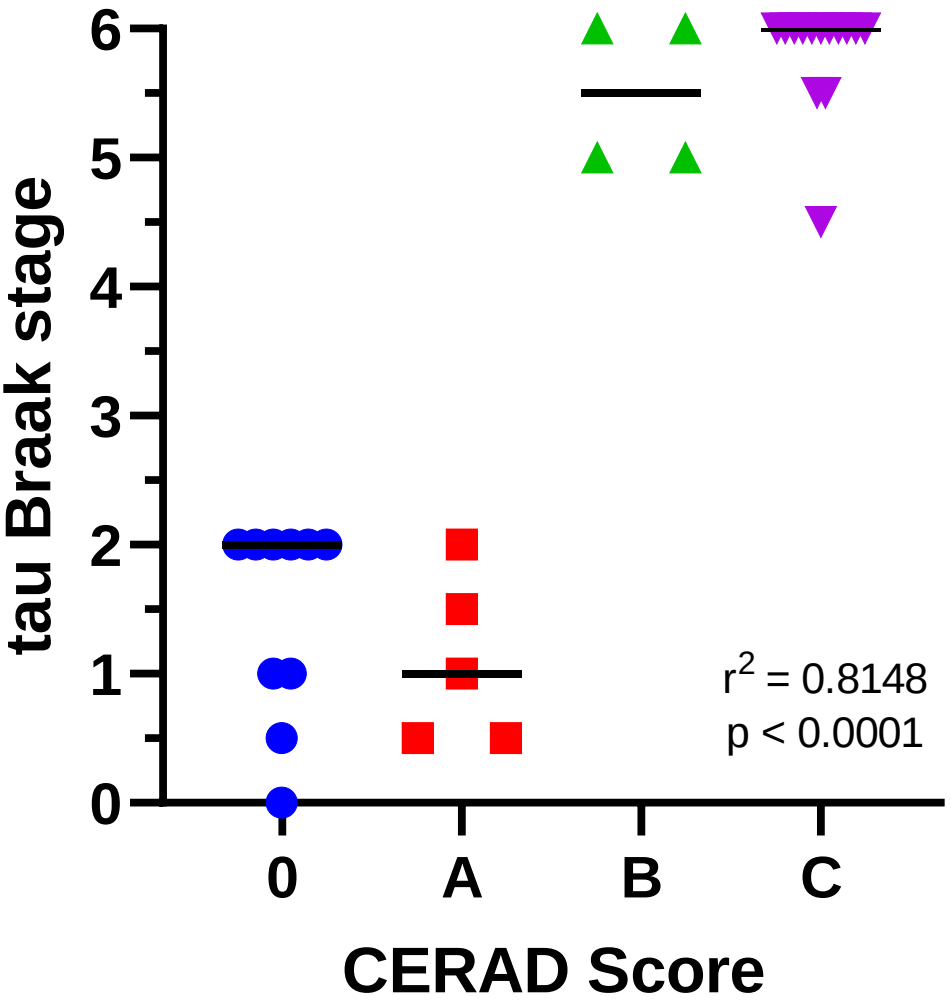

Scatter plot shows individual CERAD/Braak scores with medians. A Spearman's rank-order correlation was run to determine the relationship between CERAD score and tau Braak Stage. There was a strong positive correlation which was statistically significant (r^2 = 0.8148; $p < 0.001$).

6.3.2. Human Brain Metabolite Analysis

Following a previous analysis on the Auckland cohort (184), an investigation of two distinct cohorts from the Manchester and Newcastle brain banks was performed in order to investigate whether findings from different groups would produce similar findings. A total

of 66 unique metabolites were identified in tissue from the cingulate gyrus of nine AD cases and nine controls in both the Manchester and Newcastle cohorts.

6.3.2.1. Newcastle Cohort

Two significantly altered metabolites were identified within the Newcastle cohort: increased myo-inositol and glycerol-3-phosphate in cases compared to controls (see Figure 6.2A; see Electronic Appendix D for table of all identified metabolites). However, no separation was found between cases and controls, or between individuals of different gender, age, disease stage, PMD, CAA, or brain weight when mapped onto a (PLS–DA) plot (see Figure 6.2B). Both quality control measurements (QCs) and (QLs) were closely clustered (with the exception of the first QL; see Electronic Appendix E), consistent with a successful GC run.

6.3.2.2. Manchester Cohort

No significantly altered metabolites were identified within the Manchester cohort (see Electronic Appendix D for table of all identified metabolites). Additionally, no separation was found between cases and controls, or between individuals of different gender, age, Braak staging, CERAD staging, CAA or SVD, PMD, or brain weight when mapped on to a PLS–DA plot (see Figure 6.2C). Again, QCs were tightly clustered, suggesting an accurate GC run. There were two outliers far removed from the other samples (cases AD5 ‘09/15’ and AD9 ‘10/17’; see Electronic Appendix E, Figure E1.I., p6) within the case group, which were removed from the final analysis. These samples could not be distinguished from other individuals in the group by age, gender, disease staging, CAA/SVD, PMD, or brain weight.

Figure 6. 2. Metabolomic Analysis of Newcastle and Manchester Cohorts

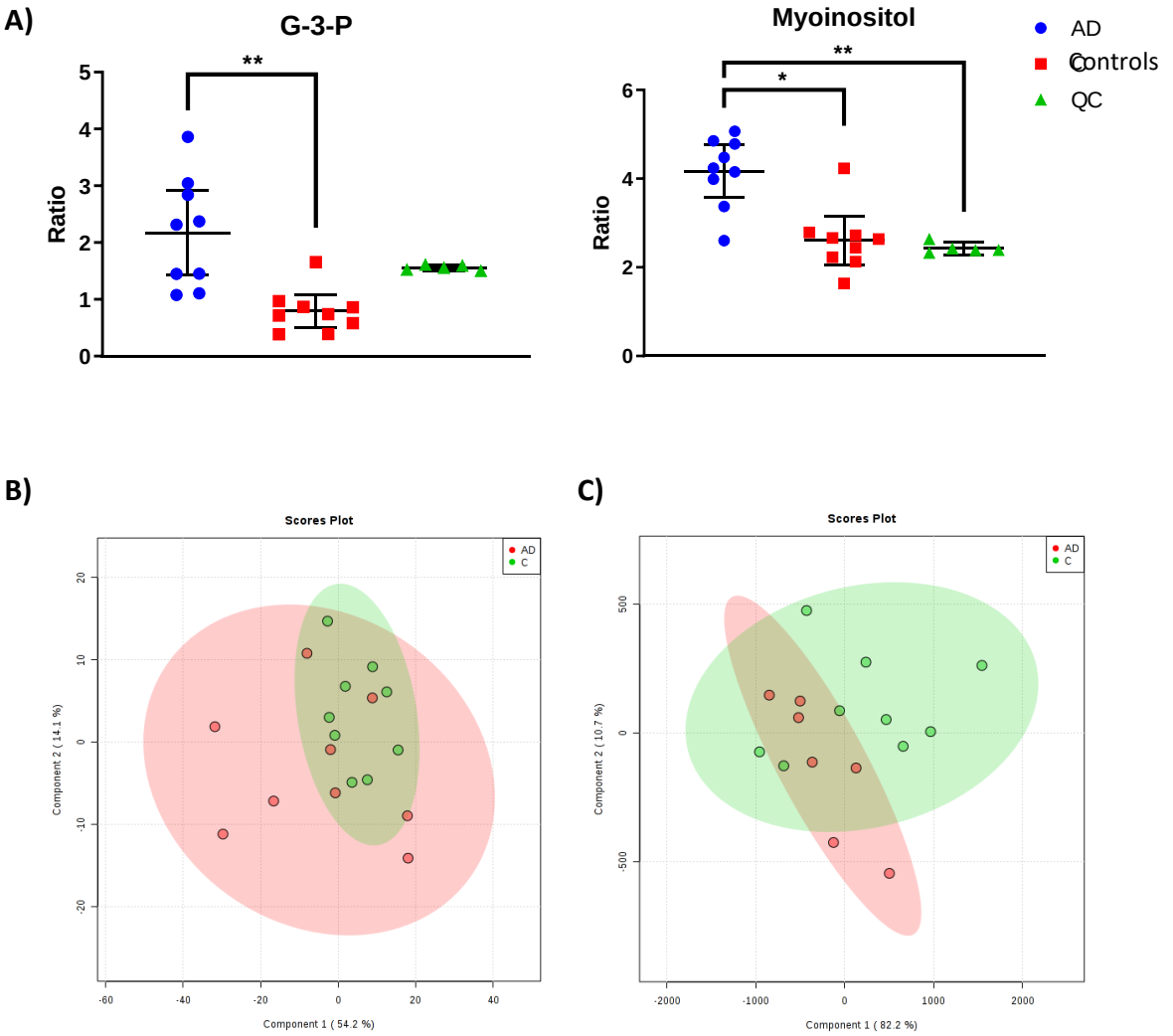

A) Glycerol-3-phosphate and myo-inositol were the only significantly altered metabolites between cases and controls in the Newcastle cohort. Graphs show ratios of significantly altered metabolites in comparison to internal standards within cingulate gyrus of cases (blue), controls (red) and quality control values (QCs; green). Error bars show ± 95% confidence intervals. Inter-group differences calculated by Kruskal-Wallis test: * $p < 0.05$; ** $p < 0.01$ **B)** PLS–DA plot of metabolites in cingulate gyrus of the Newcastle cohort. Cases are shown in red and controls in green. See Electronic Appendix E for labelled and unlabelled PCA and PLS–DA plots. **C)** PLS–DA plot of metabolites in cingulate gyrus of the Manchester cohort. Cases are shown in red and controls in green. See Electronic Appendix E for labelled and unlabelled PCA and PLS–DA plots.

6.3.2.3. Comparison of All Cohorts

Although the results of the metabolite analysis within the Newcastle and Manchester cohorts were similar, they were markedly different from those previously found within the Auckland cohort (180). Within the Auckland cohort, 28 of 69 identified metabolites were found to be significantly altered between the cingulate gyrus of cases and controls. One of these was glycerol-3-phosphate, which was 1.8-fold higher in cases than in controls; the only finding which was also present in the Newcastle cohort. However, unlike the Newcastle cohort, no significant change was found in myo-inositol between Auckland cases and controls. None of the case–control differences present in the Auckland group were found in the Manchester cohort. Significant findings in the Auckland group included large (5-fold or more) increases of several metabolites in cases compared to controls, including glucose, sorbitol, fructose, glucose-6-phosphate, and fructose-6-phosphate, all involved in glucose metabolism pathways (180). There were no significant changes in any of these metabolites found in either of the UK cohorts.

6.3.3. Effect of PMD on Metabolomic Analysis of Rat Brain Tissue

6.3.3.1. Analysis of Metabolites from Rat Brain

In order to determine any effects of PMD on metabolite levels within the brain in a more controlled manner, a metabolomics analysis was carried out on the brains of rats controlled for both age and gender, with PMDs of 0, 24, 48, and 72 hours. 63 unique metabolites were measured in the post mortem cerebral cortex and cerebellum of forty healthy adult Wistar Han rats.

Of these metabolites, 21 were unchanged in either region over the whole period of up to 72 hours PMD (see Table 6.2). Of these, four showed a coefficient of variation (CV) higher than 30% in the quality controls (QCs) in at least one of the brain regions and so were discarded (alanine, tryptophan, glutamine, hexanedioic acid). Phthalic acid was unchanged in the cortex, but was not identified in the cerebellum (see Table 6.2). Included in the 16 remaining metabolites were glucose, urea, lactic acid, and several carboxylic and fatty acids such as benzoic acid, malic acid, and phosphoric acid. Among the unaltered metabolites were molecules that have been previously associated with AD, such as glucose, urea, and n-acetylaspartic acid (NAA; see Table 6.2 and Figure 6.3).

Table 6. 2. Unaltered Metabolites in Rat Brain Tissue

Metabolite	Cortex					Cerebellum				
	Ratio at 0 Hours	Ratio at 24 Hours	Ratio at 48 Hours	Ratio at 72 Hours	P-Value (0 vs 72 Hours)	Ratio at 0 Hours	Ratio at 24 Hours	Ratio at 48 Hours	Ratio at 72 Hours	P-Value (0 vs 72 Hours)
Alternative Fuel Sources										
Lactic acid	0.6	0.5	0.6	0.6	0.9	0.4	0.5	0.5	0.5	0.8
Amino Acids and Related Compounds										
Hydroxylamine	3.0	3.7	1.6	1.8	0.8	1.9	1.4	1.5	1.2	0.5
N-acetylaspartic acid (NAA)	12.3	13.8	12.6	12.3	0.9	24.5	25.3	22.4	21.7	1.0
Pyroglutamic acid	0.02	0.02	0.02	0.02	1.0	0.002	0.002	0.002	0.002	0.8
Glucose & Related Metabolites										
Glucose	0.01	0.01	0.02	0.02	0.3	0.04	0.04	0.05	0.05	0.8
Other										
1-Methyl-N,N-bis(trimethylsilyl)-4-[(trimethylsilyl)oxy]-1H-imidazol-2-amine	41.7	42.6	45.1	47.2	0.6	2.5	2.9	2.6	2.2	0.9

1-piperidinecarboxaldehyde	0.05	0.07	0.03	0.03	0.4	0.3	0.3	0.3	0.3	0.9
7,9-Di-tert-butyl-1-oxaspiro(4,5)deca-6,9-diene-2,8-dione	0.01	0.02	0.01	0.01	0.4	0.1	0.2	0.2	0.2	1.0
Benzoic acid	0.03	0.03	0.02	0.02	0.3	0.008	0.007	0.009	0.009	0.6
Malic acid	0.6	0.7	0.7	0.7	0.4	0.06	0.06	0.07	0.07	0.7
Palmitic acid	5.4	8.0	6.4	6.7	0.3	4.2	4.8	4.8	5.8	0.2
Phthalic acid	3.3	4.1	2.8	3.0	1.0	**NI**	**NI**	**NI**	**NI**	**NI**
Phosphoric acid	0.2	0.1	0.0	0.0	0.07	0.05	0.04	0.05	0.04	0.5
Silanol	15.2	17.0	14.9	14.8	1.0	13.2	14.4	13.0	14.0	1.0
Stearic acid	2.6	4.4	2.9	3.0	0.4	5.9	6.7	6.7	8.1	0.2
Threitol	0.07	0.09	0.09	0.09	0.2	0.007	0.009	0.010	0.010	0.7
Urea	5.7	2.6	2.7	2.1	0.09	0.7	0.8	0.8	0.7	0.7

Table shows mean ratio values (full list of values can be found in Electronic Appendix F). p-value between 0 and 72 hours PMD determined by two-way ANOVA. **NI** = Not identified.

Of 57 unique metabolites identified in the cortex, four showed a CV higher than 30% in the QCs and so were discarded (proline, hypoxanthine, tryptophan, and pyruvic acid). Of the remaining 53 metabolites, 22 were found to be significantly different between 0 and 72 hours PMD. Around 75% of the altered metabolites increased in concentration from 0 to 72 hours, most markedly cysteine (7.2-fold change; see Table 6.3), propanoic acid (5.8-fold change), and glycine (4.1-fold change). Others decreased, most notably adenosine (50-fold change). Of the altered metabolites in the cortex, ten already showed statically significant changes by 24 hours (see Electronic Appendix F). Some showed continuous changes across the entire 72-hour period, such as glycine, phenylalanine (see Table 6.3), and cysteine. Others stopped increasing or decreasing after 48 hours, including adenosine and glycerol-3-phosphate (see Table 6.2). As such, 24 hours PMD was sufficient to induce changes in several metabolites, with some changes peaking at 48 hours, and others continuing to change up to 72 hours and possibly beyond.

There was a clear separation of PMD groups on the PLS–DA plot of rat cortex metabolites, with the 0, 24, 48, and 72 hours separating linearly in numeric order (see Figure 6.4A). Three samples and one quality lead (QL) were identified as outliers and removed from the plot (see Electronic Appendix G, Figure G.1.I., p6).

Fifty-four unique metabolites were identified in the rat cerebellar tissues. Of these, seven showed a CV higher than 30% in QCs (alanine, hexanedioic acid, glutamine, hypoxanthine, tyrosine, 9H-purin-6-amine, and ascorbic acid) and were excluded. Of the remaining metabolites, two-way ANOVA showed that 23 differed significantly across different time points. These all showed increases in the 72-hour PMD group compared to the 0-hour PMD group, with the exception of adenosine minor, which decreased ten-fold, and fructose, which showed a two-fold decrease (see Table 6.3 & Figure 6.3). The largest increases were seen in methionine (7.5-fold), and phenylalanine (9.0-fold; see Figure 6.3). All but two of the altered metabolites in the cerebellum (threonine and uridine) already showed significant changes by 24 hours PMD (see Electronic Appendix F).

PLS–DA plotting again showed clear separation of different PMD groups, sequentially from 0 to 72 hours (see Figure 6.4B). One sample was identified as an outlier and removed from the plot (see Electronic Appendix G, Figures G.2.F & G.2.H., p9–10 for labelled data points).

Metabolite	Fold-Change	
	Cortex	Cerebellum
Alternative Fuel Sources		
Glycerol-3-phosphate	**0.5**	0.8
Amino Acids and Related Compounds		
Aspartic acid	1.2	**2.3**
Cysteine	**7.2**	**5.9**
Ethanolamine	0.7	1.9
GABA	1.0	**2.0**
Glycine	**4.1**	**2.1**
Isoleucine	**2.1**	**3.8**
Leucine	**2.2**	**3.2**
Methionine	1.3	**6.4**
Phenylalanine	**3.2**	**9.0**
Proline	1.5	**7.2**
Serine	1.3	**2.3**
Threonine	0.5	**1.8**
Tyrosine	**3.8**	**NI**
Valine	**2.1**	**3.4**
Glucose & Related Metabolites		
Fructose	0.7	**0.5**
Ribose	**2.0**	**2.5**
Ribose-5-phosphate	1.6	**2.4**
Sorbitol	**1.7**	**1.7**
Nucleosides		
Adenosine	**0.05**	**0.1**
Uracil	**2.8**	**3.2**
Uridine	**0.3**	**0.3**

Other		
9H-purin-6-amine	**1.8**	**EXC**
Hydroxybutyric acid	1.3	**2.0**
Pantothenic acid	**1.9**	1.4
Butanedioic acid	**2.0**	**2.4**
Ethylbis(trimethylsilyl)amine	**0.2**	1.0
Ascorbic acid	**0.2**	**EXC**
Propanoic acid	**5.8**	**5.0**
Pyroglutamic acid	**0.3**	0.9
Glycerol	**3.1**	**4.4**

Table 6. 3. Metabolites Significantly Altered in Rat Brain Tissue

Significantly altered ($p < 0.05$) metabolites between rat brain tissue PMD groups in each region are highlighted in bold. Mean fold-changes are between 0 and 72-hour PMD groups. **NI** = not identified; **EXC** = excluded due to QC CoV ≥ 30%.

Figure 6. 3. Unaltered and Altered Metabolites in Rat Brain Tissue

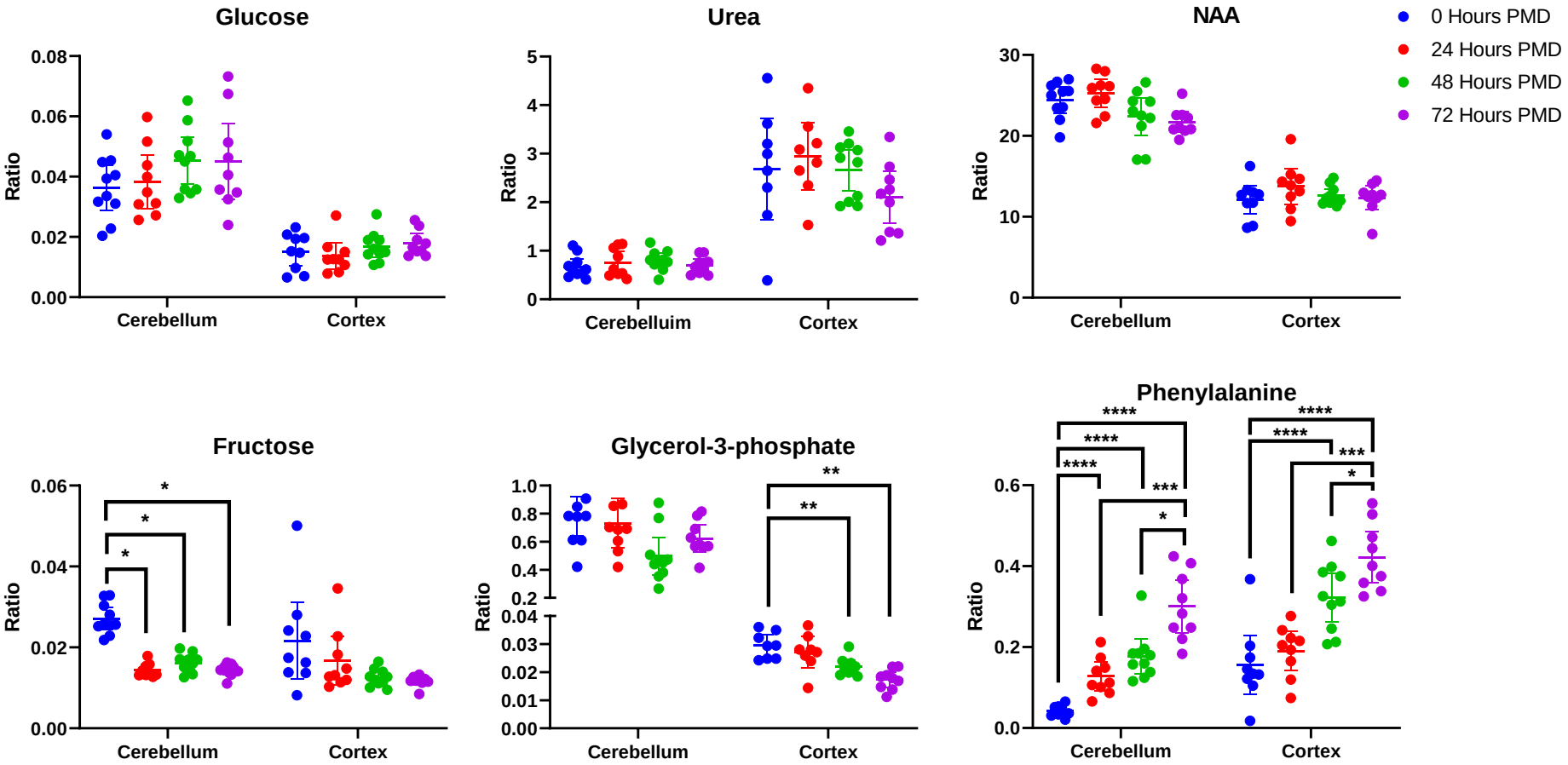

Data shown is individual metabolite ratios ± 95% confidence intervals. 23 identified unique metabolites were unchanged in either the rat cortex or cerebellum over a period of 72 hours post mortem delay (PMD), including metabolites previously associated with AD such as glucose, urea, and N-acetylaspartic acid. In the cortex, 22 metabolites were altered by 72 hours PMD including glycerol-3-phosphate and phenylalanine. 23 metabolites were altered in the cerebellum by 72 hours PMD, including fructose and phenylalanine. * < 0.05, ** < 0.01, *** < 0.001, **** < 0.0001. PMD = post mortem delay. Individual sample values, mean ratios, and fold-changes for all metabolites in the cortex and cerebellum can be found in Electronic Appendix F.

Figure 6. 4. PLS–DA Plots of Rat Brain Tissue Metabolites

A **B**

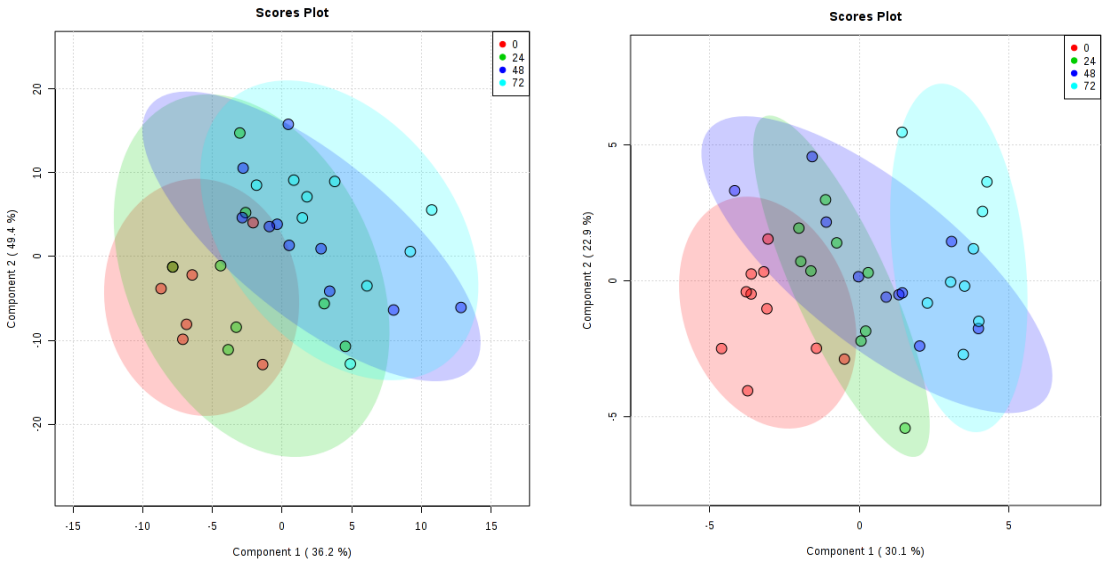

A. Rat cortex: No. of components = 4; R2 = 0.85; Q2 = 0.71. **B**. Rat cerebellum: No. of components = 4; R2 = 0.83; Q2 = 0.75. Ratios of identified metabolites in comparison to selected internal standards within rat brain tissues at 0-hour PMD (red), 24 hour PMD (green), 48 hour PMD (blue), and 72 hour PMD (purple). See Electronic Appendix G for labelled and unlabelled PCA and PLS–DA plots.

6.4. Discussion

6.4.1. Metabolomic Analysis

This study shows that measured levels of metabolites appear to be highly sensitive to variations in PMD. This finding follows a recent case–control study we conducted to investigate the effects of PMD, Braak stage, age, and brain bank location using the Auckland and Manchester cohorts. The study found no effect of any of these variables on levels of essential metals in brain tissue (348). As such it appears that brain metabolites do not show the same robustness to variability as metals do. No significant case–control differences in metabolite levels were observed in the Manchester cohort and only two metabolites were significantly different between AD cases and controls in the Newcastle group, in comparison to almost thirty metabolites within the Auckland cohort. Tight clustering of QCs in both UK cohorts suggests no errors with the running of the GC analysis, and that the given ratio values are precise. Additionally, repeats of two Auckland cases and controls that had been stored at -80°C for two years were analysed alongside the Manchester cohort and showed the same PLS–DA plot pattern as in the original analysis, consistent with reproducibility of results even when the same samples were analysed several years apart (data not shown).

As such, it appears that the lack of case–control differences observed within the groups may be due to the characteristics of the groups themselves. The Newcastle cohort was age, PMD, and gender-matched, whilst the Manchester cohort was not matched by any of these variables. Despite this, neither showed any of the case–control differences in metabolite levels observed in the Auckland cohort. This suggests that the lack of case–control differences observed in the two UK cohorts are not accounted for by case–control matching by these factors. However, both cohorts had cases and controls with higher tau Braak stage, as well as higher control ages, than the Auckland group. It is possible that the marked differences observed between the UK and Auckland cohorts could be influenced by either or both of these variables. Although there are many studies on metabolite levels in AD which go on to investigate correlations with Braak stage, few studies could be found measuring metabolite levels at individual stages (377) and comparing them directly, and

no such reports could be found which directly compared levels at Braak stage 0, I and II. As such, it is difficult to tell what the effect of Braak staging may be on metabolite levels in our own investigations, or whether differences in low Braak stages between controls in different cohorts may be exerting an effect on the metabolomic analyses.

Investigations on the effects of aging on selected metabolites in healthy brains have indicated that some metabolites are sensitive to increases in age, with reports of decreased NAA and increased myo-inositol in the brains of older healthy individuals (383). These changes are usually reported in comparisons of young (<50 years) and older (>50 years) groups, but can also be seen in investigations including only older individuals (384-386). However, to date there have been no studies on the effects of aging on the brain metabolome as a whole, with studies generally restricted to metabolites which can be imaged in living brains using MRI. This makes it difficult to assess the exact influence of control age on the findings reported here, but in combination with the present findings indicates that increased age most likely has an effect on at least some of the metabolites reported here, such as myo-inositol, even in healthy individuals.

To the author's knowledge, there have to date been no investigations on the effects of antemortem events on brain metabolite levels, although a study by Durrenberger and colleagues has observed that events such as hospitalization, coma, and ventilation prior to death are associated with lower RNA quality across six different regions of the human brain including the cerebellum (387). Several such antemortem events may be indicated by the causes of death recorded for the samples used in this study, but due to the large variations in and numbers of such events, as well as a lack of cause-of-death data for many samples, it is difficult to directly investigate any effects they may have here. However, the study by Durrenberger *et al.* also found no effect of PMD on brain RNA quality, a finding which has been replicated elsewhere (388-390). As such, these observations on the effects of antemortem effects on RNA may not be reflected in studies looking at metabolites. A previous study looking at the effects of PMD on brain metabolite levels has reported changes in the hippocampi of healthy mice as early as two hours post mortem, despite a lack of anatomical changes in neurons and glia for up to five hours (391). Another study comparing changes in nucleoside levels between rat and human brains at varying levels of

PMD observed several significant changes from two hours onwards, with similar patterns of change but differing concentrations between species (392). What is particularly lacking in the current literature is an untargeted metabolomics study comparing the effect of PMD across different brain regions within the same brain for delays of longer than 24 hours. Considering the length of PMD commonly found with human brain samples, studies of such longer periods are required to understand the effect of this variable on human brain tissue experiments. However, this is difficult to perform in human samples, as the same brain cannot be used to look at different PMDs due to the nature of sample collection, and there are too many variables involved in comparing samples from multiple donors. This type of experiment is however feasible using animal models, which can also be easily controlled for age, gender and other factors.

6.4.2. Effect of PMD on Metabolomic Analyses in Rat Brain Tissues

In this study, healthy adult rat tissues were used to look at the effect of different PMDs on cerebral metabolites; a parameter which varied greatly between different brain banks and individual human samples, whilst tightly controlling for the effects of age and gender.

The literature on the effect of PMD on rat brain tissues is limited. One study found steady decreases in catecholamine concentration in multiple rat brain regions (including the cortex and cerebellum) up to a period of 54 hours post mortem (393). Another study reported changes in proteins such as syntaxin in both human and rat cortex samples by 48 hours (394). Importantly, there were also decreases in post-synaptic density protein 95 (PSD-95) noted in human samples by 24 hours, whereas rat cortex PSD-95 remained stable for the entire measured period of 72 hours (394). This highlights the limitations that need to be kept in mind when applying animal data to human samples. Protein changes have also been observed to occur within the caudate-putamen, hippocampus, and medulla of rat brains in a period of up to 72 hours (395). These changes were not consistent across different areas of the brain, showing regional differences in susceptibility of the rat brain to such alterations, at least for protein concentrations.

A 2005 study by Kovacs and colleagues found that levels of several nucleosides were significantly altered by 24 hours PMD, and some even by as little as 2 hours in rat cortex

samples (392). In our experiment, inosine showed no significant changes in the cortex, contrary to decreases reported by Kovacs and colleagues. However, both Kovacs *et al.* and the present study observed a significant decrease in adenosine and increase in uracil concentrations by 24 hours PMD. Additionally, Kovacs *et al.* reported no changes in uridine over 24 hours; this was also observed here, with no decrease in uridine concentration until 48 hours. As such, several observations from the rat cortex were replicated here. However, this study was unable to detect all the nucleosides measured by Kovacs *et al.* (such as xanthine and hypoxanthine). It should also be noted that concurrent experiments run on human samples by Kovacs and colleagues showed similar patterns in nucleoside changes in human brain samples, although overall concentrations differed. It is unknown what effect other variables in the human tissues such as age, gender, or cause of death may have had on these results; however, this does demonstrate an applicability of observations in rat brains to human brains, although still with limitations.

Of 56 unique metabolites identified in our rat tissue samples, 23 showed no change in either the cortex or the cerebellum up to 72-hours PMD (see Table 6.2). Among these unaltered metabolites were molecules that have been previously associated with AD. For example, both glucose and urea were seen both in the Auckland cohort reported here (180), with increased glucose also observed in other reports (185). Both were unaffected by PMD in rat brains here (see Figure 6.3). However, unlike the Auckland cohort, glucose also showed no case–control differences in the Manchester and Newcastle human cohorts. This could be due to several other factors that differed between these groups, such as control age, disease staging, or cerebral vascular pathology. Alterations in glucose metabolism have been observed even in healthy aged brains (396), and glucose hypometabolism has been reported in preclinical AD cases with mild cognitive impairment and low Braak stage (397). As such, the higher age or Braak stage of UK controls could contribute to the lack of case–control changes seen in the Manchester and Newcastle cohorts. Increased measures of cerebral vascular pathology such as CAA have also been associated with higher tau Braak stage AD, independently of other variables including CERAD, age, and gender (398). This correlation between CAA score and Braak stage has also been observed in a separate cohort of samples with Braak stage 0-III pathology, with

individuals more likely to be classified as Braak stage III when they showed CAA pathology (399). Significant interactions between CAA status and measures of cognition and memory were also reported in this cohort, suggesting that CAA pathology may have contributed to cognitive impairment in these cases. However, there were no significant case–control differences in severity of CAA in either the UK cohorts, nor severity of SVD in the Manchester samples (see Table 6.1 & Supplementary Tables 6-8, p397–403). Differences in the latter could not be determined in the Newcastle cohort due to a lack of information available for samples. Likewise, neither CAA nor SVD scores were available for the Auckland samples, so it is unknown if case–control differences in either of these factors contributed to case–control separation.

NAA has been reported as decreased in AD brains (383, 400, 401), but likewise appeared unaffected by PMD in rat brains (see Figure 6.3). As such, investigations of these molecules should be robust in cohorts with PMDs of up to 72 hours or with case–control differences in PMD. However, 22 metabolites did show significant changes in the cortex over a 72-hour period, as well as 23 in the cerebellum (see Table 6.3). Many of these metabolites had already begun to show changes by 24 hours and all by 48 hours, similar to previous studies. This has significant implications on the use of brain tissues in metabolomics experiments, both human and animal. Although it cannot be assumed that human brain tissues will show all the same changes as those observed here in rat tissues, our data in combination with previous reports, suggests that the human brain metabolome will have already undergone significant alterations in a time frame as short as 24 hours. As such, it becomes imperative to limit post mortem delay in these tissues as much as possible—at least within a 24-hour period, but possibly in an even shorter time frame. Further studies looking at concentrations of the metabolites shown here to be affected by 24 hours would be necessary to determine the maximum PMD allowable for reliable determination of these analytes. Although 14 of the metabolites observed to significantly change were common to both regions, seven were only altered in the cortex and nine in the cerebellum. This also raises the importance of recognising differences in susceptibility across brain regions and how the metabolome may be affected in each. Taken together, these data suggest that although targeted analyses of certain metabolites can be performed regardless of PMD of

tissues, such as glucose and urea, untargeted analyses investigating the metabolome as a whole require careful control of PMD to at least under 24 hours.

6.5. Conclusions

Taken together, the results shown here from both human and rat tissues illustrate a marked effect of PMD and a probable effect of disease stage and age on the brain metabolome. In particular, several metabolites showed alterations by PMDs of 24 hours or more, which were not always consistent across multiple regions—making the matching of brain regions and precise dissection of tissues important if findings between patients and case–control groups are not to be ambiguous. As such, in order to maximise interpretability of metabolomics data in human brain tissue, it can be recommended that tissues should have a PMD of less than 24 hours, although even this period may be too long for reliable measurements of many metabolites. Although the exact effects of age and Braak staging are difficult to determine, it seems likely that they also contribute to the differences in findings observed between human cohorts reported here. As such, samples should also be as well-matched in these areas as possible, and consideration should be made as to whether it is suitable to include low Braak stage (Braak stage I-II) individuals in AD control cohorts.

Based on these findings, it was determined that the limited pool of PDD samples available in UK brain banks was not suitable for an untargeted metabolomics study. As such, tissues were sought from the US, where age- and sex-matched samples with low PMD could be obtained in sufficient numbers for analysis.

Chapter Seven | Substantively lowered levels of pantothenic acid (vitamin B5) in several regions of the human brain in Parkinson's disease dementia

This data has been accepted for publication by Metabolites: Scholefield M, Church SJ, Xu J, Patassini S, Hooper NM, Unwin RD, et al. Substantively Lowered Levels of Pantothenic Acid (Vitamin B5) in Several Regions of the Human Brain in Parkinson's Disease Dementia. Metabolites. 2021;11(9) (402). It is presented here in its pre-published form, which represents its state at the time of thesis submission.

Our group has previously performed analyses of AD (403) and HD (404) brains in which multi-regional decreases in pantothenic acid, a precursor molecule for coenzyme A, were observed. Following an additional analysis of pantothenic acid levels in rat brains on which I assisted with the data analysis (104), in which a potential role for vitamin B5 in myelin homeostasis was identified, the question was raised as to whether similar decreases may be present in the PDD brain. As such, pantothenic acid was added as a molecule of interest in our metabolomics analyses.

Originally pantothenic acid was to be analysed alongside other metabolites in an untargeted GC–MS analysis. However, due to an equipment malfunction and the inability of a newly-developed untargeted LC–MS method to identify pantothenic acid, a targeted LC–MS method was developed for this purpose. This data from this targeted analysis is presented here.

7.1. Introduction

Parkinson's disease (PD) is a common neurodegenerative disorder primarily characterised clinically by bradykinesia, resting tremor, and rigidity, and neuropathologically by extensive dopaminergic neuronal loss and accumulation of α-synuclein deposits known as Lewy bodies. These changes occur most severely within the substantia nigra pars compacta, but also throughout other regions of the brain (25). As well as motor dysfunction, cognitive impairment is a common symptom in PD as the disease progresses, with up to 80% of individuals going on to develop Parkinson's disease dementia (PDD) in the twenty years following initial diagnosis (405).

Despite how common the condition is, the causes and mechanisms of PDD remain poorly characterised. Most cases are sporadic with no identifiable cause, and treatments remain purely symptomatic, with even the most promising clinical trials thus far being unable to slow, stop, or reverse the progression of the disease. This is also the case with other similar neurodegenerative diseases, such as Alzheimer's (ADD) and Huntington's disease (HD), which also currently have only symptomatic treatments despite extensive interest and studies into causes, mechanisms, and potential treatments (406).

These neurodegenerative diseases share several characteristics. Age is a primary risk factor for development of symptoms (although HD is always caused by a dominant autosomal mutation in the huntingtin gene, development of symptomology generally occurs with later age), cerebral protein deposition is present in each condition (α-synuclein in PD, tau and amyloid-β in ADD, and huntingtin in HD), and clinical presentations can show significant overlap, with increased risk of psychological complaints (407), issues with sleep (408), and difficulty walking (409) as well as progressive development of cognitive impairment (410, 411).

These findings have raised the question as to whether there may be common pathogenic insults present across multiple neurodegenerative diseases contributing to these similarities in presentation. Common disruptions in multiple metabolic pathways have already been identified in ADD and HD brains, including widespread urea (180, 214, 382, 412) and glucose increases (180, 183-185), dysregulation of glucose and purine metabolism

pathways (180, 183, 184, 306, 377), and decreases in the essential nutrient pantothenic acid (403, 404), also known as vitamin B5. Pantothenic acid is essential for the synthesis of coenzyme A (CoA), a molecule with extensive roles in metabolism including in the tricarboxylic acid (TCA) cycle, fatty acid metabolism, and acetylcholine and myelin synthesis amongst others. Dysregulation of pantothenic acid could disrupt the supply of this essential molecule, with widespread downstream metabolic complications. Inborn mutations in the pantothenate kinase 2 gene (PKAN2), which is an intermediate in the CoA synthesis pathway, are associated with a disease known as pantothenate kinase-associated neurodegeneration (413); a condition characterised by severe brain damage within the basal ganglia and progressive cognitive and motor dysfunction including parkinsonism.

Levels of pantothenic acid have not to our knowledge been investigated previously in the PDD brain. Thus, this investigation is the first to report dysregulation of cerebral pantothenic acid in PDD, similar to that previously observed in ADD and HD.

7.2. Methods

7.2.1. Acquiring Tissue for Pantothenic Acid Quantification

Brain tissue from nine regions including the middle temporal gyrus (MTG); motor cortex (MCX); primary visual cortex (PVC); hippocampus (HP); anterior cingulate gyrus (CG); cerebellum, at the level of the dentate nucleus (CB); substantia nigra (SN); pons; and medulla oblongata (MED) were obtained from nine confirmed cases of PDD and nine controls from the University of Miami Brain Endowment Bank, USA (part of the National Institute of Health NeuroBioBank network). All available patient data were collected and recorded, including age at death, sex, brain weight, post mortem delay (PMD), α-synuclein Braak stage, and cause of death (see Supplementary Table 14, p411–413, for individual patient data).

7.2.2. Diagnosis & Severity of PDD Cases

Flash-frozen tissues obtained from both cases and controls were examined and diagnosed by the referring neuropathologists of the Miami Brain Endowment Bank. All were diagnosed to be of the α-synucleinopathy neocortical type, consistent with the clinical phenotype of PDD, and controls did not show any features of neurodegeneration or vascular pathology. PDD staging was assessed using either Braak staging (Braak, 2003) or McKeith's typing of Lewy body disease (McKeith 2005). Individual donor data can be found in Supplementary Table 14 (p411–413).

7.2.3. Pantothenic Acid Quantification

Pantothenic acid was quantified in brain extracts by UHPLC–MS/MS. Samples were extracted into 800 µl 50:50 (v/v) methanol:chloroform containing 1 µM labelled pantothenic acid standard ((di-β-alanine-$^{13}C_6$,$^{15}N_2$) calcium salt ≥98 atom %, ≥97% (CP); Sigma-Aldrich, MO, USA). 800 µl Methanol:chloroform:internal standard blanks were also prepared. Samples were lysed in a TissueLyser batch bead homogeniser (Qiagen, Manchester, UK) for 10 min at 25 Hz using 3 mm carbamide beads. 400 µl LC–MS grade water was added to lysed samples before centrifugation at 2400 x g for 15 minutes to separate polar and non-polar phases. 200 µl of the polar methanol phase was transferred to a fresh tube before drying overnight in a Speedvac centrifugal concentrator (Savant Speedvac, Thermo Scientific, UK).

Following drying, 400 µl of 0.1% formic acid was added to each sample and blank. 100 µl of this solution was then transferred to 300 µl autosampler vials (Thermo Fisher Scientific, MA, USA). Four blanks containing only 100 µl 0.1% (v/v) formic acid were also prepared and interleaved throughout the UHPLC–MS/MS run. 200 µl standard solutions containing the labelled pantothenic acid internal standard and unlabelled pantothenic acid external standards (D-Pantothenic acid hemicalcium salt ≥98.0%; Sigma-Aldrich, MI, USA) in 0.1% formic acid were prepared in 300 µl autosampler vials containing concentrations of 0–5000 mM pantothenic acid; these were used to create standard curves during analysis. Three 200 µl QC samples containing 20, 200, and 2000 mM unlabelled pantothenic acid standards in 0.1% (v/v) formic acid were also prepared and interleaved throughout the run.

Pantothenic acid quantification was performed on a TSQ Vantage triple quadrupole mass spectrometer coupled with an Accela UHPLC system (Thermo Fisher Scientific, Massachusetts, USA) using a Hypersil Gold AQ column with a diameter of 2.1 mm, length of 100 mm, and particle size of 1.9 µm (Thermo Fisher Scientific 25302-101130, Massachusetts, USA), with a 0.5 µm pre-column filter (Thermo Fisher Scientific 22016, Massachusetts, USA) and electrospray ionisation source. UHPLC-MS/MS was performed under the following source conditions: capillary temp 200°C, vaporiser temp 380°C, spray voltage 5000 V, auxiliary nitrogen gas pressure 45, and sheath nitrogen gas pressure 40. The column was maintained at 25°C during each run; samples were maintained at 4°C. 10 µl of sample was injected. Gradient elution was performed using 0.1% formic acid in water (A) and 0.1% formic acid in acetonitrile (B) at 300 µl/min (see Table 7.1). Two regions were analysed per run, with randomisation of cases and controls. Transitions are shown in Table 7.2.

Table 7. 1. UHPLC-MS/MS Gradient Elution Conditions

Time (mins)	A: 0.1% formic Acid in water	B: 0.1% formic acid in acetonitrile
0.0	100	0
0.8	100	0
2.0	95	5
4.0	0	100
6.5	0	100
6.5	100	0
9.0	100	0

Table 7. 2. UHPLC-MS/MS Transitions

Standard	Precursor m/z	Product m/z	Collision Energy
VB51	220	124.1	19
VB52	220	184.1	11
VB53	220	202.1	10
Labelled VB51	224.5	126.1	19
Labelled VB52	224.5	188.1	12
Labelled VB53	224.5	206.1	10

7.2.4. UHPLC–MS/MS Data Analysis

Peaks were identified based on the expected retention time (RT) derived by comparison with the RT of the spiked pantothenic acid-labelled internal standard. Peaks were manually checked to ensure correct identification by the software. Standards were only accepted when showing a % difference of < 15% of expected, with 6/10 standards required for acceptance of the standard curve. QC samples showing a % difference > 20 % of expected concentration were excluded, with 2/3 successful QC run required in each batch for the run to be accepted.

Concentrations of pantothenic acid in each sample were determined based on the standard curve. Concentrations were corrected for sample wet-weight and case–control differences analysed in GraphPad Prism v8.1.2. (Prism; La Jolla, CA). A non-parametric Mann–Whitney U test was used due to the small sample size, and a p-value < 0.05 was considered significant.

The minimum sample size required to confidently determine case–control differences at a significance level of $p < 0.05$ was calculated using the sample size calculator from SPH Analytics, Alpharetta, USA (https://www.sphanalytics.com/sample-size-calculator-using-average-values/).

Results obtained were compared to those previously reported in both ADD and HD.

7.3. Results & Discussion

7.3.1. Cohort Characterisation

Cases and controls were matched for age, sex, PMD, and brain weight, with no significant differences in any of these variables (see Table 7.3). Samples were acquired with as low a PMD as possible, at a maximum of 26 hours. Additional metadata including cause of death and disease staging were also obtained for all samples (see Supplementary Table 14, p411–413).

Due to a lack of available SN tissue for two controls, two additional, replacement SN samples (C55 and C56) were obtained from different donors to those employed for the

other brain regions. When the revised SN cohort was analysed, it was still matched for age, sex, and brain weight, but cases had a lower PMD than controls (p = 0.03; see Table 7.3).

Table 7. 3. PDD Cohort Characteristics

	Gender (% male)	Age at death (years)	PMD (hours)	Brain Weight (g)
Controls (n = 9)	44	70 (61 – 79)	19.8 (12.5 – 26.0)	1285 (1135 – 1371)
SN Controls (n = 9)	44	70 (62 – 79)	20.6 (10.8 – 26.0)	1335 (1135 – 1550)†
Cases (n = 9)	66	73 (61 – 81)	14.6 (4.3 – 21.9)	1291 (1187 – 1520)

Mean (range) age, PMD, brain weight and Braak stage. * p < 0.05 between cases and controls as determined by Mann–Whitney U Test. †Brain weight not available for one control. See Supplementary Table 14 for individual data.

7.3.2. Pantothenic Acid Analysis

Concentrations of pantothenic acid were found to be significantly lower in the CB (p = 0.008), SN (p = 0.02), and MED (p = 0.008) of cases compared to controls (see Table 7.4 and Figure 7.1a). In these three regions, there was a decrease of around 40% in PDD cases. There was also a suggestion of decreased pantothenic acid in the pons, but this did not reach significance (p = 0.0503). Inter-regional concentrations of pantothenic acid were consistent, with no significant differences between any two regions in either cases or controls (data not shown). A ROC curve was generated using values from all three regions showing significant case-control differences (SN, CB, and MED; see Figure 7.1b). The ROC curve has an area under curve (AUC) value of 0.82 (p < 0.0001), indicating good discriminatory power in distinguishing between PDD cases and controls.

Neither of the substituted SN controls showed significant differences in pantothenic acid concentrations compared to the other cases in the SN cohort (see Supplementary Table 15, p414, for individual values). Case–control differences in the SN remained significant with exclusion of substituted SN controls C10 and C11. A previous analysis by our group of

the effects of PMD on human and rat brain metabolites found no changes in pantothenic acid concentrations up to 24 hours PMD (103). Together with the data here, there appears to be no significant effect of PMD on pantothenic acid levels in the current cohort.

Statistical analyses were performed following this analysis to confirm the sample size used was sufficient to determine significant case–control differences at $p < 0.05$; the required sample size was < 10 in all regions that showed significant case–control differences, as well as in the CG and pons (see Table 7.5).

Figure 7. 1. Pantothenic Acid Concentrations in PDD Cases and Controls

a)

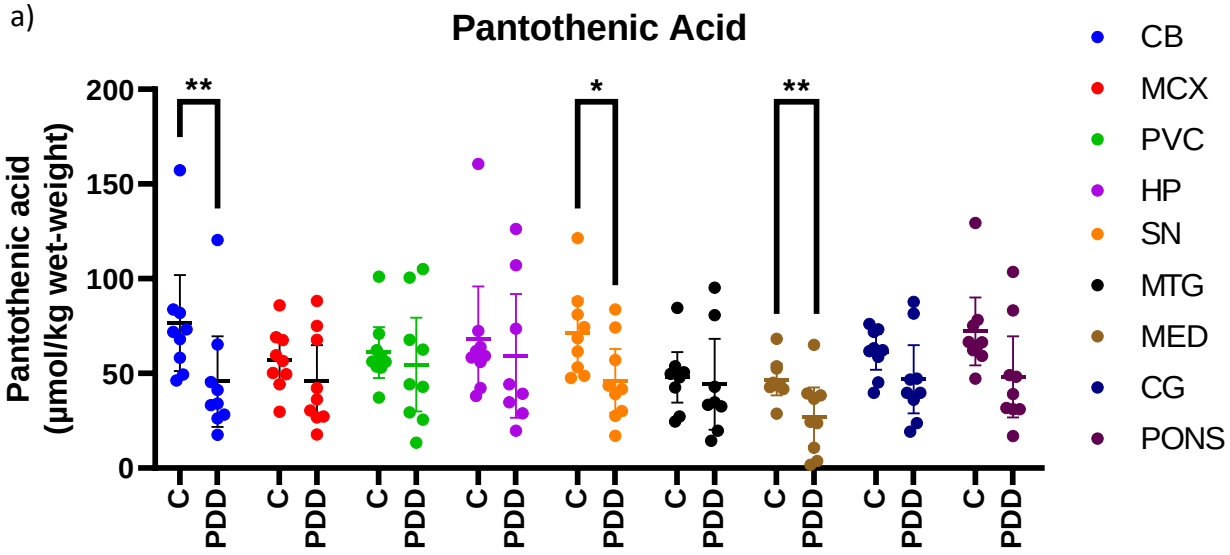

b)

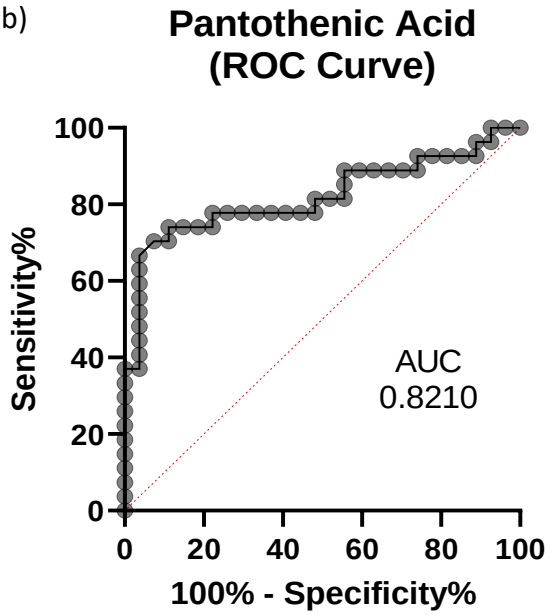

a) Mean pantothenic acid concentrations ± 95% confidence intervals in µmol/kg wet-weight. Case-control differences were determined using Mann-Whitney U test. * $p < 0.05$, ** $p < 0.01$. C = Controls; PDD = PDD cases. b) receiver-operating characteristic (ROC) curve for pantothenic acid in all brain regions showing significant case-control differences (SN, CB, and MED). Area under curve (AUC) value was 0.8210 with $p < 0.0001$.

Table 7. 4. Pantothenic Acid Concentrations in PDD Cases and Controls

Region	Controls (n = 9) (µmol/kg wet-weight)	PDD Cases (n = 9) (µmol/kg wet-weight)	Fold-Change	P-Value
CB	76.7 (51.3 – 102.0)	45.7 (21.8 – 69.7)	**0.6**	**0.008**
MCX	56.9 (44.5 – 69.4)	45.7 (26.6 – 64.9)	0.8	0.3
PVC	61.1 (47.7 – 74.5)	54.6 (29.8 – 79.4)	0.9	0.5
HP	68.1 (40.2 – 96.0)	59.3 (26.6 – 91.9)	0.9	0.4
SN	71.6 (53.6 – 89.6)	46.0 (29.2 – 62.9)	**0.6**	**0.02**
MTG	47.9 (34.6 – 61.2)	44.2 (20.2 – 68.3)	0.9	0.4
MED	46.8 (38.5 – 55.0)	27.1 (11.5 – 42.6)	**0.6**	**0.008**
CG	61.3 (51.9 – 70.8)	46.9 (28.9 – 64.9)	0.8	0.1
PONS	72.2 (54.3 – 90.1)	48.2 (26.8 – 69.7)	0.7	0.0503

Mean pantothenic acid concentrations with 95% confidence intervals in µmol/kg wet-weight. Case–control differences were determined using Mann–Whitney U test and $p < 0.05$ was considered significant. Fold-changes are cases compared to corresponding controls. See Supplementary Table 15 for individual data.

Table 7. 5. Statistical Power of Pantothenic Acid Analyses

Element	Statistical Power ($p < 0.05$)	Sample Size Required ($p < 0.05$)
CB	53.8	**6**
MCX	20.5	19
PVC	8.3	86
HP	7.8	99
SN	66.9	**4**
MTG	6.3	222
MED	73.2	**4**
CG	37.2	**9**
PONS	50.8	**6**

Bold values indicate required sample size of < 10

7.3.3. Comparisons with ADD and HD

As well as investigating case–control comparisons of pantothenic acid in PDD, we also compared the current results with those we obtained in previous analyses of other neurodegenerative diseases. Our group has previously performed analyses of pantothenic levels in ADD (403) and HD (183, 404) by methods comparable to those used in this study. Although there is some variation in the brain regions investigated, it is possible to compare findings across multiple areas of the brain in all three conditions, including the CB, MCX, PVC, HP, MTG, and CG, as well as the SN in PDD and HD (see Table 7.6 and Figure 7.2).

Notably, PDD, ADD, and HD all showed significantly decreased pantothenic acid in the CB, where the reduction was ~40-50%. This is the only region investigated in all three diseases which showed a significant alteration in every condition. Both PDD and HD show a significant reduction of around 40% in the SN, but this region was not investigated in ADD. The MED was not included in either the ADD or HD studies, and so cannot be compared to PDD. Both ADD and HD showed significantly decreased pantothenic acid in the entorhinal cortex (ENT), but this region was not investigated in the current PDD study.

Pantothenic acid dysregulations appear to be less widespread in PDD than either ADD or HD, showing changes in three of nine investigated regions, in comparison to seven of eleven regions in HD and all seven areas reported on in ADD. Where reductions occur, they are on a similar scale, at around 60% of control values.

Table 7. 6. Pantothenic acid fold-changes in PDD, ADD, and HD

Region	Fold-Change PDD	Fold-Change AD (Xu et al, 2016)	Fold-Change HD (Patassini et al, 2015)
CB	**0.6**	**0.5**	**0.6**
MCX	0.8	**0.3**	0.6
PVC	0.9	**0.4**	0.5
HP	0.9	**0.5**	**0.5**
SN	**0.6**	-	**0.6**
MTG	0.9	**0.5**	0.6
MED	**0.6**	-	**-**
CG	0.8	**0.5**	0.5
PONS	*0.7*	-	-
PUT	-	-	**0.5**
GP	-	-	**0.4**
MFG	-	-	**0.6**
ENT	-	**0.4**	**0.6**

Case–control fold-changes in pantothenic acid between three dementias. CB = cerebellum; MCX = motor cortex; PVC = primary visual cortex; HP = hippocampus; SN = substantia nigra; MTG = middle temporal gyrus; MED = medulla; CG = cingulate gyrus; PUT = putamen; GP = globus pallidus; MFG = middle frontal gyrus; ENT = entorhinal cortex. Significant intra-cohort case–control fold-changes are highlighted in bold.

Figure 7. 2. Regional Distribution of Pantothenic Acid Decreases in the PDD, ADD, and HD Brain

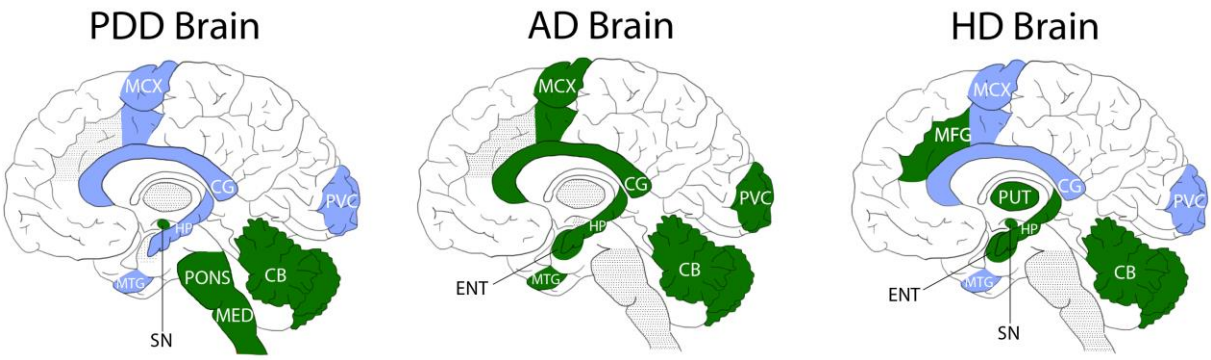

Areas shaded in green denote regions with significant decreases in pantothenic acid compared to matched cohort controls. Areas shaded in blue denote regions showing no significant case–control differences. Areas shaded in grey denote regions that were not investigated.

Outside of our own previous analyses, pantothenic acid levels have not to our knowledge been investigated in the ADD, HD, or PDD brain. Interestingly though, increased dietary intake of pantothenic acid has been associated with increased amyloid-β burden in individuals with cognitive impairment *(414)*. This may indicate that pantothenic acid deficiencies in the brain cannot be counteracted by increased dietary intake. In PD, increased microbial pantothenic acid production in patient stool samples has been positively associated with non-motor symptoms such as constipation by one group *(415)*, whereas another investigation has reported decreased pantothenic acid levels in PD patient faecal samples *(416)*. Altogether, the current literature on pantothenic acid levels in dementia is at present very limited, and the current investigation offers novel insights into disruptions in this molecule within the PDD brain.

The cohort for this investigation was carefully selected to avoid as many possible confounding factors as possible, including close matching for age, sex, PMD, and brain weight. A PMD of 26 hours or less was considered suitable, as a previous analysis carried out by our group has observed no changes in pantothenic acid concentrations in either the cerebellum or cortex of rats for up to 24 hours PMD, although a modest significant increase was observed by 48 hours in the cortex (103). To our knowledge this has not been investigated in human brains, most likely due to the high number of confounding factors

that would make getting sufficient sample sizes difficult, and the infeasibility of obtaining very low PMD brain samples from humans. As such, we take the results from the investigation on rat brains to be the best available evidence for our selected PMD timeframe, but are cognisant that human brain samples may show differences in this respect to animal models.

Pantothenic acid is required for synthesis of CoA, which plays roles in many major metabolic pathways, including several which have previously been reported to be disrupted in PD. For example, CoA is a carbon transporter in the TCA cycle, which has been reported to show downregulated gene expression and enzyme levels in PD brain (73, 335), as well as decreased metabolite intermediate levels in the PD cerebrospinal fluid (417). Reductions in pantothenic acid may lead to insufficient production of CoA for proper functioning of the TCA cycle.

It is possible that such a perturbation may converge with disruptions in other metabolic pathways. Usually, pyruvate produced by the breakdown of glucose in the glycolytic pathway would enter the TCA cycle after being converted into acetyl-CoA in the mitochondria. This process itself requires the presence of CoA. Glycolysis has been widely observed to be downregulated in PD (418), and even suggested as a possible therapeutic target in the disease (419). This dysregulation reflects increased levels of glucose (74) and overall glucose hypometabolism throughout the PD and PDD brain (418, 420), correlating with motor and cognitive symptoms (421, 422). As such, reduced pantothenic acid may link not only reduced TCA cycle activity, but also decreased glycolysis and glucose hypometabolism in the PDD brain. This may be a shared pathogenic mechanism with ADD and HD, which also show increased brain-glucose levels, impaired glycolytic and TCA cycle activity, and increased glucose hypometabolism throughout the brain (180, 183-185, 214, 306).

In order to determine whether these changes are initial drivers of metabolic dysfunction in PDD, rather than simply being a late-stage downstream result of neuronal cell death, it would be necessary to quantify pantothenic acid levels in pre-symptomatic or early-stage PD/D patients. However, as there are currently no methods available for quantifying pantothenic acid in vivo to the authors' knowledge, and as it is not yet possible to

determine who will go on to develop PD with certainty (and so take measurements from presymptomatic individuals who passed away prior to developing the disease), this cannot be investigated at this stage. However, pantothenic acid has been seen to be decreased in the brains of individuals with presymptomatic HD, which can be positively diagnosed due to the autosomal dominant huntingtin mutation present in all individuals with HD from birth, with levels most markedly lowered in highly-impacted brain regions (104). This indicates that pantothenic acid levels can decrease prior to extensive neuronal loss, but development of in vivo techniques for measuring pantothenic acid or reliable biomarkers for diagnosing presymptomatic PD would be necessary to conclude that this is also the case in PD/D.

Another possible contributor to the alterations observed here could be decreased microbial production of pantothenic acid. Over recent decades, more and more studies have been reporting observations that support the microbiota-gut-brain hypothesis of PD, wherein microbial alterations and initial accumulation of pathogenic α-synuclein deposits in the gut spreads in a prion-like manner from the peripheral to the central nervous system, resulting in inflammation, increased permeability of the blood-gut and blood-brain barriers, and the spread of α-synuclein inclusions to the PD brain itself (423-425) – in some cases prior to the development of motor symptoms (426). Indeed, α-synuclein Braak staging itself, commonly used to determine the PD disease stage, has described α-synuclein inclusions in the gastrointestinal tract of PD patients (427). Decreased microbial production of pantothenic acid has been observed in stool samples taken from PD patients, and has been associated with non-motor symptoms, particularly constipation (415), which is commonly observed in presymptomatic individuals that later go on to develop PD (428). Another study has also reported overall decreases in pantothenic acid levels in the PD gut microbiota taken from faecal samples along with reductions in anti-inflammatory bacteria (416). If faecal samples could be obtained from individuals who later go on to develop PD for quantification of pantothenic acid, it could be better determined whether pantothenic acid is likely to be a driving force in metabolic dysregulation in PD/D, or whether it is a later downstream effect of the disease – however, this remains difficult without biomarkers of presymptomatic disease.

One interesting distinction between PDD compared with ADD and HD is the variability in regions affected by lowered pantothenic acid levels. In PDD, only the SN, MED, and CB showed significant reductions in pantothenic acid levels. The SN is the region most severely affected by neuronal loss in PD, and the MED one of the first areas to show Lewy body deposition according to typical PD/PDD progression as defined by α-synuclein Braak staging (25), suggesting that more severely or earlier-affected areas of the PDD brain may show pantothenic acid reduction. However, the CB is not an area typically associated with PD, with varying reports on the degree of atrophy in this region (429), although it has been observed to show functional and morphological changes which have been theorised to include both pathological and protective functions in the disease (430). Furthermore, reduced pantothenic acid was also observed in the CB of the ADD and HD cases, indicating a shared perturbation across all three diseases in this region. This may indicate a higher degree of involvement of the cerebellum in neurodegenerative diseases than previously considered, and would benefit from further investigation with a larger sample size. HD also showed significant decreases in the SN, but otherwise there were no regional similarities observed between PDD and ADD or HD. This could suggest a regional susceptibility in pantothenic acid reductions that contributes to the variability in clinical presentations in different conditions, despite some areas of shared pathology and/or symptomology.

However, investigations of other regions of the brain that are highly impacted by neurodegeneration in both PD/D and HD such as the putamen and caudate nucleus - which were not included in this analysis as regions were selected to try and cover moderately-affected and relatively-spared regions of the PDD brain as well as highly-affected areas - may reveal more similarities between these conditions than can be observed here. Wider investigation of more highly-affected, moderately-affected, and relatively-spared regions throughout the PDD brain could also provide more evidence towards the possibility of regional susceptibility in this particular disease – which is currently limited here by sample size and limited number of investigated regions. Yet further to this, determination of α-synuclein levels within individual brain regions alongside pantothenic acid concentrations could more convincingly determine any correlation between Lewy body deposition and

changes in pantothenic acid in the PDD brain. This was not possible with the current sample set, but could provide evidence towards the hypothesis of regional susceptibility to pantothenic acid alternations in PDD suggested here.

Overall, pantothenic acid reductions present a novel and region-specific pathogenic insult in PDD, ADD, and HD, which may contribute to observed disease mechanisms such as glucose hypometabolism and other related metabolic dysfunction.

Chapter Eight | Severe and regionally widespread increases in tissue urea in the human brain represent a novel finding of pathogenic potential in Parkinson's disease dementia

The data presented in this chapter has been accepted by Frontiers in Molecular Neuroscience for consideration for publication: Scholefield M, Church SJ, Xu J, Patassini S, Roncaroli F, Hooper NM, et al. Severe and regionally-widespread increases in tissue urea in the human brain represent a novel finding of pathogenic potential in Parkinson's disease dementia. 2021 (431). It is included here with minor adjustments.

Whilst performing the systematic review for this thesis in order to identify analytes of potential interest in PDD, one metabolite which showed consistent alterations in both AD (180, 214) and HD (382, 412) was urea – which has been identified to be dramatically increased in a widespread manner in brain tissues in both diseases by multiple groups, including our own. Although urea has been found to be increased in PD plasma (317), to the author's knowledge it is yet to be investigated in the PD brain, either with or without dementia. As such, as with pantothenic acid, urea then became an analyte of interest in metabolomics analysis of the PDD brain.

Like pantothenic acid, urea was initially to be analysed alongside other metabolites with an untargeted GC–MS method, but malfunction of the GC–MS and the inability of the newly-developed untargeted LC–MS method to identify urea, a targeted LC–MS method was developed. The data from this analysis is presented here.

8.1. Background

Parkinson's disease (PD) is the second most common neurodegenerative condition after Alzheimer's disease (AD) (432). PD is characterised mainly by motor dysfunction including bradykinesia, resting tremor, and rigidity. Up to 80% of patients with PD develop cognitive dysfunction during the course of their disease, usually within twenty years from the diagnosis, designated as Parkinson's disease dementia (PDD) (405). Neuropathologically, PD and PDD are characterised by extensive loss of dopaminergic neurons in the substantia nigra, and accumulation and progressive spread of misfolded α-synuclein with formation of Lewy bodies and Lewy neuropil threads. Deposition of α-synuclein is thought to begin in the olfactory bulbs and lower brainstem and progress to the midbrain and eventually to the neocortex (25, 433). The severity of α-synuclein deposition in the post mortem brain is assessed using the Braak staging system.

A conclusive clinical diagnosis of PD/PDD can be challenging due to the heterogeneity of the condition, presence of comorbidities, and overlap with other forms of movement disorders and dementia (434, 435). The hypothesis that different forms of dementia represent a spectrum with common pathogenetic mechanisms has been suggested (436, 437). Studies that search for perturbations in different areas of the brain across different neurodegenerative conditions represent an approach to unveil potential common pathogenetic mechanisms. Previous metabolomics studies have investigated AD and HD and demonstrated widespread increases in brain-tissue urea in both these conditions despite their different clinical phenotypes and genetic alterations (180, 183, 382, 412).

Peripheral blood levels of urea have been reported in PD patients with discordant results including increase in plasma (317), no change in serum (204), decreases in the CSF (271), and decrease in whole blood concentrations (438). Additionally, none of these studies of peripheral urea distinguished between PD with or without dementia. Conclusions on cerebral tissue levels of this metabolite cannot be inferred from these studies but to our knowledge, brain-tissue urea levels have not previously been reported in PDD.

8.2. Methods

8.2.1. Obtaining Tissue for Urea Quantification

For this study, tissues from nine brain regions from nine cases with definitely diagnosed PDD and nine controls were obtained from the University of Miami Brain Endowment Bank, Miami, FL, USA (part of the National Institute of Health NeuroBioBank network). Tissues were dissected from the following human-brain regions: middle temporal gyrus (MTG); motor cortex (MCX); primary visual cortex (PVC); hippocampus (HP); anterior cingulate gyrus (CG); cerebellum, at the level of the dentate nucleus (CB); substantia nigra (SN); pons; and medulla oblongata (MED). All available patient metadata for cases and controls were obtained and are herein presented in Supplementary Table 14, p411–413.

8.2.2. Diagnosis & Severity of PDD Cases

Cases and controls were diagnosed by the referring neuropathologists of the Miami Brain Endowment Bank. All cases were diagnosed to be of the alpha-synucleinopathy neocortical type, consistent with the clinical phenotype of PDD. Controls did not show any features of neurodegeneration or vascular pathology. The brains were assessed using either Braak staging (25) and/or McKeith's staging criteria for Lewy body dementias (439) (see Supplementary Table 14, p411–413).

8.2.3. Tissue Dissection

Brain samples were cut into sections of 50 mg (± 5 mg) for urea quantification using a metal-free ceramic scalpel. Samples were stored in 'Safe-Lok' microfuge Eppendorf tubes (Eppendorf AG; Hamburg, Germany) and stored at -80^{o}C prior to extraction.

8.2.4. Urea Quantification

Urea was quantified in brain sample by UHPLC–MS/MS. Brain samples were extracted in 800 µl 50:50 (v/v) methanol:chloroform containing labelled urea internal standard (urea-$^{15}N_2$ 98 atom % ^{15}N, 99% (CP), 316830 Sigma-Aldrich, MO, USA). Extraction blanks containing only 800 µl methanol:chloroform:internal standard solvent were prepared. Samples were lysed in a TissueLyser batch bead homogeniser (Qiagen, Manchester, UK) with 3 mm carbide beads at 25 Hz for 10 min. 400 µl LC–MS grade water was then added

to samples before separation of polar and non-polar phases by centrifugation at 2400 x g for 15 minutes. The polar methanol phase was transferred to a fresh tube before being dried overnight in a Speedvac centrifugal concentrator (Savant Speedvac, Thermo Scientific, UK) at ~25°C for 16–18 hours.

Once dried, 400 µl 0.1% formic acid was added to samples. 100 µl of the resulting solution was transferred to 300 µl autosampler vials, with two blanks containing only 100 µl 0.1% (v/v) formic acid also prepared. 200 µl standard solutions containing a labelled urea internal standard and corresponding unlabelled urea external standards (urea analytical standard, 56180 Supelco, PA, USA) were prepared, containing concentrations of 0–5000 µM unlabelled urea in 0.1% v/v formic acid. Three 200 µl QC samples were also prepared containing 10 µm labelled urea and 20, 200, and 2000 µM unlabelled urea in 0.1% v/v formic acid.

Urea quantification was performed on a TSQ Vantage triple quadrupole mass spectrometer coupled with an Accela UHPLC system (Thermo Fisher Scientific, Massachusetts, USA) using a Hypersil Gold AQ column with a diameter of 2.1 mm, length of 100 mm, and particle size of 1.9 µm (Thermo Fisher Scientific 25302-101130, Massachusetts, USA), with a 0.5 µm pre-column filter (Thermo Fisher Scientific 22016, Massachusetts, USA) and electrospray ionisation source. UHPLC-MS/MS was performed under the following source conditions: capillary temp 200°C, vaporiser temp 380°C, spray voltage 5000 V, auxiliary nitrogen gas pressure 45, and sheath nitrogen gas pressure 40. The column was maintained at 25°C during each run; samples were maintained at 4°C. 10 µl of sample was injected. Gradient elution was performed using 0.1% formic acid in water (A) and 0.1% formic acid in acetonitrile (B) at 300 µl/min (see Table 8.1). Two regions were analysed per run, with randomisation of cases and controls. Transitions are shown in Table 8.2.

Table 8. 1. UHPLC-MS/MS Gradient Elution Conditions

Time (mins)	A: 0.1% formic Acid in water	B: 0.1% formic acid in acetonitrile
0.0	100	0
0.8	100	0
2.0	95	5
4.0	0	100
6.5	0	100
6.5	100	0
9.0	100	0

Table 8. 2. UHPLC-MS/MS Transitions

Standard	Precursor m/z	Product m/z	Collision Energy
Urea	61.1	44.1	18
Labelled Urea	63.1	45.1	18

8.2.5. UHPLC–MS/MS Data Analysis

UHPLC–MS/MS data were analysed using LCQuan software (Thermo Fisher Scientific, MA, USA). Chromatographic peaks were identified based on expected retention time (RT), and compared against labelled urea internal standard peak retention times for each individual QC/standard/sample. Each peak was manually checked for correct identification.

Quantification of urea in samples was performed using the ratio of urea peak area to internal standard peak area and comparison to the standard curve. These concentrations were corrected for sample wet-weight and analysed in GraphPad Prism v8.1.2. (Prism; La Jolla, CA). A non-parametric Mann–Whitney U test was used to determine the significance of case–control differences due to the relatively small sample sizes.

The minimum sample size required to confidently determine case–control differences at a significance level of $p < 0.05$ and $p < 0.01$ was calculated using the sample size calculator from SPH Analytics, Alpharetta, USA (https://www.sphanalytics.com/sample-size-calculator-using-average-values/).

8.3. Results & Discussion

8.3.1. Cohort Characterisation

Metadata were obtained for all cases and controls, including sex, age, race, ethnicity, post mortem delay (PMD), brain weight, comorbidities, and cause of death (see Supplementary Table 14, p411–413, for individual data). There were no significant case–control differences in sex, age at death, PMD or brain weight (Table 8.3). All samples had a PMD of 26 hours or less, with an average of 19.8 hours in controls and 14.6 hours in cases.

Due to a lack of available SN tissue for two of the cohort samples, two alternate SN samples were obtained from different donors. These samples were age- and sex-matched, but the cases had a lower PMD than controls (~6 hours, p = 0.03; Table 8.3). The impact of this is discussed in the section on brain tissue urea findings below.

Table 8. 3. PDD Cohort Characteristics

	Gender (% male)	Age at death (years)	PMD (hours)	Brain Weight (g)
Controls (n = 9)	44	70 (61 – 79)	19.8 (12.5 – 26.0)	1285 (1135 – 1371)
SN Controls (n = 9)	44	70 (62 – 79)	20.6 (10.8 – 26.0)	1335 (1135 – 1550)†
Cases (n = 9)	66	73 (61 – 81)	14.6 (4.3 – 21.9)	1291 (1187 – 1520)

Mean (range) age, PMD, and brain weight. No case–control differences were significant. * $p < 0.05$ between cases and controls as determined by Mann–Whitney-U Test; all other differences were not significant. †Brain weight not available for one control.

8.3.2. Brain-tissue Urea Findings in PDD

Urea levels were increased in PDD cases compared to controls in every region analysed (Table 8.4 and Figure 8.1). There was an average 5.5-fold increase in tissue-urea concentrations in the CG of cases compared with controls, and an average ~3.5 to 4.5-fold increase in cases in every other region.

Inter-regional concentrations of urea were highly consistent in both controls and cases, with no significant differences between any two regions. Control tissue-urea

concentrations averaged ~9.4 mmol/kg and case concentrations 40.0 mmol/kg, showing a substantial, ~4-fold increase in case–control urea levels across the brain overall.

Neither of the substituted SN samples showed significant differences in urea concentrations compared with other cases in the cohort (see Supplementary Table 16, p415, for individual values). Case–control differences in SN-urea levels remained significant with exclusion of substituted SN controls C10 and C11.

As sample sizes in this study were small, a study measuring the statistical power of the urea values was conducted (see Table 8.5). This found a statistical power of over 80% in the CB, MCX, PVC, MED, CG, and PONS, over 70% in the SN and MTG, and a lower value of 68.7% in the HP for $p < 0.05$. This indicates good statistical power in most regions, but highlights the necessity of larger sample sizes for more robust measurements. The same test showed a required sample size of 3 for confident identification of case–control differences at $p < 0.05$ for all regions except the HP, which showed a required sample size of 4.

Figure 8. 1. Urea Concentrations in PDD Cases and Matched Controls

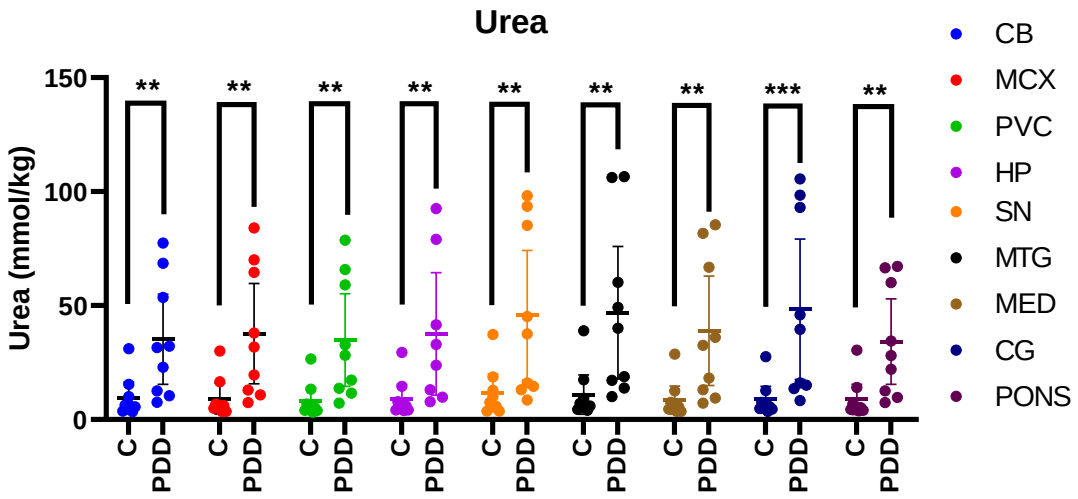

Mean tissue-urea concentrations ± 95% confidence intervals expressed in mmol/kg. Case–control differences were determined by applying the Mann–Whitney-U test. **, $p < 0.01$; ***, $p < 0.001$. C = control; PDD = Parkinson's disease dementia case

Table 8. 4. Tissue Urea Concentrations in PDD Cases and Controls

Region	Controls (n = 9) (mmol/kg)	PDD Cases (n = 9) (mmol/kg)	Fold-Change	P-Value
CB	9.6 (2.7 – 16.4)	35.2 (15.4 – 55.0)	**3.7**	**0.003**
MCX	9.2 (2.5 – 16.0)	37.7 (15.7 – 59.7)	**4.1**	**0.002**
PVC	8.1 (2.3 – 13.9)	34.9 (14.6 – 55.2)	**4.3**	**0.001**
HP	9.0 (2.6 – 15.4)	37.6 (10.7 – 64.4)	**4.2**	**0.004**
SN	11.6 (3.4 – 19.9)	45.8 (17.3 – 74.2)	**3.9**	**0.006**
MTG	11.0 (2.3 – 19.6)	46.9 (17.9 – 76.0)	**4.3**	**0.002**
MED	8.5 (2.3 – 14.7)	38.9 (14.9 – 62.9)	**4.6**	**0.002**
CG	8.8 (3.0 – 14.6)	48.4 (17.6 – 79.1)	**5.5**	**0.0008**
PONS	8.8 (2.2 – 15.5)	34.2 (15.4 – 53.0)	**3.9**	**0.003**

Mean tissue-urea concentrations ± 95% confidence intervals expressed in mmol/kg. Significance of case–control differences was determined using the Mann–Whitney-U test wherein $P < 0.05$ has been considered significant. Fold-changes are cases compared to controls.

Table 8. 5. Statistical Power of Urea Analyses

Element	Statistical Power ($p < 0.05$)	Statistical Power ($p < 0.01$)	Sample Size Required ($p < 0.05$)	Sample Size Required ($p < 0.01$)
CB	**80.6**	59.8	**3**	**6**
MCX	**81.5**	61.1	**3**	**6**
PVC	**83.4**	63.8	**3**	**6**
HP	68.7	44.9	**4**	**7**
SN	75.9	53.4	**3**	**7**
MTG	78.0	56.2	**3**	**7**
MED	**80.8**	60.0	**3**	**6**
CG	**83.1**	63.4	**3**	**6**
PONS	**83.4**	63.9	**3**	**6**

Bold values indicate statistical power of > 80% or sample size of < 10

8.3.3. Comparisons with Brain-urea Concentrations in AD and in HD

Our group has previously reported severe and regionally-widespread increases in brain-tissue urea concentrations in cases with AD dementia (180), and with HD dementia (183, 382). In these studies, AD and HD brain-tissue urea values were reported from multiple regions compared between cases and matched controls (Table 8.7, Figure 8.2; refs (8-10)).

Although there are some differences in the methodologies used in the two former studies compared with the current one (such as previous use of gas Chromatography–mass spectrometry, and some differences in the regions studied; Figure 8.2), case–control tissue-urea fold-changes can be compared between PDD, HD, and AD (Table 8.4) across several brain regions.

Cases and controls in the HD study were slightly younger than those in the current PDD cohort, at an average of around three years for controls and eight years for cases (183, 382). Moreover, PMD was significantly lower than in the current PDD cohort, at an average of ~11 hours in both cases and controls. Cause of death in the HD cohort was most commonly bronchopneumonia in cases and heart failure in controls, but data on comorbidities and other vascular pathology were unavailable. Brain tissue-urea concentrations showed a similar average fold-increase to that measured in PDD of 3.5 in HD cases compared to controls (Table 8.6, Figure 8.2). As in PDD, the increase was observed in the SN, CB, HP, MTG, CG, SCX, and MCX, as well as in other regions not included in the current PDD study, such as the putamen, globus pallidus, middle frontal gyrus, and entorhinal cortex.

The AD cases whose brain-tissue urea levels we measured were similar in age to the current PDD cohort, with an average of ~70 years in both cases and controls (180). PMD was also significantly shorter in this cohort, at an average of 9 hours in controls and 7 hours in cases. Causes of death were varied in both cases and controls, most commonly being due to heart or lung complications. Comorbidity and vascular pathology metadata were not available. Although absolute tissue-urea concentrations cannot be directly compared to the previous studies in AD brains, there was a higher average case–control fold-change in AD than that

observed here in PDD, the average being ~5.3-fold, but with increases as high as 6.5-fold in the HP (180) (Table 8.6). Tissue-urea elevations in this AD cohort were observed in the HP, MTG, SCX, MCX, CG, and CB, as well as in the entorhinal cortex (which was not included in the current study). The AD cohort was similar in age to the current PDD cohort.

Table 8. 6. Urea fold-changes in PDD, AD, and HD

Region	Fold-Change in PDD (this study)	Fold-Changes in AD (Xu et al, 2016)	Fold-Changes in HD (Patassini et al, 2015)
CB	3.7	4.9	3.6
MCX	4.1	5.0	3.4
PVC	4.3	4.9	3.4
HP	4.2	6.5	3.6
SN	3.9	-	3.5
MTG	4.3	4.7	3.4
MED	4.6	-	-
CG	5.5	5.3	3.5
PONS	3.9	-	-
PUT	-	-	3.7
GP	-	-	3.6
MFG	-	-	3.0
ENT	-	5.6	2.8
Overall	4.3 (3.9 – 4.6)	5.3 (4.8 – 5.8)	3.5 (3.2 – 3.6)

Comparisons of case–control fold-changes in human brain urea levels between PDD, AD and HD. Case–control differences were significant for every region in every disease. Overall shows mean overall fold-change with ±95% confidence intervals.

Figure 8. 2. Regional Distribution of Measured Tissue Urea Increases in the PDD, AD, and HD Brain

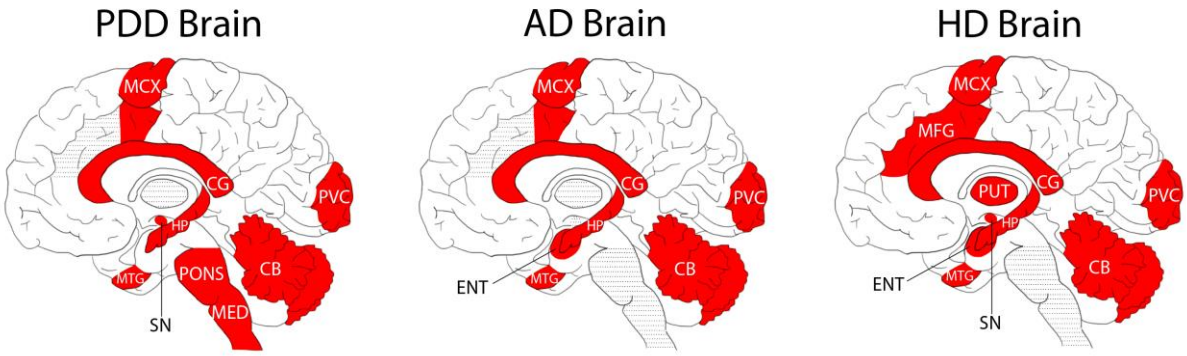

Areas shaded in red denote significant increases in urea compared to intra-cohort controls. Areas shaded in grey were not investigated in the illustrated studies.

Table 8. 7. Urea concentrations in PDD and HD

Region	PDD Controls (n = 9) (mmol/kg)	HD Controls (n = 9) (mmol/kg)	PDD Cases (n = 9) (mmol/kg	HD Cases (n = 9) (mmol/kg)
CB	9.6 (2.7 – 16.4)	7.3 (6.2 – 8.3)	35.2 (15.4 – 55.0)	26.2 (15.3 – 37.1)
MCX	9.2 (2.5 – 16.0)	7.8 (6.5 – 9.1)	37.7 (15.7 – 59.7)	26.4 (14.5 – 38.3)
PVC	8.1 (2.3 – 13.9)	7.4 (6.1 – 8.6)	34.9 (14.6 – 55.2)	24.6 (14.4 – 34.8)
HP	9.0 (2.6 – 15.4)	6.7 (5.6 – 7.8)	37.6 (10.7 – 64.4)	24.0 (12.9 – 35.1)
MTG	11.0 (2.3 – 19.6)	8.6 (7.3 – 9.8)	46.9 (17.9 – 76.0)	28.8 (17.6 – 40.0)
CG	8.8 (3.0 – 14.6)	7.1 (6.0 – 8.2)	48.4 (17.6 – 79.1)	24.8 (13.9 – 35.8)
SN	11.6 (3.4 – 19.9)	6.5 (5.3 – 7.7)	45.8 (17.3 – 74.2)	23.0 (13.3 – 32.7)

HD data acquired from Patassini et al, 2015. Absolute urea concentrations of AD samples not available.

Additional studies have also confirmed urea increases in AD *(214)* and HD *(412)* brains, although one study reported decreases in the HD striatum and no change in the HD frontal lobe *(182)*. Such discrepancies may be contributed to by differences in methods used or between cohorts, such as differences in PMD. However, we have previously observed that PMD does not affect urea levels for up to 72 hours in rat brains *(103)*, although this may not necessarily also be the case in human brains.

Together, the observations in PDD, AD, and HD suggest a shared pathogenic mechanism in these three diseases, despite apparent differences in causative processes and symptomology. There appear to be regional differences between diseases with respect to tissue-urea elevations. For example, AD showed the highest increases in the severely-affected HP (6.5-fold), whereas in HD the putamen showed slightly higher-than-average elevations (3.7-fold). These regional differences may contribute to differences in severity and pathogenesis in the different conditions. Interestingly, the CG showed the highest urea increase in PDD (5.5-fold); the anterior CG is involved in emotive states and emotionally-coded memories. All other studied regions of the PDD brain showed urea increments of around 3.5- to 4.5-fold. However, there were no statistically significant differences between different PDD-control regions or between different PDD-case regions. Greater power (by increasing the sample size), would probably be required to determine whether the fold-elevation observed in the CG is significantly greater than that of other regions of the PDD brain. If so, it is possible that the prominence of both motor and cognitive dysfunction in PDD correlates with similar tissue urea elevations in areas involved in both cognition and motor control processes – a future investigation into regional tissue urea dysregulation in PD brains without dementia could help elucidate this and would probably be a logical next step.

Urea's main metabolic function is to provide a route for the excretion of nitrogen-containing moieties derived from toxic nitrogen-containing compounds. In the urea cycle, ammonia is converted into urea, which is then excreted from the body via the urine. Urea is mainly produced in the liver and is carried to other parts of the body via the blood stream. However, it is slow to cross the blood–brain barrier (BBB) (440), leading to the question as to whether cerebral urea does in fact enter the brain through the BBB, or whether it is also

produced in the brain. There is little evidence for the presence of intracerebral urea cycle activity, although there have been limited observations of partial activity in some studies. For example, some studies have identified increased expression of arginase I (ARG1) mRNA in AD brains and the brains of the APP^{sw} mouse model of AD (441), as well as increased arginase activity in human AD brains – accompanied by concurrent decreases in ornithine (256). Arginase is the final enzyme of the urea cycle, responsible for conversion of arginine to urea – as such, increased arginase activity could result in increased urea levels. A proteomics study conducted by our own lab on several regions of the AD brain observed arginase II in the CB, but did not observe any case–control changes in the enzyme; ARGI was not identified in any region (351). Triple transgenic AD mouse models have also exhibited reduced amyloid-β deposits, microgliosis, and spatial memory deficits with administration of arginase inhibitor L-norvaline (442). Administration of an arginase-1 inhibitor has also been found to be protective against midbrain dopaminergic neuronal loss induced in rat brain slice cultures by arginase-1 promoter macelignan (443). A network analysis has also found arginine pathways be enriched in both PD and AD, as well as in amyotrophic lateral sclerosis (158), possibly resulting in downstream upregulation of nitric oxide synthesis, leading to hypoxia, which has been implicated in both PD and AD (444). Together, these results suggest a role for arginase in AD and PD pathology.

However, arginase is only one component of the urea cycle and is not sufficient for complete urea cycle activity; another urea cycle component - ornithine transcarbamylase (OTC) - the enzyme responsible for the conversion of ornithine to citrulline in the urea cycle, was initially reported to be expressed only in AD brains (445), but has also been observed in healthy control brains in limited amounts (446, 447). However, studies attempting to investigate the levels of other urea cycle enzymes in HD sheep model brains for example were unable to identify either OTC or carbamoyl phosphate synthetase I in the striatum (412). Additionally, a more recent large-scale proteomic study of six regions of human AD and control brains was unable to identify the presence of either of these urea cycle enzymes at the protein level (351). As such, it is possible that upregulation of OTC in AD brains leads to urea cycle activity in the brain that would otherwise not be present, characterized by increased urea and arginase activity and decreased ornithine, but the lack

of other urea cycle components makes definite conclusions difficult to draw at this stage. It is not yet known whether increases in OTC are also present in the PDD brain.

Some other urea cycle components such as adenosine (179-181), citrulline (256), and ornithine (214, 256) have been reported in the AD brain, as well as the HD brain (182, 183) – however, as these metabolites are also involved in other metabolic pathways, this does not necessarily indicate urea cycle activity. For example, adenosine is a core component of several widespread co-enzymes such as adenosine triphosphate (ATP), diphosphate (ADP), and monophosphate (AMP) which are crucial to a wide variety of metabolic pathways including the ETC (448), TCA cycle (449), and purine metabolism (450). As such, it seems likely that cerebral urea may be formed by an alternative process, either by itself or in addition to potential urea cycle activity in the brain.

Several urea cycle intermediates have also been reported to be dysregulated in PD serum, plasma, and CSF. Arginine has been reported by some investigations to be decreased in PD serum (213) and CSF (206), although other reports have observed no changes in either the serum (204), CSF (213, 451), or plasma (206). There is one report of increased citrulline in PD serum (207), although another investigation reported no change (204), and further reports indicated no change in the CSF (206, 451) or plasma (205, 206). Increases in PD serum ornithine have been reported (204), with varying reports in the CSF of decrease (206), increase (273), or no change (451). Moreover, no changes have been reported by several groups in studies of plasma ornithine in PD (205, 206, 273). None of these urea cycle components have been reported on in the PD/PDD brain itself, and the investigations of peripheral levels in the plasma, CSF, and serum have reported inconsistent results. As such, this entire pathway, and the possibility of partial or whole urea cycle activity in the brain, presents a novel area for future investigation of PDD.

Protein dysregulation and neuronal death may lead to greater protein breakdown, and so to increased urea production. Disruptions to the BBB, as observed in PDD (452), may result in defective urea clearance from the brain or increased entry of urea from the bloodstream via urea transporters. Urea transporters are responsible for regulating movement of urea by facilitating urea diffusion, and are expressed in astrocytes and the BBB as well as outside the brain. Urea transporter B has been shown to be upregulated in the HD CB, which may

reflect attempts to clear elevated urea levels in the HD brain (412). Urea transporters have not yet been investigated in PD/PDD, but may show similar perturbations to those reported in HD.

Urea accumulation caused by kidney failure is known to be toxic to the brain, leading to a condition called uraemic encephalopathy (453). High urea levels lead to synaptic loss and inhibition of long-term potentiation via carbamylation of mTOR in a chronic kidney disease mouse model (454). Carbamylation is a post-translational modification involving the addition of isocyanate, usually derived from urea, to protein-bound amino-acid residues, causing alterations in the structure and function of the affected proteins. Increased carbamylation has been observed in aging humans (455), and as a result of chronic kidney disease (456) as well as in AD with cerebrovascular disease (457). It has been shown that tau, which is aggregated in AD and also to a lesser degree in PDD, can be carbamylated, resulting in increased amyloid formation and tau accumulation (458). Whether α-synuclein may also be carbamylated is unknown, but it does contain several potentially-susceptible amino-acid residues, which might serve as target sites for carbamylation.

High urea levels in chronic kidney disease and renal failure have also been linked to increased oxidative stress (459). Oxidative stress is a well-recognised feature of PD, AD, and HD (182, 460) and is linked to other pathogenic mechanisms including mitochondrial dysfunction and proteinopathy (461), dysregulated glucose metabolism (462), insulin resistance and inflammation (463), and α-synuclein accumulation, oligomerisation, and phosphorylation (464, 465). As such, it is possible that elevated urea levels in PDD could contribute to one or more of these known pathogenic mechanisms.

8.4. Conclusions

In conclusion, this investigation shows widespread urea accumulation throughout the PDD brain, similar to that previously observed in AD and HD, with concentrations comparable to those seen in uremic encephalopathy. This suggests a novel shared pathogenic insult across multiple neurodegenerative conditions and may indicate a common mechanism in the development of cognitive impairment.

Chapter Nine | Untargeted Metabolomics Analysis of PDD

9.1. Introduction

As well as metallic perturbations, PD/PDD has previously been observed to show several metabolic dysregulations, which have been covered in detail in Chapter Three. However, studies of brain tissue in PD/PDD are limited, and are usually restricted to cover only the striatum or cortex. Current metabolomic perturbations reported in the PD/PDD brain include alterations in glucose (71, 74, 75), purine metabolism (181), and TCA cycle pathways (73). An updated summary of these studies can be seen in Table 9.1.

A multi-regional, untargeted metabolomic analysis of the brain, such as the ones we have previously conducted on AD (180) and HD (183) brains, has yet to be carried out in PD/PDD. The aim of this chapter is to perform such an analysis, in order firstly to investigate PDD case–control differences in cerebral metabolite levels, secondly to observe how any such changes are distributed across brain regions, and finally to see if these changes mirror those already observed in AD and HD brains.

In order to do this, it was originally planned that an untargeted GC–MS analysis was to be carried out using the methods previously used for the AD and HD analyses. However due to an equipment malfunction, this was not possible. Instead, we collaborated with another mass spectrometry group in order to develop a new LC–MS metabolomics method which would allow us to investigate the same analytes as those identified in the previous AD and HD analyses. In future when a new GC–MS is obtained, results from each method can then be compared for consistency of observed alterations and sensitivity of each method in identifying multiple analytes—although this was not possible within the timeframe of this thesis.

Metabolite	Study	Brain Region	Reported Change
Glucose Metabolism Pathways			
Glucose	Bohnen et al, 2011 (74)	Cortex	Increased
Glucose-6-Phosphate	Dunn et al, 2014 (75)	Cortex	Decreased
GSH	Sian et al, 1994 (71)	SN	Decreased
Purine Metabolism Pathways			
Adenosine	McFarland et al, 2013 (181)	Cortex, striatum	Increased (males)
Inosine	McFarland et al, 2013 (181)	Cortex, striatum	Increased (males)
Uric Acid	McFarland et al, 2013 (181)	Cortex, striatum	Decreased (males)
Xanthine	McFarland et al, 2013 (181)	Cortex, striatum	Increased (females)
TCA Cycle			
α-ketoglutarate	Gibson et al, 2003 (73)	CB	Decreased
Other			
NADPH	Dunn et al, 2014 (75)	Cortex, PUT	Increased
Phosphocreatine	Toczylowska et al, 2020 (466)	PUT	Decreased
Amino Acids			
Creatine	Pesch et al, 2019 (467)	Striatum	Decreased
Glutamine	Toczylowska et al, 2020 (466)	PUT	Increased

Table 9. 1. Summary of Metabolomic Perturbations Previously Reported in PD/PDD Brains

CB = Cerebellum; PUT = Putamen; SN = Substantia nigra

9.2. Methods

9.2.1. Obtaining Tissue for LC–MS Metabolomics

Tissues were obtained from nine brain regions, including the middle temporal gyrus (MTG); motor cortex (MCX); primary visual cortex (PVC); hippocampus (HP); anterior cingulate gyrus (CG); cerebellum, at the level of the dentate nucleus (CB); substantia nigra (SN); pons; and medulla oblongata (MED). These tissues were obtained from nine cases with neuropathologically-confirmed diagnoses of PDD, and nine controls free from any type of neurodegenerative disease from the Miami Brain Endowment Bank, Miami, FL, USA (part of the National Institute of Health NeuroBioBank network). All available patient metadata, including cause of death and comorbidities, were obtained and are presented in Supplementary Table 14 (p411–413).

9.2.2. Diagnosis & Severity of PDD Cases

Referring neuropathologists at the Miami Brain Endowment Bank diagnosed all donor tissue. All PDD cases were diagnosed to be the α-synucleinopathy neocortical type, consistent with the clinical phenotype of PDD. Controls did not show any neuropathological or clinical features of neurodegenerative disease or vascular pathology. Brains were assessed using either a-synuclein Braak staging (25) and/or McKeith's (13) staging criteria for Lewy body dementias (see Supplementary Table 14, p411–413, for individual data).

9.2.3. Tissue Dissection

Brain samples were cut into sections of 50 mg (± 5 mg) for LC–MS analysis using a metal-free ceramic scalpel. Samples were stored in 'Safe-Lok' microfuge Eppendorf tubes (Eppendorf AG; Hamburg, Germany) and stored at -80^{o}C prior to extraction.

9.2.4. LC–MS Metabolomics

Untargeted metabolic analysis was carried out on the brain samples using HPLC–MS. Samples were extracted in 800 µl 50:50 (v/v) methanol:chloroform before being lysed in a TissueLyser batch bead homogeniser (Qiagen, Manchester, UK) with a 3 mm carbamide beads at 25 Hz for 10 min. Blanks were also prepared containing only 800 µl 50:50 (v/v) methanol:chloroform. Following lysing, 200 µl of LC–MS grade water was added to samples before centrifugation at 2400 x g for 15 minutes for separation of polar and non-polar

phases. 200 µl of the polar methanol phase was transferred to a new tube before being dried overnight in a Speedvac centrifugal concentrator (Savant Speedvac, Thermo Scientific, UK) at ~25°C for 16–18 hours. Samples were resuspended in 100 µl acetonitrile and water in a ratio of 5:1. The sample was then centrifuged at 20,000 x g for 3 min and the top 80 µl was transferred to a glass autosampler vial with 300 µl insert and capped.

LC–MS analysis was performed using a Thermo-Fisher Ultimate 3000 HPLC system consisting of an HPG-3400RS high pressure gradient pump, TCC 3000SD column compartment and WPS 3000 Autosampler (Thermo Fisher, Waltham MA, USA), coupled to a SCIEX 6600 TripleTOF Q-TOF mass spectrometer with TurboV ion source (Sciex, Framingham MA, USA). The system was controlled by SCIEX Analyst 1.7.1 (Sciex), DCMS Link (Thermo Fisher) and Chromeleon Xpress software (Thermo Fisher).

A sample volume of 5 µL was injected by pulled loop onto a 5 µL sample loop with 150 µl post-injection needle wash with 9:1 acetonitrile and water. Injection cycle time was 1 min per sample. Separations were performed using an Agilent Poroshell 120 HILIC-Z PEEK-lined column with dimensions of 150 mm length, 2.1 mm diameter, and 2.7 µm particle size equipped with a guard column of the same phase (Agilent, Santa Clara CA, USA). Mobile phase A was water with 10 mM ammonium acetate adjusted to pH 9 with ammonium hydroxide and 20 µM medronic acid, mobile phase B was 85:15 acetonitrile and water with 10 mM ammonium acetate adjusted to pH 9 with ammonium hydroxide and 20 µM medronic acid. Separation was performed by gradient chromatography at a flow rate of 0.25 ml/min, starting at 96 % B for 2 min, ramping to 65 % B over 20 min, hold at 65 % B for 2 min, then back to 96 % B. Re-equilibration time was 5 min. Total run time including 1 min injection cycle was 30 min.

The mass spectrometer was run in negative mode under the following source conditions: curtain gas pressure, 50 psi; ionspray voltage, -4500 V; temperature, 400 °C; ESI nebulizer gas pressure, 50 psi; heater gas pressure, -70 psi; declustering potential, -80 V.

Data was acquired in a data-independent manner using SWATH in the range of 50–1000 m/z, split across 78 variable-size windows (79 experiments including TOF survey scan), each with an accumulation time of 20 ms. Total cycle time was 1.66 s. Collision energy of each

SWATH window was determined using the formula CE (V) = 0.084 x m/z + 12 up to a maximum of 55 V.

9.2.5. Data Analysis

Acquired data was processed in MultiQuant 3.0.2 (Sciex). Peaks from MS1 and MS2 data were picked and matched against a metabolite library of 235 standards, based on retention time and mass error of ± 0.025 Da. Data exported from MultiQuant 3.0.2 was further sorted, filtered, and scored using a custom VBA macro in Excel, based on presence, peak area, and coelution of precursor and fragment ions.

Statistical significance of individual metabolites was calculated using multiple two-tailed t-tests corrected for potential effects of multiple comparisons by applying a false-discovery rate (FDR) of 10% using GraphPad v6.04 (Prism; La Jolla, CA). Where blank values were > 10% of the lowest sample value, the analyte was removed from analysis. A list of all identified signals is included in Electronic Appendix G.

9.3. Results

9.3.1. Cohort Characteristics

Brain tissue for all nine investigated regions was obtained from the same case and control donors (see Table 9.2), with the exception of the SN, in which two control samples had to be substituted due to a lack of available tissue in the standard cohort donors (controls C55 and C56, see Supplementary Table 14, p411–413, for individual data). Controls C55 and C56 were age and gender-matched to the rest of the cohort. However, control C46 had to be excluded from the analysis due to a lack of metabolites identified in the sample during LC–MS. The resulting cohort of eight controls vs nine cases is described in Table 9.2. Cases and controls in the SN remained matched for age, gender, and brain weight, but PMD was lower in cases (mean 14.6 hours) compared to controls (mean 21.8 hours; p = 0.005). Case PDD12 and control C47 also did not have sufficient HP tissue for analysis, and so only eight cases and seven controls were analysed for this region; they were age, gender, brain weight, and PMD-matched (see Table 9.2).

PDD cases and controls showed no significant difference in age, gender distribution, or brain weight (see Table 9.2). Cases and controls were *post mortem* delay (PMD)-matched

in all brain regions except the SN, in which cases had a lower PMD than controls (p = 0.02; data not shown). PMD was kept as low as possible, at a maximum of 26.0 hours in any region and an average of 17.1 hours.

Additional metadata was also obtained for all cases and controls, including cause of death and PD disease staging (see Supplementary Table 14, p411–413). Brain weight was unavailable for control C56.

	Gender (% male)	Age at death (years)	PMD (hours)	Brain Weight (g)
Controls (n = 9)	44	70 (61 – 79)	19.8 (12.5 – 26.0)	1285 (1135 – 1371)
SN Controls (n = 8)	37.5	70 (62 – 79)	21.8 (17.8 – 26.0)	1275 (1135 – 1371)†
HP Controls (n = 7)	44	71 (61 – 79)	20.5 (12.5 – 26.0)	1263 (1135 – 1372)
Cases (n = 9)	66	73 (61 – 81)	14.6 (4.3 – 21.88)	1291 (1187 – 1520)
HP Cases (n = 8)				

Table 9. 2. Cohort Characteristics

Table shows mean (range) age, PMD, brain weight and Braak stage.

9.3.2. LC–MS Analysis

A total of 64 metabolites were identified in the samples (see Electronic Appendix H for full list). Of these, 47 (73%) showed significant case–control changes ($p < 0.05$ corrected with 10% FDR) in at least one investigated brain region (see Supplementary Figure 1, p416–421, for graphs of all altered metabolites). 31 (66%) of the altered metabolites were decreased in PDD cases compared to controls in at least one region and 21 showed increases (57%). For some analytes, results had to be excluded due to high blank values (see Table 9.3).

The regions showing the highest number of altered metabolites were the MED (25), PONS (24), and MTG (23; see Fig 1 and Table 9.3). The regions with the lowest number of altered metabolites were the MCX (7), PVC (10), and CG (11). The CB, SN, and HP showed intermediate levels of metabolite alterations at 13, 19, and 22 respectively. The number of overall metabolite changes appears to correlate with the stage at which the brain region is considered to start showing Lewy body deposition according to α-synuclein Braak staging criteria, with regions affected earlier in PDD showing higher numbers of metabolic alterations (see Fig 1). Interestingly, the CB showed a similar number of changes to the SN, despite being considered to be relatively unaffected in PDD.

The highest number of metabolite increases was observed in the HP (16), whereas the most decreased metabolites were found in the PONS (14). Interestingly, the CG showed statistically significant decreases in PDD cases for several metabolites which were observed to show significant increases in other regions (see Table 9.3), including deoxyguanosine (0.8-fold), deoxyuridine-monophosphate (0.9-fold), D-ribose-5-phosphate (0.1-fold), ethylmalonate (0.9-fold), and inosine (0.8-fold).

Some metabolites were altered in almost every observed region. Fructose was found to be significantly increased in every region except the CB and SN, with increases ranging from 1.1-fold in the CG to as high as 2.8-fold in the HP and PVC. Inosine was altered in every region except the MTG and SN, with increases ranging from 1.5 (pons) to 2.3-fold (MED) in every other region except the CG, where it was decreased by 0.8-fold. Proline was observed to be significantly decreased in every region, with decreases ranging from 0.3-fold in the CG to 0.6-fold in the pons and SN. Serine was also decreased in every region, with fold-changes ranging from 0.3-fold in the CG to 0.7-fold in the HP and SN. Deoxyguanosine was also altered in every region, with increases ranging from 1.5 (CB, pons, SN) to 2.1-fold (MED) in every region except the CG, which showed a 0.8-fold decrease.

The altered metabolites observed in the PDD brain are associated with several metabolic pathways, such as glucose (see Figure 9.2) and purine (see Figure 9.3) metabolism, as well as including multiple amino acids (see Supplementary Figure 1, p416–421, for graphs of all significantly altered metabolites). Multiple metabolites involved in glycolysis were found to be increased in at least one brain region, including glucose, fructose, fructose-6-

phosphate, and glucose-6-phosphate. Alterations in alternative glucose metabolic pathways were also observed, such as changes in ribose-5-phosphate, which is downstream of glucose-6-phosphate in the pentose phosphate pathway (PPP). As well as glucose pathways, multiple metabolite intermediates of purine metabolism were observed to be altered, including increased guanosine and inosine, and decreased hypoxanthine and xanthine.

Analyte	CG	CB	HP	MCX	MED	MTG	PONS	SN	PVC
Amino Acids									
Allothreonine	0.3	0.4	**0.5**	0.5	**0.6**	0.6	0.7	0.8	0.7
Aspartate	0.3	0.7	**0.5**	0.6	0.8	0.7	**0.7**	1.0	0.5
Creatine	0.4	0.8	**0.5**	0.7	0.8	0.7	**0.7**	1.0	0.6
Glutamate	0.6	1.1	1.1	1.1	1.2	1.0	1.1	**1.5**	1.1
Histidine	0.3	**0.5**	**0.6**	0.6	**0.6**	**0.6**	0.7	**0.6**	0.6
Isoleucine	0.3	**0.5**	**0.6**	0.6	**0.6**	**1.1**	0.7	**0.6**	0.6
Leucine	0.3	0.5	**0.6**	0.6	**0.6**	**1.1**	0.7	**0.6**	0.6
N-acetylserine	0.4	**0.5**	**0.4**	0.6	0.7	**0.6**	0.8	0.8	**0.5**
Norleucine	0.3	0.5	**0.6**	0.6	**0.6**	**0.6**	0.7	**0.6**	0.6
Norvaline	0.3	**0.5**	**0.6**	0.6	**0.6**	**0.5**	**0.7**	0.7	0.5
Proline	**0.3**	**0.5**	**0.5**	**0.5**	**0.5**	**0.4**	**0.6**	**0.6**	**0.4**
Sarcosine	0.1	0.4	0.2	0.1	0.4	**0.3**	0.8	0.7	0.6
Serine	**0.3**	**0.5**	**0.7**	**0.6**	**0.6**	**0.6**	**0.6**	**0.7**	**0.5**
Tyrosine	0.3	**0.6**	**0.7**	0.7	**0.7**	0.7	0.8	0.8	0.6
Valine	0.3	**0.5**	**0.6**	0.6	**0.6**	**0.5**	**0.7**	0.7	0.5
Glucose & Related Metabolites									
Fructose	**1.1**	1.6	**2.8**	**2.7**	**2.4**	**2.7**	**2.4**	1.2	**2.8**
Fructose-6-phosphate	**4.8**	0.9	**4.0**	3.2	1.4	**2.3**	1.2	**EXC**	1.1
Glucose	0.6	2.0	1.1	1.4	1.3	1.0	**2.1**	0.9	1.0
Glucose-6-phosphate	1.3	0.9	1.5	1.2	**EXC**	1.4	**2.3**	**EXC**	2.6

Mannose-6-phosphate	**1.9**	1.4	**3.5**	0.6	**EXC**	2.5	1.9	1.1	3.6
Ribose-5-phosphate	**0.1**	1.2	**1.9**	1.5	**2.1**	**1.6**	**1.8**	**EXC**	**2.3**
Nucleosides & Purine Metabolism									
Deoxyguanosine	**0.8**	**1.5**	**1.8**	**1.8**	**2.1**	**1.7**	**1.5**	**1.5**	**1.6**
Deoxyuridine-monophosphate	**0.9**	1.4	**1.5**	**1.8**	**1.7**	**1.7**	**2.1**	**EXC**	2.1
Guanine	0.4	0.8	0.9	0.9	0.9	0.8	0.9	**0.7**	0.9
Guanosine	0.6	**1.9**	1.3	**1.7**	**2.5**	1.5	**1.6**	1.3	1.5
Hypoxanthine	0.4	0.8	0.8	0.7	**0.8**	**0.7**	0.8	**0.7**	**0.6**
Inosine	**0.8**	**1.6**	**1.8**	**2.0**	**2.3**	1.7	**1.5**	1.1	**1.8**
Uracil	**0.3**	0.7	**0.6**	0.6	**0.7**	**0.6**	0.8	**0.5**	**0.4**
Ureidopropionate	0.5	0.9	1.1	1.1	**1.2**	1.1	**1.2**	1.1	1.0
Xanthine	0.4	0.8	0.9	0.9	0.9	0.8	0.9	**0.7**	0.8
TCA & Urea Cycles									
Malate	0.3	0.7	**0.6**	0.6	0.7	0.8	0.7	0.9	0.5
N-acetylglutamate	0.4	0.9	1.0	0.7	1.0	**0.5**	**0.3**	0.7	**0.6**
Alternative Fuel Sources									
3-hydroxymethyl-glutarate	0.6	1.7	0.2	0.9	1.0	0.5	**0.4**	0.6	0.9
Myo-inositol	0.6	1.3	1.2	1.1	1.2	1.1	1.2	**1.5**	1.2
Other									
2,3-dihydroxybenzoate	0.5	0.8	0.9	0.9	0.8	0.8	0.9	**0.6**	0.8
2-methylmalate	0.6	1.0	1.4	1.4	1.3	**1.5**	1.1	0.7	**1.2**
4-guanidinobutanoate	0.8	1.8	1.3	2.3	**2.0**	**1.8**	**2.0**	**2.2**	1.8
Decanoate	**EXC**	1.4	1.7	1.3	**1.7**	1.3	1.3	1.4	1.3

Ethylmalonate	**0.9**	1.6	1.6	2.5	**2.0**	**1.9**	**1.7**	1.3	1.5
Galactitol	0.8	**3.1**	1.5	**1.7**	**2.7**	**1.6**	**2.3**	**3.0**	1.4
L-tryptophanamide	0.3	0.6	0.6	0.6	**0.6**	**0.5**	0.7	**0.6**	0.5
N-acetylaspartate	0.6	1.3	1.2	1.2	**1.2**	1.1	**1.1**	1.1	1.2
N-acetylmethionine	0.3	0.6	0.7	0.7	0.7	0.8	1.0	**0.6**	0.7
N-acetylneuraminate	0.5	1.1	**0.6**	0.8	1.0	0.8	**1.3**	**1.8**	0.9
Pantothenate	0.3	**0.4**	0.7	0.6	**0.6**	**0.7**	**0.6**	0.6	0.7
S-adenosylhomocysteine	0.5	1.3	1.0	0.9	1.1	0.9	1.3	**1.6**	0.8
Suberate	**1.4**	0.9	**1.6**	1.2	1.5	2.1	**2.5**	1.6	1.2

Table 9. 3. Significantly Altered Metabolites in PDD Brain

EXC = Excluded from analysis due to high blank values. Significant case–control fold-changes ($p < 0.05$) were determined by multiple student's t-test corrected with 10% FDR and are highlighted in bold. See Electronic Appendix H for full list of metabolites, fold-changes, and p-values.

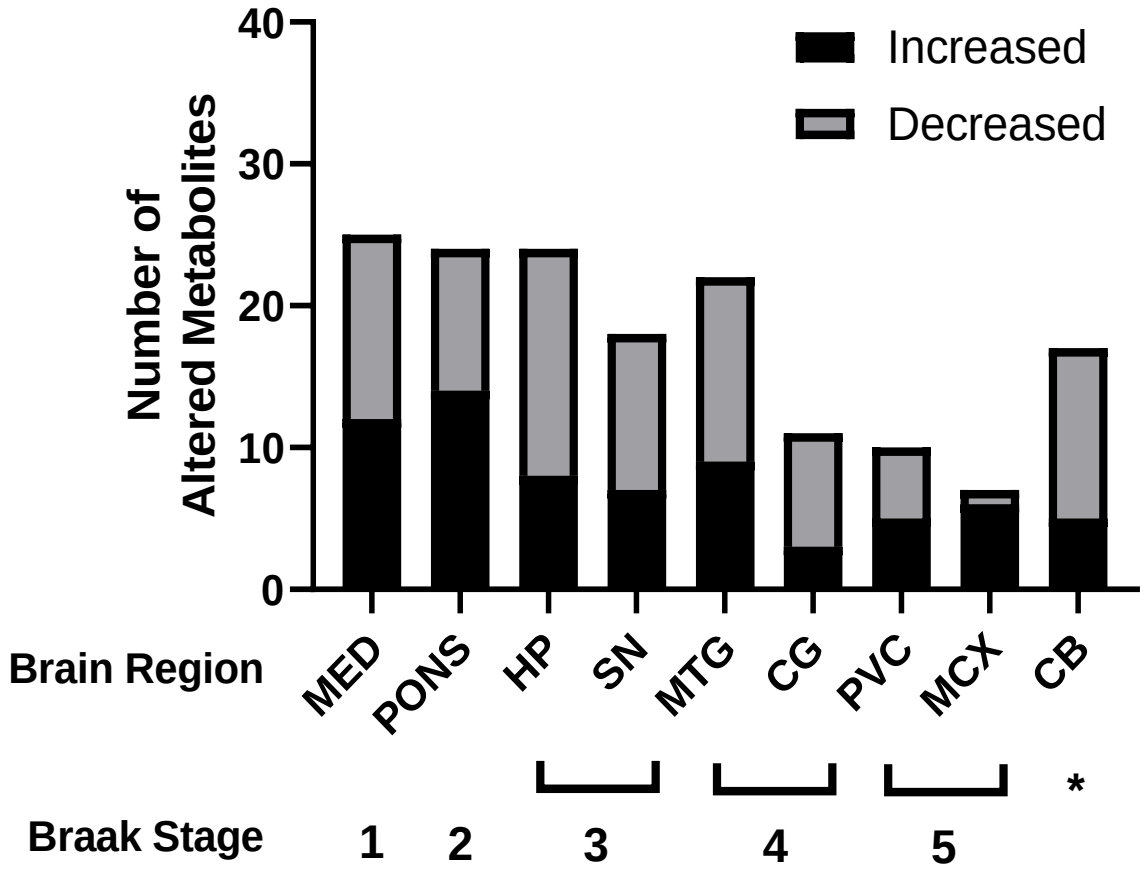

Figure 9. 1. Number of Altered Metabolites in PDD Brain Regions

CB = Cerebellum; CG = Cingulate gyrus; HP = Hippocampus; MCX = Motor cortex; MED = Medulla oblongata; MTG = Middle temporal gyrus; PVC = Primary visual cortex; SN = Substantia nigra. * CB typically considered to be free of Lewy body deposition in traditional α-synuclein Braak staging.

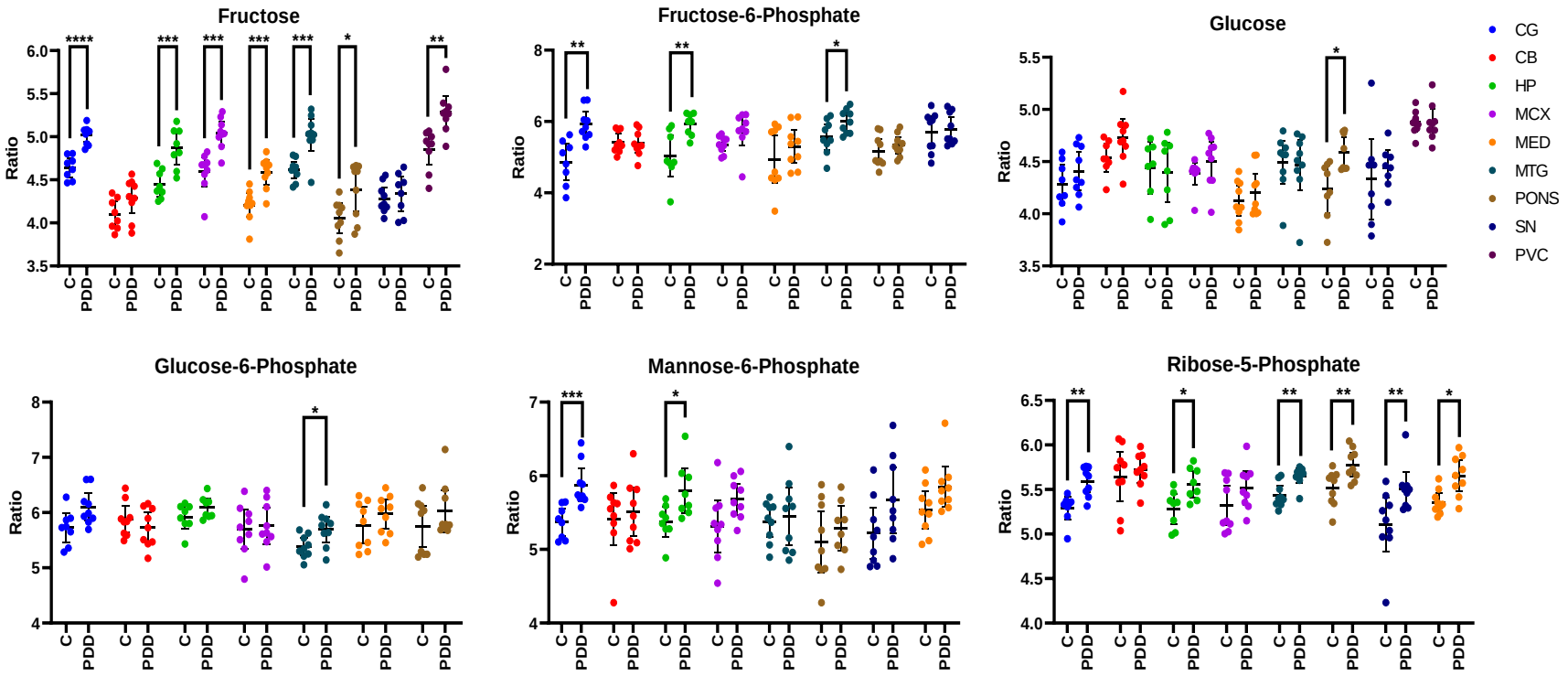

Figure 9. 2. Glucose Pathway Metabolites in the PDD Brain

C = Control; PDD = Parkinson's disease dementia. Case–control significance was determined by multiple t-tests corrected by 10% FDR. * $p < 0.05$, ** $p < 0.01$, *** $p < 0.001$, **** $p < 0.0001$.

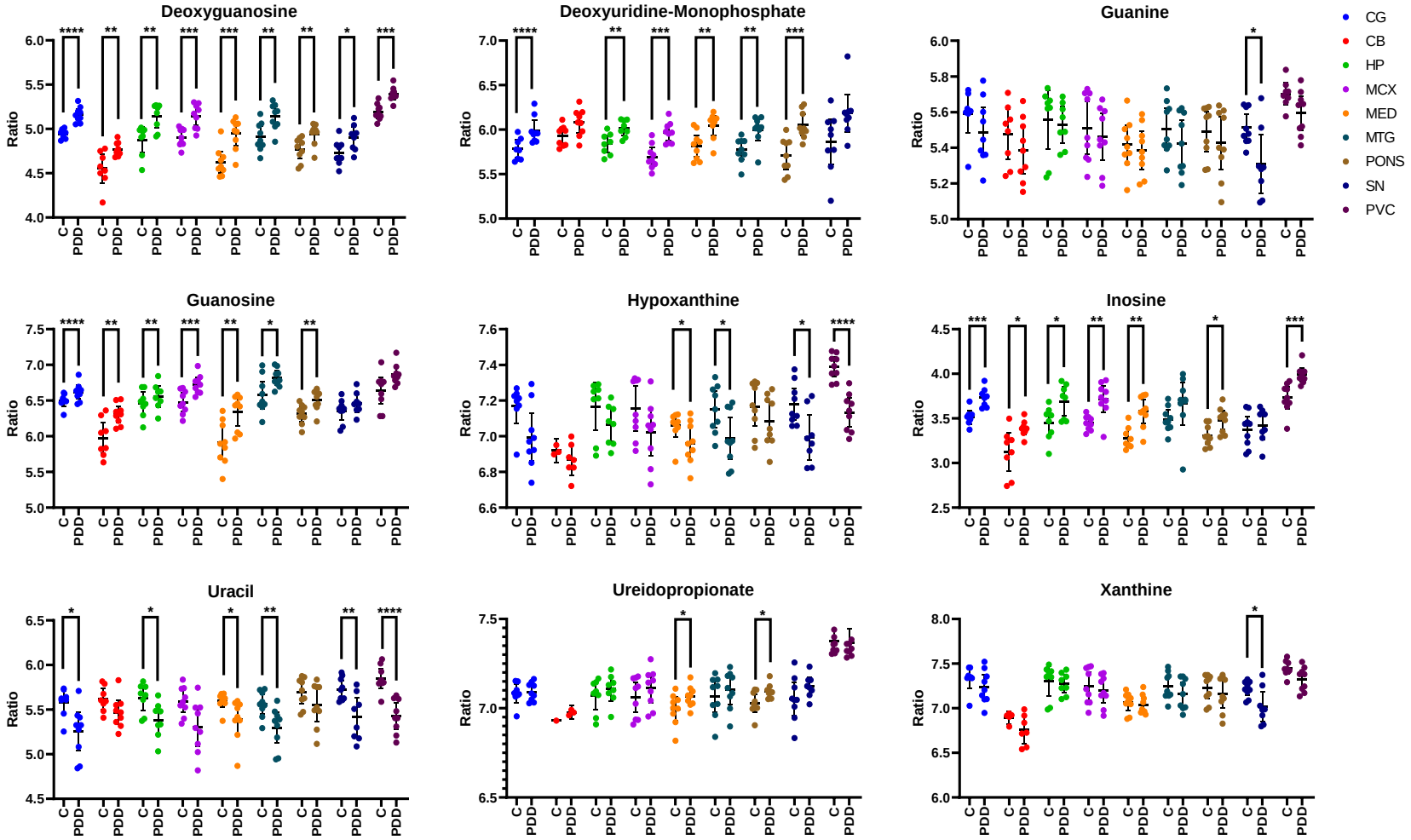
Deoxyguanosine
Deoxyuridine-Monophosphate
Guanine
Guanosine
Hypoxanthine
Inosine
Uracil
Ureidopropionate
Xanthine
Ratio
C
PDD
CG
CB
HP
MCX
MED
MTG
PONS
SN
PVC

Figure 9. 3. Purine Pathway Metabolites in the PDD Brain

C = Control; PDD = Parkinson's disease dementia. Case–control significance was determined by multiple t-tests corrected by 10% FDR. * $p < 0.05$, ** $p < 0.01$, *** $p < 0.001$, **** $p < 0.0001$.

9.3.3. Comparison to AD and HD

We have previously performed untargeted metabolomics analyses of AD (180) and HD (183) brains using GC–MS. Although the mass spectrometry methods employed are slightly different, the results should be comparable across diseases.

Each analysis investigated different brain regions. The AD investigation included six regions involved in the current analysis: the HP, MTG, SCX, MCX, CG, and CB. The HD investigation included seven regions used in the current analysis: the HP, MTG, SCX, MCX, CG, CB, and SN. As such, six regions were analysed in all three diseases: the HP, MTG, SCX, MCX, CG, and CB. Results from these regions can be compared across PDD, AD, and HD.

Of the 64 analytes identified here, 17 were also identified in the AD study, and 21 in the HD study (see Table 9.4). Of these, 16 were identified in all three studies: glucose, glucose-6-phosphate, fructose, ribose-5-phosphate, proline, serine, aspartate, uracil, hypoxanthine, n-acetylaspartate, glutamate, guanosine, valine, leucine, isoleucine, and tyrosine. As such, results for these metabolites can be compared across all three diseases. These are summarised in Table 9.4.

9.3.3.1. PDD and AD

Of 17 metabolites identified in both PDD and AD brains, fifteen showed similar changes in both; increased glucose, glucose-6-phosphate, fructose, fructose-6-phosphate, and myo-inositol; and decreased ribose-5-phosphate, proline, serine, aspartate, uracil, aspartate, n-acetylaspartate, pantothenic acid, and hypoxanthine.

Many of these shared changes did not occur within the same brain regions in both PDD and AD, suggesting regional specificity in different dementias. However, there were some changes that were shared within the same regions in both diseases, including: increased fructose in the HP, MTG, MCX, and CG; increased fructose-6-phosphate in the HP, MTG, and CB; decreased ribose-5-phosphate in the MTG; decreased proline in the HP; decreased serine in the HP and CB; decreased aspartate in the HP; decreased uracil in the CG, HP, and MTG; decreased pantothenic acid in the CB and MTG; and decreased hypoxanthine in the MTG in both PDD and AD brains. Of all comparable brain regions, the HP showed the greatest number of similarities between PDD and AD.

9.3.3.2. PDD and HD

Of the 21 metabolites identified in both PDD and HD brains, 14 showed similar changes, including increased glutamate, fructose, glucose, glucose-6-phosphate, and guanosine, and decreased aspartate, leucine, isoleucine, proline, serine, uracil, hypoxanthine, pantothenic acid and N-acetylglutamate.

Of these, only seven showed changes that were consistent across the same brain regions in both PDD and HD, including: decreased leucine in the HP, decreased isoleucine in the HP and CB, decreased proline in the HP and CB, decreased uracil in the HP, decreased serine in the CB and HP, decreased hypoxanthine in the MTG, and increased fructose in the CB of both PDD and HD brains. Once again, the HP appears to be the region showing the highest number of similarities between PDD and HD.

9.3.3.3. PDD, AD, and HD

Out of all 16 analytes observed in all three dementias, 12 showed consistent changes within PDD, AD, and HD brains; including decreased aspartate, proline, serine, hypoxanthine, uracil, N-acetylglutamate, and pantothenic acid; and increased glutamate, fructose, glucose, glucose-6-phosphate, and guanosine. Only four of these changes were consistent across all three dementias within the same region; proline was decreased in the HP, serine decreased in the CB and HP, hypoxanthine decreased in the MTG, and uracil decreased in the HP in PDD, AD, and HD.

	PDD		AD		HD	
Analyte	**Change**	**Brain Region**	**Change**	**Brain Region**	**Change**	**Brain Region**
Amino Acids						
Aspartate	**Decreased**	**HP**, *MED*	**Decreased**	**HP**, ENT	**Decreased**	*PUT*
Glutamate	**Increased**	SN	**Increased**	CG	**Increased**	GP
Isoleucine	**Decreased**	CB, **HP**, *MED*, MTG, SN	Unchanged		**Decreased**	**HP**, ENT
Leucine	**Decreased**	**HP**, *MED*, MTG, SN	Unchanged		**Decreased**	**HP**, ENT
Proline	**Decreased**	CG, CB, **HP**, MCX, *MED*, MTG, *PONS*, SN, *PVC*	**Decreased**	**HP, ENT**	**Decreased**	**HP, ENT**, SCX, *PUT*
Serine	**Decreased**	CG, **CB, HP,** MCX, *MED*, MTG, *PONS*, SN, *PVC*	**Decreased**	**CB, HP**, ENT	**Decreased**	CG, **CB, HP**, MTG, SN, SCX, *PUT*
Tyrosine	**Decreased**	CB, HP, *MED*	Unchanged		**Increased**	*PUT*
Valine	**Decreased**	CB, HP, *MED*, MTG, PONS	Unchanged		Unchanged	
Glucose & Related Metabolites						

Fructose	Increased	**CG, HP, MCX,** *MED*, **MTG,** *PONS*, *PVC*	Increased	**CG, CB, HP, MCX, MTG,** ENT, SCX	Increased	**CB,** *PUT*
Fructose-6-Phosphate	Increased	**CG, HP, MTG**	Increased	**CG,** CB, **HP,** MCX, **MTG,** ENT, SCX	Unchanged	
Glucose	Increased	*PONS*	Increased	CG, CB, HP, MCX, MTG, ENT, **SCX**	Increased	SN, **SCX,** *PUT, GP*
Glucose-6-Phosphate	Increased	*PONS*	Increased	CG, CB, **HP,** MCX, MTG, **ENT,** SCX	Increased	**HP,** SN, **ENT,** *PUT, GP*
Ribose-5-Phosphate	Decreased Increased	CG HP, *MED*, MTG, *PONS*, *PVC*	Decreased	MTG, ENT	Unchanged	
Nucleosides & Purine Metabolism						
Guanosine	Increased	CB, MCX, *MED*, *PONS*	Increased	MTG	Increased	*MFG*
Hypoxanthine	Decreased	*MED*, **MTG, SN,** *PVC*	Decreased	**CB, MTG**, ENT, **SCX**	Decreased	**CB,** HP, **MTG, SN, SCX,** *PUT*
Inosine			Not detected		Increased	*PUT*

	Decreased **Increased**	CG CB, HP, MCX, *MED*, *PONS*, *PVC*				
Uracil	**Decreased**	**CG, HP,** *MED*, **MTG,** SN, *PVC*	**Decreased**	**CG,** CB, **HP,** MCX, **MTG**, ENT, SCX	**Decreased**	**HP,** *PUT*
Xanthine	**Decreased**	SN	Not detected		**Increased**	MCX, *PUT*
TCA & Urea Cycles						
Malate	**Decreased**	HP	**Increased**	MTG, ENT	**Increased**	*PUT*
N-Acetylglutamate	**Decreased**	*MED*, *PONS*, *PVC*	**Decreased**	ENT	**Decreased**	SCX
Alternative Fuel Sources						
Myo-inositol	**Increased**	SN	**Increased**	ENT	**Decreased**	CB, MTG, SCX
Other						
N-Acetylaspartate	**Increased**	*MED*, *PONS*	Unchanged		**Decreased**	SCX, *PUT*
Pantothenic Acid	**Decreased**	**CB,** *MED*, *PONS*, **MTG**	**Decreased**	CG, **CB, HP**, MCX, **MTG,** ENT, SCX	**Decreased**	**HP,** SN, *PUT, GP*

Table 9. 4. Comparison of Metabolites in PDD, AD, and HD Brains

CB = Cerebellum; CG = Cingulate gyrus; ENT = Entorhinal cortex; GP = Globus pallidus; HP = Hippocampus; MCX = Motor cortex; MED = Medulla oblongata; MFG = Middle frontal gyrus; MTG = Middle temporal gyrus; PUT = Putamen; PVC = Primary visual cortex; SCX = Sensory cortex; SN = Substantia nigra. Italicised regions were only investigated in one dementia, and so results could not be compared across diseases. Regions highlighted in bold show similar changes across two or more dementias.

9.4. Discussion

To the authors' knowledge, this study presents the first systematic, untargeted metabolomics analysis across multiple regions of the PDD brain. Such studies are often restricted to targeted investigations of only one or two severely affected regions of the PD brain (such as the SN or PUT), and do not differentiate between PD with and without dementia. Additionally, this study includes the first comparison of metabolomic alterations identified across PDD, AD, and HD brains using comparable methodologies and multiple brain regions. Such comparisons are usually limited by differences in methodologies, cohort characteristics, and investigated brain regions; but a comparison of multiple analytes across several brain regions in PDD, AD, and HD was possible in this study.

This study identified 47 metabolic alterations in the PDD brain, including multiple amino acids as well as metabolites involved in glucose and purine metabolism. The number of alterations varied depending on the brain region investigated, with regions affected earlier in the disease or more severely by neurodegeneration (as described by α-synuclein Braak staging (25)) showing a higher number of changes. This suggests that metabolic disruptions reflect the severity of damage in PDD-affected brain regions.

One exception to this rule appears to be the CB, which showed a moderate number of metabolite alterations despite traditionally being considered to be relatively unaffected by neurodegeneration in PD/D. This may indicate a greater involvement of the CB in PDD than previously thought. Indeed, Lewy body deposition and dopaminergic neurodegeneration has been observed in the CB in PD, despite its lack of involvement in the description of typical α-synuclein Braak stage progression (430, 468-470). This also mirrors observations from our previous analyses of AD and HD, in which the CB also showed unexpectedly high levels of metabolic alterations, despite being a region considered to be relatively spared in both diseases. Taken together, these results suggest an unexpected degree of cerebellar involvement in neurodegenerative diseases.

9.4.1. Glucose Metabolism

Evidence for impaired glucose metabolism has been reported extensively in the PD and PDD brain (420, 471, 472), with previous reports of increased glucose (74) and decreased glucose-6-phosphate (75) in the PD cortex. Although the cortex as a whole was not

investigated here, we were unable to identify increased glucose in the PDD MCX, with the only glucose increase observed in the pons. Likewise we did not observe any changes in glucose-6-phosphate in the MCX, but instead found an increase in the pons. Discrepancies with previous reports in the cortex may be accounted for by differences in methodologies, with PET imaging and ELISA assay previously used to measure glucose and glucose-6-phosphate respectively, may represent differences between PD with and without dementia, or may simply be the result of differences between the PDD MCX and cortex as whole. As there have been no investigations looking at either of these metabolites in any other region of the PD/PDD brain, our results in these regions present novel findings, which are illustrated in Figure 9.4 – updated to include the findings from the current study.

Other glucose pathway metabolites, including fructose, fructose-6-phosphate, mannose-6-phosphate, and ribose-5-phosphate, have not to the authors' knowledge been previously investigated in the PD/D brain. Strikingly, fructose showed increases of up to 2.8-fold in all investigated regions except the CB and SN, and fructose-6-phosphate also showed large increases of up to 4.8-fold in the CG, HP, and MTG. Fructose elevations may indicate increased activity of the polyol pathway, which generates fructose downstream from glucose and sorbitol. This fructose may then be utilised as an energy source to compensate for decreased glycolytic activity in PDD. Likewise, widespread elevations in ribose-5-phosphate, and more limited increases in glucose-6-phosphate and fructose-6-phosphate may indicate impaired glycolysis, with a build-up of glycolytic precursor molecules. It may also indicate an increase in activity of the pentose phosphate pathway, which generates glycolysis precursor molecules from glucose.

The lack of fructose changes in the heavily-affected SN is surprising in PDD, when changes in this metabolite appear to affect every other region investigated. Unfortunately due to high blank readings, the fructose-6-phosphate, glucose-6-phosphate, and ribose-5-phosphate data for the SN had to be excluded, so it is unknown whether these analytes were altered in the SN. However, taken together, the data suggests dysregulation of glucose metabolism pathways that is widespread, but potentially absent from the SN.

Glucose metabolism not only appears to be dysregulated in PDD, but has also been reported to be altered in both AD and HD, with widespread increases in fructose in both

diseases (183, 184). Increased glucose is also present throughout the AD brain (184, 185), with more localised accumulations in the HD brain (183). Fructose-6-phosphate and glucose-6-phosphate have also been seen to be increased in AD (180), but only the latter has been found to be raised in some HD brain regions (183) in some reports, with others reporting no change (287). As such, dysregulation in glucose metabolism, with alterations in both polyol and pentose phosphate pathway intermediate metabolites, appears to be a common feature to PDD, AD, and HD.

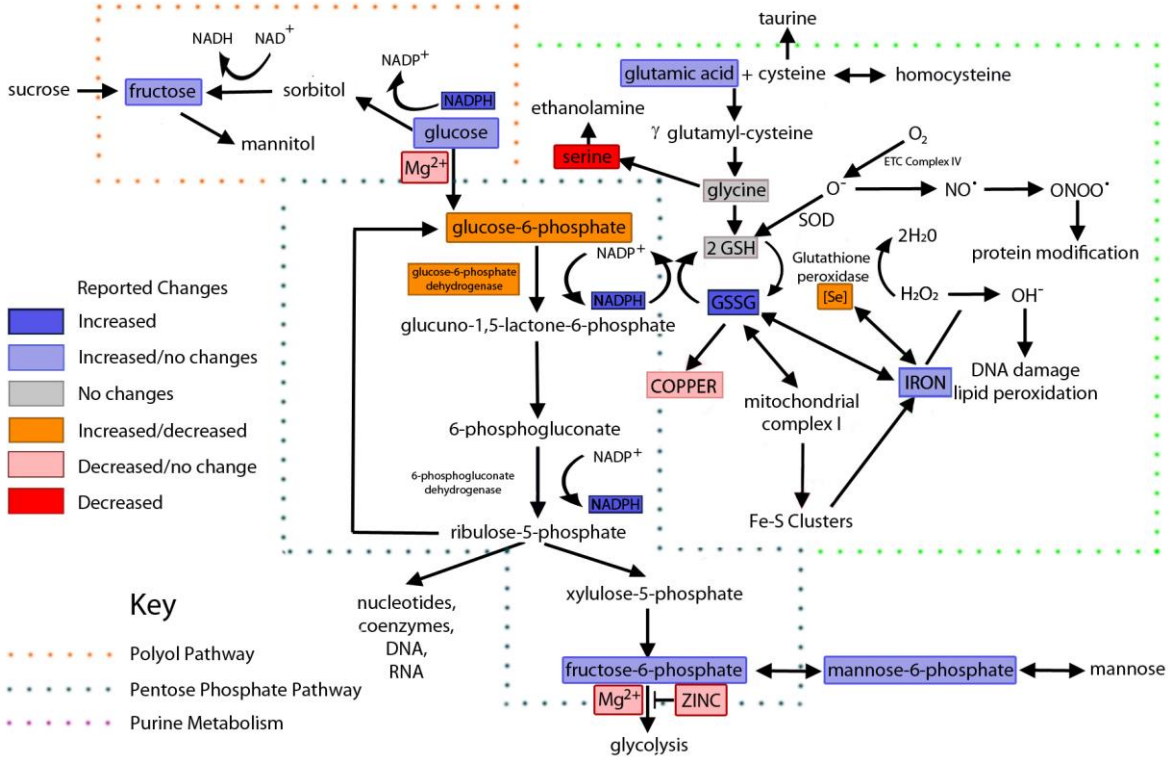

Figure 9. 4. Updated: Glucose Pathway Changes in the PDD Brain

Figure shows metabolite changes found in the current study and reported by previous investigations in the PD/PDD brain. GSH, reduced glutathione; GSSG, oxidised glutathione; H_2O_2, hydrogen peroxide; Mg^{2+}, magnesium ion; NAD, oxidised nicotinamide adenine dinucleotide^{+}; NADH, reduced nicotinamide adenine dinucleotide; $NADP^{+}$, oxidised nicotinamide adenine dinucleotide phosphate; NADPH, reduced nicotinamide adenine dinucleotide phosphate; NO^{-}, nitric oxide radical; OH^{-}, hydroxide radical; $ONOO^{-}$, peroxynitrite; Se, selenium.

9.4.2. Purine Metabolism

Purines are heterocyclic aromatic compounds which include the two purine nucleotide bases guanine and adenine, as well as purine derivatives such as hypoxanthine, xanthine,

and uric acid. The nucleotide base purines are essential components of the DNA and RNA nucleobase backbone, but purines also function as components of other metabolic molecules such as adenosine triphosphate (ATP), cyclic adenosine monophosphate (cAMP), reduced nicotinamide adenine dinucleotide (NADH), and coenzyme A (CoA). As such, purines are involved in a large number of metabolic pathways.

The purine metabolism pathway is the pathway by which purines are synthesised and broken down, and is essential for purine homeostasis. Disruptions in this pathway may lead to insufficient pools of purine components for metabolic biomolecules and downstream dysregulation of metabolic pathways that require those molecules, such as glucose metabolism, TCA cycle, the MTC, etc. Region-specific dysregulation of purine metabolism genes have been previously reported in the PD brain, with distinct alterations observed in the SN and frontal cortex (473).

Here, we report widespread increases in inosine, an intermediate in the purine metabolism pathway. Inosine was increased in the CB, HP, MCX, MED, PONS, and PVC, although it also showed a significant decrease in the CG of PDD. A similar pattern of changes was observed in deoxyguanosine, as well as increases in the MTG and SN. Region-specific increases were also observed in guanosine, deoxyuridine-monophosphate, and ureidopropionate, as well as localised decreases in guanine, hypoxanthine, uracil, and xanthine. Together, these observations suggest substantial disruption of the purine metabolism pathway in the PDD brain (see updated pathway in Fig 5.). This is supported by a previous report of increased adenosine and inosine, and decreased uric acid in the PD cortex and striatum—although the study reported these changes to be male-specific, with female-specific increases in xanthine (181). These sex-specific differences were not present in the current PDD cohort. It is possible this may be a distinguishing factor between PD with and without dementia, as the McFarland cohort was not selected based on the presence of dementia symptoms. A parallel analysis of PD without dementia using the methods employed in this investigation could investigate the effects of cognitive decline on PD brain metabolism.

Alterations in purine metabolism have also been reported in AD and HD brains. Our own analyses have observed region-specific decreases in hypoxanthine and uracil, and increases in guanosine in both AD and HD. We also reported increases in xanthine and inosine in the

HD PUT. Other reports have found increased adenosine, inosine, and guanosine in the parietal and temporal cortices (179), increased guanine in the ENT (377), decreased hypoxanthine in the frontal cortex (179), and decreased xanthine in the frontal cortex (179) and ENT (377) of the AD brain. However, another report found no changes in any of these analytes within the AD CB, striatum, frontal or parietal cortices (181). In HD, increased guanosine in the superior temporal gyrus (287), increased inosine in the striatum (182), and decreased uric acid in the inferior temporal gyrus and caudate nucleus (287) have been reported. Taken together, our own analyses as well as other existing data indicate a shared perturbation in cerebral purine metabolism in PDD, AD, and HD.

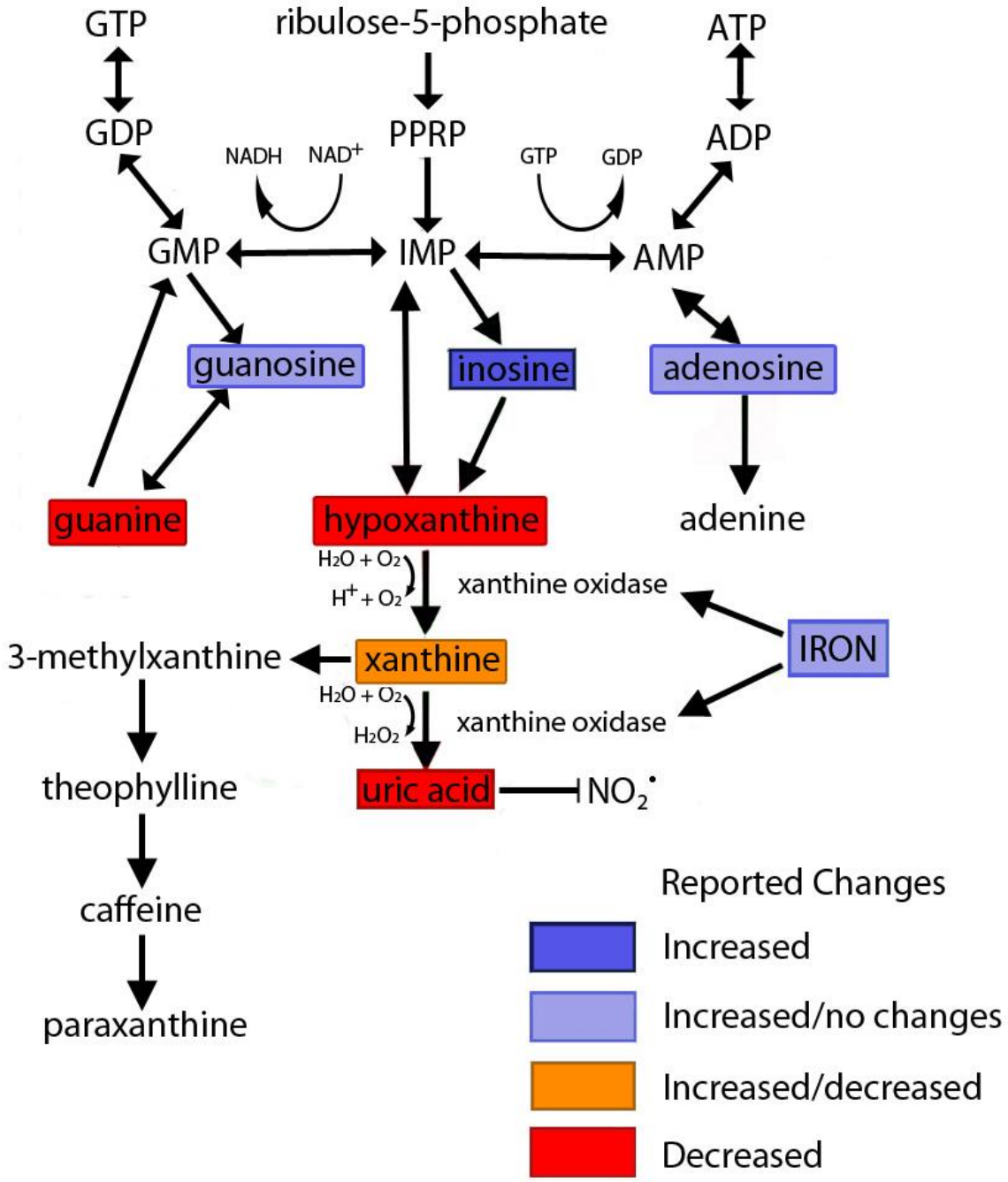

Figure 9. 5. Updated: Purine Pathway Alterations in the PDD Brain

Figure shows metabolite changes found in the current study and reported by previous investigations in the PD/PDD brain. ADP, adenosine diphosphate; AMP, adenosine monophosphate; ATP, adenosine triphosphate; GMP, guanosine monophosphate; GTP, guanosine triphosphate; IMP, inosinic acid; NAD, oxidised nicotinamide adenine dinucleotide; NADH, reduced nicotinamide adenine dinucleotide; NADP, oxidised nicotinamide adenine dinucleotide phosphate; NADPH, reduced nicotinamide adenine dinucleotide phosphate; NO^{-}, nitric oxide radical; PPRP, phosphoribosyl pyrophosphate.

9.4.3. Amino Acids

Multiple amino acids were observed to be altered in the PDD brain, with widespread decreases in serine and proline affecting every investigated region, as well as region-specific decreases in isoleucine, valine, and histidine among others. MTG-specific increases in leucine and isoleucine were also present. Amino acids provide substrates to metabolic pathways such as the TCA cycle, which produces energy through the oxidation of acetyl-CoA. Diminished amino acid levels may prevent proper functioning of the TCA cycle, leading to decreased energy production.

Amino acids may also influence neurotransmitter synthesis and function. Glutamate, which was increased in the PDD SN, is the precursor of the inhibitory neurotransmitter γ-aminobutyric acid (GABA), which has been reported to be increased in the basal ganglia (474, 475) and PUT (476) of individuals with PD. However, other reports have observed decreased GABA levels in the PD basal ganglia (477), as well as in the occipital lobe of PD patients experiencing visual hallucinations (478). As such, although there are many reports of GABA alterations in PD, further studies are required to determine whether levels are increased or decreased, or whether the nature of GABA alterations may depend on clinical presentation of particular motor, cognitive, or psychological symptoms.

9.4.4. Other

Alterations in several other metabolites were also identified here in the PDD brain. The most widespread alterations was in galactitol, which was observed to be elevated in all regions except the CG, HP, and PVC, with increases of up to 3.1-fold. Increased cerebral and ocular galactitol is a feature of galactosaemia, a rare genetic metabolic disorder in which galactose accumulates in the blood as it cannot be properly metabolised (479). This condition can result in severe cognitive impairment in sufferers if untreated.

Pantothenic acid was observed to be decreased in the CB, MED, MTG, and pons of PDD cases here. Reduced pantothenic was also found in our targeted analysis of Chapter Seven in the CB and MED, with borderline significance in the pons. However it was not observed in the MTG in the targeted analysis, although there was a non-significant trend towards decrease, and was found to be significantly decreased in the SN. This regional discrepancy must be attributed to differences in the methodologies used in the two analyses, as the

cohorts used were identical. This may point to a relative lack of accuracy in the untargeted analysis in comparison to the targeted method, which allowed for determination and comparison of absolute concentrations, and not just relative fold-changes. Such factors need to be kept in mind for similar future untargeted analyses.

9.4.5. Limitations of the Study

In this study, we present an untargeted metabolomics analysis employing a newly-developed LC–MS method. This approach has many strengths, including the ability to identify large numbers of analytes, including ones which have not been previously investigated in PDD. It is able to do so in large numbers of samples in a relatively short amount of time, using a sensitive mass spectrometry analysis which is able to detect very small concentrations of an analyte in a sample, and accurately identify it using the in-house library. This methodology is ideal for identification of polar and non-volatile molecules and does not require derivitisation of samples, with sample prep being relatively straight-forward in comparison to other approaches such as gas chromatography–mass spectrometry (GC–MS).

However, there are also limitations to this approach. Due to the large number of analytes involved, it is not feasible to include internal standards for each one. Due to this, it is not possible to determine absolute concentrations of an analyte—but only relative concentrations. This may diminish the accuracy of the analysis in comparison to more targeted methods with spiked internal standards. As a new method, this approach also requires validation to ensure that it is as accurate as previously used untargeted methods. In this case, the results from the current LC–MS analysis need to be comparable to those previously obtained in the GC–MS analyses of AD and HD, if we are to accurately compare results between these three diseases. In order to ensure this is the case, it would be ideal to perform a GC–MS analysis of the current PDD cohort and see if the results are comparable across both approaches. This was not possible within the time frame of this thesis, but may be performed in the near future if the required equipment becomes available.

A few specific issues arose during this analysis, including high blank readings for several analytes, such as glucose-6-phosphate and fructose-6-phosphate in the SN, which led to

these metabolites being excluded from the analysis. This was particularly unfortunate in this case, as the SN is a region of upmost importance in PD, and the sugar phosphates were of particular interest for comparison of changes in PDD to those in AD and HD, in which sugar phosphates were elevated. Additionally, some other analytes of interest, such as urea, could not be identified using this approach, necessitating the development of targeted methods for these metabolites. A comparison of the current LC–MS results with an already-validated GC–MS approach would help determine if the latter is a more suitable method for all future analyses, or if a mixed approach would be ideal in order to utilise the strengths of both GC–MS and LC–MS.

9.5. Conclusions

Untargeted metabolomic analysis of the PDD brain revealed multiple metabolic perturbations, in several pathways including glucose and purine metabolism, among others. Many of these alterations reflect those already observed in AD and HD, indicating shared pathogenic processes across multiple neurodegenerative diseases. Although a further analysis using GC–MS would help strengthen the observations reported here, this report represents the first systematic multi-regional investigation of the PDD brain.

Chapter Ten | Discussion

10.1. Discussion

This work aimed to address several questions: firstly, to discover how metals and metabolites in the brain are affected by tissue collection factors; secondly, whether levels of metals and metabolites in the PDD brain differ from those in non-demented brains; thirdly, if differences observed in the PDD brain mirror those previously observed in the AD and HD brain; and lastly, if similarities between multiple dementia diseases may indicate shared pathogenic mechanisms.

This thesis was able to successfully tackle these questions. Firstly, it was observed that metals are relatively unaffected by differences in tissue collection factors, but that the concentrations of many metabolites in the brain are significantly affected by increases in PMD, and possibly by other factors such as age and disease staging.

It was observed that concentrations of several metals, including magnesium, potassium, manganese, copper, zinc, and selenium, were altered in a region-specific manner in the PDD brain compared to brains without dementia. Most strikingly, decreased copper was found in all but two investigated regions, indicating widespread copper dyshomeostasis. Furthermore, these decreases in copper reflect those already reported in the AD brain, suggested a shared pathogenic alteration between these two diseases.

Targeted analysis of two metabolites of interest: pantothenic acid and urea, showed region-specific decreases in the former and widespread accumulations of the latter in all investigated brain regions. These results also mirror those previously observed in both AD and HD, presenting two additional shared pathogenic alterations in the dementia brain – this time across three different neurodegenerative conditions.

Finally, untargeted metabolomic analysis of the PDD brain uncovered multiple metabolic alterations in comparison to non-demented brains, including dysregulation of glucose and purine metabolism pathways, as well as changes in several amino acids. Together these indicate dysfunction of several essential metabolic functions, in particular energetic pathways. These again are similar to changes already reported in both AD and HD.

Overall, the data reported here indicate multiple metallomic and metabolomic alterations in the PDD brain, which mirror many of those already reported in other neurodegenerative

diseases – suggesting several shared pathogenic mechanisms which may contribute the diagnosis, monitoring, or treatment of one or all of these conditions. Most of these perturbations have never before been reported in the PDD brain, and so present novel findings.

10.2. Designing Studies for –Omics

When first beginning this study, it quickly became apparent that in order to address the *a priori* thesis hypotheses, the selection of an appropriate brain donor cohort was essential. Without controlling for factors such as age, sex, disease staging, and PMD, or otherwise knowing the effects of those factors, it would be difficult to accurately interpret the results of our metallomic and metabolomic studies – and even more difficult to compare them to those previously obtained in different cohorts.

To address this matter, we performed an investigation into the effects of as many tissue collection factors as possible, using both human AD cohorts to determine whether results were replicable across cohorts with several differing characteristics, and rat brains to perform a more focused analysis of PMD without having to simultaneously account for effects from other factors such as age or sex.

The findings from these preliminary investigations were able to assist us in the design of our following metallomic and metabolomic studies of the PDD brain. Firstly, we observed that metallomic findings were reproducible despite substantive differences in cohort characteristics. This made selecting and obtaining a cohort for the PDD metallomic analysis much simpler, and allowed for straightforward comparisons with previous studies (both our own and those performed by others) without needing to factor in differences between cohorts. This observation has not been previously reported to the authors' knowledge, with metallomic investigations rarely discussing the potential of confounding factors to affect metal observations in human tissues. This analysis has provided evidence that future metallomic studies can be performed even in cohorts that cannot be well-matched—a useful observation considering the scarcity of human tissues available for use in research, and that these factors should not affect interpretation of existing data.

However, the metabolomics investigation was less clear-cut. Metabolomic findings across different AD cohorts were not replicable, and a focused investigation of the effects of PMD on metabolite concentrations in the rat brain revealed that although many metabolites were unaffected up to a period of at least 72 hours' PMD, with many already altered by as little as 24 hours. This finding is important for both the design of future metabolomic studies and the interpretation of existing data. Using these data, we determined that in order to compare across different cohorts, we would need to keep PMD as low as possible, and match cases to controls across as many factors as possible. To achieve this objective, we determined that we needed to obtain samples from the US NIH brain-bank system, as the necessary numbers of low-PMD, age- and sex-matched PD cases with dementia (PDD) were not available from UK brain banks. Without this preliminary investigation and the subsequently modified experimental design that we adopted, our later findings would probably have been difficult to interpret, and likely inconclusive. These data can also be used to determine where such measures are not necessary in future investigations—for example, in the targeted analysis of metabolites such as urea, which were not altered by PMD. Such findings have not previously been reported to the authors' knowledge and are of use not only for our own future investigations, but also for others to consider in the designing of their own studies.

These findings are also important for the interpretation of existing metabolomic findings. Human tissue cohorts are often poorly matched, have high PMD, or sometimes contain no data on PMD at all due to the restricted availability of suitable samples and limited metadata for donors. Metabolomics analyses often produce data that differ from one another, and the influence of these cohort factors may assist in explaining such discrepancies. Although some investigations correct for certain factors, such as age and sex, many do not discuss the potential effects of any of these variables. The current study is the first to investigate the effects of these factors in an untargeted metabolomics analysis as a primary hypothesis, and the first to report the effects across multiple metabolites in multiple cohorts as well as in animal brain regions.

10.3. Metals in the PDD Brain

When considering –omics studies, there is often a lot of focus on the proteome, genome, and metabolome of tissues. However, there has been increasing interest in the potential effects of metals in neurodegenerative disease, following the identification of alterations in essential metals such as iron, copper, and zinc in AD, PD, and HD (see Chapter Three for detailed coverage of these studies). This study aimed to address a gap in the current literature, namely, the lack of data concerning metal levels across multiple brain regions in PD.

Metals play several key roles in cellular processes, acting, for example, as enzymatic and antioxidative cofactors, as well as regulators of ion gradients, apoptosis, and neurotransmitters. Previous metallomic perturbations in AD highlighted the potential for similar alterations in PDD, as well as reports of iron (76-81, 278) and copper (76, 78, 171) changes, as well as other metals (346), in PD brain studies. Here, we were able to observe multiple region-specific metallic alterations in the PDD brain. Most strikingly, we found widespread copper decreases throughout the PDD brain, akin to those previously identified in AD.

This finding presents the first report of copper changes in multiple regions of the PDD brain, and is also the first to uncover a shared perturbation in copper between PDD and AD. As a SOD1/3-cofactor, diminished copper may indicate decreased antioxidative capacity in affected brain regions, leading to increased free radical concentrations in neuronal and glial cells which may be toxic and contribute to neurodegeneration. This possibility is supported by reports of oxidative stress in both PD (480-482) and AD (462, 483, 484). Decreases in other SOD cofactors manganese (SOD2) and zinc (SOD1/3), and glutathione peroxidase cofactor selenium, may exacerbate this effect in a more region-specific manner.

The lack of changes in iron observed here in the PDD brain was unexpected, as there have been multiple reports of increased total iron in the PD SN (76-78, 80, 81, 278)—although there have also been previous reports finding no change in iron (349, 485, 486), and few investigations have looked outside the SN itself. It is possible that the lack of iron changes here reflects late-stage disease, by which point individuals have already developed dementia symptoms. This usually occurs at least a decade following the original diagnosis

of PD, and so is only involved in the later stages of disease. The degree of neuronal loss at this point in neuromelanin-heavy regions, such as the severely affected SN and LC, may negate the initial iron increases often observed in PD—as iron would usually be sequestered in neuromelanin in high amounts (487, 488). A future parallel study investigating PD without dementia could help elucidate whether this is the case. Additionally, the use of whole tissue in this study, rather than the separation of different cell types, isolation of Lewy body inclusions, or separation of smaller regions (such as the SN pars compacta and pars reticulum) may also contribute to this discrepancy with some previous studies, as changes in iron may be specific to small regions (77, 81), specific cell types (489, 490), or to Lewy body deposits themselves (491). Further studies isolating different components of PDD brain tissue would be useful in identifying the relative distribution of iron in these different parts of the brain.

10.4. Metabolites in the PDD Brain

The metabolome is of particular interest when carrying out untargeted –omics analyses of human tissues, as it can provide a functional snapshot of a tissue at the time it was collected. This differs from other –omics methodologies such as genomics or proteomics, which are subject to differences in RNA or protein translation and expression, and/or posttranslational modifications, for example. The number of metabolites within any given tissue is considerable, as they are involved in almost all essential cellular processes, from energy production to protein breakdown to apoptosis.

As such, the strength of untargeted studies of the metabolome lies in their ability to identify new metabolites of interest which may not have been previously investigated in a particular condition. To our knowledge, such a study has never been previously carried out on multiple regions of the PDD brain, and so one of the primary hypotheses of this thesis was to address this gap in the current knowledge of PDD. However, due to an unexpected equipment malfunction, it became necessary to develop new methods to do this. This also necessitated the development of targeted methods for analytes of interest, namely urea and pantothenic acid, whilst replacement untargeted methods were in development.

Neither pantothenic acid nor urea have previously been investigated in the PDD brain to the authors' knowledge. As such, this study provides novel evidence on the existence of

region-specific decreases in pantothenic acid, and widespread increases in urea. Pantothenic acid is essential for the synthesis of CoA, which in turn is necessary for almost all major metabolic pathways including the TCA cycle, amino acid metabolism, and fatty acid synthesis, among many others. As such, reductions in pantothenic acid could result in a loss of CoA, which in turn could lead to deficiencies in these metabolic pathways, with widespread consequences on cellular processes. Equivalent changes are also present in AD and HD, suggesting the existence of a region-specific shared pathogenic alteration in all three conditions.

This is also the case with urea, which has been observed to be increased in every investigated region of PDD, AD, and HD. These increases occur at levels similar to those observed in uremic encephalopathy, in which chronic urea increases in the bloodstream and brain result in symptoms similar to those seen in dementia. Due to the lack of urea cycle activity observable in the brain, these increases in urea are likely to be the result of increased cerebral protein breakdown, meaning that neurodegeneration itself could lead to urea increases, which in turn contribute to neuronal loss in a continuing cycle.

The untargeted metabolomics analysis was able to build on the metabolic alterations already identified with pantothenic acid and urea. It revealed several alterations in the PDD brain, including perturbations in glucose and purine metabolism, amino acids, and other metabolites involved in the TCA cycle, alternative energy production pathways, and others. There was previously very little metabolomic data available on the PD brain, and almost none specifically on PD with dementia (PDD). As such, these findings presented a number of novel alterations across several regions of the PDD brain.

Changes in pathways of glucose metabolism may reflect the glucose hypo/hypermetabolism previously reported in PD (420, 492, 493), providing a plausible explanation for dysregulated energy production from glucose. They also appear to reflect an increase in the activity of alternative glucose-related energy pathways, such as the pentose phosphate and polyol pathways, which may be induced to compensate for energetic losses from diminished glycolytic activity. Together with increases in alternative energy sources such as myo-inositol, these data present widespread deficiency in energy

production in the PDD brain, which may contribute to the mitochondrial dysfunction reported in PD (85, 494, 495).

Changes in purine metabolism pathways may also contribute to energy pathway dysregulation, as purines are components of several metabolites involved in a vast array of metabolic pathways; these include ATP, GTP, cAMP, NADH and CoA metabolism. As such, the perturbations observed in the purine metabolism pathways in the PDD brain here may lead to a deficiency in these essential metabolic intermediates, further contributing to disruptions in the TCA cycle, mitochondrial electron transport chain, and glucose metabolism pathways.

Strikingly, these pathways have also been reported to be disrupted previously in both AD and HD, suggesting yet more shared pathogenic mechanisms across all three of these neurodegenerative diseases. The increasing number of identifiable similarities between PDD, AD, and HD suggest that the development of dementia involves a number of common mechanisms in the brain, regardless of the neurodegenerative condition it is a part of. Such an observation could be of major significance in the treatment of these diseases, with the possibility of common therapeutic targets across multiple conditions. Additionally, where differences do occur—either in the changes observed or the regions in which they are observed in distinct diseases—these may be useful in diagnosing different conditions where clinical presentation is similar, or may contribute to (some of) the symptomatic differences observed between diseases. However, the current data are limited with respect to the former, as many of the metabolites investigated here cannot yet be identified or measured *in vivo*.

10.5. Where Metallomics and Metabolomics Meet

One of the primary justifications for a multi-omic analysis of PDD tissues in this work is that data from different -omics approaches often overlap, contributing different viewpoints to the same processes within a tissue. As such, data from one -omics approach can be combined with other data to provide a more thorough picture of what is occurring in a tissue, or on a larger scale, in a particular disease.

The findings from both these metallomic and metabolomic analyses here point to similar mechanistic changes within the PDD brain—including decreased energy production, mitochondrial dysfunction, and oxidative stress. Although all these processes have been observed to be altered in PD, there have been few studies investigating the individual components of these pathways.

In Chapter Three of this thesis an image was created to portray the current reported perturbations in metallomic and metabolomic pathways in the PD brain, and how they interact. Using the data obtained in this work, this figure can now be updated to show the new findings in the PDD brain (see Figure 10.1). This figure shows the degree of crosstalk between metals and metabolites in essential cellular processes, and how the alterations observed in one may contribute to perturbations in the other. It is only with multiple approaches that these overlaps can be observed, and a more thorough understanding of disease processes be understood.

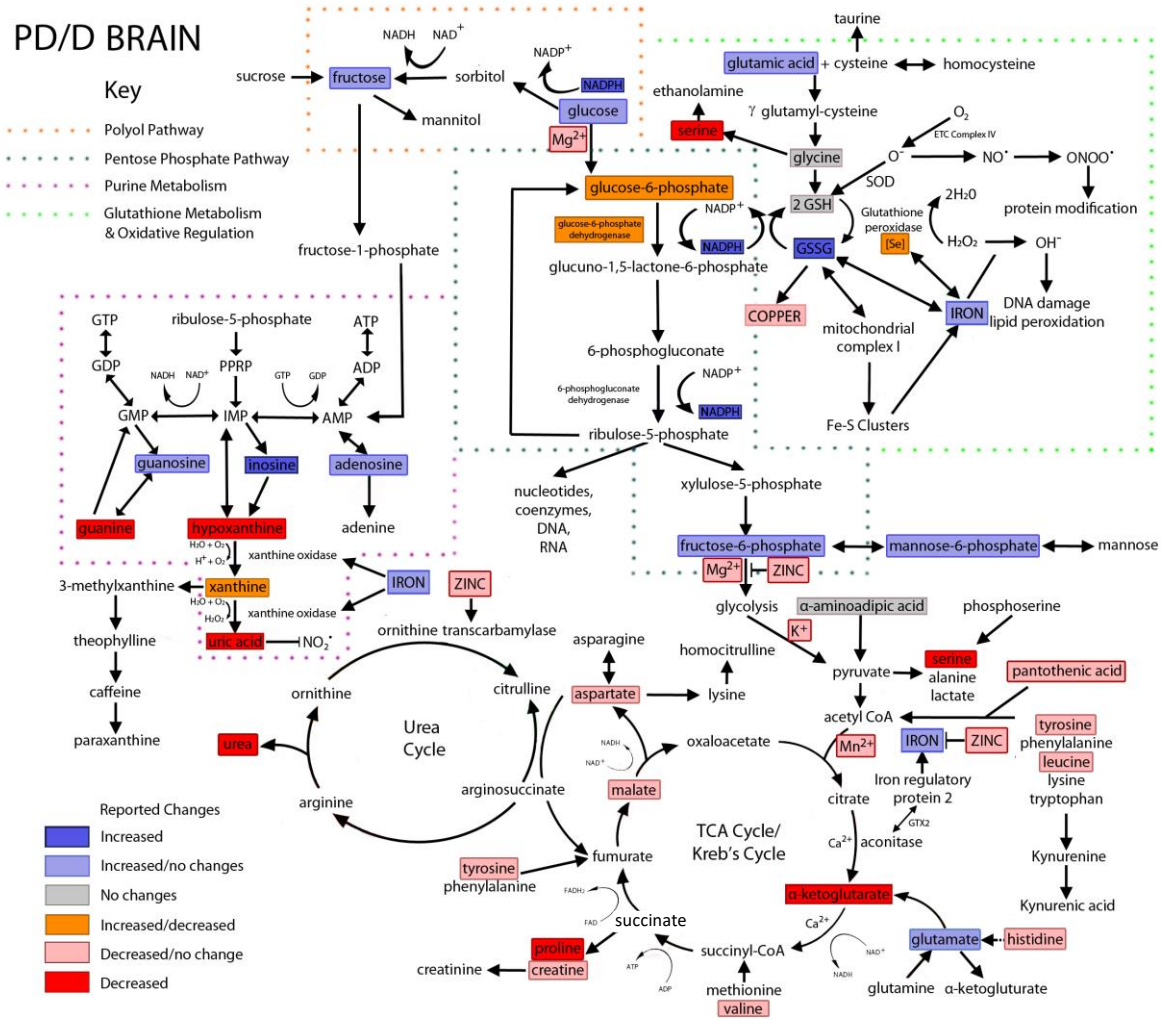

Figure 10. 1. Updated Diagram of Metabolic and Metallomic Changes Reported in the PD/D Brain

Updated summary of evidence from all reports of altered metals and metabolites in PD and PDD brains, including both the existing literature and findings from this thesis. Newly reported findings include widespread increases in fructose and urea, decreased pantothenic acid, and widespread decreases in copper. Reports of changes/lack of changes are all equally weighted. Acetyl CoA, acetyl coenzyme A; ADP, adenosine diphosphate; AMP, adenosine monophosphate; ATP, adenosine triphosphate; Ca^{2+}, calcium ion; ETC, electron transport chain; GMP, guanosine monophosphate; GSH, reduced glutathione; GSSG, oxidised glutathione; GTP, guanosine triphosphate; H_2O_2, hydrogen peroxide; IMP, inosinic acid; Mg^{2+}, magnesium ion; K^+, potassium ion; Mn^{2+}, manganese ion; NAD, oxidised nicotinamide adenine dinucleotide; NADH, reduced nicotinamide adenine dinucleotide; NADP, oxidised nicotinamide adenine dinucleotide phosphate; NADPH, reduced nicotinamide adenine dinucleotide phosphate; $NO^{\cdot}$, nitric oxide radical; $O^{\cdot}$, superoxide radical; $OH^{\cdot}$, hydroxide radical; $ONOO^{-}$, peroxynitrite; PPRP, phosphoribosyl pyrophosphate; Se, selenium; SOD, superoxide dismutase.

10.6. PDD, AD, and HD

As well as investigating dysfunction in the PDD brain, another primary aim of this thesis was to compare results with those previously obtained in two other neurodegenerative diseases which differed in clinical presentation, but shared the common symptom of dementia: namely AD and HD. These two conditions had already shown striking similarities to one another, with widespread increases in glucose, fructose, and urea, as well as region-specific decreases in pantothenic acid. As such, it became of interest to know whether this was also the case in other dementias, such as PDD.

This study was able to identify multiple pathogenic alterations in PDD shared with AD and/or HD (see Figure 10.2), including increases in fructose and urea, and decreases in pantothenic acid, as well as alterations in energetic and purine metabolism pathways. Such a number of common perturbations has never before been reported between these three diseases, and indicates a greater degree of similarity between them than may have been previously thought—despite differences in causes, clinical presentation, and neuropathological presentation.

Two observations were of particular interest with regard to shared alterations between these conditions: firstly, that some changes appeared to occur in most or all investigated brain regions, in all three diseases. This indicates shared pathogenic mechanisms that occur throughout most or all of the brain, contributing to shared symptoms, i.e. cognitive decline, regardless of the degree of neurodegeneration present in a particular area of the brain. This could point towards therapeutic targets that could be used to target cognitive symptoms in all three neurodegenerative diseases, without consideration needing to be made for targeting specific regions. This could simplify development of such treatments. These shared alterations could also provide potential targets for identification of individuals at risk of developing dementia, which could not only assist in initiating early treatment, but also in finding cohorts for preclinical disease stage studies, if these perturbations were found to occur early on in disease. For example, glucose can be imaged in the living brain (496-498) and so could be of use in such cases.

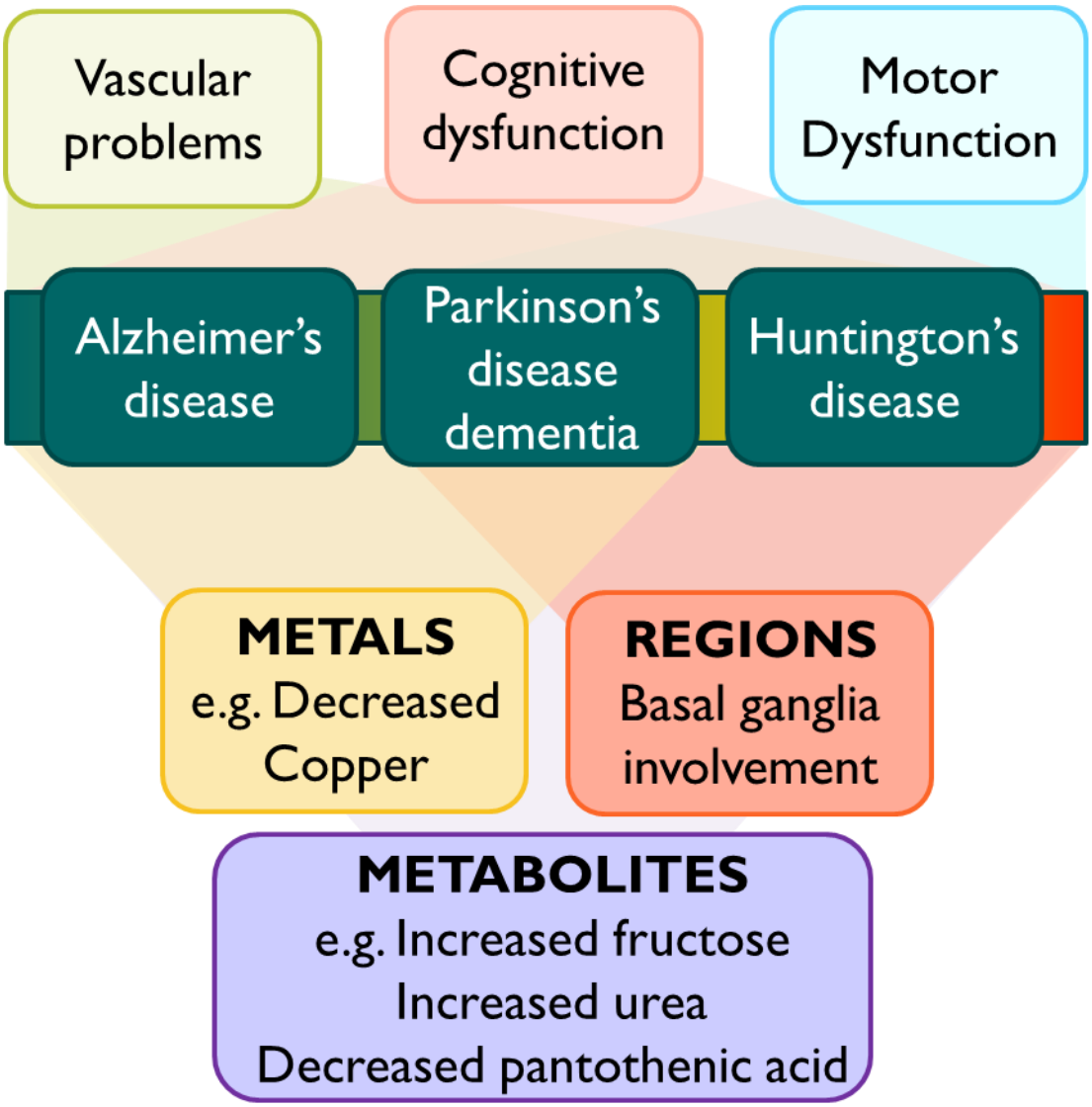

Figure 10. 2. Common features and findings between AD, PDD, and HD

Secondly, other changes were shared between conditions, but only in distinct brain regions. This points to more focused pathogenic mechanisms that, although functioning in a similar manner, may contribute to different symptoms in distinct diseases based on the region affected. For example, alterations in the SN leading to motor dysfunction, and changes in the HP resulting in cognitive decline. If this were the case, this could mean that targeting the same metabolic alterations could treat different types of symptoms in neurodegenerative disease, so long as the affected regions could be targeted. These changes could also assist in identifying people at risk of specific neurodegenerative diseases, by looking for alterations in specific brain regions e.g. widespread glucose

increases in AD and increased glucose in the pons in PDD. This could be particularly useful where clinical presentation is similar—for example, dementia with Lewy bodies, a condition which is primarily distinguished from PDD by the order of motor and cognitive symptom onset, could be more easily diagnosed if metabolomic perturbations were present in distinct regions of the PDD brain, which could have implications for treatment pathways and identification of study cohort participants.

10.7. Future Studies

Due to issues caused by delays in tissue acquisition, equipment malfunctions, and the COVID-19 pandemic, the direction of some of the investigations for this thesis had to be altered. The most disruptive of these was the loss of the GC–MS, which was used in previous metabolomics analyses. This necessitated the development of a new LC–MS method, which was itself in turn delayed by the pandemic. The LC–MS analysis was possible within the scope of this thesis, but in order to determine the reliability of the results obtained, it is desirable to carry out a parallel study using the previous GC–MS methodology, to determine if the results are consistent between methods and comparable with the previous AD and HD analyses. The necessary equipment should be available in the near future, at which point this analysis will be carried out either by myself or another PhD candidate working in this field of study.

Regardless of disruptions to any of the work carried out here, there are also several avenues of investigation which suggest themselves as logical progressions from this study. The first is the metallomic and metabolomic analysis of brain regions in PD without dementia. This thesis is unable to determine whether PD presents similar alterations before the initiation of cognitive decline, or whether some perturbations are specific to dementia once symptomatic. It would be of interest not only to note whether any observed changes are the same before and after dementia onset, but also whether the same brain regions are affected. Even where similar alterations are observed across PDD, AD, and HD, they often present in different regions—primarily in those most heavily affected in the specific condition. A comparison of PD with PDD is expected to show if this region-specificity also occurs at different stages of the same disease, with specificity relating to the symptoms themselves.

It would also be of interest to extend these studies to other neurodegenerative conditions. The most obvious starting point would be dementia with Lewy bodies (DLB), due to the high degree of similarity between this disease and PDD. It would be particularly noteworthy to see whether these diseases look very similar at the time of death, considering the almost identical presentation of signs and symptoms at this late stage, or whether there are differences between metallomic/metabolomic alterations or brain regions that can account for differences in disease progression—namely, the onset of motor symptoms before cognitive symptoms, or vice versa. This could provide insight on whether these diseases can be treated in a similar manner, or whether different approaches are required to tackle each effectively. Investigations into other less similar neurodegenerative conditions, such as vascular dementia (already being investigated by another PhD candidate), fronto-temporal dementia, amyotrophic lateral sclerosis, and multiple sclerosis, could elucidate whether these are completely distinct entities, or whether there are mechanistic similarities that may explain the occurrence of cognitive decline shared between all these conditions—as has so far been observed in PDD, AD, and HD.

10.8. Conclusions

The primary aim of this work was to identify pathogenic perturbations in the metallome and metabolome of the PDD brain, with a secondary comparison of identified alterations with those found in the AD and HD brain. Despite some setbacks, we have succeeded in these aims, with identification of multiple metallomic and metabolomics alterations in PDD which are shared with both AD and HD. The work presented here has shown that:

- Metal concentrations are unaffected by differences in cohort characteristics, such as age, sex, and PMD up to 72 h.
- Metabolomic findings cannot be replicated efficiently across cohorts with differing characteristics, as many metabolites are sensitive to PMDs of at least 24 hours.
- Several metallomic perturbations are present in the PDD brain, including widespread decreases in copper
- Multiple metabolomic alterations are also present in the PDD brain, including widespread increases in urea, region-specific decreases in pantothenic acid, and alterations in glucose and purine metabolism pathways.

- Many of these changes in metals and metabolites are shared with the AD and HD brain, either in a widespread or region-specific manner.
- Regions known to be heavily affected by neurodegeneration appear to show higher numbers of metallomic and metabolomic alterations, in their respective conditions.
- Multi-omic observations point towards pathogenic mechanisms in PDD overlapping with other dementias, including mitochondrial dysfunction, energetic pathway dysregulation, and oxidative stress.

Future investigations looking at PD without dementia, as well as other neurodegenerative diseases is expected to identify how many conditions these changes are shared by. Considering the current findings across three dementias, it is possible that all conditions sharing cognitive decline as a primary symptom may present similar findings. GC–MS analyses of the current PDD cohort can also elucidate the relative suitability of either LC–MS or GC–MS for metabolomics studies of the human brain, and validate the untargeted metabolomics findings presented in this work.

References

1. Tysnes OB, Storstein A. Epidemiology of Parkinson's disease. J Neural Transm (Vienna). 2017;124(8):901-5.
2. Hanagasi HA, Tufekcioglu Z, Emre M. Dementia in Parkinson's disease. J Neurol Sci. 2017;374:26-31.
3. Cheng HC, Ulane CM, Burke RE. Clinical progression in Parkinson disease and the neurobiology of axons. Ann Neurol. 2010;67(6):715-25.
4. Braak H, Alafuzoff I, Arzberger T, Kretzschmar H, Tredici KD. Staging of Alzheimer disease-associated neurofibrillary pathology using paraffin sections and immunocytochemistry. Acta Neuropathol. 2006;112:389-404.
5. Kalaitzakis ME, Graeber MB, Gentleman SM, Pearce RK. The dorsal motor nucleus of the vagus is not an obligatory trigger site of Parkinson's disease: a critical analysis of alpha-synuclein staging. Neuropathol Appl Neurobiol. 2008;34(3):284-95.
6. Jellinger KA. A critical evaluation of current staging of alpha-synuclein pathology in Lewy body disorders. Biochim Biophys Acta. 2009;1792(7):730-40.
7. Abeliovich A, Schmitz Y, Farinas I, Choi-Lundberg D, Ho WH, Castillo PE, et al. Mice lacking alpha-synuclein display functional deficits in the nigrostriatal dopamine system. Neuron. 2000;25(1):239-52.
8. Fujiwara H, Hasegawa M, Dohmae N, Kawashima A, Masliah E, Goldberg MS, et al. alpha-Synuclein is phosphorylated in synucleinopathy lesions. Nat Cell Biol. 2002;4(2):160-4.
9. Neumann M, Muller V, Kretzschmar HA, Haass C, Kahle PJ. Regional distribution of proteinase K-resistant alpha-synuclein correlates with Lewy body disease stage. J Neuropathol Exp Neurol. 2004;63(12):1225-35.
10. Marvian AT, Koss DJ, Aliakbari F, Morshedi D, Outeiro TF. In vitro models of synucleinopathies: informing on molecular mechanisms and protective strategies. J Neurochem. 2019;150(5):535-65.
11. Lang AE, Espay AJ. Disease modification in Parkinson's disease: Current approaches, challenges, and future considerations. Mov Disord. 2018;33(5):660-77.
12. Singh A, Kukreti R, Saso L, Kukreti S. Oxidative stress: A key modulator in neurodegenerative diseases. Molecules. 2019;24(8).
13. McKeith IG, Boeve BF, Dickson DW, Halliday G, Taylor JP, Weintraub D, et al. Diagnosis and management of dementia with Lewy bodies: Fourth consensus report of the DLB Consortium. Neurology. 2017;89(1):88-100.
14. Jellinger KA. Dementia with Lewy bodies and Parkinson's disease-dementia: current concepts and controversies. J Neural Transm (Vienna). 2018;125(4):615-50.
15. Loy CT, Schofield PR, Turner AM, Kwok JB. Genetics of dementia. Lancet. 2014;383(9919):828-40.
16. Orr HT. FTD and ALS: genetic ties that bind. Neuron. 2011;72(2):189-90.
17. Meguro K, Tanaka N, Nakatsuka M, Nakamura K, Satoh M. Vascular lesions in mixed dementia, vascular dementia, and Alzheimer disease with cerebrovascular disease: the Kurihara Project. J Neurol Sci. 2012;322(1-2):157-60.
18. Pilotto A, Turrone R, Liepelt-Scarfone I, Bianchi M, Poli L, Borroni B, et al. Vascular risk factors and cognition in Parkinson's disease. J Alzheimers Dis. 2016;51(2):563-70.
19. Profenno LA, Porsteinsson AP, Faraone SV. Meta-analysis of Alzheimer's disease risk with obesity, diabetes, and related disorders. Biol Psychiatry. 2010;67(6):505-12.
20. Pagano G, Polychronis S, Wilson H, Giordano B, Ferrara N, Niccolini F, et al. Diabetes mellitus and Parkinson disease. Neurology. 2018;90(19):e1654-e62.
21. Bougea A, Stefanis L, Paraskevas GP, Emmanouilidou E, Efthymiopoulou E, Vekrelis K, et al. Neuropsychiatric symptoms and alpha-Synuclein profile of patients with Parkinson's disease dementia, dementia with Lewy bodies and Alzheimer's disease. J Neurol. 2018;265(10):2295-301.
22. Lai L, Lee PE, Chan P, Fok MC, Hsiung GR, Sepehry AA. Prevalence of delusions in drug-naive Alzheimer disease patients: A meta-analysis. Int J Geriatr Psychiatry. 2019;34(9):1287-93.
23. Tzeng RC, Tsai CF, Wang CT, Wang TY, Chiu PY. Delusions in patients with dementia with Lewy bodies and the associated factors. Behav Neurol. 2018;2018:6707291.
24. Kazui H, Yoshiyama K, Kanemoto H, Suzuki Y, Sato S, Hashimoto M, et al. Differences of behavioral and psychological symptoms of dementia in disease severity in four major dementias. PLoS One. 2016;11(8):e0161092.
25. Braak H, Del Tredici K, Rub U, de Vos RA, Jansen Steur EN, Braak E. Staging of brain pathology related to sporadic Parkinson's disease. Neurobiol Aging. 2003;24(2):197-211.
26. Jellinger KA. Is Braak staging valid for all types of Parkinson's disease? J Neural Transm (Vienna). 2019;126(4):423-31.
27. Wakabayashi K, Tanji K, Mori F, Takahashi H. The Lewy body in Parkinson's disease: molecules implicated in the formation and degradation of alpha-synuclein aggregates. Neuropathology. 2007;27(5):494-506.
28. Lashuel HA, Overk CR, Oueslati A, Masliah E. The many faces of alpha-synuclein: from structure and toxicity to therapeutic target. Nat Rev Neurosci. 2013;14(1):38-48.
29. Chandra S, Fornai F, Kwon HB, Yazdani U, Atasoy D, Liu X, et al. Double-knockout mice for alpha- and beta-synucleins: effect on synaptic functions. Proc Natl Acad Sci U S A. 2004;101(41):14966-71.

30. Bloch A, Probst A, Bissig H, Adams H, Tolnay M. Alpha-synuclein pathology of the spinal and peripheral autonomic nervous system in neurologically unimpaired elderly subjects. Neuropathol Appl Neurobiol. 2006;32(3):284-95.
31. DelleDonne A, Klos KJ, Fujishiro H, Ahmed Z, Parisi JE, Josephs KA, et al. Incidental Lewy body disease and preclinical Parkinson disease. Arch Neurol. 2008;65(8):1074-80.
32. Mehra S, Sahay S, Maji SK. alpha-Synuclein misfolding and aggregation: Implications in Parkinson's disease pathogenesis. Biochim Biophys Acta Proteins Proteom. 2019;1867(10):890-908.
33. Stefanis L. alpha-Synuclein in Parkinson's disease. Cold Spring Harb Perspect Med. 2012;2(2):a009399.
34. Roberts RF, Wade-Martins R, Alegre-Abarrategui J. Direct visualization of alpha-synuclein oligomers reveals previously undetected pathology in Parkinson's disease brain. Brain. 2015;138(Pt 6):1642-57.
35. Conway KA, Lee SJ, Rochet JC, Ding TT, Williamson RE, Lansbury PT, Jr. Acceleration of oligomerization, not fibrillization, is a shared property of both alpha-synuclein mutations linked to early-onset Parkinson's disease: implications for pathogenesis and therapy. Proc Natl Acad Sci U S A. 2000;97(2):571-6.
36. Winner B, Jappelli R, Maji SK, Desplats PA, Boyer L, Aigner S, et al. In vivo demonstration that alpha-synuclein oligomers are toxic. Proc Natl Acad Sci U S A. 2011;108(10):4194-9.
37. Peelaerts W, Bousset L, Van der Perren A, Moskalyuk A, Pulizzi R, Giugliano M, et al. alpha-Synuclein strains cause distinct synucleinopathies after local and systemic administration. Nature. 2015;522(7556):340-4.
38. Sun J, Wang L, Bao H, Premi S, Das U, Chapman ER, et al. Functional cooperation of alpha-synuclein and VAMP2 in synaptic vesicle recycling. Proc Natl Acad Sci U S A. 2019;116(23):11113-5.
39. Choi BK, Choi MG, Kim JY, Yang Y, Lai Y, Kweon DH, et al. Large alpha-synuclein oligomers inhibit neuronal SNARE-mediated vesicle docking. Proc Natl Acad Sci U S A. 2013;110(10):4087-92.
40. Luth ES, Stavrovskaya IG, Bartels T, Kristal BS, Selkoe DJ. Soluble, prefibrillar alpha-synuclein oligomers promote complex I-dependent, Ca2+-induced mitochondrial dysfunction. J Biol Chem. 2014;289(31):21490-507.
41. Guardia-Laguarta C, Area-Gomez E, Schon EA, Przedborski S. A new role for alpha-synuclein in Parkinson's disease: Alteration of ER-mitochondrial communication. Mov Disord. 2015;30(8):1026-33.
42. Guardia-Laguarta C, Area-Gomez E, Rub C, Liu Y, Magrane J, Becker D, et al. alpha-Synuclein is localized to mitochondria-associated ER membranes. J Neurosci. 2014;34(1):249-59.
43. Colla E, Jensen PH, Pletnikova O, Troncoso JC, Glabe C, Lee MK. Accumulation of toxic alpha-synuclein oligomer within endoplasmic reticulum occurs in alpha-synucleinopathy in vivo. J Neurosci. 2012;32(10):3301-5.
44. McFarthing K, Simuni T. Clinical trial highlights: Targetting alpha-synuclein. J Parkinsons Dis. 2019;9(1):5-16.
45. Fields CR, Bengoa-Vergniory N, Wade-Martins R. Targeting alpha-synuclein as a therapy for Parkinson's disease. Front Mol Neurosci. 2019;12:299.
46. Schapira AH, Cooper JM, Dexter D, Clark JB, Jenner P, Marsden CD. Mitochondrial complex I deficiency in Parkinson's disease. J Neurochem. 1990;54(3):823-7.
47. Holper L, Ben-Shachar D, Mann JJ. Multivariate meta-analyses of mitochondrial complex I and IV in major depressive disorder, bipolar disorder, schizophrenia, Alzheimer disease, and Parkinson disease. Neuropsychopharmacology. 2019;44(5):837-49.
48. Gatt AP, Duncan OF, Attems J, Francis PT, Ballard CG, Bateman JM. Dementia in Parkinson's disease is associated with enhanced mitochondrial complex I deficiency. Mov Disord. 2016;31(3):352-9.
49. Valdez LB, Zaobornyj T, Bandez MJ, Lopez-Cepero JM, Boveris A, Navarro A. Complex I syndrome in striatum and frontal cortex in a rat model of Parkinson disease. Free Radic Biol Med. 2019;135:274-82.
50. Mimaki M, Wang X, McKenzie M, Thorburn DR, Ryan MT. Understanding mitochondrial complex I assembly in health and disease. Biochim Biophys Acta. 2012;1817(6):851-62.
51. Distelmaier F, Koopman WJ, van den Heuvel LP, Rodenburg RJ, Mayatepek E, Willems PH, et al. Mitochondrial complex I deficiency: from organelle dysfunction to clinical disease. Brain. 2009;132(Pt 4):833-42.
52. Kanazawa M, Ohba H, Nishiyama S, Kakiuchi T, Tsukada H. Effect of MPTP on serotonergic neuronal systems and mitochondrial complex I activity in the living brain: A PET study on conscious rhesus monkeys. J Nucl Med. 2017;58(7):1111-6.
53. Tsukada H, Kanazawa M, Ohba H, Nishiyama S, Harada N, Kakiuchi T. PET Imaging of Mitochondrial Complex I with 18F-BCPP-EF in the Brains of MPTP-Treated Monkeys. J Nucl Med. 2016;57(6):950-3.
54. Richardson JR, Caudle WM, Guillot TS, Watson JL, Nakamaru-Ogiso E, Seo BB, et al. Obligatory role for complex I inhibition in the dopaminergic neurotoxicity of 1-methyl-4-phenyl-1,2,3,6-tetrahydropyridine (MPTP). Toxicol Sci. 2007;95(1):196-204.
55. Sterky FH, Hoffman AF, Milenkovic D, Bao B, Paganelli A, Edgar D, et al. Altered dopamine metabolism and increased vulnerability to MPTP in mice with partial deficiency of mitochondrial complex I in dopamine neurons. Hum Mol Genet. 2012;21(5):1078-89.
56. Kim HW, Choi WS, Sorscher N, Park HJ, Tronche F, Palmiter RD, et al. Genetic reduction of mitochondrial complex I function does not lead to loss of dopamine neurons in vivo. Neurobiol Aging. 2015;36(9):2617-27.
57. Marella M, Seo BB, Matsuno-Yagi A, Yagi T. Mechanism of cell death caused by complex I defects in a rat dopaminergic cell line. J Biol Chem. 2007;282(33):24146-56.
58. Choi WS, Kruse SE, Palmiter RD, Xia Z. Mitochondrial complex I inhibition is not required for dopaminergic neuron death induced by rotenone, MPP+, or paraquat. Proc Natl Acad Sci U S A. 2008;105(39):15136-41.

59. Zhou L, Wang W, Hoppel C, Liu J, Zhu X. Parkinson's disease-associated pathogenic VPS35 mutation causes complex I deficits. Biochim Biophys Acta Mol Basis Dis. 2017;1863(11):2791-5.
60. Morais VA, Haddad D, Craessaerts K, De Bock PJ, Swerts J, Vilain S, et al. PINK1 loss-of-function mutations affect mitochondrial complex I activity via NdufA10 ubiquinone uncoupling. Science. 2014;344(6180):203-7.
61. Chinta SJ, Mallajosyula JK, Rane A, Andersen JK. Mitochondrial alpha-synuclein accumulation impairs complex I function in dopaminergic neurons and results in increased mitophagy in vivo. Neurosci Lett. 2010;486(3):235-9.
62. Perfeito R, Lazaro DF, Outeiro TF, Rego AC. Linking alpha-synuclein phosphorylation to reactive oxygen species formation and mitochondrial dysfunction in SH-SY5Y cells. Mol Cell Neurosci. 2014;62:51-9.
63. Ray PD, Huang BW, Tsuji Y. Reactive oxygen species (ROS) homeostasis and redox regulation in cellular signaling. Cell Signal. 2012;24(5):981-90.
64. Kohchi C, Inagawa H, Nishizawa T, Soma G. ROS and innate immunity. Anticancer Res. 2009;29(3):817-21.
65. Diwanji N, Bergmann A. An unexpected friend - ROS in apoptosis-induced compensatory proliferation: Implications for regeneration and cancer. Semin Cell Dev Biol. 2018;80:74-82.
66. Valko M, Leibfritz D, Moncol J, Cronin MT, Mazur M, Telser J. Free radicals and antioxidants in normal physiological functions and human disease. Int J Biochem Cell Biol. 2007;39(1):44-84.
67. Peoples JN, Saraf A, Ghazal N, Pham TT, Kwong JQ. Mitochondrial dysfunction and oxidative stress in heart disease. Exp Mol Med. 2019;51(12):1-13.
68. Chung SY, Kishinevsky S, Mazzulli JR, Graziotto J, Mrejeru A, Mosharov EV, et al. Parkin and PINK1 patient iPSC-derived midbrain dopamine neurons exhibit mitochondrial dysfunction and alpha-synuclein accumulation. Stem Cell Reports. 2016;7(4):664-77.
69. Nguyen HN, Byers B, Cord B, Shcheglovitov A, Byrne J, Gujar P, et al. LRRK2 mutant iPSC-derived DA neurons demonstrate increased susceptibility to oxidative stress. Cell Stem Cell. 2011;8(3):267-80.
70. Dolgacheva LP, Berezhnov AV, Fedotova EI, Zinchenko VP, Abramov AY. Role of DJ-1 in the mechanism of pathogenesis of Parkinson's disease. J Bioenerg Biomembr. 2019;51(3):175-88.
71. Sian J, Dexter DT, Lees AJ, Daniel S, Agid Y, Javoy-Agid F, et al. Alterations in glutathione levels in Parkinson's disease and other neurodegenerative disorders affecting basal ganglia. Ann Neurol. 1994;36(3):348-55.
72. Bellinger FP, Bellinger MT, Seale LA, Takemoto AS, Raman AV, Miki T, et al. Glutathione peroxidase 4 is associated with neuromelanin in substantia nigra and dystrophic axons in putamen of Parkinson's brain. Mol Neurodegener. 2011;6(1):8.
73. Gibson GE, Kingsbury AE, Xu H, Lindsay JG, Daniel S, Foster OJ, et al. Deficits in a tricarboxylic acid cycle enzyme in brains from patients with Parkinson's disease. Neurochem Int. 2003;43(2):129-35.
74. Bohnen NI, Koeppe RA, Minoshima S, Giordani B, Albin RL, Frey KA, et al. Cerebral glucose metabolic features of Parkinson disease and incident dementia: longitudinal study. J Nucl Med. 2011;52(6):848-55.
75. Dunn L, Allen GF, Mamais A, Ling H, Li A, Duberley KE, et al. Dysregulation of glucose metabolism is an early event in sporadic Parkinson's disease. Neurobiol Aging. 2014;35(5):1111-5.
76. Ayton S, Lei P, Duce JA, Wong BX, Sedjahtera A, Adlard PA, et al. Ceruloplasmin dysfunction and therapeutic potential for Parkinson disease. Ann Neurol. 2013;73(4):554-9.
77. Costa-Mallen P, Gatenby C, Friend S, Maravilla KR, Hu SC, Cain KC, et al. Brain iron concentrations in regions of interest and relation with serum iron levels in Parkinson disease. J Neurol Sci. 2017;378:38-44.
78. Genoud S, Roberts BR, Gunn AP, Halliday GM, Lewis SJG, Ball HJ, et al. Subcellular compartmentalisation of copper, iron, manganese, and zinc in the Parkinson's disease brain. Metallomics. 2017;9(10):1447-55.
79. Kim TH, Lee JH. Serum uric acid and nigral iron deposition in Parkinson's disease: a pilot study. PLoS One. 2014;9(11):e112512.
80. Pyatigorskaya N, Sharman M, Corvol JC, Valabregue R, Yahia-Cherif L, Poupon F, et al. High nigral iron deposition in LRRK2 and Parkin mutation carriers using R2* relaxometry. Mov Disord. 2015;30(8):1077-84.
81. Xuan M, Guan X, Gu Q, Shen Z, Yu X, Qiu T, et al. Different iron deposition patterns in early- and middle-late-onset Parkinson's disease. Parkinsonism Relat Disord. 2017;44:23-7.
82. Jiang T, Sun Q, Chen S. Oxidative stress: A major pathogenesis and potential therapeutic target of antioxidative agents in Parkinson's disease and Alzheimer's disease. Prog Neurobiol. 2016;147:1-19.
83. Nunnari J, Suomalainen A. Mitochondria: in sickness and in health. Cell. 2012;148(6):1145-59.
84. Grunewald A, Kumar KR, Sue CM. New insights into the complex role of mitochondria in Parkinson's disease. Prog Neurobiol. 2019;177:73-93.
85. Bose A, Beal MF. Mitochondrial dysfunction in Parkinson's disease. J Neurochem. 2016;139 Suppl 1:216-31.
86. Angelova PR, Esteras N, Abramov AY. Mitochondria and lipid peroxidation in the mechanism of neurodegeneration: Finding ways for prevention. Med Res Rev. 2021;41(2):770-84.
87. Gelders G, Baekelandt V, Van der Perren A. Linking neuroinflammation and neurodegeneration in Parkinson's disease. J Immunol Res. 2018;2018:4784268.
88. Lawson LJ, Perry VH, Gordon S. Turnover of resident microglia in the normal adult mouse brain. Neuroscience. 1992;48(2):405-15.
89. Wolf SA, Boddeke HW, Kettenmann H. Microglia in physiology and disease. Annu Rev Physiol. 2017;79:619-43.
90. Gerhard A, Pavese N, Hotton G, Turkheimer F, Es M, Hammers A, et al. In vivo imaging of microglial activation with [11C](R)-PK11195 PET in idiopathic Parkinson's disease. Neurobiol Dis. 2006;21(2):404-12.

91. Hamza TH, Zabetian CP, Tenesa A, Laederach A, Montimurro J, Yearout D, et al. Common genetic variation in the HLA region is associated with late-onset sporadic Parkinson's disease. Nat Genet. 2010;42(9):781-5.
92. Stokholm MG, Iranzo A, Ostergaard K, Serradell M, Otto M, Svendsen KB, et al. Assessment of neuroinflammation in patients with idiopathic rapid-eye-movement sleep behaviour disorder: a case-control study. Lancet Neurol. 2017;16(10):789-96.
93. Tu D, Gao Y, Yang R, Guan T, Hong JS, Gao HM. The pentose phosphate pathway regulates chronic neuroinflammation and dopaminergic neurodegeneration. J Neuroinflammation. 2019;16(1):255.
94. Martin-Bastida A, Tilley BS, Bansal S, Gentleman SM, Dexter DT, Ward RJ. Iron and inflammation: in vivo and post-mortem studies in Parkinson's disease. J Neural Transm (Vienna). 2021;128(1):15-25.
95. Olmedo-Diaz S, Estevez-Silva H, Oradd G, Af Bjerken S, Marcellino D, Virel A. An altered blood-brain barrier contributes to brain iron accumulation and neuroinflammation in the 6-OHDA rat model of Parkinson's disease. Neuroscience. 2017;362:141-51.
96. Zoroddu MA, Aaseth J, Crisponi G, Medici S, Peana M, Nurchi VM. The essential metals for humans: a brief overview. J Inorg Biochem. 2019;195:120-9.
97. Scholefield M, Unwin RD, Cooper GJS. Shared perturbations in the metallome and metabolome of Alzheimer's, Parkinson's, Huntington's, and dementia with Lewy bodies: A systematic review. Ageing Res Rev. 2020;63:101152.
98. Powers R, Lei S, Anandhan A, Marshall DD, Worley B, Cerny RL, et al. Metabolic investigations of the molecular mechanisms associated with Parkinson's disease. Metabolites. 2017;7(2).
99. Anandhan A, Jacome MS, Lei S, Hernandez-Franco P, Pappa A, Panayiotidis MI, et al. Metabolic dysfunction in parkinson's disease: Bioenergetics, redox homeostasis and central carbon metabolism. Brain Res Bull. 2017;133:12-30.
100. Mittal M, Kumar K, Anghore D, Rawal RK. ICP-MS: Analytical method for identification and detection of elemental impurities. Curr Drug Discov Technol. 2017;14(2):106-20.
101. Scholefield M, Church SJ, Xu J, Kassab S, Gardiner NJ, Roncaroli F, et al. Evidence that levels of nine essential metals in post-mortem human-Alzheimer's-brain and ex vivo rat-brain tissues are unaffected by differences in post-mortem delay, age, disease staging, and brain bank location. Metallomics. 2020;12(6):952-62.
102. Scholefield M, Church SJ, Xu J, Patassini S, Roncaroli F, Hooper NM, et al. Widespread decreases in cerebral copper are common to Parkinson's disease dementia and Alzheimer's disease dementia. Front Aging Neurosci. 2021;13:641222.
103. Scholefield M, Church SJ, Xu J, Robinson AC, Gardiner NJ, Roncaroli F, et al. Effects of alterations of post-mortem delay and other tissue-collection variables on metabolite levels in human and rat brain. Metabolites. 2020;10(11).
104. Ismail N, Kureishy N, Church SJ, Scholefield M, Unwin RD, Xu J, et al. Vitamin B5 (d-pantothenic acid) localizes in myelinated structures of the rat brain: Potential role for cerebral vitamin B5 stores in local myelin homeostasis. Biochem Biophys Res Commun. 2020;522(1):220-5.
105. Pritchard DE, Thompson JK. Mass Spectrometry at 100 Parts Per Trillion. In: Atutov SN, Calabrese R, Moi L, editors. Trapped Particles and Fundamental Physics. Dordrecht: Springer Netherlands; 2002. p. 245-58.
106. Thomas R. A beginner's guide to ICP-MS. Spectroscopy. 2001;16(4):38-42.
107. Rochat B. Quantitative and qualitative LC-high-resolution MS: The technological and biological reasons for a shift of paradigm. 2018 14/12/2018. In: Recent advances in analytical chemistry [Internet]. IntechOpen. Available from: https://www.intechopen.com/books/recent-advances-in-analytical-chemistry/quantitative-and-qualitative-lc-high-resolution-ms-the-technological-and-biological-reasons-for-a-sh.
108. Domingo-Almenara X, Montenegro-Burke JR, Ivanisevic J, Thomas A, Sidibe J, Teav T, et al. XCMS-MRM and METLIN-MRM: a cloud library and public resource for targeted analysis of small molecules. Nat Methods. 2018;15(9):681-4.
109. Ranque C. Electrospray ionization (ESI) mass spectrometry 2021 [updated 2021/03/2825/05/2021]. Available from: https://phys.libretexts.org/@go/page/14603.
110. Accurate mass: Fiehn Lab; 2016 [25/05/2021]. Available from: https://fiehnlab.ucdavis.edu/projects/Seven-Golden-Rules/Accurate-Mass.
111. Yates JR, Ruse CI, Nakorchevsky A. Proteomics by mass spectrometry: approaches, advances, and applications. Annu Rev Biomed Eng. 2009;11:49-79.
112. Soares R, Franco C, Pires E, Ventosa M, Palhinhas R, Koci K, et al. Mass spectrometry and animal science: protein identification strategies and particularities of farm animal species. J Proteomics. 2012;75(14):4190-206.
113. Cajka T, Hajslova J, Mastovska K. Mass Spectrometry and Hyphenated Instruments in Food Analysis. In: Ötleş S, editor. Handbook of Food Analysis Instruments: CRS Press, Taylor & Francis Group; 2008. p. 208-9.
114. Hecht ES, Scigelova M, Eliuk S, Makarov A. Fundamentals and Advances of Orbitrap Mass Spectrometry. Encyclopedia of Analytical Chemistry: Applications, Theory and Instrumentation [Internet]. 2019:[1-40 pp.].
115. Lebedev A, Zaikin V. Recent problems and advances in mass spectrometry. Inorganic Materials. 2008;44(14).
116. Bigler L. Mass spectrometry-recent applications in chemistry, pharmacology and biology. Zurich: University of Zurich; 2009.
117. Brock K. Evidence-Based to Personalized Medicine: mass Spectrometry Bridges the Gap Lab Compare2011 [25/05/2021]. Available from: https://www.labcompare.com/10-Featured-Articles/19396-Evidence-Based-to-Personalized-Medicine-Mass-Spectrometry-Bridges-the-Gap/.
118. Emwas AH. The strengths and weaknesses of NMR spectroscopy and mass spectrometry with particular focus on metabolomics research. Methods Mol Biol. 2015;1277:161-93.

119. Rudin M, Sauter A. In vivo NMR in pharmaceutical research. Magn Reson Imaging. 1992;10(5):723-31.
120. West BM. A primer for ICP-mass spectrometry. Laboratory medicine. 2004;35(12):745-7.
121. Pappas RS. Sample Preparation Problem Solving for Inductively Coupled Plasma-Mass Spectrometry with Liquid Introduction Systems I. Solubility, Chelation, and Memory Effects. Spectroscopy (Springf). 2012;27(5):20-31.
122. Dan Y, Zhang W, Xue R, Ma X, Stephan C, Shi H. Characterization of gold nanoparticle uptake by tomato plants using enzymatic extraction followed by single-particle inductively coupled plasma-mass spectrometry analysis. Environ Sci Technol. 2015;49(5):3007-14.
123. Wilschefski SC, Baxter MR. Inductively Coupled Plasma Mass Spectrometry: Introduction to Analytical Aspects. Clin Biochem Rev. 2019;40(3):115-33.
124. Todoli JL, Maestre S, Mora J, Canals A, Hernandis V. Comparison of several spray chambers operating at very low liquid flow rates in inductively coupled plasma atomic emission spectrometry. Fresenius J Anal Chem. 2000;368(8):773-9.
125. Neufeld L. ICP-MS Interface Cones: Maintaining the Critical Interface between the Mass Spectrometer and the Plasma Discharge to Optimize Performance and Maximize Instrument Productivity. SPECTROSCOPY. 2019;34(7):12-7.
126. May TW, Wiedmeyer RH. A table of polyatomic interferences in ICP-MS. Atomic Spectroscopy 1998;19:150-5.
127. Ammann AA. Inductively coupled plasma mass spectrometry (ICP MS): a versatile tool. J Mass Spectrom. 2007;42(4):419-27.
128. Tyler G, S. JY. ICP-OES, ICP-MS and AAS Techniques Compared. ICP Optical Emission Spectroscopy Technical Note [Internet]. 1995; 5. Available from: https://www.horiba.com/fileadmin/uploads/Scientific/Downloads/OpticalSchool_CN/TN/ICP/ICP-OES__ICP-MS_and_AAS_Techniques_Compared.pdf.
129. Elliott S. Comparison of ICP-QQQ and MP-AES to alternative atomic spectrometry techniques 2017 [updated 17/02/2017. Available from: https://www.labcompare.com/10-Featured-Articles/333957-Comparison-of-ICP-QQQ-and-MP-AES-to-Alternative-Atomic-Spectrometry-Techniques/.
130. Grochowski C, Blicharska E, Krukow P, Jonak K, Maciejewski M, Szczepanek D, et al. Analysis of Trace Elements in Human Brain: Its Aim, Methods, and Concentration Levels. Front Chem. 2019;7:115.
131. Iwasaki Y, Sawada T, Hatayama K, Ohyagi A, Tsukuda Y, Namekawa K, et al. Separation technique for the determination of highly polar metabolites in biological samples. Metabolites. 2012;2(3):496-515.
132. Halket JM, Waterman D, Przyborowska AM, Patel RK, Fraser PD, Bramley PM. Chemical derivatization and mass spectral libraries in metabolic profiling by GC/MS and LC/MS/MS. J Exp Bot. 2005;56(410):219-43.
133. Majors RE. Supported Liquid Extraction: The Best-Kept Secret in Sample Preparation. LC-GC Europe [Internet]. 2012 26/05/2021; 30(8). Available from: https://www.interchim.fr/cat/Article%20LCGC_SupportedLiquidExtraction.pdf.
134. Kumari C, Varughese B, Ramji S, Kapoor S. Liquid-Liquid Extraction and Solid Phase Extraction for Urinary Organic Acids: A Comparative Study from a Resource Constraint Setting. Indian J Clin Biochem. 2016;31(4):414-22.
135. Hoofnagle AN, Whiteaker JR, Carr SA, Kuhn E, Liu T, Massoni SA, et al. Recommendations for the Generation, Quantification, Storage, and Handling of Peptides Used for Mass Spectrometry-Based Assays. Clin Chem. 2016;62(1):48-69.
136. Moldoveanu SC, David V. Derivatization Methods in GC and GC/MS. 2018. In: Gas Chromatography - Derivatization, Sample Preparation, Application [Internet]. IntechOpen. Available from: https://www.intechopen.com/books/gas-chromatography-derivatization-sample-preparation-application/derivatization-methods-in-gc-and-gc-ms.
137. Orata F. Derivatization Reactions and Reagents for Gas Chromatography Analysis. In: Mohd MA, editor. Advanced Gas Chromatography - Progress in Agricultural, Biomedical and Industrial Applications. Croatia: InTech; 2012. p. 83-108.
138. Villas-Boas SG, Smart KF, Sivakumaran S, Lane GA. Alkylation or Silylation for Analysis of Amino and Non-Amino Organic Acids by GC-MS? Metabolites. 2011;1(1):3-20.
139. Sparkman DO, Penton Z, Kitson FG. Gas Chromatography: Sample Introduction. In: Gross ML, Caprioli R, editors. Gas Chromatography and Mass Spectrometry: A Practical Guide. 2nd ed. UK: Academic Press; 2011. p. 16-36.
140. Using Hydrogen Carrier Gas with Mass Spectrometric Detection: Crawford Scientific; 2019 [updated 05/08/2019. Available from: https://www.crawfordscientific.com/chromatography-blog/post/hydrogen-carrier-gas-ms-detection.
141. Sparkman DO, Penton Z, Kitson FG. Gas Chromatography: Carrier Gas Considerations. In: Gross ML, Caprioli R, editors. Gas Chromatography and Mass Spectrometry: A Practical Guide. 2nd ed. UK: Academic Press; 2011. p. 61-3.
142. Rahman MM, Abd El-Aty AM, Choi J-H, Shin H-C, Shin SC, Shim J-H. Basic overview on gas chromatography columns. Analytical Separation Science. p. 823-34.
143. The GC oven. 2020.
144. Linne U, Bezold F, Bamberger J. Coupling Methods in Mass Spectrometry Part 12019 27/05/2021. Available from: https://analyticalscience.wiley.com/do/10.1002/gitlab.18346.
145. Dolan JW. How Does It Work? Part III: Autosamplers. LCGC North America [Internet]. 2016; 34(7):[472-8 pp.].
146. Moldoveanu SC, David V. Chapter 5 - Retention Mechanisms in Different HPLC Types. In: Moldoveanu SC, David V, editors. Essentials in Modern HPLC Separations: Elsevier; 2013. p. 145-90.
147. Moldoveanu SC, David V. Chapter 9 - HPLC Analysis. In: Moldoveanu SC, David V, editors. Essentials in Modern HPLC Separations: Elsevier; 2013. p. 465-519.

148. Heaton J, Smith NW. Advantages and disadvantages of HILIC; a brief overview. Chromatogr Today. 2012;5:44-7.
149. Dass C. Modes of Ionization. Fundamentals of Contemporary Mass Spectrometry: John Wiley & Sons; 2007. p. 15-65.
150. Zhou B, Xiao JF, Tuli L, Ressom HW. LC-MS-based metabolomics. Mol Biosyst. 2012;8(2):470-81.
151. Gowda GA, Djukovic D. Overview of mass spectrometry-based metabolomics: opportunities and challenges. Methods Mol Biol. 2014;1198:3-12.
152. Stein S. Mass spectral reference libraries: an ever-expanding resource for chemical identification. Anal Chem. 2012;84(17):7274-82.
153. Torres J. To run or to fly: A comparison between HPLC and GC: BitesizeBio; 2019 [updated 14/11/2016. Available from: https://bitesizebio.com/29109/run-fly-comparison-hplc-gc/.
154. Li H, Tennessen JM. Methods for studying the metabolic basis of Drosophila development. Wiley Interdiscip Rev Dev Biol. 2017;6(5).
155. Koek MM, Bakels F, Engel W, van den Maagdenberg A, Ferrari MD, Coulier L, et al. Metabolic profiling of ultrasmall sample volumes with GC/MS: from microliter to nanoliter samples. Anal Chem. 2010;82(1):156-62.
156. Want EJ, Cravatt BF, Siuzdak G. The expanding role of mass spectrometry in metabolite profiling and characterization. Chembiochem. 2005;6(11):1941-51.
157. McAllum EJ, Finkelstein DI. Metals in Alzheimer's and Parkinson's Disease: Relevance to Dementia with Lewy Bodies. J Mol Neurosci. 2016;60(3):279-88.
158. Kori M, Aydin B, Unal S, Arga KY, Kazan D. Metabolic Biomarkers and Neurodegeneration: A Pathway Enrichment Analysis of Alzheimer's Disease, Parkinson's Disease, and Amyotrophic Lateral Sclerosis. OMICS. 2016;20(11):645-61.
159. Griffin JW, Bradshaw PC. Amino Acid Catabolism in Alzheimer's Disease Brain: Friend or Foe? Oxid Med Cell Longev. 2017;2017:5472792.
160. Chaturvedi RK, Flint Beal M. Mitochondrial diseases of the brain. Free Radic Biol Med. 2013;63:1-29.
161. Akatsu H, Hori A, Yamamoto T, Yoshida M, Mimuro M, Hashizume Y, et al. Transition metal abnormalities in progressive dementias. Biometals. 2012;25(2):337-50.
162. Stephanos JJ, Addison AW. Chemistry of metalloproteins : problems and solutions in bioinorganic chemistry. Hoboken, New Jersey: Wiley,; 2014.
163. Deibel MA, Ehmann WD, Markesbery WR. Copper, iron, and zinc imbalances in severely degenerated brain regions in Alzheimer's disease: possible relation to oxidative stress. J Neurol Sci. 1996;143(1-2):137-42.
164. Magaki S, Raghavan R, Mueller C, Oberg KC, Vinters HV, Kirsch WM. Iron, copper, and iron regulatory protein 2 in Alzheimer's disease and related dementias. Neurosci Lett. 2007;418(1):72-6.
165. Religa D, Strozyk D, Cherny RA, Volitakis I, Haroutunian V, Winblad B, et al. Elevated cortical zinc in Alzheimer disease. Neurology. 2006;67(1):69-75.
166. Rosas HD, Chen YI, Doros G, Salat DH, Chen NK, Kwong KK, et al. Alterations in brain transition metals in Huntington disease: an evolving and intricate story. Arch Neurol. 2012;69(7):887-93.
167. Corrigan FM, Reynolds GP, Ward NI. Hippocampal tin, aluminum and zinc in Alzheimer's disease. Biometals. 1993;6(3):149-54.
168. Xu J, Church SJ, Patassini S, Begley P, Waldvogel HJ, Curtis MA, et al. Evidence for widespread, severe brain copper deficiency in Alzheimer's dementia. Metallomics. 2017;9(8):1106-19.
169. Loeffler DA, LeWitt PA, Juneau PL, Sima AA, Nguyen HU, DeMaggio AJ, et al. Increased regional brain concentrations of ceruloplasmin in neurodegenerative disorders. Brain Res. 1996;738(2):265-74.
170. Szabo ST, Harry GJ, Hayden KM, Szabo DT, Birnbaum L. Comparison of Metal Levels between Postmortem Brain and Ventricular Fluid in Alzheimer's Disease and Nondemented Elderly Controls. Toxicol Sci. 2016;150(2):292-300.
171. Davies KM, Bohic S, Carmona A, Ortega R, Cottam V, Hare DJ, et al. Copper pathology in vulnerable brain regions in Parkinson's disease. Neurobiol Aging. 2014;35(4):858-66.
172. Graham SF, Nasarauddin MB, Carey M, McGuinness B, Holscher C, Kehoe PG, et al. Quantitative measurement of [Na+] and [K+] in postmortem human brain tissue indicates disturbances in subjects with Alzheimer's disease and dementia with Lewy bodies. J Alzheimers Dis. 2015;44(3):851-7.
173. Di Paola M, Phillips OR, Sanchez-Castaneda C, Di Pardo A, Maglione V, Caltagirone C, et al. MRI measures of corpus callosum iron and myelin in early Huntington's disease. Hum Brain Mapp. 2014;35(7):3143-51.
174. Bartzokis G, Lu PH, Tishler TA, Fong SM, Oluwadara B, Finn JP, et al. Myelin breakdown and iron changes in Huntington's disease: pathogenesis and treatment implications. Neurochem Res. 2007;32(10):1655-64.
175. Dumas EM, Versluis MJ, van den Bogaard SJ, van Osch MJ, Hart EP, van Roon-Mom WM, et al. Elevated brain iron is independent from atrophy in Huntington's Disease. Neuroimage. 2012;61(3):558-64.
176. Sanchez-Castaneda C, Cherubini A, Elifani F, Peran P, Orobello S, Capelli G, et al. Seeking Huntington disease biomarkers by multimodal, cross-sectional basal ganglia imaging. Hum Brain Mapp. 2013;34(7):1625-35.
177. Raven EP, Lu PH, Tishler TA, Heydari P, Bartzokis G. Increased iron levels and decreased tissue integrity in hippocampus of Alzheimer's disease detected in vivo with magnetic resonance imaging. J Alzheimers Dis. 2013;37(1):127-36.

178. Graham SF, Nasaruddin MB, Carey M, Holscher C, McGuinness B, Kehoe PG, et al. Age-associated changes of brain copper, iron, and zinc in Alzheimer's disease and dementia with Lewy bodies. J Alzheimers Dis. 2014;42(4):1407-13.
179. Alonso-Andres P, Albasanz JL, Ferrer I, Martin M. Purine-related metabolites and their converting enzymes are altered in frontal, parietal and temporal cortex at early stages of Alzheimer's disease pathology. Brain Pathol. 2018.
180. Xu J, Begley P, Church SJ, Patassini S, Hollywood KA, Jullig M, et al. Graded perturbations of metabolism in multiple regions of human brain in Alzheimer's disease: Snapshot of a pervasive metabolic disorder. Biochim Biophys Acta. 2016;1862(6):1084-92.
181. McFarland NR, Burdett T, Desjardins CA, Frosch MP, Schwarzschild MA. Postmortem brain levels of urate and precursors in Parkinson's disease and related disorders. Neurodegener Dis. 2013;12(4):189-98.
182. Graham SF, Kumar PK, Bjorndahl T, Han B, Yilmaz A, Sherman E, et al. Metabolic signatures of Huntington's disease (HD): (1)H NMR analysis of the polar metabolome in post-mortem human brain. Biochim Biophys Acta. 2016;1862(9):1675-84.
183. Patassini S, Begley P, Xu J, Church SJ, Reid SJ, Kim EH, et al. Metabolite mapping reveals severe widespread perturbation of multiple metabolic processes in Huntington's disease human brain. Biochim Biophys Acta. 2016;1862(9):1650-62.
184. Xu J, Begley P, Church SJ, Patassini S, McHarg S, Kureishy N, et al. Elevation of brain glucose and polyol-pathway intermediates with accompanying brain-copper deficiency in patients with Alzheimer's disease: metabolic basis for dementia. Sci Rep. 2016;6:27524.
185. An Y, Varma VR, Varma S, Casanova R, Dammer E, Pletnikova O, et al. Evidence for brain glucose dysregulation in Alzheimer's disease. Alzheimers Dement. 2018;14(3):318-29.
186. Annanmaki T, Muuronen A, Murros K. Low plasma uric acid level in Parkinson's disease. Mov Disord. 2007;22(8):1133-7.
187. Bogdanov M, Matson WR, Wang L, Matson T, Saunders-Pullman R, Bressman SS, et al. Metabolomic profiling to develop blood biomarkers for Parkinson's disease. Brain. 2008;131(Pt 2):389-96.
188. Johansen KK, Wang L, Aasly JO, White LR, Matson WR, Henchcliffe C, et al. Metabolomic profiling in LRRK2-related Parkinson's disease. PLoS One. 2009;4(10):e7551.
189. Sakuta H, Suzuki K, Miyamoto T, Miyamoto M, Numao A, Fujita H, et al. Serum uric acid levels in Parkinson's disease and related disorders. Brain Behav. 2017;7(1):e00598.
190. Boll MC, Alcaraz-Zubeldia M, Montes S, Rios C. Free copper, ferroxidase and SOD1 activities, lipid peroxidation and NO(x) content in the CSF. A different marker profile in four neurodegenerative diseases. Neurochem Res. 2008;33(9):1717-23.
191. Molina JA, Jimenez-Jimenez FJ, Aguilar MV, Meseguer I, Mateos-Vega CJ, Gonzalez-Munoz MJ, et al. Cerebrospinal fluid levels of transition metals in patients with Alzheimer's disease. J Neural Transm (Vienna). 1998;105(4-5):479-88.
192. Ahmed SS, Santosh W. Metallomic profiling and linkage map analysis of early Parkinson's disease: a new insight to aluminum marker for the possible diagnosis. PLoS One. 2010;5(6):e11252.
193. Alimonti A, Bocca B, Pino A, Ruggieri F, Forte G, Sancesario G. Elemental profile of cerebrospinal fluid in patients with Parkinson's disease. J Trace Elem Med Biol. 2007;21(4):234-41.
194. Bocca B, Alimonti A, Senofonte O, Pino A, Violante N, Petrucci F, et al. Metal changes in CSF and peripheral compartments of parkinsonian patients. J Neurol Sci. 2006;248(1-2):23-30.
195. Karpenko MN, Ilyicheva EY, Muruzheva ZM, Milyukhina IV, Orlov YA, Puchkova LV. Role of Copper Dyshomeostasis in the Pathogenesis of Parkinson's Disease. Bull Exp Biol Med. 2018;164(5):596-600.
196. Pall HS, Williams AC, Blake DR, Lunec J, Gutteridge JM, Hall M, et al. Raised cerebrospinal-fluid copper concentration in Parkinson's disease. Lancet. 1987;2(8553):238-41.
197. Sanyal J, Ahmed SS, Ng HK, Naiya T, Ghosh E, Banerjee TK, et al. Metallomic Biomarkers in Cerebrospinal fluid and Serum in patients with Parkinson's disease in Indian population. Sci Rep. 2016;6:35097.
198. Bostrom F, Hansson O, Gerhardsson L, Lundh T, Minthon L, Stomrud E, et al. CSF Mg and Ca as diagnostic markers for dementia with Lewy bodies. Neurobiol Aging. 2009;30(8):1265-71.
199. Maetzler W, Schmid SP, Wurster I, Liepelt I, Gaenslen A, Gasser T, et al. Reduced but not oxidized cerebrospinal fluid glutathione levels are lowered in Lewy body diseases. Mov Disord. 2011;26(1):176-81.
200. Molina JA, Leza JC, Ortiz S, Moro MA, Perez S, Lizasoain I, et al. Cerebrospinal fluid and plasma concentrations of nitric oxide metabolites are increased in dementia with Lewy bodies. Neurosci Lett. 2002;333(2):151-3.
201. Molina JA, Gomez P, Vargas C, Ortiz S, Perez-Rial S, Uriguen L, et al. Neurotransmitter amino acid in cerebrospinal fluid of patients with dementia with Lewy bodies. J Neural Transm (Vienna). 2005;112(4):557-63.
202. Wennstrom M, Nielsen HM, Orhan F, Londos E, Minthon L, Erhardt S. Kynurenic Acid levels in cerebrospinal fluid from patients with Alzheimer's disease or dementia with lewy bodies. Int J Tryptophan Res. 2014;7:1-7.
203. Ruiz PJG, Mena MA, Bernardos VS, Neira WD, Roldan SG, Benitez J, et al. Cerebrospinal-fluid homovanillic-acid is reduced in untreated Huntington's disease. Clin Neuropharmacol. 1995;18(1):58-63.
204. Hatano T, Saiki S, Okuzumi A, Mohney RP, Hattori N. Identification of novel biomarkers for Parkinson's disease by metabolomic technologies. J Neurol Neurosurg Psychiatry. 2016;87(3):295-301.
205. Iwasaki Y, Ikeda K, Shiojima T, Kinoshita M. Increased plasma concentrations of aspartate, glutamate and glycine in Parkinson's disease. Neurosci Lett. 1992;145(2):175-7.

206. Molina JA, Jimenez-Jimenez FJ, Gomez P, Vargas C, Navarro JA, Orti-Pareja M, et al. Decreased cerebrospinal fluid levels of neutral and basic amino acids in patients with Parkinson's disease. J Neurol Sci. 1997;150(2):123-7.
207. Han W, Sapkota S, Camicioli R, Dixon RA, Li L. Profiling novel metabolic biomarkers for Parkinson's disease using in-depth metabolomic analysis. Mov Disord. 2017;32(12):1720-8.
208. Czech C, Berndt P, Busch K, Schmitz O, Wiemer J, Most V, et al. Metabolite profiling of Alzheimer's disease cerebrospinal fluid. PLoS One. 2012;7(2):e31501.
209. Molina JA, Jimenez-Jimenez FJ, Vargas C, Gomez P, de Bustos F, Orti-Pareja M, et al. Cerebrospinal fluid levels of non-neurotransmitter amino acids in patients with Alzheimer's disease. J Neural Transm (Vienna). 1998;105(2-3):279-86.
210. Fonteh AN, Harrington RJ, Tsai A, Liao P, Harrington MG. Free amino acid and dipeptide changes in the body fluids from Alzheimer's disease subjects. Amino Acids. 2007;32(2):213-24.
211. Gruber B, Klaczkow G, Jaworska M, Krzyszton-Russjan J, Anuszewska EL, Zielonka D, et al. Huntington' disease--imbalance of amino acid levels in plasma of patients and mutation carriers. Ann Agric Environ Med. 2013;20(4):779-83.
212. Cheng ML, Chang KH, Wu YR, Chen CM. Metabolic disturbances in plasma as biomarkers for Huntington's disease. J Nutr Biochem. 2016;31:38-44.
213. Mally J, Szalai G, Stone TW. Changes in the concentration of amino acids in serum and cerebrospinal fluid of patients with Parkinson's disease. J Neurol Sci. 1997;151(2):159-62.
214. Gueli MC, Taibi G. Alzheimer's disease: amino acid levels and brain metabolic status. Neurol Sci. 2013;34(9):1575-9.
215. Olazaran J, Gil-de-Gomez L, Rodriguez-Martin A, Valenti-Soler M, Frades-Payo B, Marin-Munoz J, et al. A blood-based, 7-metabolite signature for the early diagnosis of Alzheimer's disease. J Alzheimers Dis. 2015;45(4):1157-73.
216. Nambron R, Silajdzic E, Kalliolia E, Ottolenghi C, Hindmarsh P, Hill NR, et al. A Metabolic Study of Huntington's Disease. PLoS One. 2016;11(1):e0146480.
217. Wen M, Zhou B, Chen YH, Ma ZL, Gou Y, Zhang CL, et al. Serum uric acid levels in patients with Parkinson's disease: A meta-analysis. PLoS One. 2017;12(3):e0173731.
218. Schlesinger I, Schlesinger N. Uric acid in Parkinson's disease. Mov Disord. 2008;23(12):1653-7.
219. Gonzalez-Dominguez R, Garcia-Barrera T, Gomez-Ariza JL. Metabolite profiling for the identification of altered metabolic pathways in Alzheimer's disease. J Pharm Biomed Anal. 2015;107:75-81.
220. Mangialasche F, Baglioni M, Cecchetti R, Kivipelto M, Ruggiero C, Piobbico D, et al. Lymphocytic mitochondrial aconitase activity is reduced in Alzheimer's disease and mild cognitive impairment. J Alzheimers Dis. 2015;44(2):649-60.
221. Rinaldi P, Polidori MC, Metastasio A, Mariani E, Mattioli P, Cherubini A, et al. Plasma antioxidants are similarly depleted in mild cognitive impairment and in Alzheimer's disease. Neurobiol Aging. 2003;24(7):915-9.
222. Baldeiras I, Santana I, Proenca MT, Garrucho MH, Pascoal R, Rodrigues A, et al. Peripheral oxidative damage in mild cognitive impairment and mild Alzheimer's disease. J Alzheimers Dis. 2008;15(1):117-28.
223. Cervellati C, Romani A, Seripa D, Cremonini E, Bosi C, Magon S, et al. Oxidative balance, homocysteine, and uric acid levels in older patients with Late Onset Alzheimer's Disease or Vascular Dementia. J Neurol Sci. 2014;337(1-2):156-61.
224. Trushina E, Dutta T, Persson XMT, Mielke MM, Petersen RC. Identification of altered metabolic pathways in plasma and CSF in Mild Cognitive Impairment and Alzheimer's disease using metabolomics. Plos One. 2013;8(6).
225. Rosas HD, Doros G, Bhasin S, Thomas B, Gevorkian S, Malarick K, et al. A systems-level "misunderstanding": the plasma metabolome in Huntington's disease. Ann Clin Transl Neurol. 2015;2(7):756-68.
226. Hyder F, Rothman DL. Advances in imaging brain metabolism. Annu Rev Biomed Eng. 2017;19:485-515.
227. Dusek P, Dezortova M, Wuerfel J. Imaging of iron. Int Rev Neurobiol. 2013;110:195-239.
228. Adams JD, Jr., Klaidman LK, Odunze IN, Shen HC, Miller CA. Alzheimer's and Parkinson's disease. Brain levels of glutathione, glutathione disulfide, and vitamin E. Mol Chem Neuropathol. 1991;14(3):213-26.
229. Mandal PK, Saharan S, Tripathi M, Murari G. Brain glutathione levels--a novel biomarker for mild cognitive impairment and Alzheimer's disease. Biol Psychiatry. 2015;78(10):702-10.
230. Bermejo P, Martin-Aragon S, Benedi J, Susin C, Felici E, Gil P, et al. Peripheral levels of glutathione and protein oxidation as markers in the development of Alzheimer's disease from Mild Cognitive Impairment. Free Radic Res. 2008;42(2):162-70.
231. Puertas MC, Martinez-Martos JM, Cobo MP, Carrera MP, Mayas D, Ramirez-Exposito J. Plasma oxidative stress parameters in men and women with early stage Alzheimer type dementia. Exp Gerontol. 2012;47(8):625-30.
232. Rani P, Krishnan S, Rani Cathrine C. Study on analysis of peripheral biomarkers for Alzheimer's disease diagnosis. Front Neurol. 2017;8:328.
233. Cardoso BR, Hare DJ, Bush AI, Li QX, Fowler CJ, Masters CL, et al. Selenium Levels in Serum, Red Blood Cells, and Cerebrospinal Fluid of Alzheimer's Disease Patients: A Report from the Australian Imaging, Biomarker & Lifestyle Flagship Study of Ageing (AIBL). J Alzheimers Dis. 2017;57(1):183-93.
234. Giacoppo S, Galuppo M, Calabro RS, D'Aleo G, Marra A, Sessa E, et al. Heavy Metals and Neurodegenerative Diseases: An Observational Study. Biol Trace Elem Res. 2014;161(2):151-60.
235. Gonzalez-Dominguez R, Garcia A, Garcia-Barrera T, Barbas C, Gomez-Ariza JL. Metabolomic profiling of serum in the progression of Alzheimer's disease by capillary electrophoresis-mass spectrometry. Electrophoresis. 2014;35(23):3321-30.

236. Aybek H, Ercan F, Aslan D, Sahiner T. Determination of malondialdehyde, reduced glutathione levels and APOE4 allele frequency in late-onset Alzheimer's disease in Denizli, Turkey. Clin Biochem. 2007;40(3-4):172-6.
237. Koc ER, Ilhan A, Zubeyde A, Acar B, Gurler M, Altuntas A, et al. A comparison of hair and serum trace elements in patients with Alzheimer disease and healthy participants. Turk J Med Sci. 2015;45(5):1034-9.
238. Meseguer I, Molina JA, Jimenez-Jimenez FJ, Aguilar MV, Mateos-Vega CJ, Gonzalez-Munoz MJ, et al. Cerebrospinal fluid levels of selenium in patients with Alzheimer's disease. J Neural Transm (Vienna). 1999;106(3-4):309-15.
239. Vaz FNC, Fermino BL, Haskel MVL, Wouk J, de Freitas GBL, Fabbri R, et al. The Relationship Between Copper, Iron, and Selenium Levels and Alzheimer Disease. Biol Trace Elem Res. 2018;181(2):185-91.
240. Xu JS, Church SJ, Patassini S, Begley P, Kellett KAB, Vardy ERLC, et al. Plasma metals as potential biomarkers in dementia: a case-control study in patients with sporadic Alzheimer's disease. Biometals. 2018;31(2):267-76.
241. Kaddurah-Daouk R, Rozen S, Matson W, Han X, Hulette CM, Burke JR, et al. Metabolomic changes in autopsy-confirmed Alzheimer's disease. Alzheimers Dement. 2011;7(3):309-17.
242. Agarwal R, Kushwaha SS, Tripathi CB, Singh N, Chhillar N. Serum copper in Alzheimer's disease and vascular dementia. Indian J Clin Biochem. 2008;23(4):369-74.
243. Brewer GJ, Kanzer SH, Zimmerman EA, Celmins DF, Heckman SM, Dick R. Copper and ceruloplasmin abnormalities in Alzheimer's disease. Am J Alzheimers Dis Other Demen. 2010;25(6):490-7.
244. Gonzalez C, Martin T, Cacho J, Brenas MT, Arroyo T, Garcia-Berrocal B, et al. Serum zinc, copper, insulin and lipids in Alzheimer's disease epsilon 4 apolipoprotein E allele carriers. Eur J Clin Invest. 1999;29(7):637-42.
245. Park JH, Lee DW, Park KS. Elevated serum copper and ceruloplasmin levels in Alzheimer's disease. Asia Pac Psychiatry. 2014;6(1):38-45.
246. Squitti R, Lupoi D, Pasqualetti P, Dal Forno G, Vernieri F, Chiovenda P, et al. Elevation of serum copper levels in Alzheimer's disease. Neurology. 2002;59(8):1153-61.
247. Wang ZX, Tan L, Wang HF, Ma J, Liu JY, Tan MS, et al. Serum Iron, Zinc, and Copper Levels in Patients with Alzheimer's Disease: A Replication Study and Meta-Analyses. Journal of Alzheimers Disease. 2015;47(3):565-81.
248. Baum L, Chan IH, Cheung SK, Goggins WB, Mok V, Lam L, et al. Serum zinc is decreased in Alzheimer's disease and serum arsenic correlates positively with cognitive ability. Biometals. 2010;23(1):173-9.
249. Rembach A, Doecke JD, Roberts BR, Watt AD, Faux NG, Volitakis I, et al. Longitudinal analysis of serum copper and ceruloplasmin in Alzheimer's disease. J Alzheimers Dis. 2013;34(1):171-82.
250. Snaedal J, Kristinsson J, Gunnarsdottir S, Olafsdottir, Baldvinsson M, Johannesson T. Copper, ceruloplasmin and superoxide dismutase in patients with Alzheimer's disease . a case-control study. Dement Geriatr Cogn Disord. 1998;9(5):239-42.
251. Sun Q, Hu H, Wang W, Jin H, Feng G, Jia N. Taurine attenuates amyloid beta 1-42-induced mitochondrial dysfunction by activating of SIRT1 in SK-N-SH cells. Biochem Biophys Res Commun. 2014;447(3):485-9.
252. Du L, Zhao Z, Cui A, Zhu Y, Zhang L, Liu J, et al. Increased iron deposition on brain quantitative susceptibility mapping correlates with decreased cognitive function in Alzheimer's disease. ACS Chem Neurosci. 2018;9(7):1849-57.
253. Mueller C, Schrag M, Crofton A, Stolte J, Muckenthaler MU, Magaki S, et al. Altered serum iron and copper homeostasis predicts cognitive decline in Mild Cognitive Impairment. Journal of Alzheimers Disease. 2012;29(2):341-50.
254. Vural H, Demirin H, Kara Y, Eren I, Delibas N. Alterations of plasma magnesium, copper, zinc, iron and selenium concentrations and some related erythrocyte antioxidant enzyme activities in patients with Alzheimer's disease. J Trace Elem Med Biol. 2010;24(3):169-73.
255. Torsdottir G, Kristinsson J, Snaedal J, Johannesson T. Ceruloplasmin and iron proteins in the serum of patients with Alzheimer's disease. Dement Geriatr Cogn Dis Extra. 2011;1(1):366-71.
256. Liu P, Fleete MS, Jing Y, Collie ND, Curtis MA, Waldvogel HJ, et al. Altered arginine metabolism in Alzheimer's disease brains. Neurobiol Aging. 2014;35(9):1992-2003.
257. Graham SF, Chevallier OP, Roberts D, Holscher C, Elliott CT, Green BD. Investigation of the human brain metabolome to identify potential markers for early diagnosis and therapeutic targets of Alzheimer's disease. Anal Chem. 2013;85(3):1803-11.
258. Muguruma Y, Tsutsui H, Noda T, Akatsu H, Inoue K. Widely targeted metabolomics of Alzheimer's disease postmortem cerebrospinal fluid based on 9-fluorenylmethyl chloroformate derivatized ultra-high performance liquid chromatography tandem mass spectrometry. J Chromatogr B. 2018;1091:53-66.
259. Basun H, Forssell LG, Almkvist O, Cowburn RF, Eklof R, Winblad B, et al. Amino acid concentrations in cerebrospinal fluid and plasma in Alzheimer's disease and healthy control subjects. J Neural Transm Park Dis Dement Sect. 1990;2(4):295-304.
260. Martinez M, Frank A, Diez-Tejedor E, Hernanz A. Amino acid concentrations in cerebrospinal fluid and serum in Alzheimer's disease and vascular dementia. J Neural Transm Park Dis Dement Sect. 1993;6(1):1-9.
261. Oresic M, Hyotylainen T, Herukka SK, Sysi-Aho M, Mattila I, Seppanan-Laakso T, et al. Metabolome in progression to Alzheimer's disease. Transl Psychiatry. 2011;1:e57.
262. Jimenez-Jimenez FJ, Molina JA, Vargas C, Gomez P, Navarro JA, Benito-Leon J, et al. Neurotransmitter amino acids in cerebrospinal fluid of patients with Parkinson's disease. J Neurol Sci. 1996;141(1-2):39-44.
263. Kumudini N, Uma A, Devi YP, Naushad SM, Mridula R, Borgohain R, et al. Association of Parkinson's disease with altered serum levels of lead and transition metals among South Indian subjects. Indian J Biochem Biophys. 2014;51(2):121-6.

264. Fukushima T, Tan X, Luo Y, Wang P, Song J, Kanda H, et al. Heavy metals in blood and urine and its relation to depressive symptoms in Parkinson's disease patients. Fukushima J Med Sci. 2013;59(2):76-80.
265. Kim MJ, Oh SB, Kim J, Kim K, Ryu HS, Kim MS, et al. Association of metals with the risk and clinical characteristics of Parkinson's disease. Parkinsonism Relat Disord. 2018;55:117-21.
266. Younes-Mhenni S, Aissi M, Mokni N, Boughammoura-Bouatay A, Chebel S, Frih-Ayed M, et al. Serum copper, zinc and selenium levels in Tunisian patients with Parkinson's disease. Tunis Med. 2013;91(6):402-5.
267. Verma AK, Keshari AK, Raj J, Kumari R, Kumar T, Sharma V, et al. Prolidase-associated trace elements (Mn, Zn, Co, and Ni) in the patients with Parkinson's Disease. Biol Trace Elem Res. 2016;171(1):48-53.
268. Brewer GJ, Kanzer SH, Zimmerman EA, Molho ES, Celmins DF, Heckman SM, et al. Subclinical zinc deficiency in Alzheimer's disease and Parkinson's disease. Am J Alzheimers Dis Other Demen. 2010;25(7):572-5.
269. Hegde ML, Shanmugavelu P, Vengamma B, Rao TS, Menon RB, Rao RV, et al. Serum trace element levels and the complexity of inter-element relations in patients with Parkinson's disease. J Trace Elem Med Biol. 2004;18(2):163-71.
270. Zhao HW, Lin J, Wang XB, Cheng X, Wang JY, Hu BL, et al. Assessing plasma levels of selenium, copper, iron and zinc in patients of Parkinson's disease. PLoS One. 2013;8(12):e83060.
271. Trezzi JP, Galozzi S, Jaeger C, Barkovits K, Brockmann K, Maetzler W, et al. Distinct metabolomic signature in cerebrospinal fluid in early parkinson's disease. Mov Disord. 2017;32(10):1401-8.
272. Wu JF, Wuolikainen A, Trupp M, Jonsson P, Marklund SL, Andersen PM, et al. NMR analysis of the CSF and plasma metabolome of rigorously matched amyotrophic lateral sclerosis, Parkinson's disease and control subjects. Metabolomics. 2016;12(6).
273. Wuolikainen A, Jonsson P, Ahnlund M, Antti H, Marklund SL, Moritz T, et al. Multi-platform mass spectrometry analysis of the CSF and plasma metabolomes of rigorously matched amyotrophic lateral sclerosis, Parkinson's disease and control subjects. Mol Biosyst. 2016;12(4):1287-98.
274. Aasly JO, Saether O, Johansen KK, Bathen TF, Giskeodegard GF, White LR. Changes to Intermediary Metabolites in Sporadic and LRRK2 Parkinson's Disease Demonstrated by Proton Magnetic Resonance Spectroscopy. Parkinsons Dis. 2015;2015:264896.
275. Marques A, Dutheil F, Durand E, Rieu I, Mulliez A, Fantini ML, et al. Glucose dysregulation in Parkinson's disease: Too much glucose or not enough insulin? Parkinsonism Relat Disord. 2018;55:122-7.
276. Bharucha KJ, Friedman JK, Vincent AS, Ross ED. Lower serum ceruloplasmin levels correlate with younger age of onset in Parkinson's disease. J Neurol. 2008;255(12):1957-62.
277. Ling H, Bhidayasiri R. Reduced serum caeruloplasmin levels in non-wilsonian movement disorders. Eur Neurol. 2011;66(3):123-7.
278. Dexter DT, Carayon A, Javoy-Agid F, Agid Y, Wells FR, Daniel SE, et al. Alterations in the levels of iron, ferritin and other trace metals in Parkinson's disease and other neurodegenerative diseases affecting the basal ganglia. Brain. 1991;114 (Pt 4):1953-75.
279. Zucca FA, Segura-Aguilar J, Ferrari E, Munoz P, Paris I, Sulzer D, et al. Interactions of iron, dopamine and neuromelanin pathways in brain aging and Parkinson's disease. Progress in Neurobiology. 2017;155:96-119.
280. Xu SL, Chan P. Interaction between neuromelanin and alpha-synuclein in Parkinson's disease. Biomolecules. 2015;5(2):1122-42.
281. Cabrera-Valdivia F, Jimenez-Jimenez FJ, Molina JA, Fernandez-Calle P, Vazquez A, Canizares-Liebana F, et al. Peripheral iron metabolism in patients with Parkinson's disease. J Neurol Sci. 1994;125(1):82-6.
282. Farhoudi M, Taheraghdam A, Farid GA, Talebi M, Pashapou A, Majidi J, et al. Serum iron and ferritin level in idiopathic Parkinson. Pak J Biol Sci. 2012;15(22):1094-7.
283. Madenci G, Bilen S, Arli B, Saka M, Ak F. Serum iron, vitamin B12 and folic acid levels in Parkinson's disease. Neurochem Res. 2012;37(7):1436-41.
284. de Lau LM, Koudstaal PJ, Hofman A, Breteler MM. Serum uric acid levels and the risk of Parkinson disease. Ann Neurol. 2005;58(5):797-800.
285. Pena-Sanchez M, Riveron-Forment G, Zaldivar-Vaillant T, Soto-Lavastida A, Borrero-Sanchez J, Lara-Fernandez G, et al. Association of status redox with demographic, clinical and imaging parameters in patients with Huntington's disease. Clin Biochem. 2015;48(18):1258-63.
286. Markianos M, Panas M, Kalfakis N, Vassilopoulos D. Plasma homovanillic acid and prolactin in Huntington's disease. Neurochem Res. 2009;34(5):917-22.
287. Beal MF, Swartz KJ, Finn SF, Bird ED, Martin JB. Amino acid and neuropeptide neurotransmitters in Huntington's disease cerebellum. Brain Res. 1988;454(1-2):393-6.
288. Ruiz PJG, Mena MA, Bernardos VS, Neira WD, Roldan SG, Benitez J, et al. Cerebrospinal-Fluid Homovanillic-Acid Is Reduced in Untreated Huntingtons-Disease. Clinical Neuropharmacology. 1995;18(1):58-63.
289. Martin WR, Wieler M, Hanstock CC. Is brain lactate increased in Huntington's disease? J Neurol Sci. 2007;263(1-2):70-4.
290. Aguilar MV, Jimenez-Jimenez FJ, Molina JA, Meseguer I, Mateos-Vega CJ, Gonzalez-Munoz MJ, et al. Cerebrospinal fluid selenium and chromium levels in patients with Parkinson's disease. J Neural Transm (Vienna). 1998;105(10-12):1245-51.
291. Ebenau-Jehle C, Thomas M, Scharf G, Kockelkorn D, Knapp B, Schuhle K, et al. Anaerobic metabolism of indoleacetate. J Bacteriol. 2012;194(11):2894-903.

292. Blennow K, Wallin A, Gottfries CG, Lekman A, Karlsson I, Skoog I, et al. Significance of decreased lumbar CSF levels of HVA and 5-HIAA in Alzheimer's disease. Neurobiol Aging. 1992;13(1):107-13.
293. Shurubor YI, D'Aurelio M, Clark-Matott J, Isakova EP, Deryabina YI, Beal MF, et al. Determination of coenzyme a and acetyl-coenzyme a in biological samples using HPLC with UV detection. Molecules. 2017;22(9).
294. Wijesekara N, Goncalves RA, De Felice FG, Fraser PE. Impaired peripheral glucose homeostasis and Alzheimer's disease. Neuropharmacology. 2018;136(Pt B):172-81.
295. Szablewski L. Glucose transporters in brain: In health and in Alzheimer's disease. J Alzheimers Dis. 2017;55(4):1307-20.
296. Zilberter Y, Zilberter M. The vicious circle of hypometabolism in neurodegenerative diseases: Ways and mechanisms of metabolic correction. J Neurosci Res. 2017;95(11):2217-35.
297. Nedelska Z, Senjem ML, Przybelski SA, Lesnick TG, Lowe VJ, Boeve BF, et al. Regional cortical perfusion on arterial spin labeling MRI in dementia with Lewy bodies: Associations with clinical severity, glucose metabolism and tau PET. Neuroimage Clin. 2018;19:939-47.
298. Morea V, Bidollari E, Colotti G, Fiorillo A, Rosati J, De Filippis L, et al. Glucose transportation in the brain and its impairment in Huntington disease: one more shade of the energetic metabolism failure? Amino Acids. 2017;49(7):1147-57.
299. Herholz K. Cerebral glucose metabolism in preclinical and prodromal Alzheimer's disease. Expert Rev Neurother. 2010;10(11):1667-73.
300. Gonzalez de Vega R, Fernandez-Sanchez ML, Fernandez JC, Alvarez Menendez FV, Sanz-Medel A. Selenium levels and Glutathione peroxidase activity in the plasma of patients with type II diabetes mellitus. J Trace Elem Med Biol. 2016;37:44-9.
301. Maryon EB, Molloy SA, Kaplan JH. Cellular glutathione plays a key role in copper uptake mediated by human copper transporter 1. Am J Physiol Cell Physiol. 2013;304(8):C768-79.
302. Aliaga ME, Lopez-Alarcon C, Bridi R, Speisky H. Redox-implications associated with the formation of complexes between copper ions and reduced or oxidized glutathione. Journal of Inorganic Biochemistry. 2016;154:78-88.
303. van Duijn S, Bulk M, van Duinen SG, Nabuurs RJA, van Buchem MA, van der Weerd L, et al. Cortical iron reflects severity of Alzheimer's disease. J Alzheimers Dis. 2017;60(4):1533-45.
304. Moon Y, Han SH, Moon WJ. Patterns of brain iron accumulation in vascular dementia and Alzheimer's dementia using quantitative susceptibility mapping imaging. J Alzheimers Dis. 2016;51(3):737-45.
305. Firbank MJ, Yarnall AJ, Lawson RA, Duncan GW, Khoo TK, Petrides GS, et al. Cerebral glucose metabolism and cognition in newly diagnosed Parkinson's disease: ICICLE-PD study. J Neurol Neurosurg Psychiatry. 2017;88(4):310-6.
306. Martin WR, Clark C, Ammann W, Stoessl AJ, Shtybel W, Hayden MR. Cortical glucose metabolism in Huntington's disease. Neurology. 1992;42(1):223-9.
307. Ishii K, Hosokawa C, Hyodo T, Sakaguchi K, Usami K, Shimamoto K, et al. Regional glucose metabolic reduction in dementia with Lewy bodies is independent of amyloid deposition. Ann Nucl Med. 2015;29(1):78-83.
308. Calsolaro V, Edison P. Alterations in glucose metabolism in alzheimer's disease. Recent Pat Endocr Metab Immune Drug Discov. 2016;10(1):31-9.
309. De Pablo-Fernandez E, Goldacre R, Pakpoor J, Noyce AJ, Warner TT. Association between diabetes and subsequent Parkinson disease A record-linkage cohort study. Neurology. 2018;91(2):E139-E42.
310. Chen Z, Zhong C. Decoding Alzheimer's disease from perturbed cerebral glucose metabolism: implications for diagnostic and therapeutic strategies. Prog Neurobiol. 2013;108:21-43.
311. Ames BN, Cathcart R, Schwiers E, Hochstein P. Uric acid provides an antioxidant defense in humans against oxidant- and radical-caused aging and cancer: a hypothesis. Proc Natl Acad Sci U S A. 1981;78(11):6858-62.
312. Enroth C, Eger BT, Okamoto K, Nishino T, Nishino T, Pai EF. Crystal structures of bovine milk xanthine dehydrogenase and xanthine oxidase: Structure-based mechanism of conversion. P Natl Acad Sci USA. 2000;97(20):10723-8.
313. Kvietys PR, Inauen W, Bacon BR, Grisham MB. Xanthine oxidase-induced injury to endothelium - role of intracellular iron and hydroxyl radical. Am J Physiol. 1989;257(5):H1640-H6.
314. Gokce Cokal B, Yurtdas M, Keskin Guler S, Gunes HN, Atac Ucar C, Aytac B, et al. Serum glutathione peroxidase, xanthine oxidase, and superoxide dismutase activities and malondialdehyde levels in patients with Parkinson's disease. Neurol Sci. 2017;38(3):425-31.
315. Ghio AJ, Kennedy TP, Stonehuerner J, Carter JD, Skinner KA, Parks DA, et al. Iron regulates xanthine oxidase activity in the lung. Am J Physiol Lung Cell Mol Physiol. 2002;283(3):L563-72.
316. Yuan YS, Zhou XJ, Tong Q, Zhang L, Zhang L, Qi ZQ, et al. Change in plasma levels of amino acid neurotransmitters and its correlation with clinical heterogeneity in early Parkinson's disease patients. CNS Neurosci Ther. 2013;19(11):889-96.
317. Glaab E, Trezzi JP, Greuel A, Jager C, Hodak Z, Drzezga A, et al. Integrative analysis of blood metabolomics and PET brain neuroimaging data for Parkinson's disease. Neurobiol Dis. 2019;124:555-62.
318. Pompella A, Visvikis A, Paolicchi A, De Tata V, Casini AF. The changing faces of glutathione, a cellular protagonist. Biochem Pharmacol. 2003;66(8):1499-503.
319. Zitka O, Skalickova S, Gumulec J, Masarik M, Adam V, Hubalek J, et al. Redox status expressed as GSH:GSSG ratio as a marker for oxidative stress in paediatric tumour patients. Oncol Lett. 2012;4(6):1247-53.

320. Giil LM, Midttun O, Refsum H, Ulvik A, Advani R, Smith AD, et al. Kynurenine pathway metabolites in Alzheimer's disease. J Alzheimers Dis. 2017;60(2):495-504.
321. Smith JB, Cusumano JC, Babbs CF. Quantitative effects of iron chelators on hydroxyl radical production by the superoxide-driven fenton reaction. Free Radic Res Commun. 1990;8(2):101-6.
322. Garcia-Beltran O, Mena NP, Aguirre P, Barriga-Gonzalez G, Galdamez A, Nagles E, et al. Development of an iron-selective antioxidant probe with protective effects on neuronal function. PLoS One. 2017;12(12):e0189043.
323. Gutteridge JM. Reduction of low molecular mass iron by reducing molecules present in plasma and the protective action of caeruloplasmin. J Trace Elem Electrolytes Health Dis. 1991;5(4):279-81.
324. Crichton RR, Charloteaux-Wauters M. Iron transport and storage. Eur J Biochem. 1987;164(3):485-506.
325. Harris ED. Copper as a cofactor and regulator of copper, zinc superoxide-dismutase. J Nutr. 1992;122(3):636-40.
326. McLimans KE, Clark BE, Plagman A, Pappas C, Klinedinst B, Anatharam V, et al. Is cerebrospinal fluid superoxide dismutase 1 a biomarker of tau but not amyloid-induced neurodegeneration in Alzheimer's disease? Antioxid Redox Signal. 2019;31(8):572-8.
327. Kish SJ, Bergeron C, Rajput A, Dozic S, Mastrogiacomo F, Chang LJ, et al. Brain cytochrome oxidase in Alzheimer's disease. J Neurochem. 1992;59(2):776-9.
328. Kenney PM, Bennett JP, Jr. Alzheimer's disease frontal cortex mitochondria show a loss of individual respiratory proteins but preservation of respiratory supercomplexes. Int J Alzheimers Dis. 2019;2019:4814783.
329. Prakash R, Gandotra S, Singh LK, Das B, Lakra A. Rapid resolution of delusional parasitosis in pellagra with niacin augmentation therapy. Gen Hosp Psychiat. 2008;30(6):581-4.
330. Wakade C, Chong R. A novel treatment target for Parkinson's disease. Journal of the Neurological Sciences. 2014;347(1-2):34-8.
331. Gasperi V, Sibilano M, Savini I, Catani MV. Niacin in the central nervous system: An update of biological aspects and clinical applications. Int J Mol Sci. 2019;20(4).
332. Alisky JM. Niacin improved rigidity and bradykinesia in a Parkinson's disease patient but also caused unacceptable nightmares and skin rash - A case report. Nutr Neurosci. 2005;8(5-6):327-9.
333. Kaddurah-Daouk R, Zhu H, Sharma S, Bogdanov M, Rozen SG, Matson W, et al. Alterations in metabolic pathways and networks in Alzheimer's disease. Transl Psychiatry. 2013;3:e244.
334. Santpere G, Garcia-Esparcia P, Andres-Benito P, Lorente-Galdos B, Navarro A, Ferrer I. Transcriptional network analysis in frontal cortex in Lewy body diseases with focus on dementia with Lewy bodies. Brain Pathol. 2018;28(3):315-33.
335. Wang Q, Li WX, Dai SX, Guo YC, Han FF, Zheng JJ, et al. Meta-Analysis of Parkinson's Disease and Alzheimer's Disease Revealed Commonly Impaired Pathways and Dysregulation of NRF2-Dependent Genes. J Alzheimers Dis. 2017;56(4):1525-39.
336. Graham SF, Pan X, Yilmaz A, Macias S, Robinson A, Mann D, et al. Targeted biochemical profiling of brain from Huntington's disease patients reveals novel metabolic pathways of interest. Biochim Biophys Acta Mol Basis Dis. 2018;1864(7):2430-7.
337. Schrag M, Mueller C, Oyoyo U, Smith MA, Kirsch WM. Iron, zinc and copper in the Alzheimer's disease brain: a quantitative meta-analysis. Some insight on the influence of citation bias on scientific opinion. Prog Neurobiol. 2011;94:296-306.
338. Xu J, Church SJ, Patassini S, Begley P, Waldvogel HJ, Curtis MA, et al. Evidence for widespread, severe brain copper deficiency in Alzheimer's dementia Metallomics. 2017;9:1106-19.
339. Deibel M, Ehmann W, Markesbery W. Copper, iron and zinc imbalances in severely degenerated brain regions in Alzheimer's disease: possible relation to oxidative stress. J Neurol Sci. 1996;143:137-42.
340. Plantin L, Lying-Tunell U, Kristensson K. Trace elements in the human central nervous system studied with neutron activation analysis. Biol Trace Elem Res. 1987;13:69-75.
341. Oliveri V. Toward the discovery and development of effective modulators of alpha-synuclein amyloid aggregation. Eur J Med Chem. 2019;167:10-36.
342. Rocha EM, De Miranda B, Sanders LH. Alpha-synuclein: Pathology, mitochondrial dysfunction and neuroinflammation in Parkinson's disease. Neurobiol Dis. 2018;109(Pt B):249-57.
343. Cerri S, Blandini F. Role of autophagy in Parkinson's Disease. Curr Med Chem. 2019;26(20):3702-18.
344. Raza C, Anjum R, Shakeel NUA. Parkinson's disease: Mechanisms, translational models and management strategies. Life Sci. 2019;226:77-90.
345. Xicoy H, Wieringa B, Martens GJM. The role of lipids in Parkinson's Disease. Cells. 2019;8(1).
346. Bjorklund G, Stejskal V, Urbina MA, Dadar M, Chirumbolo S, Mutter J. Metals and Parkinson's disease: Mechanisms and biochemical processes. Curr Med Chem. 2018;25(19):2198-214.
347. Reetz K, Romanzetti S, Dogan I, Sass C, Werner CJ, Schiefer J, et al. Increased brain tissue sodium concentration in Huntington's Disease - a sodium imaging study at 4 T. Neuroimage. 2012;63(1):517-24.
348. Scholefield M, Church SJ, Xu J, Kassab S, Gardiner NJ, Roncaroli F, et al. Evidence that levels of nine essential metals in post-mortem human-Alzheimer's-brain and ex vivo rat-brain tissues are unaffected by differences in post-mortem delay, age, disease staging, and brain bank location. Metallomics. 2020.
349. Uitti RJ, Rajput AH, Rozdilsky B, Bickis M, Wollin T, Yuen WK. Regional metal concentrations in Parkinson's disease, other chronic neurological diseases, and control brains. Can J Neurol Sci. 1989;16(3):310-4.

350. Association LBD. Recognizing when it is not Parkinson's or Alzheimer's disease 2014 [
351. Xu J, Patassini S, Rustogi N, Riba-Garcia I, Hale BD, Phillips AM, et al. Regional protein expression in human Alzheimer's brain correlates with disease severity. Commun Biol. 2019;2:43.
352. Winterbourn CC. Toxicity of iron and hydrogen peroxide: the Fenton reaction. Toxicol Lett. 1995;82-83:969-74.
353. Bisaglia M, Bubacco L. Copper ions and parkinson's disease: Why is homeostasis so relevant? Biomolecules. 2020;10(2).
354. Dias V, Junn E, Mouradian MM. The role of oxidative stress in Parkinson's disease. J Parkinsons Dis. 2013;3(4):461-91.
355. Trist BG, Davies KM, Cottam V, Genoud S, Ortega R, Roudeau S, et al. Amyotrophic lateral sclerosis-like superoxide dismutase 1 proteinopathy is associated with neuronal loss in Parkinson's disease brain. Acta Neuropathol. 2017;134(1):113-27.
356. Trist BG, Fifita JA, Freckleton SE, Hare DJ, Lewis SJG, Halliday GM, et al. Accumulation of dysfunctional SOD1 protein in Parkinson's disease is not associated with mutations in the SOD1 gene. Acta Neuropathol. 2018;135(1):155-6.
357. Kumar A, Ganini D, Mason RP. Role of cytochrome c in alpha-synuclein radical formation: implications of alpha-synuclein in neuronal death in Maneb- and paraquat-induced model of Parkinson's disease. Mol Neurodegener. 2016;11(1):70.
358. Perl DP, Olanow CW. The neuropathology of manganese-induced Parkinsonism. J Neuropathol Exp Neurol. 2007;66(8):675-82.
359. Koller WC, Lyons KE, Truly W. Effect of levodopa treatment for parkinsonism in welders: A double-blind study. Neurology. 2004;62(5):730-3.
360. Brouillet EP, Shinobu L, McGarvey U, Hochberg F, Beal MF. Manganese injection into the rat striatum produces excitotoxic lesions by impairing energy metabolism. Exp Neurol. 1993;120(1):89-94.
361. Cordova FM, Aguiar AS, Jr., Peres TV, Lopes MW, Goncalves FM, Pedro DZ, et al. Manganese-exposed developing rats display motor deficits and striatal oxidative stress that are reversed by Trolox. Arch Toxicol. 2013;87(7):1231-44.
362. Dusek P, Roos PM, Litwin T, Schneider SA, Flaten TP, Aaseth J. The neurotoxicity of iron, copper and manganese in Parkinson's and Wilson's diseases. J Trace Elem Med Biol. 2015;31:193-203.
363. Kawamata H, Manfredi G. Different regulation of wild-type and mutant Cu, Zn superoxide dismutase localization in mammalian mitochondria. Hum Mol Genet. 2008;17(21):3303-17.
364. Hall H, Reyes S, Landeck N, Bye C, Leanza G, Double K, et al. Hippocampal Lewy pathology and cholinergic dysfunction are associated with dementia in Parkinson's disease. Brain. 2014;137(Pt 9):2493-508.
365. Liu Z, Jing Y, Yin J, Mu J, Yao T, Gao L. Downregulation of thioredoxin reductase 1 expression in the substantia nigra pars compacta of Parkinson's disease mice. Neural Regen Res. 2013;8(35):3275-83.
366. Oyanagi K, Kawakami E, Kikuchi-Horie K, Ohara K, Ogata K, Takahama S, et al. Magnesium deficiency over generations in rats with special references to the pathogenesis of the Parkinsonism-dementia complex and amyotrophic lateral sclerosis of Guam. Neuropathology. 2006;26(2):115-28.
367. La Piana G, Gorgoglione V, Laraspata D, Marzulli D, Lofrumento NE. Effect of magnesium ions on the activity of the cytosolic NADH/cytochrome c electron transport system. FEBS J. 2008;275(24):6168-79.
368. Shah NH, Aizenman E. Voltage-gated potassium channels at the crossroads of neuronal function, ischemic tolerance, and neurodegeneration. Transl Stroke Res. 2014;5(1):38-58.
369. Jellinger K, Paulus W, Grundke-Iqbal I, Riederer P, Youdim MB. Brain iron and ferritin in Parkinson's and Alzheimer's diseases. J Neural Transm Park Dis Dement Sect. 1990;2(4):327-40.
370. Loeffler DA, Connor JR, Juneau PL, Snyder BS, Kanaley L, DeMaggio AJ, et al. Transferrin and iron in normal, Alzheimer's disease, and Parkinson's disease brain regions. J Neurochem. 1995;65(2):710-24.
371. Galazka-Friedman J, Bauminger ER, Friedman A, Barcikowska M, Hechel D, Nowik I. Iron in parkinsonian and control substantia nigra--a Mossbauer spectroscopy study. Mov Disord. 1996;11(1):8-16.
372. Friedman A, Galazka-Friedman J, Koziorowski D. Iron as a cause of Parkinson disease - a myth or a well established hypothesis? Parkinsonism Relat Disord. 2009;15 Suppl 3:S212-4.
373. Dashtipour K, Liu M, Kani C, Dalaie P, Obenaus A, Simmons D, et al. Iron accumulation is not homogenous among patients with Parkinson's disease. Parkinsons Dis. 2015;2015:324843.
374. Prince MW, A.; Guerchet, M.; Ali, G. C.; Wu, Y. T.; Prima, M. World Alzheimer Report 2015 The global impact of dementia an analysis of prevalence, incidence, cost and trends. 2014.
375. Statistics OfN. Deaths registered in England and Wales: 2018. 2019:1-15.
376. Mehta D, Jackson R, Paul G, Shi J, Sabbagh M. Why do trials for Alzheimer's disease drugs keep failing? A discontinued drug perspective for 2010-2015. Expert Opin Inv Drug. 2017;26(6):735-9.
377. Ansoleaga B, Jove M, Schluter A, Garcia-Esparcia P, Moreno J, Pujol A, et al. Deregulation of purine metabolism in Alzheimer's disease. Neurobiol Aging. 2015;36(1):68-80.
378. Abolhassani N, Leon J, Sheng Z, Oka S, Hamasaki H, Iwaki T, et al. Molecular pathophysiology of impaired glucose metabolism, mitochondrial dysfunction, and oxidative DNA damage in Alzheimer's disease brain. Mech Ageing Dev. 2017;161(Pt A):95-104.
379. Toledo JB, Arnold M, Kastenmuller G, Chang R, Baillie RA, Han X, et al. Metabolic network failures in Alzheimer's disease: A biochemical road map. Alzheimers Dement. 2017;13(9):965-84.

380. Beach TG. Alzheimer's disease and the "valley of death": not enough guidance from human brain tissue? J Alzheimers Dis. 2013;33:S219-S33.
381. Braak H, Braak E. Staging of Alzheimer's disease-related neurofibrillary changes. Neurobiol Aging. 1995;16:271-84.
382. Patassini S, Begley P, Reid SJ, Xu J, Church SJ, Curtis M, et al. Identification of elevated urea as a severe, ubiquitous metabolic defect in the brain of patients with Huntington's disease. Biochem Biophys Res Commun. 2015;468(1-2):161-6.
383. Cleeland C, Pipingas A, Scholey A, White D. Neurochemical changes in the aging brain: A systematic review. Neurosci Biobehav Rev. 2019;98:306-19.
384. Sijens PE, den Heijer T, Origgi D, Vermeer SE, Breteler MM, Hofman A, et al. Brain changes with aging: MR spectroscopy at supraventricular plane shows differences between women and men. Radiology. 2003;226(3):889-96.
385. Kochunov P, Coyle T, Lancaster J, Robin DA, Hardies J, Kochunov V, et al. Processing speed is correlated with cerebral health markers in the frontal lobes as quantified by neuroimaging. Neuroimage. 2010;49(2):1190-9.
386. Ross AJ, Sachdev PS, Wen W, Valenzuela MJ, Brodaty H. Cognitive correlates of 1H MRS measures in the healthy elderly brain. Brain Res Bull. 2005;66(1):9-16.
387. Durrenberger PF, Fernando S, Kashefi SN, Ferrer I, Hauw JJ, Seilhean D, et al. Effects of antemortem and postmortem variables on human brain mRNA quality: a BrainNet Europe study. J Neuropathol Exp Neurol. 2010;69(1):70-81.
388. Ervin JF, Heinzen EL, Cronin KD, Goldstein D, Szymanski MH, Burke JR, et al. Postmortem delay has minimal effect on brain RNA integrity. J Neuropathol Exp Neurol. 2007;66(12):1093-9.
389. White K, Yang P, Li L, Farshori A, Medina AE, Zielke HR. Effect of postmortem interval and years in storage on RNA quality of tissue at a repository of the NIH Neurobiobank. Biopreserv Biobank. 2018;16(2):148-57.
390. Robinson AC, Palmer L, Love S, Hamard M, Esiri M, Ansorge O, et al. Extended post-mortem delay times should not be viewed as a deterrent to the scientific investigation of human brain tissue: a study from the Brains for Dementia Research Network Neuropathology Study Group, UK. Acta Neuropathol. 2016;132(5):753-5.
391. Gonzalez-Riano C, Tapia-Gonzalez S, Garcia A, Munoz A, DeFelipe J, Barbas C. Metabolomics and neuroanatomical evaluation of post-mortem changes in the hippocampus. Brain Struct Funct. 2017;222(6):2831-53.
392. Kovacs Z, Kekesi KA, Bobest M, Torok T, Szilagyi N, Szikra T, et al. Post mortem degradation of nucleosides in the brain: comparison of human and rat brains for estimation of in vivo concentration of nucleosides. J Neurosci Methods. 2005;148(1):88-93.
393. Roubein IF, Embree LJ. Post mortem stability of catecholamines in discrete regions of rat brain. Res Commun Chem Pathol Pharmacol. 1979;23(1):143-53.
394. Siew LK, Love S, Dawbarn D, Wilcock GK, Allen SJ. Measurement of pre- and post-synaptic proteins in cerebral cortex: effects of post-mortem delay. J Neurosci Methods. 2004;139(2):153-9.
395. Machaalani R, Gozal E, Berger F, Waters KA, Dematteis M. Effects of post-mortem intervals on regional brain protein profiles in rats using SELDI-TOF-MS analysis. Neurochemistry International. 2010;57(6):655-61.
396. Mosconi L. Glucose metabolism in normal aging and Alzheimer's disease: Methodological and physiological considerations for PET studies. Clin Transl Imaging. 2013;1(4).
397. Mosconi L, Pupi A, De Leon MJ. Brain glucose hypometabolism and oxidative stress in preclinical Alzheimer's disease. Ann N Y Acad Sci. 2008;1147:180-95.
398. Robinson AC, Roncaroli F, Chew-Graham S, Davidson YS, Minshull J, Horan MA, et al. The contribution of vascular pathology toward cognitive impairment in older individuals with intermediate Braak stage tau pathology. J Alzheimers Dis. 2020.
399. Malek-Ahmadi M, Perez SE, Chen K, Mufson EJ. Braak stage, Cerebral Amyloid Angiopathy, and cognitive decline in early Alzheimer's disease. J Alzheimers Dis. 2020;74(1):189-97.
400. Schuff N, Capizzano AA, Du AT, Amend DL, O'Neill J, Norman D, et al. Different patterns of N-acetylaspartate loss in subcortical ischemic vascular dementia and AD. Neurology. 2003;61(3):358-64.
401. Glodzik L, Sollberger M, Gass A, Gokhale A, Rusinek H, Babb JS, et al. Global N-acetylaspartate in normal subjects, mild cognitive impairment and Alzheimer's disease patients. J Alzheimers Dis. 2015;43(3):939-47.
402. Scholefield M, Church SJ, Xu J, Patassini S, Hooper NM, Unwin RD, et al. Substantively Lowered Levels of Pantothenic Acid (Vitamin B5) in Several Regions of the Human Brain in Parkinson's Disease Dementia. Metabolites. 2021;11(9).
403. Xu J, Patassini S, Begley P, Church S, Waldvogel HJ, Faull RLM, et al. Cerebral deficiency of vitamin B5 (d-pantothenic acid; pantothenate) as a potentially-reversible cause of neurodegeneration and dementia in sporadic Alzheimer's disease. Biochem Biophys Res Commun. 2020;527(3):676-81.
404. Patassini S, Begley P, Xu J, Church SJ, Kureishy N, Reid SJ, et al. Cerebral Vitamin B5 (D-Pantothenic Acid) Deficiency as a Potential Cause of Metabolic Perturbation and Neurodegeneration in Huntington's Disease. Metabolites. 2019;9(6).
405. Hely MA, Reid WG, Adena MA, Halliday GM, Morris JG. The Sydney multicenter study of Parkinson's disease: the inevitability of dementia at 20 years. Mov Disord. 2008;23(6):837-44.
406. McColgan P, Tabrizi SJ. Huntington's disease: a clinical review. Eur J Neurol. 2018;25(1):24-34.
407. Cummings J. The role of neuropsychiatric symptoms in research diagnostic criteria for neurodegenerative diseases. Am J Geriatr Psychiatry. 2020.

408. Fifel K, Videnovic A. Circadian and sleep dysfunctions in neurodegenerative disorders - an update. Front Neurosci. 2020;14:627330.
409. Moon Y, Sung J, An R, Hernandez ME, Sosnoff JJ. Gait variability in people with neurological disorders: A systematic review and meta-analysis. Hum Mov Sci. 2016;47:197-208.
410. Ding W, Ding LJ, Li FF, Han Y, Mu L. Neurodegeneration and cognition in Parkinson's disease: a review. Eur Rev Med Pharmacol Sci. 2015;19(12):2275-81.
411. Mestre TA, Bachoud-Levi AC, Marinus J, Stout JC, Paulsen JS, Como P, et al. Rating scales for cognition in Huntington's disease: Critique and recommendations. Mov Disord. 2018;33(2):187-95.
412. Handley RR, Reid SJ, Brauning R, Maclean P, Mears ER, Fourie I, et al. Brain urea increase is an early Huntington's disease pathogenic event observed in a prodromal transgenic sheep model and HD cases. Proc Natl Acad Sci U S A. 2017;114(52):E11293-E302.
413. Hayflick SJ. Defective pantothenate metabolism and neurodegeneration. Biochem Soc Trans. 2014;42(4):1063-8.
414. Lee JH, Ahn SY, Lee HA, Won KS, Chang HW, Oh JS, et al. Dietary intake of pantothenic acid is associated with cerebral amyloid burden in patients with cognitive impairment. Food Nutr Res. 2018;62.
415. Baldini F, Hertel J, Sandt E, Thinnes CC, Neuberger-Castillo L, Pavelka L, et al. Parkinson's disease-associated alterations of the gut microbiome predict disease-relevant changes in metabolic functions. BMC Biol. 2020;18(1):62.
416. Vascellari S, Palmas V, Melis M, Pisanu S, Cusano R, Uva P, et al. Gut microbiota and metabolome alterations associated with Parkinson's disease. mSystems. 2020;5(5).
417. Willkommen D, Lucio M, Moritz F, Forcisi S, Kanawati B, Smirnov KS, et al. Metabolomic investigations in cerebrospinal fluid of Parkinson's disease. PLoS One. 2018;13(12):e0208752.
418. Tang BL. Glucose, glycolysis, and neurodegenerative diseases. J Cell Physiol. 2020;235(11):7653-62.
419. Foltynie T. Glycolysis as a therapeutic target for Parkinson's disease. Lancet Neurol. 2019;18(12):1072-4.
420. Peppard RF, Martin WR, Carr GD, Grochowski E, Schulzer M, Guttman M, et al. Cerebral glucose metabolism in Parkinson's disease with and without dementia. Arch Neurol. 1992;49(12):1262-8.
421. Bohnen NI, Minoshima S, Giordani B, Frey KA, Kuhl DE. Motor correlates of occipital glucose hypometabolism in Parkinson's disease without dementia. Neurology. 1999;52(3):541-6.
422. Selnes P, Stav AL, Johansen KK, Bjornerud A, Coello C, Auning E, et al. Impaired synaptic function is linked to cognition in Parkinson's disease. Ann Clin Transl Neurol. 2017;4(10):700-13.
423. Fitzgerald E, Murphy S, Martinson HA. Alpha-Synuclein Pathology and the Role of the Microbiota in Parkinson's Disease. Front Neurosci. 2019;13:369.
424. Mulak A, Bonaz B. Brain-gut-microbiota axis in Parkinson's disease. World J Gastroenterol. 2015;21(37):10609-20.
425. Van Den Berge N, Ferreira N, Gram H, Mikkelsen TW, Alstrup AKO, Casadei N, et al. Evidence for bidirectional and trans-synaptic parasympathetic and sympathetic propagation of alpha-synuclein in rats. Acta Neuropathol. 2019;138(4):535-50.
426. Scheperjans F, Derkinderen P, Borghammer P. The Gut and Parkinson's Disease: Hype or Hope? J Parkinsons Dis. 2018;8(s1):S31-S9.
427. Braak H, de Vos RA, Bohl J, Del Tredici K. Gastric alpha-synuclein immunoreactive inclusions in Meissner's and Auerbach's plexuses in cases staged for Parkinson's disease-related brain pathology. Neurosci Lett. 2006;396(1):67-72.
428. Hustad E, Aasly JO. Clinical and Imaging Markers of Prodromal Parkinson's Disease. Front Neurol. 2020;11:395.
429. Gellersen HM, Guo CC, O'Callaghan C, Tan RH, Sami S, Hornberger M. Cerebellar atrophy in neurodegeneration-a meta-analysis. J Neurol Neurosurg Psychiatry. 2017;88(9):780-8.
430. Wu T, Hallett M. The cerebellum in Parkinson's disease. Brain. 2013;136(Pt 3):696-709.
431. Scholefield M, Church SJ, Xu J, Patassini S, Roncaroli F, Hooper NM, et al. Severe and regionally-widespread increases in tissue urea in the human brain represent a novel finding of pathogenic potential in Parkinson's disease dementia. 2021.
432. Erkkinen MG, Kim MO, Geschwind MD. Clinical neurology and epidemiology of the major neurodegenerative diseases. Cold Spring Harb Perspect Biol. 2018;10(4).
433. Jellinger KA. Is Braak staging valid for all types of Parkinson's disease? Journal of Neural Transmission. 2019;126(4):423-31.
434. Walker L, Stefanis L, Attems J. Clinical and neuropathological differences between Parkinson's disease, Parkinson's disease dementia and dementia with Lewy bodies - current issues and future directions. J Neurochem. 2019;150(5):467-74.
435. Irwin DJ, Lee VM, Trojanowski JQ. Parkinson's disease dementia: convergence of alpha-synuclein, tau and amyloid-beta pathologies. Nat Rev Neurosci. 2013;14(9):626-36.
436. Jellinger KA, Korczyn AD. Are dementia with Lewy bodies and Parkinson's disease dementia the same disease? BMC Med. 2018;16(1):34.
437. Perl DP, Olanow CW, Calne D. Alzheimer's disease and Parkinson's disease: distinct entities or extremes of a spectrum of neurodegeneration? Ann Neurol. 1998;44(3 Suppl 1):S19-31.
438. Troisi J, Landolfi A, Vitale C, Longo K, Cozzolino A, Squillante M, et al. A metabolomic signature of treated and drug-naive patients with Parkinson's disease: a pilot study. Metabolomics. 2019;15(6):90.

439. McKeith IG, Dickson DW, Lowe J, Emre M, O'Brien JT, Feldman H, et al. Diagnosis and management of dementia with Lewy bodies: third report of the DLB Consortium. Neurology. 2005;65(12):1863-72.
440. Sterns RH, Silver SM, Hix JK. Urea for hyponatremia? Kidney Int. 2015;87(2):268-70.
441. Colton CA, Mott RT, Sharpe H, Xu Q, Van Nostrand WE, Vitek MP. Expression profiles for macrophage alternative activation genes in AD and in mouse models of AD. J Neuroinflammation. 2006;3:27.
442. Polis B, Srikanth KD, Elliott E, Gil-Henn H, Samson AO. L-Norvaline Reverses Cognitive Decline and Synaptic Loss in a Murine Model of Alzheimer's Disease. Neurotherapeutics. 2018;15(4):1036-54.
443. Kiyofuji K, Kurauchi Y, Hisatsune A, Seki T, Mishima S, Katsuki H. A natural compound macelignan protects midbrain dopaminergic neurons from inflammatory degeneration via microglial arginase-1 expression. Eur J Pharmacol. 2015;760:129-35.
444. Virarkar M, Alappat L, Bradford PG, Awad AB. L-arginine and nitric oxide in CNS function and neurodegenerative diseases. Crit Rev Food Sci Nutr. 2013;53(11):1157-67.
445. Bensemain F, Hot D, Ferreira S, Dumont J, Bombois S, Maurage CA, et al. Evidence for induction of the ornithine transcarbamylase expression in Alzheimer's disease. Mol Psychiatry. 2009;14(1):106-16.
446. Bernstein HG, Jager K, Dobrowolny H, Steiner J, Keilhoff G, Bogerts B, et al. Possible sources and functions of L-homoarginine in the brain: review of the literature and own findings. Amino Acids. 2015;47(9):1729-40.
447. Bernstein HG, Dobrowolny H, Keilhoff G, Steiner J. In human brain ornithine transcarbamylase (OTC) immunoreactivity is strongly expressed in a small number of nitrergic neurons. Metab Brain Dis. 2017;32(6):2143-7.
448. Nolfi-Donegan D, Braganza A, Shiva S. Mitochondrial electron transport chain: Oxidative phosphorylation, oxidant production, and methods of measurement. Redox Biol. 2020;37:101674.
449. Madeira VMC. Overview of Mitochondrial Bioenergetics. Methods Mol Biol. 2018;1782:1-6.
450. Ichida K, Hosoyamada M, Hosoya T, Endou H. Primary Metabolic and Renal Hyperuricemia. 2009. In: Genetic Diseases of the Kidney [Internet]. Academic Press; [651-60].
451. Engelborghs S, Marescau B, De Deyn PP. Amino acids and biogenic amines in cerebrospinal fluid of patients with Parkinson's disease. Neurochem Res. 2003;28(8):1145-50.
452. Sweeney MD, Sagare AP, Zlokovic BV. Blood-brain barrier breakdown in Alzheimer disease and other neurodegenerative disorders. Nat Rev Neurol. 2018;14(3):133-50.
453. Seifter JL, Samuels MA. Uremic encephalopathy and other brain disorders associated with renal failure. Semin Neurol. 2011;31(2):139-43.
454. Wang H, Huang B, Wang W, Li J, Chen Y, Flynn T, et al. High urea induces depression and LTP impairment through mTOR signalling suppression caused by carbamylation. EBioMedicine. 2019;48:478-90.
455. Gorisse L, Pietrement C, Vuiblet V, Schmelzer CE, Kohler M, Duca L, et al. Protein carbamylation is a hallmark of aging. Proc Natl Acad Sci U S A. 2016;113(5):1191-6.
456. Long J, Vela Parada X, Kalim S. Protein carbamylation in chronic kidney disease and dialysis. Adv Clin Chem. 2018;87:37-67.
457. Gallart-Palau X, Serra A, Lee BST, Guo X, Sze SK. Brain ureido degenerative protein modifications are associated with neuroinflammation and proteinopathy in Alzheimer's disease with cerebrovascular disease. J Neuroinflammation. 2017;14(1):175.
458. Guru KrishnaKumar V, Baweja L, Ralhan K, Gupta S. Carbamylation promotes amyloidogenesis and induces structural changes in Tau-core hexapeptide fibrils. Biochim Biophys Acta Gen Subj. 2018;1862(12):2590-604.
459. Vaziri ND. Oxidative stress in uremia: nature, mechanisms, and potential consequences. Semin Nephrol. 2004;24(5):469-73.
460. Yan MH, Wang X, Zhu X. Mitochondrial defects and oxidative stress in Alzheimer disease and Parkinson disease. Free Radic Biol Med. 2013;62:90-101.
461. Ganguly G, Chakrabarti S, Chatterjee U, Saso L. Proteinopathy, oxidative stress and mitochondrial dysfunction: cross talk in Alzheimer's disease and Parkinson's disease. Drug Des Devel Ther. 2017;11:797-810.
462. Butterfield DA, Halliwell B. Oxidative stress, dysfunctional glucose metabolism and Alzheimer disease. Nat Rev Neurosci. 2019;20(3):148-60.
463. Verdile G, Keane KN, Cruzat VF, Medic S, Sabale M, Rowles J, et al. Inflammation and oxidative stress: The molecular connectivity between insulin resistance, obesity, and Alzheimer's disease. Mediators Inflamm. 2015;2015:105828.
464. Scudamore O, Ciossek T. Increased oxidative stress exacerbates alpha-synuclein aggregation in vivo. J Neuropathol Exp Neurol. 2018;77(6):443-53.
465. Wang R, Wang Y, Qu L, Chen B, Jiang H, Song N, et al. Iron-induced oxidative stress contributes to alpha-synuclein phosphorylation and up-regulation via polo-like kinase 2 and casein kinase 2. Neurochem Int. 2019;125:127-35.
466. Toczylowska B, Zieminska E, Michalowska M, Chalimoniuk M, Fiszer U. Changes in the metabolic profiles of the serum and putamen in Parkinson's disease patients - In vitro and in vivo NMR spectroscopy studies. Brain Res. 2020;1748:147118.
467. Pesch B, Casjens S, Woitalla D, Dharmadhikari S, Edmondson DA, Zella MAS, et al. Impairment of motor function correlates with neurometabolite and brain iron alterations in Parkinson's disease. Cells. 2019;8(2).
468. Seidel K, Bouzrou M, Heidemann N, Kruger R, Schols L, den Dunnen WFA, et al. Involvement of the cerebellum in Parkinson disease and dementia with Lewy bodies. Ann Neurol. 2017;81(6):898-903.

469. Solano SM, Miller DW, Augood SJ, Young AB, Penney JB, Jr. Expression of alpha-synuclein, parkin, and ubiquitin carboxy-terminal hydrolase L1 mRNA in human brain: genes associated with familial Parkinson's disease. Ann Neurol. 2000;47(2):201-10.
470. Piao YS, Mori F, Hayashi S, Tanji K, Yoshimoto M, Kakita A, et al. Alpha-synuclein pathology affecting Bergmann glia of the cerebellum in patients with alpha-synucleinopathies. Acta Neuropathol. 2003;105(4):403-9.
471. Kuhl DE, Metter EJ, Riege WH, Markham CH. Patterns of cerebral glucose utilization in Parkinson's disease and Huntington's disease. Ann Neurol. 1984;15 Suppl:S119-25.
472. Borghammer P, Chakravarty M, Jonsdottir KY, Sato N, Matsuda H, Ito K, et al. Cortical hypometabolism and hypoperfusion in Parkinson's disease is extensive: probably even at early disease stages. Brain Struct Funct. 2010;214(4):303-17.
473. Garcia-Esparcia P, Hernandez-Ortega K, Ansoleaga B, Carmona M, Ferrer I. Purine metabolism gene deregulation in Parkinson's disease. Neuropathol Appl Neurobiol. 2015;41(7):926-40.
474. O'Gorman Tuura RL, Baumann CR, Baumann-Vogel H. Beyond dopamine: GABA, glutamate, and the axial symptoms of Parkinson disease. Front Neurol. 2018;9:806.
475. Kish SJ, Rajput A, Gilbert J, Rozdilsky B, Chang LJ, Shannak K, et al. Elevated gamma-aminobutyric acid level in striatal but not extrastriatal brain regions in Parkinson's disease: correlation with striatal dopamine loss. Ann Neurol. 1986;20(1):26-31.
476. Emir UE, Tuite PJ, Oz G. Elevated pontine and putamenal GABA levels in mild-moderate Parkinson disease detected by 7 tesla proton MRS. PLoS One. 2012;7(1):e30918.
477. Elmaki EEA, Gong T, Nkonika DM, Wang G. Examining alterations in GABA concentrations in the basal ganglia of patients with Parkinson's disease using MEGA-PRESS MRS. Jpn J Radiol. 2018;36(3):194-9.
478. Firbank MJ, Parikh J, Murphy N, Killen A, Allan CL, Collerton D, et al. Reduced occipital GABA in Parkinson disease with visual hallucinations. Neurology. 2018;91(7):e675-e85.
479. Ridel KR, Leslie ND, Gilbert DL. An updated review of the long-term neurological effects of galactosemia. Pediatr Neurol. 2005;33(3):153-61.
480. Hemmati-Dinarvand M, Saedi S, Valilo M, Kalantary-Charvadeh A, Alizadeh Sani M, Kargar R, et al. Oxidative stress and Parkinson's disease: conflict of oxidant-antioxidant systems. Neurosci Lett. 2019;709:134296.
481. Subramaniam SR, Chesselet MF. Mitochondrial dysfunction and oxidative stress in Parkinson's disease. Prog Neurobiol. 2013;106-107:17-32.
482. Trist BG, Hare DJ, Double KL. Oxidative stress in the aging substantia nigra and the etiology of Parkinson's disease. Aging Cell. 2019;18(6):e13031.
483. Tobore TO. On the central role of mitochondria dysfunction and oxidative stress in Alzheimer's disease. Neurol Sci. 2019;40(8):1527-40.
484. Tonnies E, Trushina E. Oxidative stress, synaptic dysfunction, and Alzheimer's disease. J Alzheimers Dis. 2017;57(4):1105-21.
485. Wypijewska A, Galazka-Friedman J, Bauminger ER, Wszolek ZK, Schweitzer KJ, Dickson DW, et al. Iron and reactive oxygen species activity in parkinsonian substantia nigra. Parkinsonism Relat Disord. 2010;16(5):329-33.
486. Genoud S, Senior AM, Hare DJ, Double KL. Meta-analysis of copper and iron in Parkinson's disease brain and biofluids. Mov Disord. 2020;35(4):662-71.
487. Zecca L, Fariello R, Riederer P, Sulzer D, Gatti A, Tampellini D. The absolute concentration of nigral neuromelanin, assayed by a new sensitive method, increases throughout the life and is dramatically decreased in Parkinson's disease. FEBS Lett. 2002;510(3):216-20.
488. Fasano M, Bergamasco B, Lopiano L. Modifications of the iron-neuromelanin system in Parkinson's disease. J Neurochem. 2006;96(4):909-16.
489. Bishop GM, Dang TN, Dringen R, Robinson SR. Accumulation of non-transferrin-bound iron by neurons, astrocytes, and microglia. Neurotox Res. 2011;19(3):443-51.
490. Gerlach M, Double KL, Youdim MB, Riederer P. Potential sources of increased iron in the substantia nigra of parkinsonian patients. J Neural Transm Suppl. 2006(70):133-42.
491. Castellani RJ, Siedlak SL, Perry G, Smith MA. Sequestration of iron by Lewy bodies in Parkinson's disease. Acta Neuropathol. 2000;100(2):111-4.
492. Meles SK, Renken RJ, Pagani M, Teune LK, Arnaldi D, Morbelli S, et al. Abnormal pattern of brain glucose metabolism in Parkinson's disease: replication in three European cohorts. Eur J Nucl Med Mol Imaging. 2020;47(2):437-50.
493. Lyoo CH, Jeong Y, Ryu YH, Rinne JO, Lee MS. Cerebral glucose metabolism of Parkinson's disease patients with mild cognitive impairment. Eur Neurol. 2010;64(2):65-73.
494. Park JS, Davis RL, Sue CM. Mitochondrial dysfunction in Parkinson's disease: New mechanistic insights and therapeutic perspectives. Curr Neurol Neurosci Rep. 2018;18(5):21.
495. Ryan BJ, Hoek S, Fon EA, Wade-Martins R. Mitochondrial dysfunction and mitophagy in Parkinson's: from familial to sporadic disease. Trends Biochem Sci. 2015;40(4):200-10.
496. Cummings JL, Silverman D, Small G, Phelps M. The role of positron emission tomography in the diagnosis of Alzheimer's disease. J Am Geriatr Soc. 2004;52(3):467-8; author reply 8-9.
497. Kleinridders A, Ferris HA, Reyzer ML, Rath M, Soto M, Manier ML, et al. Regional differences in brain glucose metabolism determined by imaging mass spectrometry. Mol Metab. 2018;12:113-21.

498. Su J, Huang Q, Ren S, Xie F, Zhai Y, Guan Y, et al. Altered brain glucose metabolism assessed by (18)F-FDG PET imaging is associated with the cognitive impairment of CADASIL. Neuroscience. 2019;417:35-44.

Supplementary Material

Supplementary Table 1 – Search Terms

Disease Term	AND	Analyte Term
Alzheimer's		Metals
Alzheimer disease		Metallomics
Alzheimer's disease		Metallome
Alzheimer dementia disease		Calcium
Parkinson's		Ceruloplasmin
Parkinson disease		Copper
Parkinson's disease		Iron
Parkinson's disease dementia		Magnesium
Huntington's		Manganese
Huntington disease		Potassium
Huntington's disease		Selenium
Dementia with Lewy bodies		Sodium
Lewy body dementia		Zinc
DLB		
Dementia		Metabolites
		Metabolomics
		Metabolome
		6-phosphogluconate
		Acetyl CoA
		Aconitase
		Adenine
		Adenosine
		Alanine
		Arginine
		Arginosuccinate
		Arginosuccinic acid

Asparagine
Aspartate
Aspartic acid
Caffeine
Carnitine
Citrate
Citric acid
Citrulline
Creatine
Creatinine
Cysteine
Ethanolamine
Fructose
Fructose-6-phosphate
Fumarate
Fumaric acid
Glucono-1,5-lactone-6-phosphate
Glucose
Glucose-6-phosphate
Glutamate
Glutamic Acid
Glutamine
Glycine
GSH
GSSG
Guanine
Guanosine
Histidine
Homocitrulline
Homocysteine

Homovanillate
Homovanillic acid
Hypoxanthine
Indoleacetate
Indolacetic acid
Inosine
Isoleucine
Kynurenic Acid
Kynurenine
Lactate
Lactic acid
Leucine
Lysine
Malate
Malic acid
Mannitol
Mannose
Methionine
NADP+
NADPH
Ornithine
Oxaloacetate
Oxaloacetic acid
Paraxanthine
Phenylalanine
Phosphoserine
Proline
Pyruvate
Ribose-5-phosphate
Sarcosine

Serine
Sorbitol
Succinate
Succinic acid
Succinyl-CoA
Sucrose
Taurine
Theophylline
Threonine
Tryptophan
Tyrosine
Urea
Uric Acid
Valine
Xanthine
Xylulose-5-phosphate
α-aminoadipic acid
α-aminobutyric acid
α-ketoglutarate
γ glutamyl-cysteine

Supplementary Table 2A – Metals in AD

Metal	Source	Change	Tissue	Region	N (cases v controls)	Method
Calcium	Corrigan et al., 1993	**Decreased**	Brain	HP	12 v 12	ICP–MS
	Xu et al., 2017	**Increased** No change	Brain	ENT HP, MTG, SC, MC, CG, CB	9 v 13	ICP–MS
	Xu et al., 2018	No change	Plasma	N/A	42 v 43	ICP–MS
Ceruloplasmin	Park et al., 2013	**Increased**	Serum	N/A	89 v 118	Immunoassay
	Rembach et al., 2013	No change	Serum	N/A	186 v 695	Immunoassay
	Torsdottir et al., 2011	No change	Serum	N/A	41 v 41	Immunoassay
	Loeffler et al., 1996	**Increased** No change	Brain	HP, ENT, FC, PUT CN, TC, PC, CB	12 v 13	ELISA
	Snaedal et al., 1998	No change	Plasma	N/A	44 v 44	Immunoassay
Copper	Agarwal et al., 2008	**Increased**	Serum	N/A	50 v 30	Colorimetric Assay
	Akatsu et al., 2012	**Decreased**	Brain	HP, AMG	18 v 16	ICP–MS
	Baum et al., 2010	No change	Serum	N/A	44 v 41	ICP–MS
	Boll et al., 2008	No change	CSF	N/A	8 v 11	AAS
	Brewer et al., 2010a	**Increased**	Serum	N/A	28 v 29	AAS
	Corrigan et al., 1993	**Decreased**	Brain	HP	12 v 12	ICP–MS
	Deibel et al., 1996	**Decreased** No change	Brain	HP, AMG SG, MTG, IPL, CB	10 v 11	INAA

	Giacoppo et al., 2014	**Decreased**	Plasma	N/A	12 v 23	ICP–MS
	Gonzalez et al., 1999	**Increased**	Serum	N/A	51 v 40	AAS
	Gonzalez-Dominguez et al., 2014	**Increased**	Serum	N/A	25 v 25	ICP–MS
	Koc et al., 2015	No change	Serum	N/A	41 v 33	ICP–MS
	Loeffler et al., 1996	**Increased** No change	Brain	FC CN, PUT, SN	12 v 13	AAS
	Molina et al., 1998a	No change No change	CSF Serum	N/A	26 v 28	AAS
	Mueller et al., 2012	**Decreased**	Serum	N/A	19 v 19	AAS
	Park et al., 2013	**Increased**	Serum	N/A	89 v 118	ICP–MS
	Religa et al., 2006	No change	Brain	NC	10 v 14	ICP–MS
	Rembach et al., 2013	No change	Serum	N/A	186 v 695	ICP–MS
	Shere et al., 2018	**Decreased**	Serum	N/A	44 v 52	Colorimetric Assay
	Snaedal et al., 1998	No change	Plasma	N/A	44 v 44	AAS
	Squitti et al., 2002	**Increased**	Serum	N/A	79 v 76	ICP–MS
	Szabo et al., 2016	No change	Brain	FC	13 v 13	ICP–MS
	Tong et al., 2014	No change	Plasma	N/A	40 v 10	ICP–MS
	Vaz et al., 2018	**Increased**	Plasma	N/A	32 v 32	ICP–MS
	Vural et al., 2010	**Decreased**	Plasma	N/A	50 v 50	AAS
	Wang et al., 2015	**Increased**	Serum	N/A	83 v 83	ICP–MS
	Xu et al., 2017	**Decreased**	Brain	HP, ENT, MTG, SC, MC, CG, CB	9 v 13	ICP–MS

	Xu et al., 2018	No change	Plasma	N/A	42 v 43	ICP–MS
Iron	Akatsu et al., 2012	No change Increased	Brain	HP AMG	18 v 16	ICP–MS
	Baum et al., 2010	Decreased	Serum	N/A	44 v 41	ICP–MS
	Corrigan et al., 1993	Decreased	Brain	HP	12 v 13	ICP–MS
	Deibel et al., 1996	Increased No change	Brain	HP AMG, SG, MTG, IPL, CB	10 v 11	INAA
	Gonzalez-Dominguez et al., 2014	Increased	Serum	N/A	25 v 25	ICP–MS
	Koc et al., 2015	No change	Serum	N/A	41 v 33	ICP–MS
	Molina et al., 1998a	No change No change	CSF Serum	N/A	26 v 28	AAS
	Mueller et al., 2012	No change	Serum	N/A	19 v 19	AAS
	Raven et al., 2013	Increased	Brain	HP	31 v 68	MRI
	Szabo et al., 2016	Increased	Brain	FC	13 v 13	ICP–MS
	Torsdottir et al., 2011	No change	Serum	N/A	41 v 41	Clinical Assay
	Vaz et al., 2018	Increased	Plasma	N/A	32 v 32	ICP–MS
	Vural et al., 2010	Decreased	Plasma	N/A	50 v 50	AAS
	Wang et al., 2015	Decreased	Serum	N/A	83 v 83	ICP–MS
	Xu et al., 2017	Increased No change	Brain	HP, ENT, MTG SC, MC, CG, CB	8 v 13	ICP–MS
	Xu et al., 2018	No change	Plasma	N/A	43 v 43	ICP–MS
Magnesium	Barbagallo et al., 2011	No change Decreased	Serum (ionised)	N/A	36 v 65	Clinical Assay

	Koc et al., 2015	No change	Serum	N/A	41 v 33	ICP–MS
	Vural et al., 2010	**Decreased**	Plasma	N/A	50 v 50	AAS
	Xu et al., 2017	**Increased** No change **Decreased**	Brain	ENT, MTG GP, SC, MC, CG CB	9 v 13	ICP–MS
	Akatsu et al., 2012	No change	Brain	HP, AMG	18 v 16	ICP–MS
Manganese	Baum et al., 2010	No change	Serum	N/A	44 v 41	ICP–MS
	Corrigan et al., 1993	No change	Brain	HP	12 v 12	ICP–MS
	Gonzalez-Dominguez et al., 2014	**Decreased**	Serum	N/A	25 v 25	ICP–MS
	Molina et al., 1998a	No change No change	CSF Serum	N/A	26 v 28	AAS
	Szabo et al., 2016	No change	Brain	FC	13 v 13	ICP–MS
	Xu et al., 2017	**Increased** No change **Decreased**	Brain	HP ENT, MTG, SC, MC, CG CB	9 v 13	ICP–MS
	Xu et al., 2018	No change	Plasma	N/A	42 v 43	ICP–MS
Potassium	Roberts et al., 2016	**Decreased** **Increased** No change	Brain Serum CSF	FC N/A N/A	30 v 30	ICP–MS
	Vitvitsky et al., 2012	**Increased** No change	Brain	CB FC, PC	16 v 12	Flame photometry
	Xu et al., 2017	No change **Decreased**	Brain	HP, ENT, MTG, SC, MC CG, CB	9 v 13	ICP–MS
	Xu et al., 2018	No change	Plasma	N/A	42 v 43	ICP–MS

Selenium	Baum et al., 2010	**Increased**	Serum	N/A	44 v 41	ICP–MS
	Cardoso et al., 2017	No change **Decreased** No change	Serum Plasma CSF	N/A	36 v 39	SEC-ICP–MS
	Corrigan et al., 1993	**Decreased**	Brain	HP	12 v 12	ICP–MS
	Giacoppo et al., 2014	**Decreased**	Plasma	N/A	15 v 23	ICP–MS
	Gonzalez-Dominguez et al., 2014	**Decreased**	Serum	N/A	25 v 25	ICP–MS
	Koc et al., 2015	No change	Serum	N/A	41 v 33	ICP–MS
	Meseguer et al., 1999	No change No change	CSF Serum	N/A	27 v 34	AAS
	Vaz et al., 2018	No change	Plasma	N/A	32 v 32	ICP–MS
	Vural et al., 2010	**Decreased**	Plasma	N/A	50 v 50	AAS
	Xu et al., 2017	No change **Decreased**	Brain	HP, ENT, MTG, SC, MC CG, CB	9 v 13	ICP–MS
	Xu et al., 2018	No change	Plasma	N/A	42 v 43	ICP–MS
Sodium	Vitvitsky et al., 2012	**Increased**	Brain	FC, PC, CB	16 v 12	Flame photometry
	Xu et al., 2017	**Increased** No change	Brain	HP, ENT, MTG SC, MC, CG, CB	9 v 13	ICP–MS
	Xu et al., 2018	No change	Plasma	N/A	42 v 43	ICP–MS
Zinc	Akatsu et al., 2012	No change	Brain	HP, AMG	18 v 16	ICP–MS
	Baum et al., 2010	**Decreased**	Serum	N/A	44 v 41	ICP–MS
	Corrigan et al., 1993	**Decreased**	Brain	HP, MTG, SFG, SPG	12 v 12	ICP–MS

	Deibel et al., 1996	Increased No change	Brain	HP, AMG, IPL SG, MTG, CB	10 v 11	INAA
	Dong et al., 2008	No change	Serum	N/A	18 v 16	ICP–MS
	Giacoppo et al., 2014	Decreased (males only)	Plasma	N/A	15 v 23	ICP–MS
	Gonzalez et al., 1999	No change	Serum	N/A	51 v 40	AAS
	Gonzalez-Dominguez et al., 2014	Decreased	Serum	N/A	25 v 25	ICP–MS
	Koc et al., 2015	No change	Serum	N/A	41 v 33	ICP–MS
	Molina et al., 1998a	Decreased	CSF	N/A	26 v 28	AAS
	Panayi et al., 2002	Decreased	Brain	N/A	11 v 10	ICP–MS
	Religa et al., 2006	Increased	Brain	PFC	10 v 14	ICP–MS
	Rulon et al., 2000	No change Increased	Brain Serum	AMG, HP, CB, SG, MTG N/A	9 v 8	AAS
	Szabo et al., 2016	No change	Brain	FC	13 v 13	ICP–MS
	Vural et al., 2010	Decreased	Plasma	N/A	50 v 50	AAS
	Wang et al., 2015	No change	Serum	N/A	83 v 83	ICP–MS
	Xu et al., 2017	Increased No change Decreased	Brain	ENT, MTG HP, SC, MC, CG CB	9 v 13	ICP–MS
	Xu et al., 2018	Increased	Plasma	N/A	42 v 43	ICP–MS

Supplementary Table 2B – Metabolites in AD

Metabolite	Source	Change	Tissue	Region	N (cases v controls)	Method
6-phosphogluconate	X					
Acetyl CoA	X					
Aconitase	Raukas et al., 2012	No change	Brain	FC, OPC	12 v 12	Enzymatic Assay
	Mangialasche et al., 2015	**Decreased**	Plasma	N/A	28 v 21	Enzymatic Assay
Adenine	Xu et al., 2016a	**Increased** No change	Brain	CB HP, ENT, MTG, SC, MC, CG	9 v 9	GC/MS
	Muguruma et al., 2018	No change	CSF (PM)	N/A	10 v 10	UHPLC–MS/MS
Adenosine	Alonso-Andres et al., 2018	**Decreased** **Increased**	Brain	FC PC, TC	47 v 47	HPLC
	Gonzalez-Dominguez et al., 2015	**Increased**	Serum	N/A	23 v 21	GC/MS
	McFarland et al., 2013	No change	Brain	FC, TC, STR, CB	19 v 13	HPLC
	Muguruma et al., 2018	No change	CSF (PM)	N/A	10 v 10	UHPLC–MS/MS
	Selley, ML., 2004	**Decreased**	Plasma	N/A	25 v 25	Enzymatic Assay

	Xu et al., 2016a	No change	Brain	N/A	9 v 9	GC/MS
Alanine	Basun et al., 1990	No change No change	CSF Plasma	N/A	22 v 11	LC/MS
	Czech et al., 2012	No change	CSF	N/A	79 v 51	GC/MS & LC/MS
	Ellison et al., 1987	No change	Brain	HP, CN, PUT, NA, FC	10 v 10	HPLC
	Lowe et al., 1990	No change	Brain	PC	16 v 16	HPLC
	Martinez et al., 1993	No change No change	CSF Serum	N/A	13 v 15	HPLC
	Molina et al., 1998b	No change No change	CSF Plasma	N/A	37 v 32	Ion exchange chromatography
	Muguruma et al., 2018	No change	CSF (PM)	N/A	10 v 10	UHPLC–MS/MS
	Olazaran et al., 2015	**Increased**	Plasma	N/A	100 v 93	UPLC–MS
	Xu et al., 2016a	No change	Brain	HP, ENT, MTG, SC, MC, CG, CB	9 v 9	GC–MS
Arginine	Basun et al., 1990	No change No change	CSF Plasma	N/A	22 v 11	LC–MS
	Czech et al., 2012	No change	CSF	N/A	79 v 51	GC–MS & LC–MS
	Fonteh et al., 2007	No change No change No change	CSF Plasma Urine	N/A	8 v 8	LC–MS
	Graham et al., 2015	No change	Plasma	N/A	19 v 37	HRMS
	Gueli & Taibi, 2013	**Decreased**	Brain	TC	13 v 13	HPLC
	Liu et al., 2014	**Increased** **No change**	Brain	SFG HP, CB	12 v 12	LC–MS

	Martinez et al., 1993	No change No change	CSF Serum	N/A	13 v 15	HPLC
	Molina et al., 1998	**Increased** No change	CSF Plasma	N/A	37 v 32	Ion exchange chromatography
	Muguruma et al., 2018	No change	CSF (PM)	N/A	10 v 10	UHPLC–MS/MS
	Olazaran et al., 2015	**Increased**	Plasma	N/A	100 v 93	UPLC–MS
	Ravaglia et al., 2004	No change	Plasma	N/A	51 v 29	IEC Analysis
	Trushina et al., 2013	No change **Decreased**	CSF Plasma	N/A	15 v 15	HPLC-TOF/MS
Arginosuccinate	Corso et al., 2017	**Increased**	Serum	N/A	29 v 46	MS/MS
Asparagine	Fonteh et al., 2007	No change No change No change	CSF Plasma Urine	N/A	8 v 8	LC–MS
	Gonzalez-Dominguez et al., 2015	**Decreased**	Serum	N/A	23 v 21	GC–MS
	Jimenez-Jimenez et al., 1998	No change **Decreased**	CSF Plasma	N/A	37 v 32	Ion exchange chromatography
	Lowe et al., 1990	No change	Brain	PC	16 v 16	HPLC
	Martinez et al., 1993	No change No change	CSF Serum	N/A	13 v 15	HPLC
	Olazaran et al., 2015	**Increased**	Plasma	N/A	100 v 93	UPLC–MS
Aspartate	Corso et al., 2017	**Decreased**	Serum	N/A	29 v 46	MS/MS
	Ellison et al., 1987	No change	Brain	HP, CN, PUT, NA, FC	10 v 10	HPLC

	Gueli & Taibi, 2013	**Decreased**	Brain	TC	13 v 13	HPLC
	Jimenez-Jimenez et al., 1998	**Increased**	Plasma	N/A	37 v 32	Ion exchange chromatography
	Lowe et al., 1990	No change	Brain	PC	16 v 16	HPLC
	Martinez et al., 1993	**Increased** No change	CSF Serum	N/A	13 v 15	HPLC
	Muguruma et al., 2018	No change	CSF (PM)	N/A	10 v 10	UHPLC–MS/MS
Caffeine	X					
Carnitine	Czech et al., 2012	No change	CSF	N/A	79 v 51	GC–MS & LC–MS
	Rubio et al., 1998	**Decreased** No change	Plasma CSF	N/A	28 v 28	GC–MS
	Makar et al., 1995	No change **Decreased (with age)**	Brain	SFG, CB HP	13 v 13	Enzymatic Assay
Citrate	Czech et al., 2012	No change	CSF	N/A	79 v 51	GC–MS
	Xu et al., 2016a	**Increased** No change	Brain	HP, ENT MTG, SC, MC, CG, CB	9 v 9	GC–MS
Citrulline	Corso et al., 2017	**Increased**	Serum	N/A	29 v 46	MS/MS
	Czech et al., 2012	**Increased**	CSF	N/A	79 v 51	GC–MS & LC–MS
	Fonteh et al., 2007	No change No change No change	CSF Plasma Urine	N/A	8 v 8	LC–MS
	Liu et al., 2014	No change	Brain	SFG, HP, CB	12 v 12	LC–MS

	Molina et al., 1998b	Decreased Increased	CSF Plasma	N/A	37 v 32	Ion exchange chromatography
	Muguruma et al., 2018	No change	CSF (PM)	N/A	10 v 10	UHPLC–MS/MS
Creatine	Czech et al., 2012	No change	CSF	N/A	79 v 51	GC–MS & LC–MS
	Graham et al., 2015	Increased	Plasma	N/A	19 v 37	HRMS
	Pfefferbaum et al., 1999	Increased	Brain	GM	16 v 19	MRI
	Trushina et al., 2013	Decreased Increased	CSF Plasma	N/A	15 v 15	HPLC/TOF-MS
Creatinine	Czech et al., 2012	Increased	CSF	N/A	79 v 51	GC–MS & LC–MS
	Evlice & Ulusu, 2017	Increased	Serum	N/A	30 v 30	Clinical Assay
	Ravaglia et al., 2004	No change	Plasma	N/A	51 v 29	IEC Analysis
	Trushina et al., 2013	Decreased No change	CSF Plasma	N/A	15 v 15	HPLC-TOF/MS
	Xu et al., 2016a	Increased No change	Brain	MTG, CB HP, CG, ENT, SC, MC	9 v 9	GC–MS
Cysteine	Czech et al., 2012	Increased	CSF	N/A	79 v 51	GC–MS & LC–MS
	Fonteh et al., 2007	No change No change No change	CSF Plasma Urine	N/A	8 v 8	LC–MS
	Xu et al., 2016a	Increased No change	Brain	HP, CG ENT, MTG, SC, MC, CB	9 v 9	GC–MS
Ethanolamine	Lowe et al., 1990	No change	Brain	PC	16 v 16	HPLC

	Molina et al., 1998b	Decreased Decreased	CSF Plasma	N/A	37 v 32	Ion exchange chromatography
	Muguruma et al., 2018	No change	CSF (PM)	N/A	10 v 10	UHPLC–MS/MS
	Xu et al., 2016a	Decreased	Brain	HP, ENT, MTG, SC, MC, CG, CB	9 v 9	GC–MS
Fructose	Czech et al., 2012	No change	CSF	N/A	79 v 51	GC–MS & LC–MS
	Xu et al., 2016a	Increased	Brain	HP, ENT, MTG, SC, MC, CG, CB	9 v 9	GC–MS
	Xu et al., 2016b	Increased	Brain	HP, ENT, MTG, SC, MC, CG, CB	9 v 9	GC–MS
Fructose-6-phosphate	Xu et al., 2016a	Increased No change	Brain	MTG, CG HP, ENT, SC, MC, CB	9 v 9	GC–MS
Fumarate	Xu et al., 2016a	Increased No change	Brain	CG HP, ENT, MTG, SC, MC, CB	9 v 9	GC–MS
Glucono-1,5-lactone-6-phosphate	X					
Glucose	An et al., 2018	Increased No change Increased	Brain Plasma	ITG, MFG CB N/A	14 v 14	LC–MS
	Czech et al., 2012	No change	CSF	N/A	79 v 51	GC–MS & LC–MS
	Gonzalez-Dominguez et al., 2015	Increased	Serum	N/A	23 v 21	GC–MS

	Xu et al., 2016a	Increased	Brain	HP, ENT, MTG, SC, MC, CG, CB	9 v 9	GC–MS
	Xu et al., 2016b	Increased	Brain	HP, ENT, MTG, SC, MC, CG, CB	9 v 9	GC–MS
Glucose-6-phosphate	Xu et al., 2016a	Increased	Brain	HP, ENT, MTG, SC, MC, CG, CB	9 v 9	GC–MS
Glutamate	Ellison et al., 1987	Decreased No change	Brain	FC, PC, ITG HP, CN, PUT, NA	10 v 10	HPLC
	Gueli & Taibi, 2013	Decreased	Brain	TC	13 v 13	HPLC
	Hudd et al., 2019	Increased	Serum	N/A	11 v 28	LC–MS/MS
	Jimenez-Jimenez et al., 1998	Increased No change	CSF Plasma	N/A	37 v 32	Ion exchange chromatography
	Liu et al., 2014	Decreased Increased No change	Brain	HP CB SFG	12 v 12	LC–MS
	Lowe et al., 1990	Increased	Brain	PC	16 v 16	HPLC
	Martinez et al., 1993	Decreased No change	CSF Serum	N/A	13 v 15	HPLC
	Muguruma et al., 2018	No change	CSF (PM)	N/A	10 v 10	UHPLC–MS/MS
	Vitvitsky et al., 2012	No change	Brain	FC, PC, CB	16 v 12	HPLC
Glutamic Acid	Basun et al., 1990	No change Decreased	CSF Plasma	N/A	22 v 11	LC–MS
	Fonteh et al., 2007	No change No change No change	CSF Plasma Urine	N/A	8 v 8	LC–MS

	Olazaran et al., 2015	**Decreased**	Plasma	N/A	100 v 93	UPLC–MS
	Oresic et al., 2011	No change	Serum	N/A	47 v 46	GC–MS
	Wang et al., 2014	**Decreased**	Plasma	N/A	57 v 57	GC-TOFMS
	Xu et al., 2016a	**Increased** No change	Brain	CG HP, ENT, MTG, SC, MC, CB	9 v 9	GC–MS
Glutamine	Basun et al., 1990	No change No change	CSF Plasma	N/A	22 v 11	LC–MS
	Corso et al., 2017	No change	Serum	N/A	29 v 46	MS/MS
	Czech et al., 2012	No change	CSF	N/A	79 v 51	GC–MS & LC–MS
	Fonteh et al., 2007	No change No change No change	CSF Plasma Urine	N/A	8 v 8	LC–MS
	Gonzalez et al., 1999	No change	Serum	N/A	51 v 40	Colorimetric Assay
	Gonzalez-Dominguez et al., 2015	**Decreased**	Serum	N/A	23 v 21	GC–MS
	Gueli & Taibi, 2013	**Increased**	Brain	TC	13 v 13	HPLC
	Jimenez-Jimenez et al., 1998	No change No change	CSF Plasma	N/A	37 v 32	Ion exchange chromatography
	Liu et al., 2014	**Increased** No change	Brain	SFG, CB HP	12 v 12	LC–MS
	Lowe et al., 1990	No change	Brain	PC	16 v 16	HPLC
	Martinez et al., 1993	No change No change	CSF Serum	N/A	13 v 15	HPLC

	Oresic et al., 2011	No change	Serum	N/A	47 v 46	GC–MS
	Vitvitsky et al., 2012	No change	Brain	FC, PC, CB	16 v 12	HPLC
	Wang et al., 2014	**Increased**	Plasma	N/A	57 v 57	GC-TOF/MS
Glycine	Ansoleaga et al., 2015	**Decreased**	Brain	ETC	57 v 35	LC–MS
	Basun et al., 1990	**Decreased** No change	CSF Plasma	N/A	22 v 11	LC–MS
	Fonteh et al., 2007	No change No change **Increased**	CSF Plasma Urine	N/A	8 v 8	LC–MS
	Jimenez-Jimenez et al., 1998	**Increased** **Increased**	CSF Plasma	N/A	37 v 32	Ion exchange chromatography
	Lowe et al., 1990	No change	Brain	PC	16 v 16	HPLC
	Martinez et al., 1993	No change No change	CSF Serum	N/A	13 v 15	HPLC
	Muguruma et al., 2018	No change	CSF (PM)	N/A	10 v 10	UHPLC–MS/MS
	Olazaran et al., 2015	**Increased**	Plasma	N/A	100 v 93	UPLC–MS
	Oresic et al., 2011	No change	Serum	N/A	47 v 46	GC–MS
	Xu et al., 2016a	**Decreased** No change	Brain	ENT, MTG HP, SC, MC, CG, CB	9 v 9	GC–MS
GSH	Adams et al., 1991	**Decreased** No change	Brain	HP, MB FC, MED, PUT, CN	9 v 9	HPLC
	Aybek et al., 2007	No change	Serum	N/A	62 v 56	Colorimetric Assay
	Baldeiras et al., 2008	No change	Plasma	N/A	42 v 37	Fluorimetric Assay

	Bermejo et al., 2008	Decreased	Plasma	N/A	45 v 28	Fluorimetric Assay
	Kaddurah-Daouk et al., 2011	No change	CSF	N/A	15 v 15	LC–MS
	Mandal et al., 2015	Decreased	Brain	HP, FC	21 v 21	MRS
	Puertas et al., 2012	Decreased	Plasma	N/A	46 v 46	Colorimetric Assay
	Rani et al., 2017	Decreased	Plasma	N/A	45 v 45	Colorimetric Assay
GSSG	Adams et al., 1991	No change	Brain	HP, MB, FC, MED, PUT, CN	9 v 9	HPLC
	Baldeiras et al., 2008	Increased	Plasma	N/A	42 v 37	Fluorimetric Assay
	Bermejo et al., 2008	No change	Plasma	N/A	45 v 28	Fluorimetric Assay
	Kaddurah-Daouk et al., 2011	No change	CSF	N/A	15 v 15	LC–MS
	Rani et al., 2017	Increased	Plasma	N/A	45 v 45	Colorimetric Assay
Guanine	Ansoleaga et al., 2015	Increased	Brain	ETC	57 v 35	LC–MS
	Muguruma et al., 2018	No change	CSF (PM)	N/A	10 v 10	UHPLC–MS/MS
Guanosine	Alonso-Andres et al., 2018	Decreased Increased	Brain	FC PC, TC	47 v 47	HPLC
	Kaddurah-Daouk et al., 2011	No change	CSF	N/A	15 v 15	LC–MS
	Muguruma et al., 2018	No change	CSF (PM)	N/A	10 v 10	UHPLC–MS/MS
	Xu et al., 2016a	Increased No change	Brain	MTG HP, ENT, SC, CG, CB	9 v 9	GC–MS

Histidine	Basun et al., 1990	No change No change	CSF Plasma	N/A	22 v 11	LC–MS
	Fonteh et al., 2007	No change No change No change	CSF Plasma Urine	N/A	8 v 8	LC–MS
	Gonzalez-Dominguez et al., 2015	**Decreased**	Serum	N/A	23 v 21	GC–MS
	Martinez et al., 1993	No change No change	CSF Serum	N/A	13 v 15	HPLC
	Molina et al., 1998b	**Increased** No change	CSF Plasma	N/A	37 v 32	Ion exchange chromatography
	Ravaglia et al., 2004	No change	Plasma	N/A	51 v 29	IEC Analysis
Homocitrulline	Corso et al., 2017	**Increased**	Serum	N/A	29 v 46	MS/MS
Homocysteine	Cervellati et al., 2014	No change	Serum	N/A	89 v 48	Enzymatic Assay
	Luchsinger et al., 2004	No change	Plasma	N/A	237 v 679	Enzymatic Assay
	Selley, M. L., 2004	**Increased**	Plasma	N/A	25 v 25	Enzymatic Assay
	Serot et al., 2005	No change	CSF	N/A	38 v 20	Enzymatic Assay
Homovanillate	Blennow et al., 1992	**Decreased**	CSF	N/A	123 v 57	GC–MS
	Janssens et al., 2018	No change No change	CSF Serum	N/A	52 v 88	HPLC
	Zubenko et al., 1986	**Increased**	CSF	N/A	13 v 15	LC–MS

Hypoxanthine	Alonso-Andres et al., 2018	**Decreased** No change	Brain	FC PC, TC	47 v 47	HPLC
	Kaddurah-Daouk et al., 2011	No change	CSF	N/A	15 v 15	LC–MS
	McFarland et al., 2013	No change	Brain	FC, PC, STRI, CB	19 v 13	HPLC
	Trushina et al., 2013	**No change** Decreased	CSF Plasma	N/A	15 v 15	HPLC-TOF/MS
	Wang et al., 2014	**Increased**	Plasma	N/A	57 v 57	GC-TOF-MS
	Xu et al., 2016a	**Decreased** No change	Brain	ENT, MTG, SC, CB HP, MC, CG	9 v 9	GC–MS
Indoleacetate	Blennow et al., 1992	**Decreased**	CSF	N/A	123 v 57	GC–MS
Inosine	Alonso-Andres et al., 2018	No change **Increased**	Brain	FC PC, TC	47 v 47	HPLC
	McFarland et al., 2013	No change	Brain	FC, PC, STRI, CB	19 v 13	HPLC
Isoleucine	Basun et al., 1990	No change No change	CSF Plasma	N/A	22 v 11	LC–MS
	Czech et al., 2012	No change	CSF	N/A	79 v 51	GC–MS & LC–MS
	Fonteh et al., 2007	No change No change No change	CSF Plasma Urine	N/A	8 v 8	LC–MS
	Hudd et al., 2019	No change	Serum	N/A	11 v 28	LC–MS/MS
	Martinez et al., 1993	No change No change	CSF Serum	N/A	13 v 15	HPLC

	Molina et al., 1998b	No change **Decreased**	CSF Plasma	N/A	37 v 32	Ion exchange chromatography
	Muguruma et al., 2018	No change	CSF (PM)	N/A	10 v 10	UHPLC–MS/MS
	Oresic et al., 2011	No change	Serum	N/A	47 v 46	GC–MS
	Xu et al., 2016a	No change	Brain	HP, ENT, MTG, SC, MC, CG, CB	9 v 9	GC–MS
Kynurenic Acid	Giil et al., 2017	No change	Plasma	N/A	65 v 65	LC–MS/MS
	Gulaj et al., 2010	**Decreased**	Plasma	N/A	34 v 18	HPLC
	Hartai et al., 2007	**Decreased**	Plasma	N/A	28 v 31	HPLC
	Oxenkrug et al., 2017	No change	Serum	N/A	20 v 24	HPLC
	Wennstrom et al., 2014	No change	CSF	N/A	19 v 20	HPLC
Kynurenine	Czech et al., 2012	No change	CSF	N/A	79 v 51	GC–MS & LC–MS
	Giil et al., 2017	**Decreased**	Plasma	N/A	65 v 65	LC–MS/MS
	Gulaj et al., 2010	No change	Plasma	N/A	34 v 18	HPLC
	Hartai et al., 2007	No change	Plasma	N/A	28 v 31	HPLC
	Kaddurah-Daouk et al., 2011	No change	CSF	N/A	15 v 15	LC–MS
	Oxenkrug et al., 2017	No change	Serum	N/A	20 v 24	HPLC
Lactate	Liguori et al., 2015	**Increased**	CSF	N/A	145 v 80	Enzymatic Assay
Leucine	Basun et al., 1990	**Decreased** **No change**	CSF Plasma	N/A	22 v 11	LC–MS
	Czech et al., 2012	No change	CSF	N/A	79 v 51	GC–MS & LC–MS

	Fonteh et al., 2007	No change No change No change	CSF Plasma Urine	N/A	8 v 8	LC–MS
	Hudd et al., 2019	No change	Serum	N/A	11 v 28	LC–MS/MS
	Martinez et al., 1993	No change No change	CSF Serum	N/A	13 v 15	HPLC
	Molina et al., 1998b	No change Decreased	CSF Plasma	N/A	37 v 32	Ion exchange chromatography
	Muguruma et al., 2018	No change	CSF	N/A	10 v 10	UHPLC–MS/MS
	Oresic et al., 2011	No change	Serum	N/A	47 v 46	GC–MS
	Xu et al., 2016a	No change	Brain	HP, ENT, MTG, SC, MC, CG, CB	9 v 9	GC–MS
Lysine	Basun et al., 1990	No change No change	CSF Plasma	N/A	22 v 11	LC–MS
	Czech et al., 2012	No change	CSF	N/A	79 v 51	GC–MS & LC–MS
	Fonteh et al., 2007	No change No change No change	CSF Plasma Urine	N/A	8 v 8	LC–MS
	Martinez et al., 1993	Increased No change	CSF Serum	N/A	13 v 15	HPLC
	Molina et al., 1998b	Increased No change	CSF Plasma	N/A	37 v 32	Ion exchange chromatography
	Trushina et al., 2013	No change Increased	CSF Plasma	N/A	11 v 14	TOF-MS

	Xu et al., 2016a	Decreased No change	Brain	HP ENT, MTG, SC, MC, CG, CB	9 v 9	GC–MS
Malate	Xu et al., 2016a	Increased No change	Brain	ENT, MTG HP, SC, MC, CG, CB	9 v 9	GC–MS
Mannitol	Xu et al., 2016a	No change	Brain	HP, ENT, MTG, SC, MC, CG, CB	9 v 9	GC–MS
Mannose	Czech et al., 2012	No change	CSF	N/A	79 v 51	GC–MS & LC–MS
	Wang et al., 2014	Increased	Plasma	N/A	57 v 57	GC-TOF-MS
Methionine	Basun et al., 1990	No change No change	CSF Plasma	N/A	22 v 11	LC–MS
	Corso et al., 2017	No change	Serum	N/A	29 v 46	MS/MS
	Czech et al., 2012	Increased	CSF	N/A	79 v 51	GC–MS & LC–MS
	Gueli & Taibi, 2013	Decreased	Brain	TC	13 v 13	HPLC
	Kaddurah-Daouk et al., 2011	No change	CSF	N/A	15 v 15	LC–MS
	Martinez et al., 1993	No change No change	CSF Serum	N/A	13 v 15	HPLC
	Molina et al., 1998b	Decreased Decreased	CSF Plasma	N/A	37 v 32	Ion exchange chromatography
	Muguruma et al., 2018	No change	CSF (PM)	N/A	10 v 10	UHPLC–MS/MS
	Olazaran et al., 2015	Increased	Plasma	N/A	100 v 93	UPLC–MS
	Ravaglia et al., 2004	No change	Plasma	N/A	51 v 29	IEC Analysis
	Vitvitsky et al., 2012	Decreased No change	Brain	CB FC, PC	16 v 12	HPLC

	Xu et al., 2016a	No change	Brain	HP, ENT, MTG, SC, MC, CG, CB	9 v 9	GC–MS
NADP+				X		
NADPH				X		
Ornithine	Basun et al., 1990	No change No change	CSF Plasma	N/A	22 v 11	LC–MS
	Fonteh et al., 2007	No change No change No change	CSF Plasma Urine	N/A	8 v 8	LC–MS
	Gonzalez-Dominguez et al., 2015	**Decreased**	Serum	N/A	23 v 21	GC–MS
	Graham et al., 2013	**Decreased**	Plasma	N/A	19 v 37	HRMS
	Gueli & Taibi, 2013	**Decreased**	Brain	TC	13 v 13	HPLC
	Liu et al., 2014	**Decreased**	Brain	SFG, HP, CB	12 v 12	LC–MS
	Martinez et al., 1993	No change No change	CSF Serum	N/A	13 v 15	HPLC
	Muguruma et al., 2018	**Decreased**	CSF (PM)	N/A	10 v 10	UHPLC–MS/MS
	Oresic et al., 2011	No change	Serum	N/A	47 v 46	GC–MS
Oxaloacetate				X		
Paraxanthine				X		
Phenylalanine	Basun et al., 1990	No change No change	CSF Plasma	N/A	22 v 11	LC–MS
	Corso et al., 2017	**Decreased**	Serum	N/A	29 v 46	MS/MS

	Czech et al., 2012	Increased	CSF	N/A	79 v 51	GC–MS & LC–MS
	Fonteh et al., 2007	No change No change No change	CSF Plasma Urine	N/A	8 v 8	LC–MS
	Gonzalez-Dominguez et al., 2015	Decreased	Serum	N/A	23 v 21	GC–MS
	Hudd et al., 2019	No change	Serum	N/A	11 v 28	LC–MS/MS
	Martinez et al., 1993	No change No change	CSF Serum	N/A	13 v 15	HPLC
	Molina et al., 1998b	No change No change	CSF Plasma	N/A	37 v 32	Ion exchange chromatography
	Muguruma et al., 2018	Decreased	CSF (PM)	N/A	10 v 10	UHPLC–MS/MS
	Ravaglia et al., 2004	Increased	Plasma	N/A	51 v 29	IEC Analysis
	Xu et al., 2016a	Increased No change	Brain	MTG, CG HP, ENT, SC, MC, CB	9 v 9	GC–MS
Phosphoserine	Molina et al., 1998b	Decreased Increased	CSF Plasma	N/A	37 v 32	Ion exchange chromatography
Proline	Fonteh et al., 2007	No change No change No change	CSF Plasma Urine	N/A	8 v 8	LC–MS
	Martinez et al., 1993	No change No change	CSF Serum	N/A	13 v 15	HPLC
	Molina et al., 1998b	Increased	Plasma	N/A	37 v 32	Ion exchange chromatography

	Wang et al., 2014	Increased	Plasma	N/A	57 v 57	GC-TOFMS
	Xu et al., 2016a	Decreased No change	Brain	HP, ENT MTG, SC, MC, CG, CB	9 v 9	GC–MS
Pyruvate	Czech et al., 2012	Increased	CSF	N/A	79 v 51	GC–MS & LC–MS
Ribose-5-phosphate	Xu et al., 2016a	Increased No change	Brain	ENT, MTG HP, SC, MC, CG, CB	9 v 9	GC–MS
	Oresic et al., 2011	No change	Serum	N/A	47 v 46	GC–MS
Sarcosine	Muguruma et al., 2018	No change	CSF (PM)	N/A	10 v 10	UHPLC–MS/MS
Serine	Basun et al., 1990	No change No change	CSF Plasma	N/A	22 v 11	LC–MS
	Czech et al., 2012	Increased	CSF	N/A	79 v 51	GC–MS & LC–MS
	Fonteh et al., 2007	No change No change No change	CSF Plasma Urine	N/A	8 v 8	LC–MS
	Lowe et al., 1990	Increased	Brain	PC	16 v 16	HPLC
	Martinez et al., 1993	No change No change	CSF Serum	N/A	13 v 15	HPLC
	Molina et al., 1998b	Increased No change	CSF Plasma	N/A	37 v 32	Ion exchange chromatography
	Muguruma et al., 2018	No change	CSF (PM)	N/A	10 v 10	UHPLC–MS/MS
	Xu et al., 2016a	Decreased No change	Brain	HP, ENT MTG, SC, MC, CG, CB	9 v 9	GC–MS
Sorbitol	Czech et al., 2012	Increased	CSF	N/A	79 v 51	GC–MS & LC–MS

	Xu et al., 2016a	Increased	Brain	HP, ENT, MTG, SC, MC, CG, CB	9 v 9	GC–MS
	Xu et al., 2016b	Increased	Brain	HP, ENT, MTG, SC, MC, CG, CB	9 v 9	GC–MS
Succinate	X					
Succinyl-CoA	X					
Sucrose	X					
Taurine	Basun et al., 1990	No change Decreased	CSF Plasma	N/A	22 v 11	LC–MS
	Czech et al., 2012	No change	CSF	N/A	79 v 51	GC–MS & LC–MS
	Ellison et al., 1986	No change	Brain	HP, CN, PUT, NA, FC	10 v 10	HPLC
	Lowe et al., 1990	No change	Brain	PC	16 v 16	HPLC
	Martinez et al., 1993	No change No change	CSF Serum	N/A	13 v 15	HPLC
	Molina et al., 1998b	No change No change	CSF Plasma	N/A	37 v 32	Ion exchange chromatography
	Muguruma et al., 2018	No change	CSF (PM)	N/A	10 v 10	UHPLC–MS/MS
	Ravaglia et al., 2004	No change	Plasma	N/A	51 v 29	IEC Analysis
	Trushina et al., 2013	Increased No change	CSF Plasma	N/A	15 v 15	HPLC-TOF/MS
Theophylline	X					
Threonine	Basun et al., 1990	No change No change	CSF Plasma	N/A	22 v 11	LC–MS

	Czech et al., 2012	No change	CSF	N/A	79 v 51	GC–MS & LC–MS
	Fonteh et al., 2007	No change No change No change	CSF Plasma Urine	N/A	8 v 8	LC–MS
	Martinez et al., 1993	No change No change	CSF Serum	N/A	13 v 15	HPLC
	Molina et al., 1998b	**Increased** **Increased**	CSF Plasma	N/A	37 v 32	Ion exchange chromatography
	Muguruma et al., 2018	No change	CSF (PM)	N/A	10 v 10	UHPLC–MS/MS
	Xu et al., 2016a	**Increased** No change	Brain	MTG HP, ENT, SC, MC, CG, CB	9 v 9	GC–MS
Tryptophan	Basun et al., 1990	No change	Plasma	N/A	22 v 11	LC–MS
	Czech et al., 2012	No change	CSF	N/A	79 v 51	GC–MS & LC–MS
	Fonteh et al., 2007	No change No change No change	CSF Plasma Urine	N/A	8 v 8	LC–MS
	Giil et al., 2017	**Decreased**	Plasma	N/A	65 v 65	LC–MS/MS
	Gonzalez-Dominguez et al., 2015	**Decreased**	Serum	N/A	23 v 21	GC–MS
	Gulaj et al., 2010	**Decreased**	Plasma	N/A	34 v 18	HPLC
	Janssens et al., 2018	**Decreased**	CSF	N/A	52 v 88	HPLC
	Kaddurah-Daouk et al., 2011	No change	CSF	N/A	15 v 15	LC–MS

	Martinez et al., 1993	No change No change	CSF Serum	N/A	13 v 15	HPLC
	Molina et al., 1998b	No change No change	CSF Plasma	N/A	37 v 32	Ion exchange chromatography
	Muguruma et al., 2018	**Decreased**	CSF (PM)	N/A	10 v 10	UHPLC–MS/MS
	Oxenkrug et al., 2017	No change	Serum	N/A	20 v 24	HPLC
	Trushina et al., 2013	No change **Decreased**	CSF Plasma	N/A	15 V 15	HPLC-TOF/MS
	Xu et al., 2016a	**Increased** No change	Brain	HP, ENT, MTG, MC, CG SC, CB	9 v 9	GC–MS
Tyrosine	Basun et al., 1990	No change No change	CSF Plasma	N/A	22 v 11	LC–MS
	Corso et al., 2017	No change	Serum		29 v 46	MS/MS
	Czech et al., 2012	**Increased**	CSF	N/A	79 v 51	GC–MS & LC–MS
	Fonteh et al., 2007	No change No change No change	CSF Plasma Urine	N/A	8 v 8	LC–MS
	Gonzalez-Dominguez et al., 2015	**Decreased**	Serum	N/A	23 v 21	GC–MS
	Hudd et al., 2019	No change	Serum	N/A	11 v 28	LC–MS/MS
	Kaddurah-Daouk et al., 2011	No change	CSF	N/A	15 v 15	LC–MS

	Martinez et al., 1993	No change No change	CSF Serum	N/A	13 v 15	HPLC
	Molina et al., 1998b	No change No change	CSF Plasma	N/A	37 v 32	Ion exchange chromatography
	Muguruma et al., 2018	No change	CSF (PM)	N/A	10 v 10	UHPLC–MS/MS
	Ravaglia et al., 2004	No change	Plasma		51 v 29	IEC Analysis
	Xu et al., 2016a	No change	Brain	HP, ENT, MTG, SC, MC, CG, CB	9 v 9	GC–MS
Urea	Czech et al., 2012	No change	CSF	N/A	79 v 51	GC–MS & LC–MS
	Gonzalez-Dominguez et al., 2015	**Decreased**	Serum	N/A	23 v 21	GC–MS
	Gueli & Taibi, 2013	**Increased**	Brain	TC	13 v 13	HPLC
	Trushina et al., 2013	**No change** **Decreased**	CSF Plasma	N/A	15 v 15	HPLC-TOF/MS
	Xu et al., 2016a	**Increased**	Brain	HP, ENT, MTG, SC, MC, CG, CB	9 v 9	GC–MS
Uric Acid	Baldeiras et al., 2008	No change	Plasma	N/A	42 v 37	Colorimetric Assay
	Cervellati et al., 2014	No change	Serum	N/A	89 v 48	Enzymatic Assay
	Czech et al., 2012	No change	CSF	N/A	79 v 51	GC–MS & LC–MS
	Gonzalez-Dominguez et al., 2015	**Decreased**	Serum	N/A	23 v 21	GC–MS

	Kaddurah-Daouk et al., 2011	No change	CSF	N/A	15 v 15	LC–MS
	Mangialasche et al., 2015	**Decreased**	Plasma	N/A	28 v 21	Enzymatic Assay
	McFarland et al., 2013	No change	Brain	FC, PC, STR, CB	19 v 13	HPLC
	Rinaldi et al., 2003	**Decreased**	Plasma	N/A	63 v 56	HPLC
	Trushina et al., 2013	No change **Increased**	CSF Plasma	N/A	15 v 15	HPLC-TOF/MS
Valine	Basun et al., 1990	**Decreased** No change	CSF Plasma	N/A	22 v 11	LC–MS
	Czech et al., 2012	No change	CSF	N/A	79 v 51	GC–MS & LC–MS
	Fonteh et al., 2007	No change No change No change	CSF Plasma Urine	N/A	8 v 8	LC–MS
	Gonzalez-Dominguez et al., 2015	**Decreased**	Serum	N/A	23 v 21	GC–MS
	Hudd et al., 2019	No change	Serum	N/A	11 v 28	LC–MS/MS
	Martinez et al., 1993	No change No change	CSF Serum	N/A	13 v 15	HPLC
	Molina et al., 1998b	No change No change	CSF Plasma	N/A	37 v 32	Ion exchange chromatography
	Muguruma et al., 2018	No change	CSF (PM)	N/A	10 v 10	UHPLC–MS/MS
	Oresic et al., 2011	No change	Serum	N/A	47 v 46	GC–MS

	Xu et al., 2016a	No change	Brain	HP, ENT, MTG, SC, MC, CG, CB	9 v 9	GC–MS
Xanthine	Alonso-Andres et al., 2018	**Decreased** No change	Brain	FC PC, TC	47 v 47	HPLC
	Ansoleaga et al., 2015	**Decreased**	Brain	ETC	57 v 35	LC–MS
	Kaddurah-Daouk et al., 2011	No change	CSF	N/A	15 v 15	LC–MS
	McFarland et al., 2013	No change	Brain	FC, PC, STRI, CB	19 v 13	HPLC
	Trushina et al., 2013	No change **Decreased**	CSF Plasma	N/A	15 v 15	HPLC-TOF/MS
Xylulose-5-phosphate	X					
α-aminoadipic acid	Wang et al., 2014	**Increased**	Plasma	N/A	57 v 57	GC-TOF-MS
	Molina et al., 1998b	No change	Plasma	N/A	37 v 32	Ion exchange chromatography
α-aminobutyric acid	Molina et al., 1998b	**Decreased** **Decreased**	CSF Plasma	N/A	37 v 32	Ion exchange chromatography
α-ketoglutarate	Gonzalez-Dominguez et al., 2015	**Increased**	Serum	N/A	23 v 21	GC–MS
γ glutamyl-cysteine	X					

Supplementary Table 3A – Metals in PD

Metal	Source	Change	Tissue	Region	N (cases v controls)	Method
Calcium	Alimonti et al., 2007	No change	CSF	N/A	42 v 20	ICP-AES
	Bocca et al., 2006	No change **Increased** No change **Increased**	CSF Plasma Serum Urine	N/A	91 v 18	ICP–MS / ICP-AES
	Hegde et al., 2004	**Increased (early PD)**	Serum	N/A	52 v 25	ICP-AES
	Sanyal et al., 2016	**Increased** **Increased**	CSF Serum	N/A	60 v 50 250 v 280	AAS
Ceruloplasmin	Annanmaki et al., 2007	No change	Plasma	N/A	40 v 29	Immunoassay
	Ayton et al., 2013	No change	Brain	SN, Cortex	10 v 10	AAS
	Bharucha et al., 2008	**Decreased (early-onset only)**	Serum	N/A	62 v 40	MRI
	Boll et al., 2008	**Decreased**	Plasma	N/A	22 v 11	Colorimetric Assay
	Loeffler et al., 1996	**Increased** No change	Brain	HP, TC, GC, PC SN, CAUD, PUT, CB	10 v 10	ELISA/IHC

	Ling & Bhidayasiri, 2011	**Decreased**	Serum	N/A	71 v 26	Immunoassay
Copper	Ahmed et al., 2010	No change	CSF	N/A	45 v 42	ICP–MS
	Alimonti et al., 2007	No change	CSF	N/A	42 v 20	ICP-AES
	Ayton et al., 2013	**Decreased** No change	Brain	SN Cortex	10 v 10	AAS
	Bharucha et al., 2008	**Decreased**	Serum	N/A	49 v 28	Clinical Assay
	Bocca et al., 2006	No change **Increased** **Decreased** No change	CSF Plasma Serum Urine	N/A	91 v 18	ICP–MS/ICP-AES
	Boll et al., 2008	**Increased**	CSF	N/A	22 v 11	AAS
	Davies et al., 2014	**Decreased**	Brain	SN, CN, LC	10 v 10	X-ray Emission Microscopy; ICP–MS
	Fukushima et al., 2013	**Increased** No change	Serum Urine	N/A	82 v 82 71 v 70	ICP–MS
	Genoud et al., 2017	**Decreased** No change	Brain	SN OCC, FG	11 v 11	ICP–MS
	Hegde et al., 2004	**Increased**	Serum	N/A	52 v 25	ICP-AES
	Karpenko et al., 2018	No change	CSF	N/A	11 v 22	AAS
	Kim et al., 2018	**Decreased**	Serum	N/A	325 v 304	ICP–MS

	Kumudini et al., 2014	Increased	Serum	N/A	150 v 170	ICP–MS
	Ling & Bhidayasiri, 2011	No change	Serum	N/A	71 v 26	Clinical Assay
	Pall et al., 1987	Increased	CSF	N/A	31 v 37	AAS
	Sanyal et al., 2016	Decreased Decreased	CSF Serum	N/A	60 v 50 250 v 280	AAS
	Younes-Mhenni et al., 2013	Decreased	Serum	N/A	48 v 36	AAS
	Zhao et al., 2013	Decreased	Plasma	N/A	238 v 302	AAS
Iron	Ahmed et al., 2010	No change	Serum	N/A	45 v 42	ICP–MS
	Alimonti et al., 2007	Decreased	CSF	N/A	42 v 20	ICP-AES
	Annanmaki et al., 2007	No change	Plasma	N/A	40 v 29	Colorimetric Assay
	Ayton et al., 2013	Increased No change	Brain	SN Cortex	10 v 10	AAS
	Bocca et al., 2006	Decreased Increased No change Increased	CSF Plasma Serum Urine	N/A	91 v 18	ICP–MS / ICP-AES
	Cabrera-Valdivia et al., 1994	No change No change	Serum Urine	N/A	68 v 68	AAS
		Increased	Brain	SNpc	24 v 27	MRI

Costa-Mallen et al., 2017	Unchanged **Decreased**	Brain Serum	SNr, RN, GP, WM, PUT N/A		Assay
Dexter et al., 1991	**Increased** No change	Brain	SN, GP Cortex, CN, PUT, CB	27 v 34	ICP–MS
Farhoudi et al., 2012	No change	Serum	N/A	50 v 50	Enzymatic & Colorimetric Assay
Fukushima et al., 2013	No change No change	Serum Urine	N/A	82 v 82 71 v 70	ICP–MS
Gazziniga et al., 1992	No change	CSF	N/A	11 v 22	AAS
Genoud et al., 2017	**Increased** No change	Brain Brain	SN OCC, FG	11 v 11	ICP–MS
Hegde et al., 2004	**Decreased**	Serum	N/A	52 v 25	ICP-AES
Kim & Lee, 2014	**Increased**	Brain	SN	30 v 25	MRI
Kim et al., 2018	No change	Serum	N/A	325 v 304	ICP–MS
Kumudini et al., 2014	**Increased**	Serum	N/A	150 v 170	ICP–MS
Ling & Bhidayasiri, 2011	No change	Serum	N/A	71 v 26	Clinical Assay
Madenci et al., 2012	No change	Serum	N/A	60 v 42	Clinical Assay
Pyatigorska et al., 2015	**Increased**	Brain	SN	20 v 20	MRI

	Sanyal et al., 2016	**Decreased** **Decreased**	CSF Serum	N/A	50 v 60 250 v 280	AAS
	Xuan et al., 2017	**Increased** No change	Brain Brain	SNc, SNr, PUT (late-onset only) GP, CN, RN	68 v 46	MRI
	Zhao et al., 2013	**Increased**	Plasma	N/A	238 v 302	AAS
Magnesium	Alimonti et al., 2007	No change	CSF	N/A	42 v 20	ICP-AES
	Bocca et al., 2006	No change No change No change **Decreased**	CSF Plasma Serum Urine	N/A	91 v 18	ICP–MS / ICP-AES
	Fukushima et al., 2013	No change	Urine	N/A	71 v 70	AAS
	Gazzaniga et al., 1992	No change	CSF	N/A	11 v 22	AAS
	Genoud et al., 2017	No change	Brain	SN, OCC, FG	11 v 11	ICP–MS
	Jimenez-Jimenez et al., 1996	No change No change	Serum Urine	N/A	29 v 27	AAS
	Kumudini et al., 2014	No change	Serum	N/A	150 v 170	ICP–MS
	Sanyal et al., 2016	**Decreased**	CSF	N/A	60 v 50	AAS

		No change	Serum		250 v 280	
	Verma et al., 2016	**Increased**	Plasma	N/A	225 v 125	ICP–MS
Manganese	Alimonti et al., 2007	No change	CSF	N/A	42 v 20	ICP-AES
	Bocca et al., 2006	No change No change No change **Decreased**	CSF Plasma Serum Urine	N/A	91 v 18	ICP–MS / ICP-AES
	Fukushima et al., 2013	No change	Urine	N/A	71 v 70	AAS
	Gazzaniga et al., 1992	No change	CSF	N/A	11 v 22	AAS
	Genoud et al., 2017	No change	Brain	SN, OCC, FG	11 v 11	ICP–MS
	Jimenez-Jimenez et al., 1996	No change No change	Serum Urine	N/A	29 v 27	AAS
	Kumudini et al., 2014	No change	Serum	N/A	150 v 170	ICP–MS
	Sanyal et al., 2016	**Decreased** No change	CSF Serum	N/A	60 v 50 250 v 280	AAS
	Verma et al., 2016	**Increased**	Plasma	N/A	225 v 125	ICP–MS
Potassium	Ahmed et al., 2010	**Increased**	Serum	N/A	45 v 42	ICP–MS

	Hegde et al., 2004	Increased	Serum	N/A	52 v 25	ICP-AES
Selenium	Aguilar et al., 1998	No change	Serum	N/A	28 v 43	AAS
	Ahmed et al., 2010	No change	Serum	N/A	45 v 42	ICP–MS
	Younes-Mhenni et al., 2013	No change	Serum	N/A	48 v 36	AAS
	Zhao et al., 2013	Increased	Plasma	N/A	328 v 302	AAS
Sodium	Ahmed et al., 2010	Increased	Serum	N/A	45 v 42	ICP–MS
	Hegde et al., 2004	Increased	Serum	N/A	52 v 25	ICP-AES
Zinc	Ahmed et al., 2010	No change	Serum	N/A	45 v 42	ICP–MS
	Alimonti et al., 2007	No change	CSF	N/A	42 v 20	ICP-AES
	Bocca et al., 2006	No change Increased No change No change	CSF Plasma Serum Urine	N/A	91 v 18	ICP–MS / ICP-AES
	Brewer et al., 2010b	Decreased Decreased	Serum Urine	N/A	29 v 30	AAS AAS
	Fukushima et al., 2013	No change No change	Serum Urine	N/A	82 v 82 71 v 70	ICP–MS
	Genoud et al., 2017	No change	Brain	SN, OCC, FG	11 v 11	ICP–MS
	Hegde et al., 2004	Decreased	Serum	N/A	52 v 25	ICP-AES
	Kim et al., 2018	No change	Serum	N/A	325 v 304	ICP–MS

	Sanyal et al., 2016	**Decreased** No change	CSF Serum	N/A	60 v 50 250 v 280	AAS
	Younes-Mhenni et al., 2013	No change	Serum	N/A	48 v 36	AAS
	Zhao et al., 2013	**Decreased**	Plasma	N/A	238 v 302	AAS

Supplementary Table 3B – Metabolites in PD

Metabolite	Source	Change	Tissue	Region	N (cases v controls)	Method
6-phosphogluconate			X			
Aconitase			X			
Adenine	Luan et al., 2015a	**Increased**	Urine	N/A	297 v 104	LC–MS
Adenosine	McFarland et al., 2013	**Increased (males)**	Brain	Cortex, striatum	17 v 13	HPLC
Alanine	Aasly et al., 2015	No change	CSF	N/A	17 v 19	MRS
	Babu et al., 2018	**Increased**	Serum	N/A	17 v 22	NMR
	Engelborghs et al., 2003	No change	CSF	N/A	28 v 30	HPLC
	Iwasaki et al., 1992	No change	Plasma	N/A	20 v 20	Ion exchange chromatography
	Luan et al., 2015b	**Increased**	Urine	N/A	92 v 65	GC–MS
	Mally et al., 1997	**Increased** No change	CSF Serum	N/A	10 v 10	HPLC
	Molina et al., 1997	**Decreased** No change	CSF Plasma	N/A	31 v 45	Ion exchange chromatography
	Wu et al., 2016	**Increased**	CSF	N/A	22 v 28	NMR
Arginine	Engelborghs et al., 2003	No change	CSF	N/A	28 v 30	HPLC
	Hatano et al., 2016	No change	Serum	N/A	35 v 15	UPLC
	Mally et al., 1997	No change	CSF	N/A	10 v 10	HPLC

		Decreased	Serum			
	Molina et al., 1997	Decreased No change	CSF Plasma	N/A	31 v 45	Ion exchange chromatography
Arginosuccinate	X					
Asparagine	Iwasaki et al., 1992	No change	Plasma	N/A	20 v 20	Ion exchange chromatography
	Jimenez-Jimenez et al., 1996	No change Decreased	CSF Plasma	N/A	31 v 45	Ion exchange chromatography
	Mally et al., 1997	No change No change	CSF Serum	N/A	10 v 10	HPLC
Aspartate	Engelborghs et al., 2003	No change	CSF	N/A	28 v 30	HPLC
	Iwasaki et al., 1992	Increased	Plasma	N/A	20 v 20	Ion exchange chromatography
	Jimenez-Jimenez et al., 1996	No change	Plasma	N/A	31 v 45	Ion exchange chromatography
	Yuan et al., 2013	Decreased	Plasma	N/A	92 v 60	HPLC
Caffeine	Fujimaki et al., 2018	Decreased	Serum	N/A	108 v 31	HPLC
	Hatano et al., 2016	Decreased	Serum	N/A	35 v 15	UPLC
Carnitine	Zhao et al., 2018	Decreased	Plasma	N/A	28 v 18	LC–MS
Citrate	Aasly et al., 2015	No change	CSF	N/A	17 v 19	MRS
	Ahmed et al., 2009	Decreased	Plasma	N/A	43 v 37	NMR
	Babu et al., 2018	Increased	Serum	N/A	17 v 22	NMR
	Glaab et al., 2019	Increased	Plasma	N/A	60 v 15	GC–MS
	Hatano et al., 2016	No change	Serum	N/A	35 v 15	GC–MS
		No change	CSF	N/A	22 v 28	GC–MS & LC–MS

	Wuolikainen et al., 2016	Increased	Plasma			
Citrulline	Engelborghs et al., 2003	No change	CSF	N/A	28 v 30	HPLC
	Han et al., 2017	Increased	Serum	N/A	43 v 42	LC–MS
	Hatano et al., 2016	No change	Serum	N/A	35 v 15	UPLC
	Iwasaki et al., 1992	No change	Plasma	N/A	20 v 20	Ion exchange chromatography
	Molina et al., 1997	Decreased No change	CSF Plasma	N/A	31 v 45	Ion exchange chromatography
Creatine	Aasly et al., 2015	No change	CSF	N/A	17 v 19	MRS
	Hatano et al., 2016	No change	Serum	N/A	35 v 15	UPLC
	Wu et al., 2016	Increased	CSF	N/A	22 v 28	NMR
Creatinine	Aasly et al., 2015	No change	CSF	N/A	17 v 19	MRS
	Annanmaki et al., 2007	No change	Plasma	N/A	40 v 29	Enzymatic Assay
	Hatano et al., 2016	Decreased	Serum	N/A	35 v 15	UPLC
	Wu et al., 2016	No change	CSF	N/A	22 v 28	NMR
	Wuolikainen et al., 2016	Decreased No change	CSF Plasma	N/A	22 v 28	GC–MS & LC–MS
Cysteine			X			
Ethanolamine	Molina et al., 1997	Decreased No change	CSF Plasma	N/A	31 v 45	Ion exchange chromatography
	Stoessel et al., 2018	Decreased No change	Plasma CSF	N/A	76 v 38	LC–MS
Fructose	Hatano et al., 2016	No change	Plasma	N/A	43 v 37	NMR

	Trezzi et al., 2017	Increased	CSF	N/A	44 v 43	GC–MS
	Troisi et al., 2019	Decreased	Blood	N/A	84 v 42	GC–MS
	Wu et al., 2016	Increased	CSF	N/A	22 v 28	NMR
Fructose-6-phosphate	X					
Fumarate	Hatano et al., 2016	No change	Serum	N/A	35 v 15	GC–MS
Glucono-1,5-lactone-6-phosphate	X					
Glucose	Aasly et al., 2015	No change	CSF	N/A	17 v 19	MRS
	Bohnen et al., 2011	Increased	Brain	Cortex	23 v 27	PET
	Hatano et al., 2016	Decreased	Serum	N/A	35 v 15	GC–MS
	Marques et al., 2018	No change (fasting) Decreased (fasting) Increased (after intake) No change (after intake)	Plasma Urine Plasma Urine	N/A	50 v 50	Spectrophotometry
	Trezzi et al., 2017	Increased	CSF	N/A	44 v 43	GC–MS
	Wu et al., 2016	Increased	CSF	N/A	22 v 28	NMR
	Wuolikainen et al., 2016	Increased No change	CSF Plasma	N/A	22 v 28	GC–MS & LC–MS
Glucose-6-phosphate	Dunn et al., 2014	Decreased	Brain	Cortex	21 v 13	ELISA
Glutamate	Babu et al., 2018	Increased	Serum	N/A	17 v 22	NMR
	Engelborghs et al., 2003	No change	CSF	N/A	28 v 30	HPLC

	Iwasaki et al., 1992	Increased	Plasma	N/A	20 v 20	Ion exchange chromatography
	Jimenez-Jimenez et al., 1996	No change No change	CSF Plasma	N/A	31 v 45	Ion exchange chromatography
	Mally et al., 1997	Decreased No change	CSF Serum	N/A	10 v 10	HPLC
	Yuan et al., 2013	Decreased	Plasma	N/A	51 v 48	HPLC
Glutamic acid	Fiandaca et al., 2018	Decreased	Serum	N/A	40 v 20	UPLC–MS
	Troisi et al., 2019	Decreased	Blood	N/A	16 v 42	GC–MS
Glutamine	Aasly et al., 2015	Increased	CSF	N/A	17 v 19	MRS
	Babu et al., 2018	Increased	Serum	N/A	17 v 22	NMR
	Engelborghs et al., 2003	No change	CSF	N/A	28 v 30	HPLC
	Iwasaki et al., 1992	No change	Plasma	N/A	20 v 20	Ion exchange chromatography
	Jimenez-Jimenez et al., 1996	No change Decreased	CSF Plasma	N/A	31 v 45	Ion exchange chromatography
	Mally et al., 1997	Increased No change	CSF Serum	N/A	10 v 10	HPLC
	Wu et al., 2016	No change	CSF	N/A	22 v 28	NMR
	Yuan et al., 2013	No change	Plasma	N/A	51 v 48	HPLC
Glycine	Engelborghs et al., 2003	No change	CSF	N/A	28 v 30	HPLC
	Hatano et al., 2016	Increased	Serum	N/A	35 v 15	UPLC
	Iwasaki et al., 1992	Increased	Plasma	N/A	20 v 20	Ion exchange chromatography
		No change	CSF	N/A	31 v 45	

	Jimenez-Jimenez et al., 1996	Decreased	Plasma			Ion exchange chromatography
	Luan et al., 2015a	Increased	Urine	N/A	297 v 104	LC–MS
	Luan et al., 2015b	Increased	Urine	N/A	92 v 65	GC–MS
	Mally et al., 1997	No change No change	CSF Serum	N/A	10 v 10	HPLC
	Yuan et al., 2013	No change	Plasma	N/A	51 v 48	HPLC
GSH	Bogdanov et al., 2008	Increased	Plasma	N/A	66 v 25	LCECA
	Sian et al., 1994	Decreased	Brain	SN	9 v 9	Enzymatic Assay
GSSG	Sian et al., 1994	No change	Brain	SN	9 v 9	Enzymatic Assay
Guanosine	Johansen et al., 2009	No change	Plasma	N/A	84 v 15	LCECA
Histidine	Babu et al., 2018	Increased	Serum	N/A	17 v 22	NMR
	Engelborghs et al., 2003	No change	CSF	N/A	28 v 30	HPLC
	Luan et al., 2015a	Increased	Urine	N/A	297 v 104	LC–MS
	Mally et al., 1997	No change No change	CSF Serum	N/A	10 v 10	HPLC
	Molina et al., 1997	Decreased No change	CSF Plasma	N/A	31 v 45	Ion exchange chromatography
	Wu et al., 2016	Increased	CSF	N/A	22 v 28	NMR
Homocitrulline	Hatano et al., 2016	No change	Serum	N/A	35 v 15	UPLC

Homovanillate	Chia et al., 1995	Unchanged (with L-DOPA) **Decreased (following L-DOPA withdrawal)**	CSF	N/A	22 v 26 22 v 26	HPLC
	Hatano et al., 2016	**Increased**	Serum	N/A	35 v 15	UPLC
	Zubenko et al., 1986	No change	CSF	N/A	10 v 15	LC–MS
Hypoxanthine	Johansen et al., 2009	**Decreased**	Plasma	N/A	84 v 15	LCECA
	Luan et al., 2015b	**Increased**	Urine	N/A	297 v 104	LC–MS
	McFarland et al., 2013	No change	Brain	Cortex, STR	17 v 13	HPLC
	Troisi et al., 2019	**Decreased**	Blood	N/A	16 v 42	GC–MS
	Wuolikainen et al., 2016	No change **Decreased**	CSF Plasma	N/A	22 v 28	GC–MS & LC–MS
Indolacetate	Hatano et al., 2016	**Decreased**	Serum	N/A	35 v 15	UPLC
Inosine	McFarland et al., 2013	**Increased (males)**	Brain	Cortex, striatum	17 v 13	HPLC
Isoleucine	Babu et al., 2018	**Increased**	Serum	N/A	17 v 22	NMR
	Engelborghs et al., 2003	No change	CSF	N/A	28 v 30	HPLC
	Iwasaki et al., 1992	No change	Plasma	N/A	20 v 20	Ion exchange chromatography
	Luan et al., 2015b	**Increased**	Urine	N/A	92 v 65	GC–MS
	Mally et al., 1997	**Decreased** No change	CSF Serum	N/A	10 v 10	HPLC

	Molina et al., 1997	Decreased No change	CSF Plasma	N/A	31 v 45	Ion exchange chromatography
	Wu et al., 2016	Increased	CSF	N/A	22 v 28	NMR
	Wuolikainen et al., 2016	Increased Increased	CSF Plasma	N/A	22 v 28	GC–MS & LC–MS
Kynurenic Acid	Oxenkrug et al., 2017	Increased	Serum	N/A	18 v 24	HPLC
Kynurenine	Chang et al., 2018	Decreased	Plasma	N/A	82 v 82	LC-TOF-MS
	Fiandaca et al., 2018	Decreased	Plasma	N/A	40 v 20	UPLC–MS
	Hatano et al., 2016	No change	Serum	N/A	35 v 15	UPLC
	Luan et al., 2015a	Increased	Urine	N/A	297 v 104	LC–MS
	Oxenkrug et al., 2017	Increased	Serum	N/A	18 v 24	HPLC
Lactate	Aasly et al., 2015	No change	CSF	N/A	17 v 19	MRS
	Babu et al., 2018	Increased	Serum	N/A	17 v 22	NMR
	Hatano et al., 2016	No change	Serum	N/A	35 v 15	UPLC
Leucine	Aasly et al., 2015	No change	CSF	N/A	17 v 19	MRS
	Engelborghs et al., 2003	No change	CSF	N/A	28 v 30	HPLC
	Fiandaca et al., 2018	Decreased	Serum	N/A	40 v 20	UPLC–MS
	Iwasaki et al., 1992	No change	Plasma	N/A	20 v 20	Ion exchange chromatography
	Luan et al., 2015b	Increased	Urine	N/A	92 v 65	GC–MS
	Mally et al., 1997	No change No change	CSF Serum	N/A	10 v 10	HPLC
	Molina et al., 1997	Decreased Decreased	CSF Plasma	N/A	31 v 45	Ion exchange chromatography

	Troisi et al., 2019	Increased	Blood	N/A	16 v 42	GC–MS
	Wu et al., 2016	Increased	CSF	N/A	22 v 28	NMR
Lysine	Engelborghs et al., 2003	No change	CSF	N/A	28 v 30	HPLC
	Luan et al., 2015b	Increased	Urine	N/A	92 v 65	GC–MS
	Mally et al., 1997	Decreased No change	CSF Serum	N/A	10 v 10	HPLC
	Molina et al., 1997	Decreased No change	CSF Plasma	N/A	31 v 45	Ion exchange chromatography
	Wu et al., 2016	No change	CSF	N/A	22 v 28	NMR
Malate	Ahmed et al., 2009	Decreased	Plasma	N/A	43 v 37	NMR
	Hatano et al., 2016	No change	Serum	N/A	35 v 15	GC–MS
Mannitol	Hatano et al., 2016	Increased	Serum	N/A	35 v 15	GC–MS
Mannose	Glaab et al., 2019	Increased	Plasma	N/A	60 v 15	GC–MS
	Hatano et al., 2016	Decreased	Serum	N/A	35 v 15	GC–MS
	Trezzi et al., 2017	Increased	CSF	N/A	44 v 43	GC–MS
	Wu et al., 2016	Decreased	CSF	N/A	22 v 28	NMR
Methionine	Engelborghs et al., 2003	No change	CSF	N/A	28 v 30	HPLC
	Fiandaca et al., 2018	Decreased	Serum	N/A	40 v 20	UPLC–MS
	Iwasaki et al., 1992	No change	Plasma	N/A	20 v 20	Ion exchange chromatography
	Mally et al., 1997	No change Decreased	CSF Serum	N/A	10 v 10	HPLC
	Molina et al., 1997	No change Increased	CSF Plasma	N/A	31 v 45	Ion exchange chromatography

	Wuolikainen et al., 2016	No change Increased	CSF Plasma	N/A	22 v 28	GC–MS & LC–MS
NADP+			X			
NADPH	Dunn et al., 2014	Increased	Brain	Cortex, PUT	21 v 13	Colorimetric Assay
Ornithine	Engelborghs et al., 2003	No change	CSF	N/A	28 v 30	HPLC
	Hatano et al., 2016	Increased	Serum	N/A	35 v 15	UPLC
	Iwasaki et al., 1992	No change No change	Plasma Plasma	N/A	20 v 20	Ion exchange chromatography
	Molina et al., 1997	Decreased No change	CSF Plasma	N/A	31 v 45	Ion exchange chromatography
	Wuolikainen et al., 2016	Increased No change	CSF Plasma	N/A	22 v 28	GC–MS & LC–MS
Paraxanthine	Fujimaki et al., 2018	Decreased	Serum	N/A	108 v 31	HPLC
	Hatano et al., 2016	Decreased	Serum	N/A	35 v 15	UPLC
Phenylalanine	Engelborghs et al., 2003	No change	CSF	N/A	28 v 30	HPLC
	Fiandaca et al., 2018	Decreased	Serum	N/A	40 v 20	UPLC–MS
	Hatano et al., 2016	No change	Serum	N/A	35 v 15	UPLC
	Iwasaki et al., 1992	No change	Plasma	N/A	20 v 20	Ion exchange chromatography
	Luan et al., 2015b	Increased	Urine	N/A	92 v 65	GC–MS
	Mally et al., 1997	No change No change	CSF Serum	N/A	10 v 10	HPLC
	Wu et al., 2016	No change	CSF	N/A	22 v 28	NMR
	Zhao et al., 2018	Increased	Plasma	N/A	28 v 18	LC–MS

Phosphoserine	Molina et al., 1997	No change Increased	CSF Plasma	N/A	31 v 45	LC–MS
Proline	Iwasaki et al., 1992	No change	Plasma	N/A	20 v 20	Ion exchange chromatography
	Luan et al., 2015b	Increased	Urine	N/A	92 v 65	GC–MS
Pyruvate	Aasly et al., 2015	No change	CSF	N/A	17 v 19	MRS
	Ahmed et al., 2009	Increased	Plasma	N/A	43 v 37	NMR
	Hatano et al., 2016	No change	Serum	N/A	35 v 15	GC–MS
Ribulose-5-phosphate	X					
Sarcosine	Molina et al., 1997	No change Increased	CSF Plasma	N/A	31 v 45	Ion exchange chromatography
	Stoessel et al., 2018	Increased Decreased	Plasma CSF	N/A	76 v 38	LC–MS
Serine	Engelborghs et al., 2003	No change	CSF	N/A	28 v 30	HPLC
	Iwasaki et al., 1992	No change	Plasma	N/A	20 v 20	Ion exchange chromatography
	Mally et al., 1997	No change No change	CSF Plasma	N/A	10 v 10	HPLC
	Troisi et al., 2019	Decreased	Blood	N/A	16 v 42	GC–MS
Sorbitol	Ahmed et al., 2009	Increased	Plasma	N/A	43 v 37	NMR
	Hatano et al., 2016	No change	Serum	N/A	35 v 15	GC–MS
	Troisi et al., 2019	Increased	Blood	N/A	84 v 42	GC–MS
	Wuolikainen et al., 2016	Increased No change	CSF Plasma	N/A	22 v 28	GC–MS & LC–MS

Succinate	Ahmed et al., 2009	**Decreased**	Plasma	N/A	43 v 37	NMR
	Glaab et al., 2019	**Increased**	Plasma	N/A	60 v 15	GC–MS
	Hatano et al., 2016	No change	Serum	N/A	35 v 15	GC–MS
Sucrose	Hatano et al., 2016	**Increased**	Serum	N/A	35 v 15	UPLC
Taurine	Engelborghs et al., 2003	**Decreased**	CSF	N/A	24 v 30	HPLC
	Iwasaki et al., 1992	No change	Plasma	N/A	20 v 20	Ion exchange chromatography
	Molina et al., 1997	**Decreased** No change	CSF Plasma	N/A	31 v 45	Ion exchange chromatography
	Yuan et al., 2013	**Decreased**	Plasma	N/A	51 v 48	HPLC
Theophylline	Fujimaki et al., 2018	**Decreased**	Serum	N/A	108 v 31	HPLC
	Hatano et al., 2016	**Decreased**	Serum	N/A	35 v 15	UPLC
Threonine	Babu et al., 2018	**Increased**	Serum	N/A	17 v 22	NMR
	Engelborghs et al., 2003	No change	CSF	N/A	28 v 30	HPLC
	Iwasaki et al., 1992	No change	Plasma	N/A	20 v 20	Ion exchange chromatography
	Molina et al., 1997	No change **Increased**	CSF Plasma	N/A	31 v 45	Ion exchange chromatography
	Troisi et al., 2019	**Decreased**	Blood	N/A	16 v 42	GC–MS
Tryptophan	Chang et al., 2018	**Decreased**	Plasma	N/A	82 v 82	LC-TOF-MS
	D'Andrea et al., 2019	No change	Plasma	N/A	48 v 10	UPLC–MS/MS
	Fiandaca et al., 2018	**Decreased**	Serum	N/A	40 v 20	UPLC–MS
	Iwasaki et al., 1992	No change	Plasma	N/A	20 v 20	UPLC
	Luan et al., 2015b	**Increased**	Urine	N/A	92 v 65	GC–MS

	Molina et al., 1997	No change Decreased	CSF Plasma	N/A	31 v 45	Ion exchange chromatography
	Oxenkrug et al., 2017	Decreased	Serum	N/A	18 v 24	HPLC
	Wuolikainen et al., 2016	No change Increased	CSF Plasma	N/A	22 v 28	GC–MS & LC–MS
Tyrosine	D'Andrea et al., 2019	Increased	Plasma	N/A	48 v 10	UPLC–MS/MS
	Engelborghs et al., 2003	No change	CSF	N/A	28 v 30	HPLC
	Hatano et al., 2016	No change	Serum	N/A	35 v 35	UPLC
	Iwasaki et al., 1992	No change	Plasma	N/A	20 v 20	Ion exchange chromatography
	Luan et al., 2015b	Increased	Urine	N/A	92 v 65	GC–MS
	Mally et al., 1997	No change No change	CSF Serum	N/A	10 v 10	HPLC
	Molina et al., 1997	No change Increased	CSF Plasma	N/A	31 v 45	Ion exchange chromatography
	Wu et al., 2016	Increased	CSF	N/A	22 v 28	NMR
Urea	Glaab et al., 2019	Increased	Plasma	N/A	60 v 15	GC–MS
	Hatano et al., 2016	No change	Serum	N/A	35 v 15	GC–MS
	Trezzi et al., 2017	Decreased	CSF	N/A	44 v 43	GC–MS
	Troisi et al., 2019	Decreased	Blood	N/A	84 v 42	GC–MS
Uric Acid	Annanmaki et al., 2007	Decreased	Plasma	N/A	40 v 29	Enzymatic Assay
	Bogdanov et al., 2008	Decreased	Plasma	N/A	66 v 25	LCECA
	Johansen et al., 2009	Decreased	Plasma	N/A	84 v 15	LCECA
	Kim & Lee, 2014	Decreased	Serum	N/A	30 v 25	Enzymatic Assay

	McFarland et al., 2013	Decreased (males)	Brain	Cortex, STR	17 v 13	HPLC
	Sakuta et al., 2017	Decreased	Serum	N/A	100 v 100	Enzymatic Assay
Valine	Aasly et al., 2015	No change	CSF	N/A	17 v 19	MRS
	Babu et al., 2018	Increased	Serum	N/A	17 v 22	NMR
	Engelborghs et al., 2003	No change	CSF	N/A	28 v 30	HPLC
	Hatano et al., 2016	Decreased	Serum	N/A	35 v 15	UPLC
	Iwasaki et al., 1992	No change	Plasma	N/A	20 v 20	Ion exchange chromatography
	Mally et al., 1997	No change Increased	CSF Serum	N/A	10 v 10	HPLC
	Molina et al., 1997	Decreased Decreased	CSF Plasma	N/A	31 v 45	Ion exchange chromatography
	Wu et al., 2016	Increased	CSF	N/A	22 v 28	NMR
	Wuolikainen et al., 2016	No change Increased	CSF Plasma	N/A	22 v 28	GC–MS & LC–MS
Xanthine	Johansen et al., 2009	No change	Plasma	N/A	84 v 15	LCECA
	McFarland et al., 2013	Increased (females)	Brain	Cortex, STR	17 v 13	HPLC
	Wu et al., 2016	No change	CSF	N/A	22 v 28	NMR
Xylulose-5-phosphate	x					
α-aminoadipic acid	Molina et al., 1997	No change Increased	CSF Plasma	N/A	31 v 45	Ion exchange chromatography
	Troisi et al., 2019	Increased	Blood	N/A	84 v 42	GC–MS

α-aminobutyric acid	Luan et al., 2015a	**Increased**	Urine	N/A	297 v 104	LC–MS
	Molina et al., 1997	**Decreased** No change	CSF Plasma	N/A	31 v 45	Ion exchange chromatography
α-ketoglutarate	Gibson et al., 2003	**Decreased**	Brain	CB	19 v 18	Enzymatic Assay
γ glutamyl-cysteine	x					

Supplementary Table 4A – Metals in DLB

Metal	Source	Change	Tissue	Regions	N (cases v controls)	Methods
Calcium	Bostrom et al., 2009	**Increased** **Increased**	CSF Plasma	N/A	29 v 51	ICP–MS
Ceruloplasmin	x					
Copper	Akatsu et al., 2012	**Decreased** No change	Brain	HP AMG	11 v 16	ICP–MS
	Bostrom et al., 2009	**Increased** No change	CSF Plasma	N/A	29 v 51	ICP–MS
	Graham et al., 2014	No change	Brain	NC	15 v 26	ICP–MS
	Magaki et al., 2007	**Decreased** No change	Brain	FC HP	6 v 6	GFAAS
Iron	Akatsu et al., 2012	No change	Brain	HP, AMG	11 v 16	ICP–MS
	Bostrom et al., 2009	No change **Decreased**	CSF Plasma	N/A	29 v 51	ICP–MS
	Graham et al., 2014	No change	Brain	NC	15 v 26	ICP–MS
Magnesium	Bostrom et al., 2009	**Increased** **Increased**	CSF Plasma	N/A	29 v 51	ICP–MS
Manganese	Akatsu et al., 2012	No change	Brain	HP, AMG	11 v 16	ICP–MS
	Bostrom et al., 2009	No change No change	CSF Plasma	N/A	29 v 51	ICP–MS
Potassium	Graham et al., 2015	No change	Brain	PC	15 v 28	ICP–MS
Selenium	x					

Sodium	Graham et al., 2015	No change	Brain	PC	15 v 28	ICP–MS
Zinc	Akatsu et al., 2012	No change	Brain	HP, AMG	11 v 16	ICP–MS
	Bostrom et al., 2009	No change **Decreased**	CSF Plasma	N/A	29 v 51	ICP–MS
	Graham et al., 2014	No change	Brain	NC	15 v 26	ICP–MS

Supplementary Table 4B – Metabolites in DLB

Metabolite	Source	Change	Tissue	Regions	N (cases v controls)	Methods
6-phosphogluconate				X		
Acetyle CoA				X		
Aconitase				X		
Adenine				X		
Adenosine	McFarland et al., 2013	**Increased (males only)**	Brain	FC, TC, STRI	13 v 13	HPLC
Alanine				X		
Arginine	Molina et al., 2002	No change No change	CSF Plasma	N/A	22 v 13	Ion exchange chromatography
Arginosuccinate				X		
Asparagine	Molina et al., 2005	**Increased**	CSF	N/A	21 v 26	Ion exchange chromatography
Aspartate	Molina et al., 2005	No change	CSF	N/A	21 v 26	Ion exchange chromatography
Brain				X		
Caffeine				X		
Carnitine				X		
Citrate				X		
Citrulline	Molina et al., 2002	No change No change	CSF Plasma	N/A	22 v 13	Ion exchange chromatography
Creatine	Zhong et al., 2014	No change	Brain	OL, OCC	19 v 18	MRS
Creatinine				X		

Cysteine	X					
Ethanolamine	X					
Fructose	X					
Fructose-6-phosphate	X					
Fumarate	X					
Glucono-1,5-lactone-6-phosphate	X					
Glucose	X					
Glucose-6-phosphate	X					
Glutamate	Molina et al., 2005	No change	CSF	N/A	21 v 26	Ion exchange chromatography
	Zhong et al., 2014	**Decreased**	Brain	N/A	19 v 18	MRI
Glutamine	X	X	X	X	X	X
GSH	Maetzler et al., 2011	**Decreased**	CSF	N/A	21 v 35	Fluorimetric Assay
GSSG	Maetzler et al., 2011	No change	CSF	N/A	21 v 35	Fluorimetric Assay
Guanine	X					
Guanosine	X					
Histidine	X					
Homocitrulline	X					
Homocysteine	X					
Homovanillate	X					

Hypoxanthine	McFarland et al., 2013	No change	Brain	FC, TC, STR	13 v 13	HPLC
Indolacetate				X		
Inosine	McFarland et al., 2013	**Increased (males only)**	Brain	FC, TC, STR	13 v 13	HPLC
Isoleucine				X		
Kynurenic Acid	Wennstrom et al., 2014	No change	CSF	N/A	18 v 20	HPLC
Kynurenine				X		
Lactate				X		
Leucine				X		
L-serine				X		
Lysine				X		
Malate				X		
Mannitol				X		
Mannose				X		
Methionine				X		
NADP+				X		
NADPH				X		
Ornithine				X		
Paraxanthine				X		
Phenylalanine				X		
Phosphoserine				X		

Proline	X					
Pyruvate	X					
Ribulose-5-phosphate	X					
Sarcosine	X					
Serine	X					
Sorbitol	X					
Succinate	X					
Succinyl-CoA	X					
Sucrose	X					
Taurine	X					
Theophylline	X					
Threonine	X					
Tryptophan	X					
Tyrosine	X					
Urea	X					
Uric Acid	McFarland et al., 2013	**Increased**	Brain	FC, TC, STR	13 v 13	HPLC
Valine						
Xanthine	McFarland et al., 2013	No change	Brain	FC, TC, STR	13 v 13	HPLC
Xylulose-5-phosphate	X					
α-aminoadipic acid	X					
α-aminobutyric acid	X					

α-ketoglutarate	X

Supplementary Table 5A – Metals in HD

Metal	Source	Change	Tissue	Region	N (cases v controls)	Method
Calcium				X		
Ceruloplasmin				X		
Copper	Rosas et al., 2012	**Decreased** No change	Brain	AntCG SFG, PCG, OCC, CB, PALL, PUT	25 v 12	ICP–MS
	Boll et al., 2008	No change	CSF	N/A	23 v 11	AAS
Iron	Di Paola et al., 2014	**Decreased**	Brain	Corpus Callosum	25 v 50	MRI
	Bartzokis et al., 2007	**Increased** **Decreased** No change	Brain	CAUD, PUT, GP FWM, GenuWM HP, THAL, SpleWM	11 v 27	MRI
	Dumas et al., 2012	**Increased**	Brain	CAUD, PUT	27 v 25	MRI
	Rosas et al., 2012	**Increased** No change **Increased** No change	Brain	PALL, CAUD, PUT, Cortex SFG, MFG, AntCG, PCG, SPG, precuneus, OCC SFG, PCG, OCC, PALL, PUT AntCG, CB	25 v 12	ICP–MS
	Sanchez-Casteneda et al., 2013	**Increased**	Brain	GP	12 v 17	MRI
Magnesium				X		
Manganese	Rosas et al., 2012	**Decreased** No change	Brain	SFG, AntCG PCG, OCC, CB, PALL, PUT	25 v 12	ICP–MS

Potassium	X					
Selenium	X					
Sodium	Reetz et al., 2012	**Increased** No change	Brain	Total, CAUD, PUT, PALL, THAL, precuneus, CG, PCG, HP, Insula, PFC, FC, TC, OC AMG, CB, PC	13 v 13	MRI
Zinc	Rosas et al., 2012	**Increased** No change	Brain	PALL, PUT SFG, AntCG, PCG, OCC, CB	25 v 12	ICP–MS

Supplementary Table 5B – Metabolites in HD

Metabolite	Source	Change	Tissue	Region	N (cases v controls)	Method
6-phosphogluconate				X		
Acetyl CoA				X		
Aconitase	Cheng et al., 2016	Decreased	Plasma	N/A	28 v 25	Western Blot
	Naseri et al., 2016	No change	Serum	N/A	8 v 8	Enzymatic Assay
Adenine	Graham et al., 2016	No change	Brain	FL, STRI	14 v 28	NMR
	Patassini et al., 2016	No change	Brain	PUT, MC, SC, GP, CG, SN, MFG, MTG, CB, HP, ENT	9 v 9	GC–MS
Adenosine	Patassini et al., 2016	No change	Brain	PUT, MC, SC, GP, CG, SN, MFG, MTG, CB, HP, ENT	9 v 9	GC–MS
Alanine	Beal et al., 1992	No change	Brain	CB, DN	27 v 20	HPLC
	Bonilla et al., 1988	No change	Brain	PUT, BD10	12 v 13	HPLC
	Cheng et al., 2016	No change	Plasma	N/A	15 v 17	LC-TOF/MS
	Graham et al., 2016	No change	Brain	FL, STRI	14 v 28	NMR
	Nambron et al., 2016	No change	Plasma	N/A	26 v 14	HPLC + Ion exchange chromatography

	Patassini et al., 2016	No change	Brain	PUT, MC, SC, GP, CG, SN, MFG, MTG, CB, HP, ENT	9 v 9	GC–MS
	Reilmann et al., 1995	**Decreased**	Plasma	N/A	16 v 21	HPLC
Arginine	Cheng et al., 2016	No change	Plasma	N/A	15 v 17	LC-TOF/MS
	Gruber et al., 2013	**Decreased**	Plasma	N/A	30 v 29	HPLC
	Nambron et al., 2016	No change **Increased**	Plasma	N/A	26 v 14	HPLC Ion exchange chromatography
	Reilmann et al., 1995	No change	Plasma	N/A	16 v 21	HPLC
Arginosuccinate				X		
Asparagine	Bonilla et al., 1988	No change	Brain	PUT, BD10	12 v 13	HPLC
	Cheng et al., 2016	No change	Plasma	N/A	15 v 17	LC-TOF/MS
	Gruber et al., 2013	**Decreased**	Plasma	N/A	30 v 29	HPLC
	Nambron et al., 2016	No change	Plasma	N/A	26 v 14	HPLC + Ion exchange chromatography
	Beal et al., 1992	**Increased** No change	Brain	CB DN	27 v 20	HPLC
Aspartate	Bonilla et al., 1988	No change **Increased**	Brain	PUT BD10	12 v 13	HPLC

	Cheng et al., 2016	No change	Plasma	N/A	15 v 17	LC-TOF/MS
	Graham et al., 2016	No change **Decreased**	Brain	FL STR	14 v 28	NMR
	Nambron et al., 2016	No change	Plasma	N/A	26 v 14	HPLC + Ion exchange chromatography
Carnitine	X					
Citrate	X					
Citrulline	Cheng et al., 2016	No change	Plasma	N/A	15 v 17	LC-TOF/MS
	Gruber et al., 2013	**Increased**	Plasma	N/A	30 v 29	HPLC
	Graham et al., 2016	No change	Brain	FL, STRI	14 v 28 14 v 14	NMR LC-LTQ-Orbitrap-MS
Creatine	Nambron et al., 2016	No change	Plasma	N/A	26 v 14	HPLC + Ion exchange chromatography
	Unschuld et al., 2012	No change	Brain	PCC	12 v 12	MRS
Creatinine	Cheng et al., 2016	No change	Plasma	N/A	15 v 17	LC-TOF/MS
	Gruber et al., 2013	**Increased**	Plasma	N/A	30 v 29	HPLC
	Patassini et al., 2016	**Decreased** No change	Brain	PUT MC, SC, GP, CG, SN, MFG, MTG, CB, HP, ENT	9 v 9	GC–MS

	Pena-Sanchez et al., 2015	No change	Plasma	N/A	14 v 29	Enzymatic Assay
Cysteine	Nambron et al., 2016	No change	Plasma	N/A	26 v 14	Western Blot
	Patassini et al., 2016	No change	Brain	PUT, MC, SC, GP, CG, SN, MFG, MTG, CB, HP, ENT	9 v 9	GC–MS
Ethanolamine	Beal et al., 1988	No change	Brain	CB, DN	27 v 20	HPLC
	Graham et al., 2016	No change	Brain	FL, STRI	14 v 28	NMR
	Patassini et al., 2016	**Decreased** No change	Brain	PUT, CG, SN, MTG, CB, HP MC, SC, GP, MFG, TN	9 v 9	GC–MS
Fructose	Patassini et al., 2016	**Increased** No change	Brain	PUT, CB MC, SC, GP, CG, MFG, MTG, HP, ENT	9 v 9	GC–MS
Fructose-6-phosphate				X		
Fumarate				X		
Glucono-1,5-lactone-6-phosphate				X		
Glucose	Nambron et al., 2016	No change	Plasma	N/A	27 v 15	Enzymatic Assay
	Patassini et al., 2016	**Increased** No change	Brain	PUT, SC, GP, SN MC, CG, MFG, MTG, CB, HP, ENT	9 v 9	GC–MS
	Pena-Sanchez et al., 2015	No change	Plasma	N/A	14 v 29	Enzymatic Assay
Glucose-6-phosphate	Beal et al., 1992	No change	Brain	CB, DN	27 v 20	HPLC

Glutamate	Bonilla et al., 1988	**Decreased**	Brain	PUT, BD10	12 v 13	HPLC
	Cheng et al., 2016	No change	Plasma	N/A	15 v 17	LC-TOF/MS
	Patassini et al., 2016	**Increased** No change	Brain	PUT, GP, SN, HP, ENT MC, SC, CG, MFG, MTG, CB	9 v 9	GC–MS
	Patassini et al., 2016	**Increased** No change	Brain	GP PUT, MC, SC, CG, SN, MFG, MTG, CB, HP, ENT	9 v 9	GC–MS
	Graham et al., 2016	No change **Decreased** No change	Brain	FL STRI FL, STRI	14 v 28	NMR LC-LTQ-Orbitrap-MS
Glutamic Acid	Gruber et al., 2013	**Decreased**	Plasma	N/A	30 v 29	HPLC
	Nambron et al., 2016	No change	Plasma	N/A	26 v 14	HPLC + Ion exchange chromatography
	Bonilla et al., 1988	No change	Brain	PUT, BD10	12 v 13	HPLC
Glutamine	Cheng et al., 2016	No change	Plasma	N/A	15 v 17	LC-TOF/MS
	Graham et al., 2016	No change	Brain	FL, STRI	14 v 28	NMR
	Gruber et al., 2013	**Decreased**	Plasma	N/A	30 v 29	HPLC
	Nambron et al., 2016	No change	Plasma	N/A	26 v 14	HPLC + Ion exchange chromatography

	Unschuld et al., 2012	Decreased	Brain	PCC	12 v 12	MRS
	Unschuld et al., 2012	No change	Brain	PCC	12 v 12	MRS
Glycine	Bonilla et al., 1988	No change Increased	Brain	PUT BD10	12 v 13	HPLC
	Cheng et al., 2016	Increased	Plasma	N/A	15 v 17	LC-TOF/MS
	Graham et al., 2016	No change Decreased	Brain	FL STRI	14 v 28	NMR
	Nambron et al., 2016	No change	Plasma	N/A	26 v 14	HPLC + Ion exchange chromatography
	Patassini et al., 2016	Increased Decreased No change	Brain	PUT CB MC, SC, GP, CG, SN, MFG, MTG, HP, ENT	9 v 9	GC–MS
GSH	Beal et al., 1992	Decreased No change	Brain	FP, ITG, MTG PCG, FC, STG, CBC, CAUD	Various	HPLC
	Klepac et al., 2007	Decreased	Plasma	N/A	19 v 47	Spectrophotometry
	Pena-Sanchez et al., 2015	No change	Plasma	N/A	14 v 29	Enzymatic Assay
	Unschuld et al., 2012	No change	Brain	PCC	12 v 12	MRS
GSSG	X					
Guanine	X					

Guanosine	Beal et al., 1992	**Increased** No change	Brain	STG PCG, FC, GP, ITG, MTG, CBC, CAUD	Various	HPLC
	Patassini et al., 2016	**Increased** No change	Brain	MFG PUT, MC, SC, GP, CG, SN, MTG, CB, HP, ENT	9 v 9	GC–MS
	Rosas et al., 2015	No change	Plasma	N/A	102 v 140	LC–MS
Histidine	Bonilla et al., 1988	No change **Decreased**	Brain	PUT BD10	12 v 13	HPLC
	Cheng et al., 2016	No change	Plasma	N/A	15 v 17	LC-TOF/MS
	Gruber et al., 2013	**Decreased**	Plasma	N/A	30 v 29	HPLC
	Nambron et al., 2016	No change	Plasma	N/A	26 v 14	HPLC + Ion exchange chromatography
	Reilmann et al., 1995	No change	Plasma	N/A	16 v 21	HPLC
Homocitrulline	Graham et al., 2016	No change	Brain	FL, STR	14 v 28	NMR
Homocysteine				X		
Homovanillate	Beal et al., 1992	No change	Brain	PCG, FC, FP, ITG, MTG, STG, CBC, CAUD	Various	HPLC
	Markianos et al., 2009	**Increased**	Plasma	N/A	90 v 60	HPLC

	Rosas et al., 2015	Increased	Plasma	N/A	102 v 40	LC–MS
	Ruiz et al., 1995	Decreased	CSF	N/A	38 v 15	LC–MS
Hypoxanthine	Graham et al., 2016	No change	Brain	FL, STR	14 v 28	NMR
	Patassini et al., 2016	Decreased No change	Brain	PUT, SC, SN, MTG, CB, HP MC, GP, CG, MFG, ENT	9 v 9	GC–MS
	Rosas et al., 2015	No change	Plasma	N/A	102 v 140	LC–MS
Indolacetate				X		
Inosine	Graham et al., 2016	No change Increased	Brain	FL STR	14 v 28	NMR
	Bonilla et al., 1988	No change	Brain	PUT, BD10	12 v 13	HPLC
Isoleucine	Cheng et al., 2016	Decreased	Plasma	N/A	15 v 17	LC-TOF/MS
	Graham et al., 2016	No change	Brain	FL, STR	14 v 28	NMR
	Nambron et al., 2016	No change	Plasma	N/A	26 v 14	HPLC + Ion exchange chromatography
	Patassini et al., 2016	Increased No change	Brain	PUT MC, SC, GP, CG, SN, MFG, MTG, CB, HP, ENT	9 v 9	GC–MS
	Patassini et al., 2016	Decreased No change	Brain	PUT, MC, SC, GP, CG, SN, MFG, MTG, ENT CB, HP	9 v 9	GC–MS

	Reilmann et al., 1995	Decreased	Plasma	N/A	16 v 21	HPLC
Kynurenic Acid	Beal et al., 1992	Decreased No change	Brain	PCG, FC, ITG, MTG, STG FP, CBC, CAUD	Various	HPLC
	Beal et al., 1988	Decreased No change	Brain	ITG, MTG PCG, FC, FP, STG, CBC, CAUD	Various	HPLC
Kynurenine	Cheng et al., 2016	No change	Plasma	N/A	15 v 17	LC-TOF/MS
	Graham et al., 2016	No change Decreased	Brain	FL STR	14 v 14	LC-LTQ-Orbitrap-MS
Kynurenine	Rosas et al., 2015	Decreased	Plasma	N/A	102 v 140	LC–MS
Lactate	Martin et al., 2007	Increased No change	Brain CSF	P-OL, CB N/A	23 v 28	MRS
	Nambron et al., 2016	No change	Plasma	N/A	12 v 12	Clinical Assay
Leucine	Bonilla et al., 1988	No change	Brain	PUT, BD10	12 v 13	HPLC
	Cheng et al., 2016	No change	Plasma	N/A	15 v 17	LC-TOF/MS
	Graham et al., 2016	Decreased	Brain	FL, STR	14 v 28	NMR
	Gruber et al., 2013	Decreased	Plasma	N/A	30 v 29	HPLC

	Nambron et al., 2016	No change	Plasma	N/A	26 v 14	HPLC + Ion exchange chromatography
	Patassini et al., 2016	**Decreased** No change	Brain	PUT, MC, SC, GP, CG, SN, MFG, MTG, ENT CB, HP	9 v 9	GC–MS
	Reilmann et al., 1995	No change	Plasma	N/A	16 v 21	HPLC
Lysine	Bonilla et al., 1988	No change **Decreased**	Brain	PUT BD10	12 v 13	HPLC
	Cheng et al., 2016	No change	Plasma	N/A	15 v 17	LC-TOF/MS
	Nambron et al., 2016	No change	Plasma	N/A	26 v 14	HPLC + Ion exchange chromatography
	Patassini et al., 2016	**Decreased** No change	Brain	PUT, GP, MFG, HP MC, SC, CG, SN, MTG, CB, ENT	9 v 9	GC–MS
	Reilmann et al., 1995	No change	Plasma	N/A	16 v 21	HPLC
Malate	X					
Mannitol	Patassini et al., 2016	No change	Brain	PUT, MC, SC, GP, CG, SN, MFG, MTG, CB, HP, ENT	9 v 9	GC–MS
Mannose	X					
Methionine	Bonilla et al., 1988	No change	Brain	PUT, BD10	12 v 13	HPLC
	Cheng et al., 2016	No change	Plasma	N/A	15 v 17	LC-TOF/MS

	Gruber et al., 2013	Decreased	Plasma	N/A	30 v 29	HPLC
	Nambron et al., 2016	No change	Plasma	N/A	26 v 14	HPLC + Ion exchange chromatography
	Patassini et al., 2016	Decreased No change	Brain	HP PUT, MC, SC, GP, CG, SN, MFG, MTG, CB, ENT	9 v 9	GC–MS
NADP+	X					
NADPH	X					
Ornithine	Cheng et al., 2016	No change	Plasma	N/A	15 v 17	LC-TOF/MS
	Gruber et al., 2013	Increased	Plasma	N/A	30 v 29	HPLC
	Nambron et al., 2016	No change	Plasma	N/A	26 v 14	HPLC + Ion exchange chromatography
	Patassini et al., 2016	Decreased No change	Brain	PUT, GP, HP MC, SC, CG, SN, MFG, MTG, CB, ENT	9 v 9	GC–MS
	Reilmann et al., 1995	No change	Plasma	N/A	16 v 21	HPLC
Oxaloacetate	X					
Paraxathine	Rosas et al., 2015	No change	Plasma	N/A	102 v 140	LC–MS
Phenylalanine	Bonilla et al., 1988	No change	Brain	PUT, BD10	12 v 13	HPLC

	Cheng et al., 2016	No change	Plasma	N/A	15 v 17	LC-TOF/MS
	Graham et al., 2016	**Decreased**	Brain	FL, STR	14 v 28	NMR
	Nambron et al., 2016	**Increased**	Plasma	N/A	26 v 14	HPLC + Ion exchange chromatography
	Patassini et al., 2016	**Increased** No change	Brain	PUT MC, SC, GP, CG, SN, MFG, MTG, CB, HP, ENT	9 v 9	GC–MS
Phosphoserine	X					
Proline	Cheng et al., 2016	No change	Plasma	N/A	15 v 17	LC-TOF/MS
	Gruber et al., 2013	**Increased**	Plasma	N/A	30 v 29	HPLC
	Nambron et al., 2016	No change	Plasma	N/A	26 v 14	HPLC + Ion exchange chromatography
	Patassini et al., 2016	**Decreased** No change	Brain	PUT, SC, CB, HP MC, GP, CG, SN, MFG, MTG, ENT	9 v 9	GC–MS
	Reilmann et al., 1995	No change	Plasma	N/A	16 v 21	HPLC
Pyruvate	Patassini et al., 2016	No change	Brain	PUT, MC, SC, GP, CG, SN, MFG, MTG, CB, HP, ENT	9 v 9	GC–MS
Ribulose-5-phosphate	Patassini et al., 2016	No change	Brain	PUT, MC, SC, GP, CG, SN, MFG, MTG, CB, HP, ENT	9 v 9	GC–MS

Sarcosine	Cheng et al., 2016	No change	Plasma	N/A	15 v 17	LC-TOF/MS
Serine	Bonilla et al., 1988	No change **Increased**	Brain	PUT BD10	12 v 13	HPLC
	Cheng et al., 2016	No change	Plasma	N/A	15 v 17	LC-TOF/MS
	Gruber et al., 2013	**Decreased**	Plasma	N/A	30 v 29	HPLC
	Nambron et al., 2016	No change	Plasma	N/A	26 v 14	HPLC + Ion exchange chromatography
	Patassini et al., 2016	**Decreased** No change	Brain	PUT, SC, SN, MTG, CB, HP MC, GP, CG, MFG, ENT	9 v 9	GC–MS
	Reilmann et al., 1995	No change	Plasma	N/A	16 v 21	HPLC
Sorbitol	Patassini et al., 2016	**Increased** No change	Brain	PUT, SC, MFG MC, GP, CG, SN, MTG, CB, HP, ENT	9 v 9	GC–MS
Succinate	Graham et al., 2016	No change	Brain	FL, STR	14 v 28	NMR
	Patassini et al., 2016	No change	Brain	PUT, MC, SC, GP, CG, SN, MFG, MTG, CB, HP, ENT	9 v 9	GC–MS
Succinyl-CoA				X		
Sucrose				X		
Taurine	Beal et al., 1992	No change	Brain	CB, DN	27 v 20	HPLC
	Bonilla et al., 1988	No change	Brain	PUT, MC, SC, GP, CG, SN, MFG, MTG, CB, HP, ENT	9 v 9	GC–MS

	Cheng et al., 2016	**Decreased**	Plasma	N/A	15 v 17	LC-TOF/MS
	Graham et al., 2016	No change **Increased** No change	Brain	FL STR FL, STR	14 v 28	NMR LC-LTQ-Orbitrap-MS
	Nambron et al., 2016	No change	Plasma	N/A	26 v 14	HPLC + Ion exchange chromatography
Theophylline				X		
Threonine	Bonilla et al., 1988	No change	Brain	PUT, BD10	12 v 13	HPLC
	Cheng et al., 2016	No change	Plasma	N/A	15 v 17	LC-TOF/MS
	Graham et al., 2016	No change	Brain	FL, STR	14 v 28	NMR
	Gruber et al., 2013	**Decreased**	Plasma	N/A	30 v 29	HPLC
	Nambron et al., 2016	No change	Plasma	N/A	26 v 14	HPLC + Ion exchange chromatography
	Patassini et al., 2016	**Decreased** No change	Brain	SN, MTG, CB, HP PUT, MC, SC, GP, CG, MFG, ENT	9 v 9	GC–MS
	Reilmann et al., 1995	No change	Plasma	N/A	16 v 21	HPLC
Tryptophan	Beal et al., 1992	**Decreased** No change	Brain	ITG PCG, FC, FP, MTG, STG, CBC, CAUD	Various	HPLC

	Bonilla et al., 1998	No change	Brain	PUT, BD10	12 v 13	HPLC
	Cheng et al., 2016	No change	Plasma	N/A	15 v 17	LC-TOF/MS
	Nambron et al., 2016	No change	Plasma	N/A	26 v 14	Ion exchange chromatography
	Patassini et al., 2016	Increased No change	Brain	PUT MC, SC, GP, CG, SN, MFG, MTG, CB, HP, ENT	9 v 9	GC–MS
	Rosas et al., 2015	No change	Plasma	N/A	102 v 140	LC–MS
Tyrosine	Beal et al., 1992	Decreased No change	Brain	ITG, MTG PCG, FC, FP, STG, CBC, CAUD	Various	HPLC
	Bonilla et al., 1988	No change	Brain	PUT, BD10	12 v 13	HPLC
	Cheng et al., 2016	No change	Plasma	N/A	15 v 17	LC-TOF/MS
	Graham et al., 2016	Decreased	Brain	FL, STR	14 v 28	NMR
	Nambron et al., 2016	Increased No change	Plasma	N/A	26 v 14	HPLC Ion exchange chromatography
	Patassini et al., 2016	Increased No change	Brain	PUT MC, SC, GP, CG, SN, MFG, MTG, CB, HP, ENT	9 v 9	GC–MS

	Reilmann et al., 1995	No change	Plasma	N/A	16 v 21	HPLC
	Rosas et al., 2015	No change	Plasma	N/A	102 v 140	LC–MS
Urea	Graham et al., 2016	No change **Decreased**	Brain	FL STR	14 v 28	NMR
	Gruber et al., 2013	**Increased**	Plasma	N/A	30 v 29	HPLC
	Handley et al., 2017	**Increased**	Brain	CB, SFG	22 v 14	Assay
	Patassini et al., 2016	**Increased**	Brain	PUT, MC, SC, GP, CG, SN, MFG, MTG, CB, HP, ENT	9 v 9	GC–MS
Uric Acid	Beal et al., 1992	**Decreased** No change	Brain	ITG, CAUD PCG, FC, FP, MTG, STG, CBC	Various	HPLC
	Graham et al., 2016	**Decreased** No change	Brain	FL STR	14 v 14	LC-LTQ-Orbitrap-MS
	Rosas et al., 2015	No change	Plasma	N/A	102 v 140	LC–MS
Valine	Bonilla et al., 1988	No change	Brain	PUT, BD10	12 v 13	HPLC
	Cheng et al., 2016	**Decreased**	Plasma	N/A	15 v 17	LC-TOF/MS
	Graham et al., 2016	No change **Decreased**	Brain	FL STR	14 v 28	NMR
	Gruber et al., 2013	**Decreased**	Plasma	N/A	30 v 29	HPLC

	Nambron et al., 2016	No change	Plasma	N/A	26 v 14	HPLC + Ion exchange chromatography
	Patassini et al., 2016	No change	Brain	PUT, MC, SC, GP, CG, SN, MFG, MTG, CB, HP, ENT	9 v 9	GC–MS
	Reilmann et al., 1995	No change	Plasma	N/A	16 v 21	HPLC
Xanthine	Beal et al., 1992	No change	Brain	PCG, FC, FP, ITG, MTG, STG, CBC, CAUD	Various	HPLC
	Patassini et al., 2016	**Increased** No change	Brain	PUT, MC SC, GP, CG, SN, MFG, MTG, CB, HP, ENT	9 v 9	GC–MS
	Rosas et al., 2015	**Decreased**	Plasma	N/A	102 v 140	LC–MS
Xylulose-5-phosphate	X					
α-aminoadipic acid	X					
α-aminobutyric acid	Bonilla et al., 1998	**Decreased** No change	Brain	PUT BD10	12 v 13	HPLC
	Nambron et al., 2016	No change	Plasma	N/A	26 v 14	HPLC + Ion exchange chromatography
α-ketoglutarate	X					
γ glutamyl-cysteine	X					

Supplementary Table 6: Characteristics of individuals in the Manchester AD cohort

Code	Sex	Age at death	Clinical diagnosis	Braak stage (AD)	APOE Status	Post mortem Delay (hours)	Whole-brain weight (g)	Brain pH	Cause of Death
AD1	M	88	Alzheimer's Disease	V	3/4	75	1027	NA	NA
AD2	M	69	Alzheimer's disease	VI	3/3	96	1160†	NA	NA
AD3	M	65	Alzheimer's disease	VI	3/3	*72**	NA	NA	NA
AD4	F	61	Alzheimer's disease	VI	3/4	130	1120	NA	NA
AD5	F	89	Alzheimer's disease	V-VI	3/3	72	NA	NA	NA
AD6	M	76	Alzheimer's disease	V-VI	3/4	*96**	1359	NA	NA
AD7	M	83	Alzheimer's disease	IV-V	3/3	96	1046†	NA	NA
AD8	F	88	Alzheimer's disease	VI	3/3	72	900†	NA	NA
AD9	M	87	Alzheimer's disease	IV	3/4	49	1066	NA	NA
MC1	F	92	No dementia or brain disease	II	3/4	37	1080†	NA	Myocardial infarction

MC2	F	87	No dementia or brain disease	I-II	3/3	39	1160†	NA	Anteroseptal myocardial infarction; coronary atherosclerosis; left ventricular hypertrophy
MC3	M	89	No dementia or brain disease	II	3/3	27	1400†	NA	Multi-organ failure, septicaemia, cellulitis, heart failure
MC4	M	95	No dementia or brain disease	I-II	3/3	12	1200†	NA	Prostatic carcinoma
MC5	F	87	No dementia or brain disease	0-I	3/4	24	1152	NA	Cardiac failure, COPD, renal impairment, osteoarthritis
MC6	M	84	No dementia or brain disease	I	3/3	69.5	1494	5.84	NA
MC7	F	90	No dementia or brain disease	0-I	3/3	39	1050	NA	Frailty of old age
MC8	F	82	No dementia or brain disease	0-I	3/3	61	1020†	NA	Metastatic ovarian cancer

MC9	F	94	No dementia or brain disease	I-II	3/3	70	1276	5.87	Carcinoma of the Electronic Appendix

*Estimated PMD (provided by the Manchester Brain Bank); †brain weighed at point of fixation by brain bank. Abbreviation: NA, not available

Supplementary Table 7: Characteristics of individuals in the Newcastle cohort

Code	Sex	Age at death	Clinical diagnosis	Braak stage (AD)	APOE Status	Post mortem Delay (hours)	Whole-brain weight (g)	CERAD	Brain pH	Cause of Death
AD19	M	81	Alzheimer's Disease	6	3/4	41	1351	High	7.08	Chest infection
AD20	M	87	Alzheimer's disease	6	3/4	21	1200	High	6.23	Pneumonia
AD21	F	80	Alzheimer's disease	6	4/4	10	985	High	5.35	Bronchopneumonia & Alzheimer’s disease
AD22	F	95	Alzheimer's disease	6	3/4	23	968	Moderate	6.21	Stroke
AD23	M	84	Alzheimer's disease	6	3/4	40	1166	Moderate	6.70	-
AD24	M	86	Alzheimer's disease	6	2/4	9	1066	High	6.47	Bronchopneumonia & metastatic bladder cancer
AD25	M	90	Alzheimer's disease	6	2/3	13	1303	High	6.43	Frailty old age & chest infection & Alzheimer’s disease
AD26	M	86	Alzheimer's disease	6	3/3	40	1043	High	6.34	-
AD27	F	70	Alzheimer's disease	6	4/4	24	959	High	6.46	Alzheimer’s disease
C28	M	88	No dementia or brain disease	1	2/3	28	1400	None	6.30	Chronic lymphocytic leukaemia
C29	M	80	No dementia or brain disease	2	3/3	16	1406	None	6.36	Prostate cancer

C30	M	88	No dementia or brain disease	2	3/3	26	1362	None	6.10	Chronic COPD
C31	F	81	No dementia or brain disease	1	3/3	40	-	-	-	-
C32	M	94	No dementia or brain disease	2	3/4	25	1175	None	6.66	Bronchopneumonia
C33	F	91	No dementia or brain disease	2	3/3	14	1238	None	6.55	Aspiration pneumonia + severe inoperable pharyngeal pouch
C34	M	76	No dementia or brain disease	2	3/4	34	1363	None	6.52	Pneumonic exacerbation of COPD
C35	F	81	No dementia or brain disease	1	-	19	1064	None	6.09	Metastatic liver cancer
C36	M	92	No dementia or brain disease	2	2/3	9	1319	None	6.28	Uro-sepsis + metastatic prostate cancer, liver and adrenal metastasis + CKD3

Presence of a dash – indicates that data is not available.

Supplementary Table 8: Characteristics of individuals in the Auckland AD cohort

Code	Sex	Age at death	Clinical diagnosis	Braak stage (AD)	APOE Status	Post mortem Delay (hours)	Whole-brain weight (g)	Brain pH	Cause of Death
AD19	M	60	Alzheimer's Disease	6	NA	7.0	1020	7.0	Alzheimer’s disease
AD20	F	62	Alzheimer's disease	6	NA	6.0	831	6.0	Alzheimer’s disease
AD21	F	63	Alzheimer's disease	6	NA	7.0	1080	7.0	Bronchopneumonia
AD22	F	70	Alzheimer's disease	5	NA	7.0	1044	7.0	Lung cancer
AD23	M	73	Alzheimer's disease	4	NA	4.0	1287	4.0	GI haemorrhage
AD24	F	74	Alzheimer's disease	5	NA	8.5	1062	8.5	Metastatic cancer
AD25	M	74	Alzheimer's disease	6	NA	12.0	1355	12.0	Pseudomonas bacteraemia
AD26	M	77	Alzheimer's disease	6	NA	4.5	1180	4.5	Myocardial infarction
AD27	M	80	Alzheimer's disease	5	NA	5.5	1039	5.5	Bronchopneumonia/ pulmonary oedema
C19	M	61	No dementia or brain disease	0	NA	7.0	1258	7.0	Ischaemic heart disease
C20	F	64	No dementia or brain disease	0	NA	5.5	1260	5.5	Pulmonary embolism

C21	F	63	No dementia or brain disease	0	NA	12.0	1280	12.0	Ruptured aorta
C22	F	72	No dementia or brain disease	0	NA	9.0	1230	9.0	Emphysema
C23	M	66	No dementia or brain disease	0	NA	9.0	1461	9.0	Ischaemic heart disease
C24	F	76	No dementia or brain disease	2	NA	12.0	1094	12.0	Metastatic carcinoma
C25	M	73	No dementia or brain disease	0	NA	13.0	1315	13.0	Ischaemic heart disease
C26	M	78	No dementia or brain disease	0	NA	7.5	1260	7.5	Ruptured aortic aneurysm
C27	M	78	No dementia or brain disease	0	NA	12.0	1416	12.0	Ruptured MI

Abbreviation: NA = Not available

Supplementary Table 9: Characteristics of Manchester AD experimental cohort

Variable	Controls	AD Cases
Number	9	9
Age	89 (82-95)	83 (61-89)*
Male Sex, n (%)	6 (66.7)	3 (33.3)
Braak Stage	I-II	IV-V****
PMD (hours)	75 (49 – 130)	39 (12 – 70)***
Whole-brain weight (g) †	1160 (1020 – 1494)	1066 (900 – 1359)

Values are: age, PMD, Braak stage, and whole-brain weight median (range); * $p < 0.05$, *** $p < 0.001$, **** $p < 0.0001$. † Whole-brain weights were unavailable for two AD cases.

Supplementary Table 10: Characteristics of Newcastle experimental cohort

Variable	Controls	AD Cases
Number	9	9
Age	85 (76-94)	83 (70-95)
Male Gender, n (%)	6 (66.7)	6 (66.7)
Braak Stage	I-II	VI****
PMD (hours)	25 (9 – 40)	25 (9 – 41)
Whole-brain weight (g) †	1235 (1064 – 1406)	1155 (959 – 1351)*
Brain pH	6.4 (6.1 – 6.7)	6.2 (5.4 – 7.1)
CERAD†	None	Moderate – High

Values are: age, PMD, Braak stage, pH, and whole brain weight median (range); * $p < 0.05$, *** $p < 0.001$, **** $p < 0.0001$. Abbreviations: PMD, post mortem delay; CERAD, Consortium to Establish a Registry for Alzheimer's disease. † Whole-brain weight and CERAD stage was not available for one control.

Supplementary Table 11: Characteristics of Auckland AD experimental cohort

Variable	Controls	AD Cases
Number	9	9
Age	72 (61 – 78)	73 (60 – 80)
Male Sex, n (%)	5 (55.6)	5 (55.6)
Braak Stage	0 (0 – II)****	VI (IV – VI)
PMD (hours)	9 (7 – 13)*	7 (4 – 12)
Whole-brain weight (g) †	1062 (831 – 1355)	1260 (1094 – 1461)
Brain pH	7.0 (4.0 – 12)*	9.0 (5.5 – 13.0)

Values are: age, PMD, Braak stage, pH, and whole brain weight median (range); * $p < 0.05$, **** $p < 0.0001$.

Abbreviations: PMD, post mortem delay.

Supplementary Table 12: Characteristics of individuals in the PDD Metallomics cohort

Code	Sex	Age at death	Clinical diagnosis	a-syn Braak stage	Tau Braak stage	Post mortem Delay (hours)	Whole-brain weight (g)	CERAD	Thal	Disease Duration (years)
PDD1	Male	65	PDD	5	0	39	1642	0	2	7
PDD2	Male	80	PDD	6	2	26	1165	0	0	11
PDD3	Male	75	PDD	6	1	48	1399	0	1	6
PDD4	Female	93	PDD	6	3	10	1222	1	3	15
PDD5	Male	66	PDD	6	4	27	1371	2	5	17
PDD6	Female	80	PDD	6	2	20	1152	1	3	23
PDD7	Male	80	PDD	5	2	31	1402	0	0	13
PDD8	Female	78	PDD	6	3	47	1386	0	2	10
PDD9	Female	76	PDD	6	1	9	960	0	2	22
C28	Female	82	No dementia or brain disease	0	2	15	946	0	-	N/A
C29	Female	95	No dementia or brain disease	0	3	28	1126	1	2	N/A
C30	Male	91	No dementia or brain disease	0	2	18	1338	0	2	N/A
C31	Male	85	No dementia or brain disease	0	2	29	989	1	3	N/A
C32	Male	79	No dementia or brain disease	0	2	25	1331	0	1	N/A
C33	Female	87	No dementia or brain disease	0	2	15	978	0	3	N/A

C34	Female	94	No dementia or brain disease	0	2	40	1158	0	5	N/A
C35	Female	88	No dementia or brain disease	0	3	23	1033	0	2	N/A
C36	Male	87	No dementia or brain disease	0	1	48	1301	0	3	N/A

Abbreviation: N/A = not applicable. Presence of a dash – indicates that data is not available.

Supplementary Table 13: Recorded comorbidities, causes of death, and neuropathological diagnoses of PDD Metallomics cohort

Code	Combordities	Cause of Death	Neuropathological Diagnosis
PDD1	Depression; anxiety; halluci-tions	Dementia with Lewy Bodies	Limbic type of Lewy body disease
PDD2	Depression; epilepsy	Bronchopneumonia; PD	Neocortical Lewy body disease
PDD3	Anxiety and depression	Bronchopneumonia; PD	Parkinson's disease; diffuse neocortical Lewy body pathology
PDD4	Osteoperosis; asymptomatic CVD; osteoarthritis	Myocardial infarction; PD	Parkinson's disease; diffuse neocortical Lewy body pathology
PDD5	Actinic keratosis; Depression; Anxiety; Carcinoma	Bronchopneumonia	Neocortical Lewy body disease
PDD6	Depression; hyperthyroid; epilepsy	PD	Neocortical Lewy body disease
PDD7	Depression; anxiety; COPD	Stroke	Limbic type of Lewy body disease
PDD8	Osteoporosis; RBD; hallucinations	Abdominal obstruction; PD	Neocortical lewy body disease
PDD9	Hallucinations; epilepsy; arthritis; glaucoma	PD	Neocortical Lewy body disease
C37	Hypertension; hyperlipidaemia; alcoholism	Lung cancer	Neuritic Braak stage II
C38	Hypertension; hypothyroidism; CKD	Pneumonia; chronic kidney disease	Low AD neuropathologic change
C39	Postural hypotension; bradychardia; scoliosis	Unknown	Low AD neuropathologic change
C40	Pacemaker fitted following aortic valve replacement; bradychardia	Lobar pneumonia	Low AD neuropathologic change
C41	Type 2 diabetes; ischaemic heart disease; family history of PD	Brainstem stroke; bronchopneumonia	Low AD neuropathologic change

C42	CKD, gout, osteoarthritis, polymalgia rheumatica; sleep apnoea; atrial fibrillation; gout	Acutely ischaemic left leg – unsalvageable; cellulitis left foot; atrial fibrillation; cerebrovascular event; COPD; peripheral vascular disease; heart failure	Low AD neuropathologic change; cerebellar infarct
C43	CKD stage 3, osteoperosis, hypercholesterolemia; postural hypotension	Respiratory failure; bronchopneumonia; fractured sternum due to fall	Low AD neuroprehologic change; CAA type II
C44	Osteoperosis, type 2 diabetes, atrial fibrillation, hypertension; short term memory problems (determined to be stress-related)	Old age	Intermediate AD neuropathologic change
C45	Hypertension; arthritis; minor stroke; prostatism; atrial fibrillation	Congestive cardiac failure; atrial fibrillation; mitral regurgitation; chronic kidney disease Stage 5	Low AD neuropathologic change

Supplementary Table 14: Characteristics of individuals in the PDD Metabolomics cohort

Code	Sex	Age at death	Clinical diagnosis	PD Neuropathology	Post mortem Delay (hours)	Whole-brain weight (g)	Cause of Death
C46	Male	61	No dementia present	None observed	12.5	1182	Respiratory failure; heart failure; coronary artery disease
C47	Male	71	No dementia present	None observed	23.9	1371	Acute myocardial infarction; severe coronary artery disease; pulmonary oedema; diabetes mellitus; cardiopulmonary arrest
C48	Male	74	No dementia present	None observed	25.5	1300	Aortic dissection
C49	Male	70	No dementia present	None observed	12.7	1350	Atherosclerotic and hypertensive heart disease
C50	Female	68	No dementia present	None observed	19.1	1270	Acute myocardial infarction; coronary artery disease
C51	Female	65	No dementia present	None observed	19.4	1372	Hypertensive arteriosclerotic cardiovascular disease; morbid obesity; respiratory arrest; suspected embolus
C52	Female	77	No dementia present	None observed	21.4	1135	Pending death certificate

C53	Female	79	No dementia present	None observed	17.8	1300	Acute myocardial infarction; coronary artery disease; atrial fibrillation; COPD
C54	Female	67	No dementia present	None observed	25.9	1382	Pending death certificate
C55 (SN ONLY)	Male	68	No dementia present	0	10.8	1550	Pending death certificate
C56 (SN ONLY)	Male	62	No dementia present	0	21.3	Not available	Diabetes; triple vessel disease of the heart; hyperlipidaemia
PDD10	Male	61	Parkinson's disease dementia	Limbic (transitional)	13.8	1188	Cardiopulmonary arrest; probable acute myocardial infarction; Parkinson's disease
PDD11	Male	79	Parkinson's disease dementia	Limbic (transitional)	16.2	1250	End stage Parkinson's disease
PDD12	Male	71	Parkinson's disease dementia	Brainstem predominant; Braak stage III-IV	16.2	1262	Pending death certificate
PDD13	Male	78	Parkinson's disease dementia	Diffuse neocortical; Braak stage VI	20.4	1520	Respiratory failure; aspiration pneumonia; dysphagia; Parkinson's disease
PDD14	Male	70	Parkinson's disease dementia	Diffuse neocortical	4.3	1218	Aspiration pneumonia; Parkinson's disease

PDD15	Female	69	Parkinson’s disease dementia	Braak stage IV-V	17.5	1187	Pending death certificate
PDD16	Female	81	Parkinson’s disease dementia	Diffuse neocortical	7.0	1415	End stage Parkinson’s disease
PDD17	Female	79	Parkinson’s disease dementia	Limbic (transitional)	21.9	1200	Respiratory failure; Parkinson’s disease
PDD18	Female	67	Parkinson’s disease dementia	Diffuse neocortical	14.5	Not available	Lewy body disease; Parkinson's disease

Supplementary Table 15: Individual Pantothenic Acid Concentrations in PDD Cohort

Sample ID	Status	CB	MCX	PVC	HP	SN	MTG	MED	CG	PONS
C1/C10	C	46.2	50.2	56	59.3	53.2	47.9	43.8	58.7	62.3
C2	C	81.9	49.6	56.2	61.8	61.6	42.5	45.1	45.2	66.4
C3	C	83.7	67.5	62.2	56	68.6	49.8	42.7	61.7	78.3
C4/C11	C	68.1	69.1	53	63.9	48.8	53.8	52.5	63.3	75.3
C5	C	49.4	29.7	37.3	38.1	47.5	24.6	28.7	39.8	47.3
C6	C	157.2	85.9	101.1	160.6	121.4	84.6	53.8	76	129.4
C7	C	58.2	56.5	59.4	58.4	81	50.3	44.2	62.2	64.7
C8	C	73.2	59.6	70.9	72.4	74.4	50.6	68.2	71.9	66.6
C9	C	71.9	44.3	53.6	42.3	88	27.2	41.8	73.3	59.3
PDD1	PDD	45.4	30.4	42.9	44.3	57.1	95.3	36.5	46.8	49.1
PDD2	PDD	28.2	26.7	25.6	28.9	27.6	32.5	24.4	23.8	39
PDD3	PDD	34.1	27.3	29.4	*	30.1	19.7	1.8	36	31
PDD4	PDD	120.4	75.1	105	107.1	83.8	42.9	65	81.6	103.5
PDD5	PDD	65.2	88.3	100.6	126.3	74.3	80.8	39.4	87.7	83.3
PDD6	PDD	33.3	36.2	67.7	73.6	39.1	33.4	3.8	39.7	48.3
PDD7	PDD	26.2	42.3	44.3	34.8	41.8	34.8	23.7	39.8	31.1
PDD8	PDD	17.5	17.8	13.4	19.8	17.1	*	10.7	19.3	16.9
PDD9	PDD	41.2	67.8	62.6	39.3	43.5	14.4	38.4	47.3	31.7
	Fold-Change	0.6	0.8	0.9	0.9	0.6	0.9	0.6	0.8	0.7
	P-Value (Mann–Whitney U)	**0.008**	0.3	0.5	0.4	**0.02**	0.4	**0.008**	0.1	0.0503

*There was insufficient HP tissue for this sample to be included in analysis. Samples highlighted in blue were used in the SN only.

Supplementary Table 16: Individual Urea Concentrations in PDD Cohort

Sample ID	Status	CB	MCX	PVC	HP	SN	MTG	MED	CG	PONS
C1/C10	C	5.5	6.2	5.4	6.2	10	6.3	5.6	7.6	5.6
C2	C	31.1	30.1	26.6	29.4	37.3	38.9	28.7	27.6	30.4
C3	C	15.4	16.6	13.3	14.6	18.7	17.4	12.5	12.7	14
C4/C11	C	4.5	5.2	3.9	4.2	12.8	5.6	4.6	4.6	4.4
C5	C	3.7	3.6	4	4.2	3.7	4.4	3.5	4.8	4
C6	C	3.4	3.6	3.2	3.9	3.7	4	3.5	3.6	3.8
C7	C	10.1	4.9	4.6	5.1	5.5	5.9	4.6	5.6	5.2
C8	C	6.3	6.8	6.8	7.8	5.8	9.3	7.5	7.3	6.8
C9	C	6	6	5.2	6.1	7.5	7	5.7	5.3	5.2
PDD1	PDD	10.4	10.8	11.5	9.8	13	10.1	9.4	13.6	9.7
PDD2	PDD	31.6	31.8	28.2	32.9	37.5	13.8	32.6	39.5	28
PDD3	PDD	53.5	64.6	59.1	*	85.2	40.1	66.8	93	60
PDD4	PDD	12.6	12.9	13.7	13.1	14.5	49.2	13.1	15	12.5
PDD5	PDD	7.6	7.4	7.2	7.8	8.6	17.2	7.2	8.3	7.4
PDD6	PDD	32.2	37.9	32.8	41.6	45.2	106.5	36	45.9	34.4
PDD7	PDD	68.6	70	65.8	79	93.6	106.2	81.7	98.4	67.2
PDD8	PDD	22.9	19.5	17.3	23.8	16	60.2	18.2	16.1	22
PDD9	PDD	77.4	84.1	78.7	92.5	98.2	18.8	85.4	105.6	66.6
	Fold-Change	3.7	4.1	4.3	4.1	3.9	4.3	4.6	5.5	3.9
	P-Value (Mann–Whitney U)	**0.003**	**0.002**	**0.001**	**0.004**	**0.006**	**0.002**	**0.002**	**0.0008**	**0.003**

*There was insufficient HP tissue for this sample to be included in analysis. Samples highlighted in blue were used in the SN only.

Supplementary Figure 1: Significantly Altered Metabolites in PDD

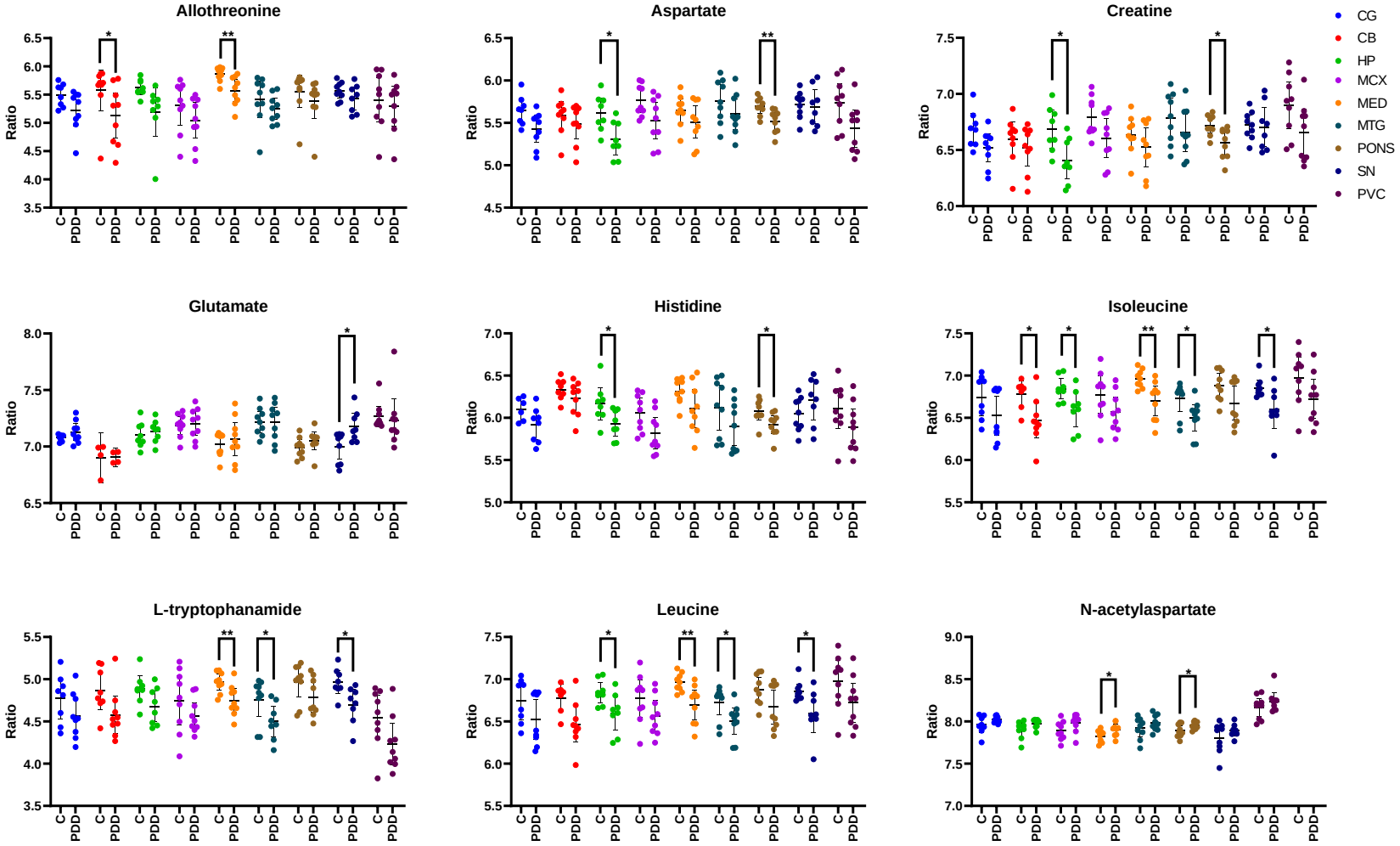

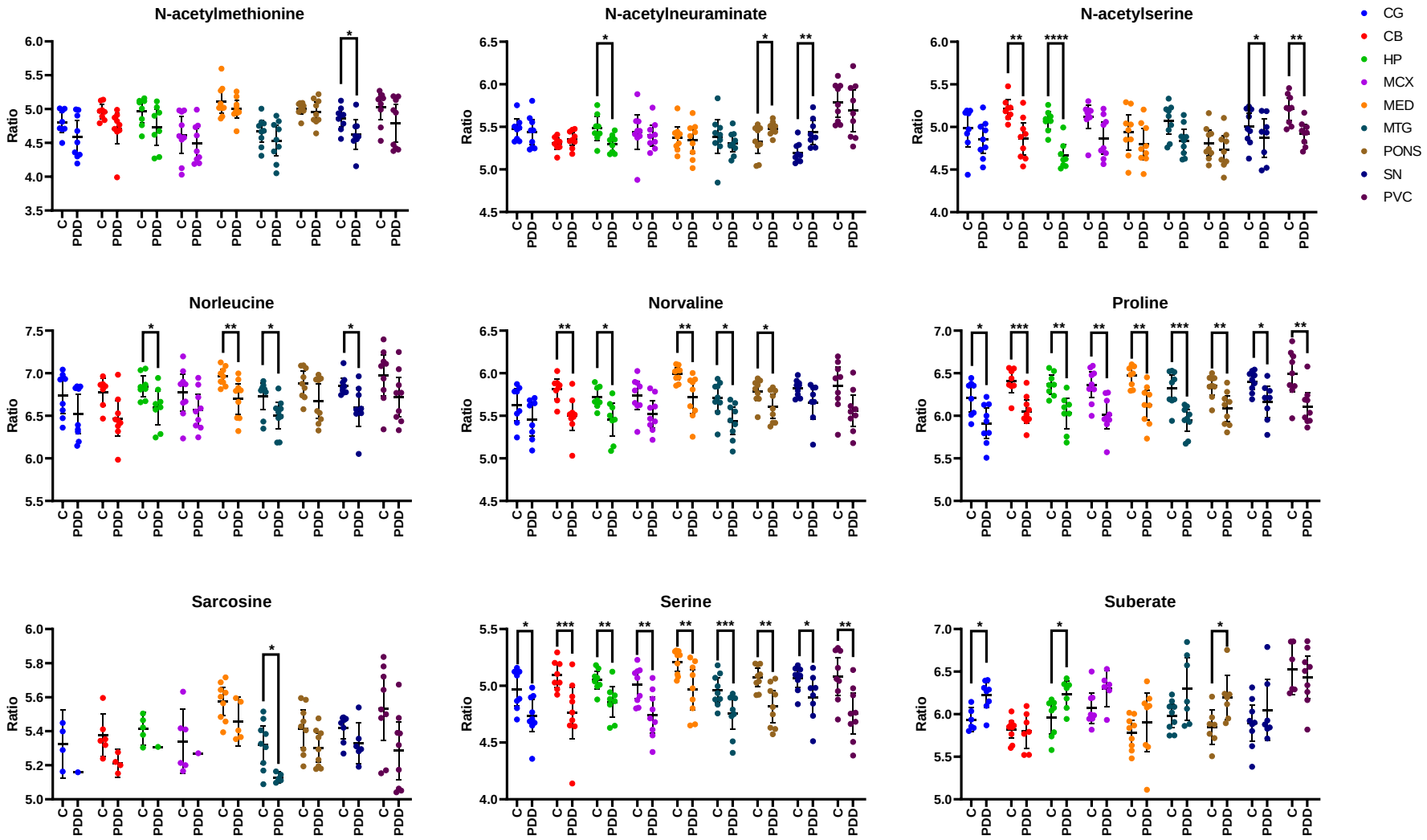
N-acetylmethionine
N-acetylneuraminate
N-acetylserine
Norleucine
Norvaline
Proline
Sarcosine
Serine
Suberate
Ratio
C
PDD
CG
CB
HP
MCX
MED
MTG
PONS
SN
PVC

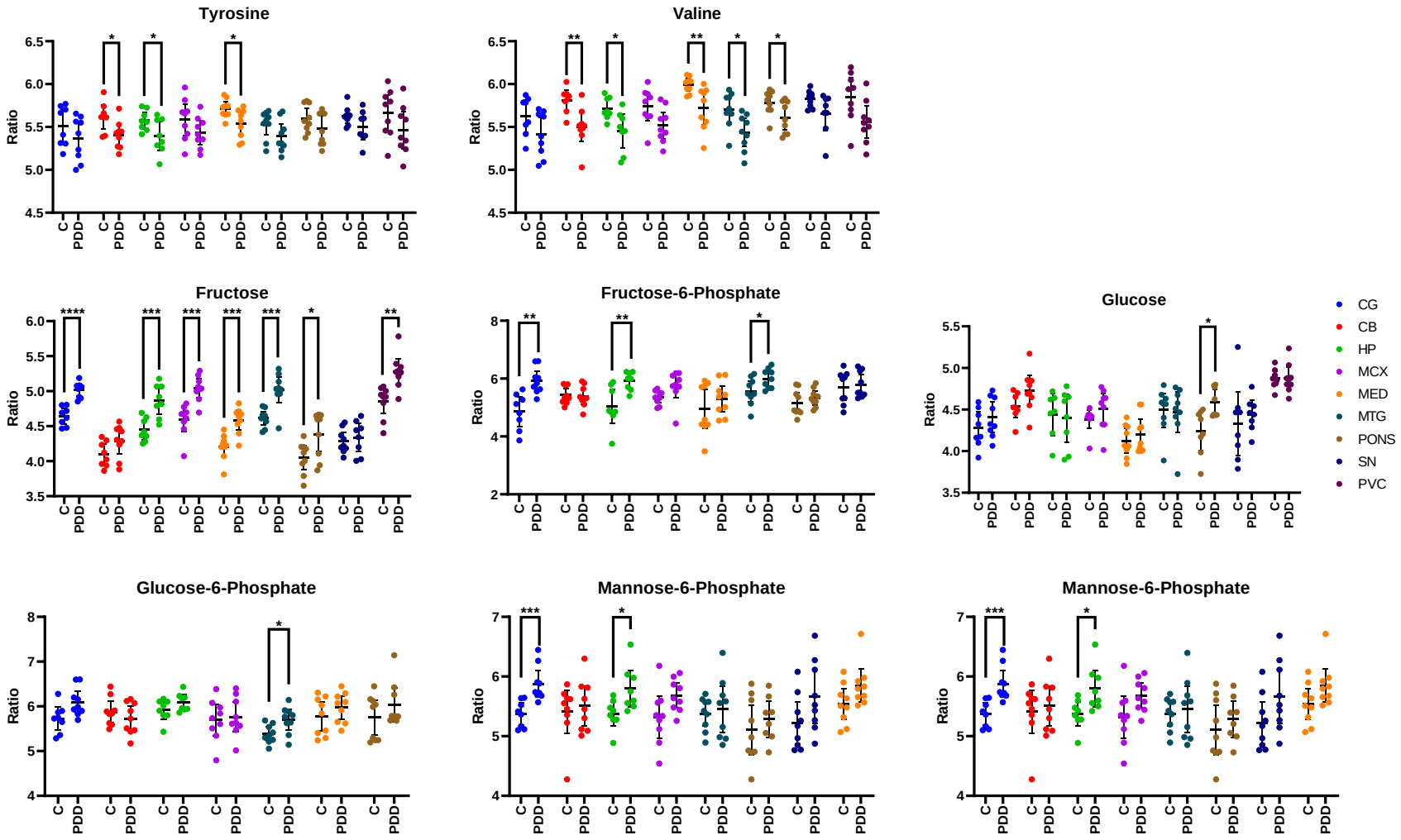
Tyrosine
Valine
Fructose
Fructose-6-Phosphate
Glucose
Glucose-6-Phosphate
Mannose-6-Phosphate
Mannose-6-Phosphate
Ratio
C
PDD
CG
CB
HP
MCX
MED
MTG
PONS
SN
PVC

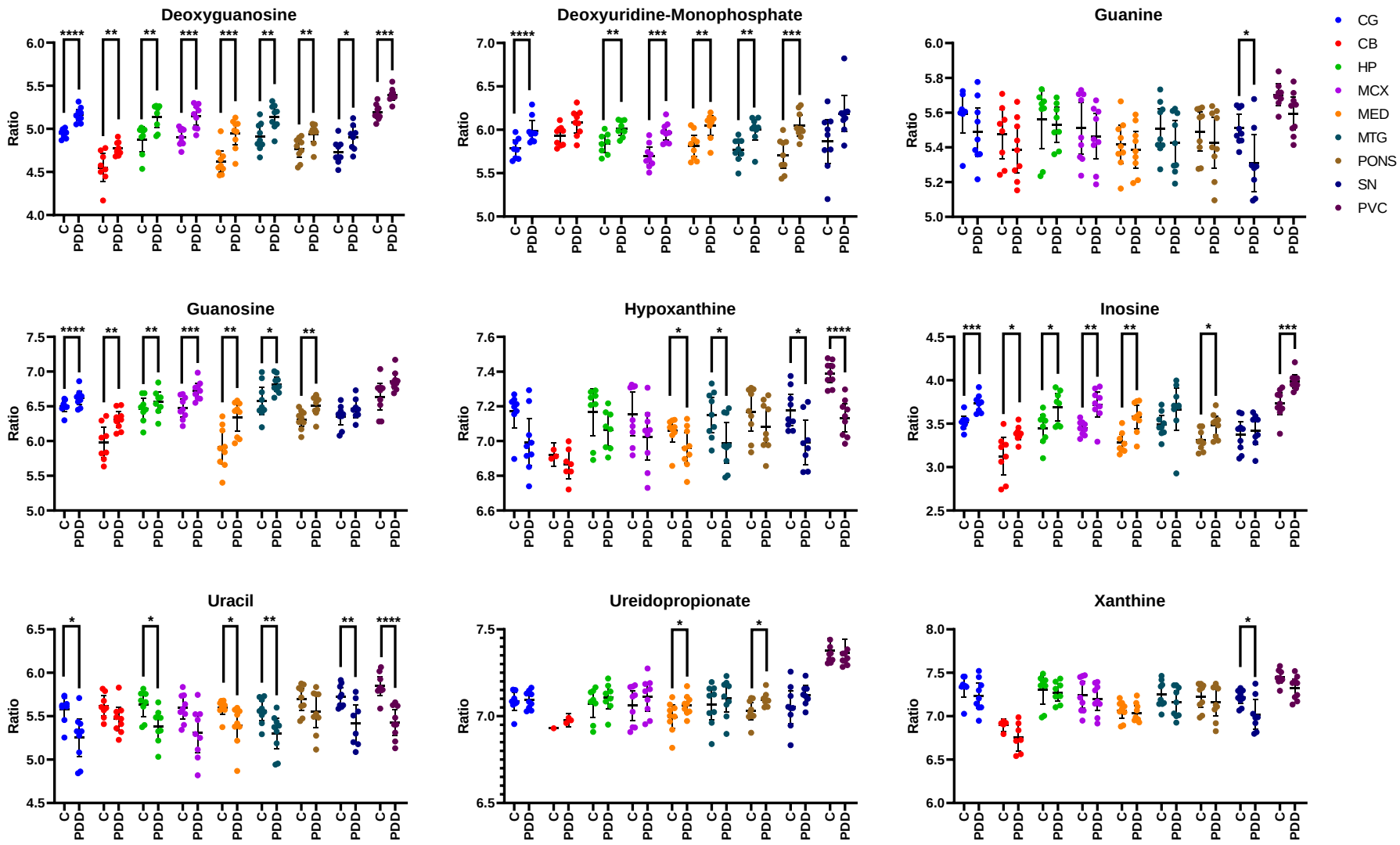
Deoxyguanosine
Deoxyuridine-Monophosphate
Guanine
Guanosine
Hypoxanthine
Inosine
Uracil
Ureidopropionate
Xanthine
Ratio
C
PDD
CG
CB
HP
MCX
MED
MTG
PONS
SN
PVC

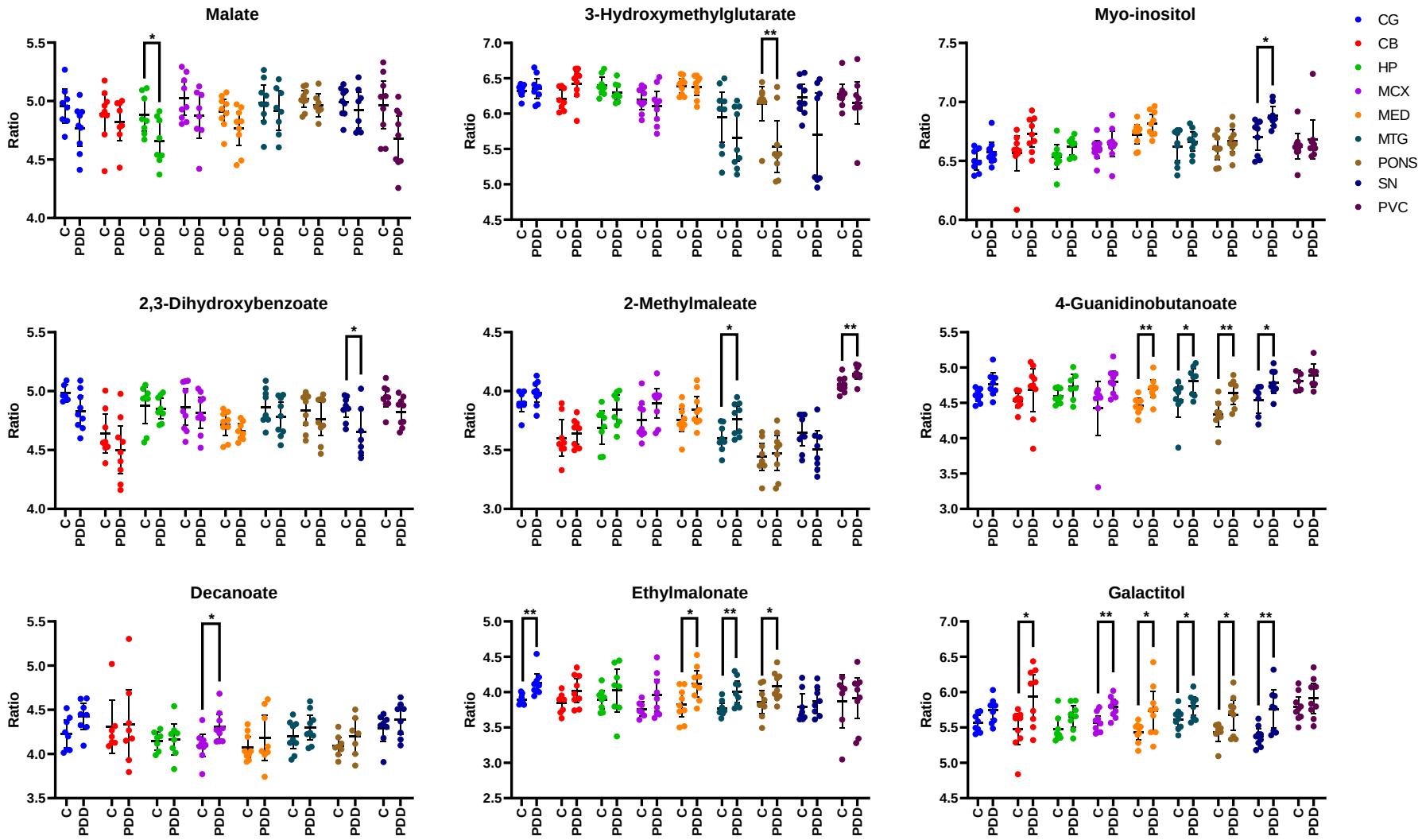
Malate
3-Hydroxymethylglutarate
Myo-inositol
2,3-Dihydroxybenzoate
2-Methylmaleate
4-Guanidinobutanoate
Decanoate
Ethylmalonate
Galactitol
Ratio
C
PDD
CG
CB
HP
MCX
MED
MTG
PONS
SN
PVC

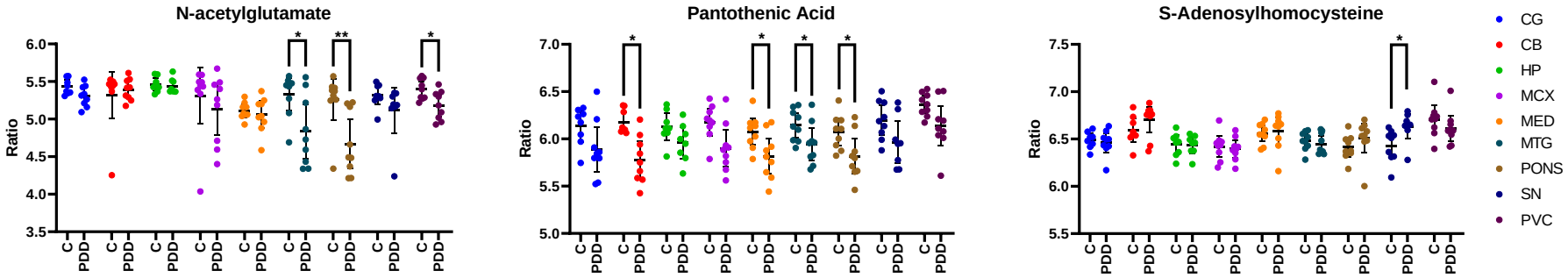
N-acetylglutamate
Pantothenic Acid
S-Adenosylhomocysteine
Ratio
C
PDD
CG
CB
HP
MCX
MED
MTG
PONS
SN
PVC

Electronic Appendix

Further data are provided electronically in Appendices A–F:

Electronic Appendix A:	Chapter Four	AD Metals Background Data
Electronic Appendix B:	Chapter Five	PDD Metals Background Data
Electronic Appendix C:	Chapter Five	PDD Metals PCA & PLS-DA Plots & Graphs
Electronic Appendix D:	Chapter Six	Human Metabolites Raw Data
Electronic Appendix E:	Chapter Six	Human Metabolite PCA & PLS-DA Plots
Electronic Appendix F:	Chapter Six	Rat Metabolite Raw Data
Electronic Appendix G:	Chapter Six	Raw Metabolite PCA & PLS-DA Plots
Electronic Appendix H:	Chapter Nine	SWATH Raw Data